A World Leading SFI Research Centre

Science Foundation Ireland For what's next

iCRAG 2019

Resources for a Sustainable Future

Monday 2nd December 2019

Croke Park, Jones' Rd, Drumcondra, Dublin 3

Poster Presentations

HOST INSTITUTION

UCD DUBLIN

PARTNER INSTITUTIONS

Trinity College Dublin, The University of Dublin

DIAS Dublin Institute for Advanced Studies

NUI Galway OÉ Gaillimh

UCC University College Cork, Ireland Coláiste na hOllscoile Corcaigh

Maynooth University National University of Ireland Maynooth

Teagasc Agriculture and Food Development Authority

DCU Dublin City University

Geological Survey Ireland Suirbhéireacht Gheolaíochta Ireland | Éireann

FUNDED BY:

Ireland's European Structural and Investment Funds Programmes 2014-2020 Co-funded by the Irish Government and the European Union

European Union European Regional Development Fund

Science Foundation Ireland For what's next

iCRAG 2019

Resources for a Sustainable Future

SUPPLY OF RAW MATERIALS

Lithium pegmatites in southeast Ireland: A storehouse for critical metals

D. Kaeter[1], R. Barros[1,2], J. Harrop[3], J. Menuge[1]

[1]SCHOOL OF EARTH SCIENCES, UNIVERSITY COLLEGE DUBLIN [2]PRESENT ADDRESS: GEOLOGICAL SURVEY OF BELIGIUM

[3]BLACKSTAIRS LITHIUM LTD & COAST MOUNTAN GEOLOGICAL

CONTACT:
david.kaeter@icrag-centre.org
@DavidKaeter

IRISH CENTRE FOR RESEARCH IN APPLIED GEOSCIENCES

BACKGROUND

INTRODUCTION

Lithium is a key element for electromobility and renewable energy storage due to its use in long-life high-energy-density batteries. Lithium is, therefore, important to attain a range of UN Sustainable Development Goals (SDGs) [1] in Ireland and the EU:

- Lithium batteries are an integral part of sustainable energy and transport infrastructures (SDG 9)
- These infrastructures are essential for sustainable cities (SDG 11).
- A domestic, European lithium supply chain would allow responsible production and consumption with a lower carbon footprint and less environmental impact than current production (SDG 12).
- Moving from fossil fuels to renewable energies (decarbonisation) is an essential part of climate action (SDG 13).

Currently, lithium is mined from only two types of deposits: Li-Cs-Ta-enriched (LCT) pegmatites and subsurface brines in salt flats (dry lakes) [2]. High emissions and energy consumption of long-distance transport in current supply chains strongly contribute to their CO_2 footprint and environmental impact. Brine production poses additional threats to local ecology and agriculture. Understanding how domestic lithium deposits formed and how they may be found are therefore crucial steps towards sustainable lithium supply. Other valuable metals typically enriched in LCT pegmatites include tantalum and tin, which are often deemed critical because of their requirement in modern electronics.

RESEARCH OPPORTUNITIES

Ore geology, mineralogy and geochemistry research is the fundament of the life cycle of any mined resource. Research outcomes directly feed into the first four domains of the supply chain – exploration, mining, processing and raw product.

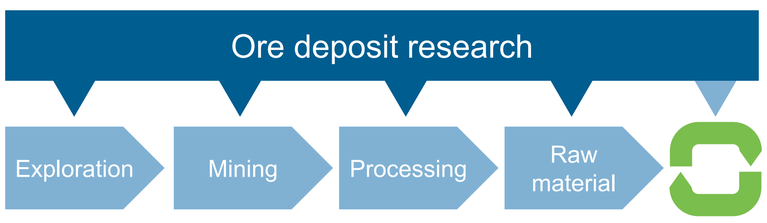

The fundamental steps in a raw material life cycle.

Research opportunities for LCT pegmatites include:

- Deposit models not nearly as advanced as for high demand metals such as copper.
- Current exploration models are limited and not widely applicable.
- Vegetated and glaciated terrain as typical for central and northern Europe poses additional challenges to exploration.
- Heterogeneous internal structure of deposits with direct implications for mining and processing.

KEY OBSERVATIONS

GEOLOGY

A belt of unexposed anatectic LCT pegmatites containing the ore mineral spodumene is emplaced within the East Carlow Deformation Zone along the margin of the Caledonian S-type Leinster Batholith, southeast Ireland [e.g. 3, 4]. In drill cores, these LCT pegmatites show ore grades, up to 1–2 wt.% Li.

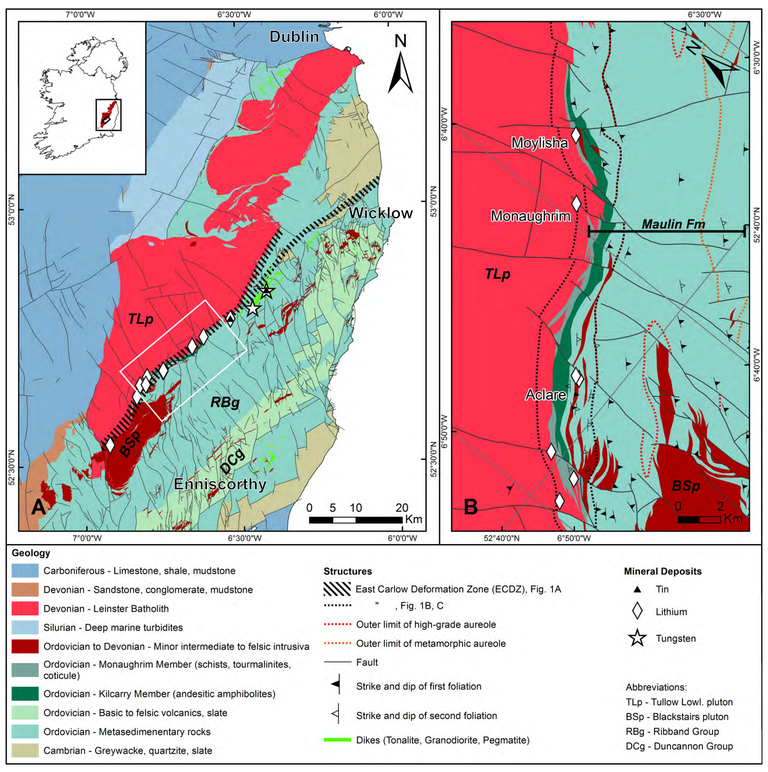

Geologic setting of the Leinster lithium pegmatites. Compiled with data from Geological Survey Ireland [5].

MINERAL CHEMISTRY

Pegmatites form from melts. Growing crystals of minerals record the changing physical and chemical conditions of a crystallising liquid by changes in their chemistry. Studying mineral chemistry allows reconstruction of melt and fluid evolution.

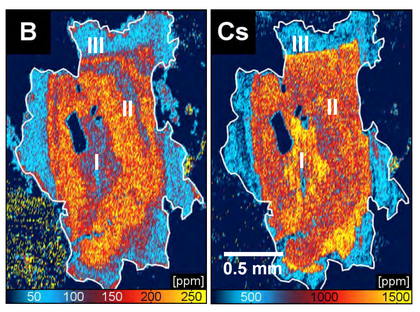

Muscovite (left) is a rock-forming mineral and shows three distinct growth stages recorded for example by boron and caesium [6]. Columbite (bottom left) is the main host for tantalum in the rocks and records a similar crystallisation history. Cassiterite (bottom right) is the main host for tin and shows at least two growth stages.

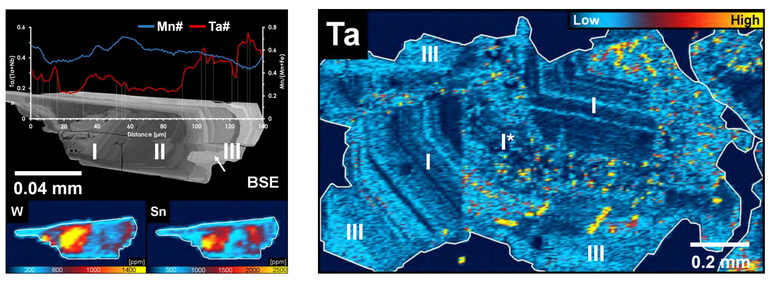

TELLUS STREAM SEDIMENTS

Southeast Ireland stream sediment data was released to the public as part of the Tellus project by Geological Survey Ireland [5]. Catchments with LCT pegmatites show anomalous tantalum and tin. Columbite and cassiterite in sediments show the same chemical zoning as in LCT pegmatites.

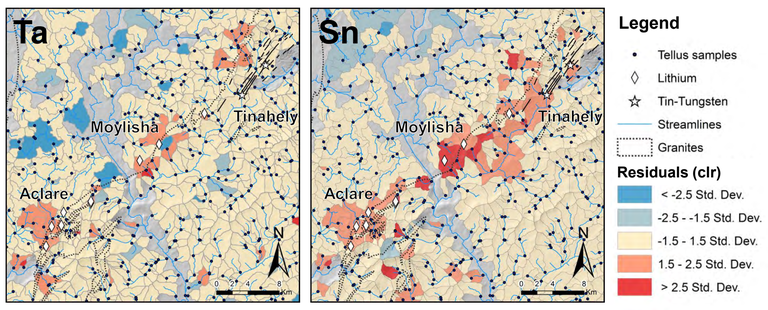

Residuals of tantalum (Ta) and tin (Sn) are high in catchments associated with lithium pegmatites [7]. Raw data: Geological Survey Ireland [5].

RESULTS

THE MODEL

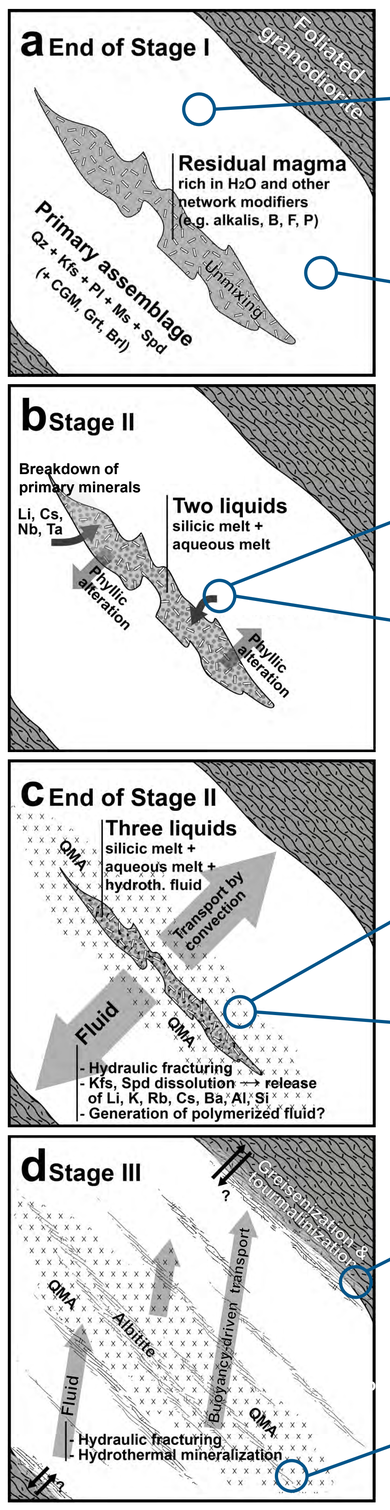

Schematic model of the magmatic–hydrothermal transition in the Leinster lithium pegmatites [6].

TYPICAL LITHOLOGIES

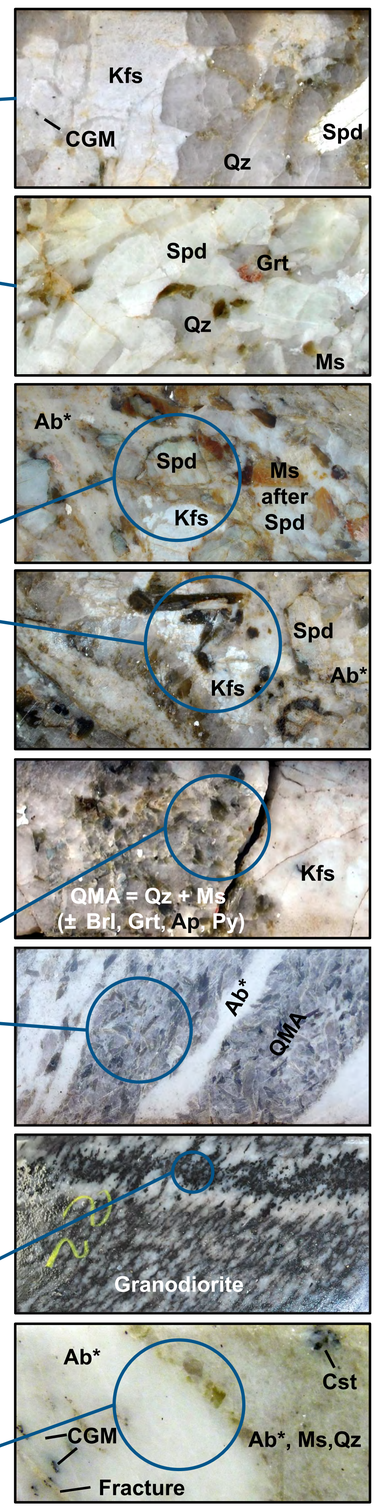

Examples of macroscopic textures typical for each stage. Field of view in all images is about 8 cm.

Abbreviations: Ab*: Albite; Ap: Apatite; Brl: Beryl; Cst: Cassiterite; CGM: Columbite; Kfs: K feldspar; Ms: Muscovite; Py: Pyrite; Qz: Quartz; Trm: Tourmaline

PRINCIPAL CONCLUSIONS

- Magmatic crystallisation in LCT pegmatites is followed by processes which remobilise and (re-) deposit critical elements.
- Lithium was deposited in early magmatic units (Stage I); tantalum and tin are enriched in late subsolidus units (Stages II–III).
- Cassiterite, columbite and other tantalum oxides in stream sediments can be used as indicator minerals in LCT pegmatite exploration.

The results allow refinement of deposit models and support exploration in Europe contributing towards responsible lithium production (SDG 12).

Understanding distribution of critical metals in LCT pegmatites allows optimisation of efficiency and by-product output of mining activities (SDGs 9, 12, 13).

REFERENCES
[1] UN 2019, Sustainable Development Goals, www.un.org.
[2] USGS 2019, Mineral commodity summaries, www.usgs.gov.
[3] Barros, 2017, PhD Thesis, UCD.
[4] Barros, Menuge, 2016, *CanMin* 54
[5] GSI, 2007, 2016, www.gsi.ie/en-ie/data-and-maps/
[6] Kaeter et al., 2018, *GCA* 240.
[7] Kaeter et al., 2019, SGA 2019 Abstr.

This publication has emanated from research supported in part by a research grant from Science Foundation Ireland (SFI) under Grant Number 13/RC/2092 and co-funded under the European Regional Development Fund and by iCRAG industry partners.

Ireland's European Structural and Investment Funds Programmes 2014-2020
Co-funded by the Irish Government and the European Union
European Union
European Regional Development Fund
Science Foundation Ireland sfi For what's next

ACKNOWLEDGEMENTS
We would like to thank E. Badenszki (UCD) and D. Chew (TCD) for technical assistance with LA-ICP-MS, and T. Culligan (UCD) for sample preparation.

PIP Petroleum Infrastructure Programme
GEOSCIENCE IRELAND Exploring Developing Sustaining
lundin mining
GROUP ELEVEN RESOURCES LTD.
international lithium corp. Power of Blue Sky Discoveries + Green Technology ILC.v
srk consulting
CIÊNCIA SEM FRONTEIRAS

Trace element study of sulfides from Irish Zn-Pb deposits: Potential vector towards mineralization

Aileen L. Doran[1]*, Steven P. Hollis[1,2], Julian F. Menuge[1], Stephen J. Piercey[3]

[1]Irish Centre for Research in Applied Geosciences (iCRAG) & University College Dublin, Department of Earth Sciences, [2]Geological Survey Ireland, Dublin, [3]Memorial University of Newfoundland, Department of Earth Sciences, St. John's, Canada

1. Irish Zn-Pb Ores: Background

- Since the 1960s, Ireland has seen 5 carbonate-hosted Zn-Pb orebodies mined and over 20 sub-economic prospects discovered (Fig. 1). After the closure of Lisheen mine in 2015, only 1 operational mine remains: Tara mines in Navan.
- Ireland is in a position to become a leader in Zn production, but for more targeted Zn exploration, our current understanding of ore formation needs to be improved.
- EMPA trace element analysis can be used to understand hydrothermal fluid processes. This will help **identify geochemical haloes around orebodies** and thereby enhance exploration strategy.

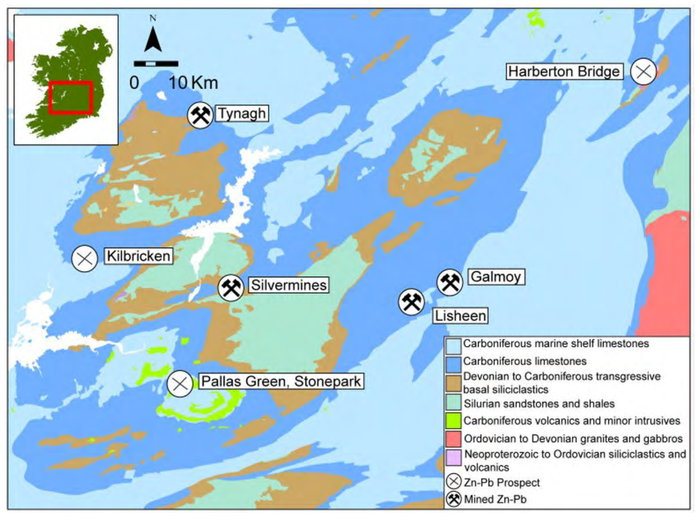

Figure 1. A simplified geological map of Ireland, with the significant Zn-Pb deposits highlighted. Geology adapted from GSI, Bedrock 1:500,000 series. Images from Doran et al. (in prep.)

2. The Lisheen deposit: Background

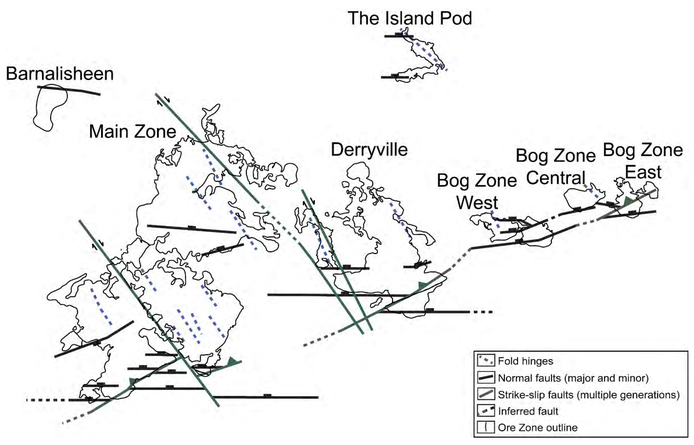

Figure 2. The orebodies of the Lisheen deposit, with key structural features shown. Structure adapted from Kyne et al., 2019 and Torremans et al., 2018). Image from Doran et al. (in prep.).

- The Lisheen deposit (Fig. 2; 23 Mt at 13.3 % Zn and 2.3 % Pb) in the southern Irish ore field formed by the replacement of Lower Carboniferous limestone, triggered primarily by fluid mixing (Wilkinson et al., 2005).
- Lisheen mine was active for over 15 years, leaving a wealth of deposit understanding. It offers an excellent testing ground for potential geochemical vectors.
- This poster presents work on the high-grade Island Pod orebody in the northern part of the mine.

3. Electron microprobe analysis (EMPA): Results

- Several generations of sphalerite, galena and pyrite were analysed by EPMA from the Island Pod orebody and its sub-economic halo (n = 574).
- EPMA data for Fe, Mn, Co, Ni, Zn, As, Pb, Bi, Mo, Ag, Cd, Tl, S, Si, Se, Cu, Au and Sb were collected at Memorial University Newfoundland and the Natural History Museum, London.
- **Sphalerite** Fe content was the most variable, with a maximum value of 6.09 wt. % (Fig. 3a). Elevated Fe correlates with low S isotope ratio (not shown), interpreted to be derived from bacteriogenic reduction of seawater sulfate.
- **Pyrite**, commonly growth-zoned, showed most variation with significant values of Co (maximum 15.1 wt. %), As (maximum 9.64 wt. %), Ni (maximum 11.2 wt. %), and Tl (maximum 1.0 wt. %) (Fig. 3b). Concentrations of Co, As, Pb and Tl are distinctly higher in main ore stage pyrite than in pre-ore (diagenetic) pyrite (Fig. 3b)
- **Galena** was relatively clean, with Zn and Fe being the most common trace elements, likely due to inclusions of sphalerite and Fe sulfides.

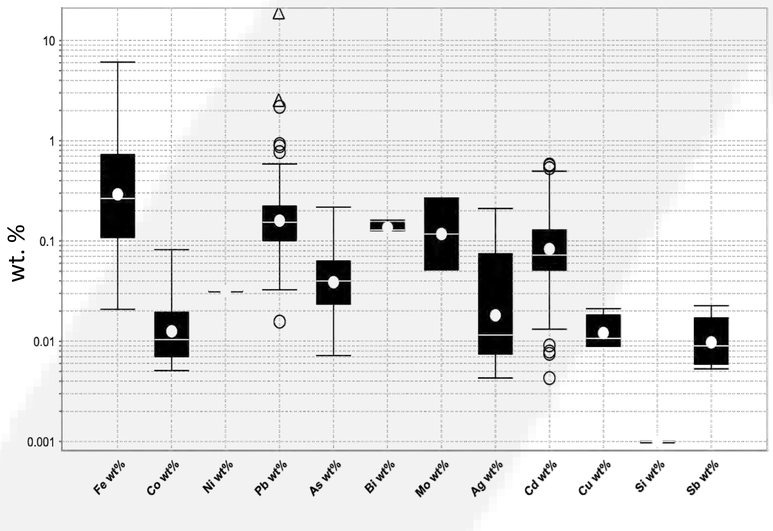

Figure 3a. (above) Sphalerite trace element data from the Island Pod orebody and its sub-economic halo. Note the large range Fe concentration in sphalerite.

Figure 3b. (below) Trace element data for main ore stage pyrite and pre-ore stage (diagenetic) pyrite.

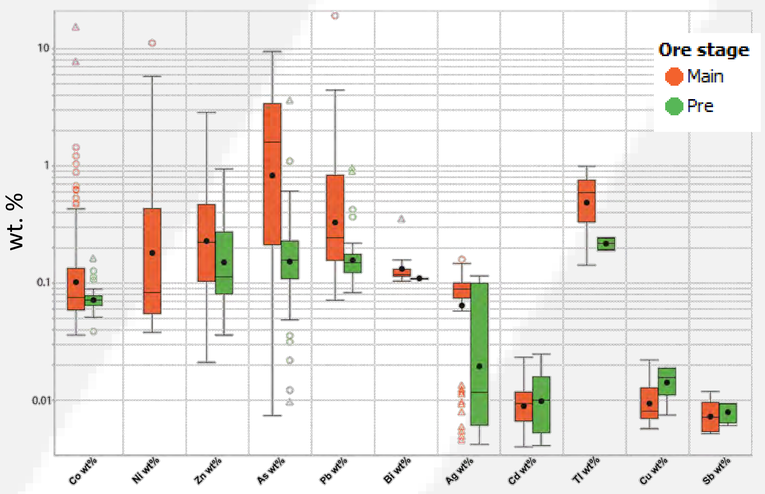

4. Pyrite trace element variation: Orebody vs halo

- Mean concentrations of As, Tl, Ni and Co are about 40-80% lower in the sub-economic halo than in the orebody (Fig. 4a, Table 1):

	Orebody mean (wt.%)	n above detection limit	Halo mean (wt.%)	n above detection limit
Co	0.34	111	0.12	151
As	2.03	104	1.25	138
Tl	0.54	55	0.24	4
Ni	1.45	13	0.34	5

Table 1 (above). Mean pyrite trace element concentrations in orebody and halo samples. Where the number of analyses (n) is low, most were below detection limits.

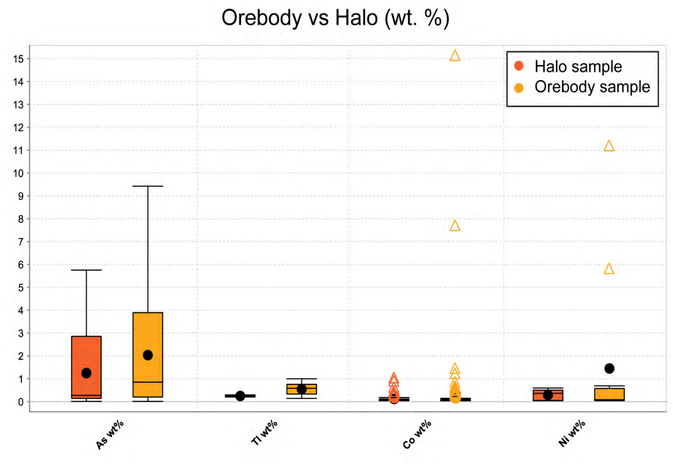

Figure 4a (above). Pyrite trace element data separated into orebody vs halo samples.

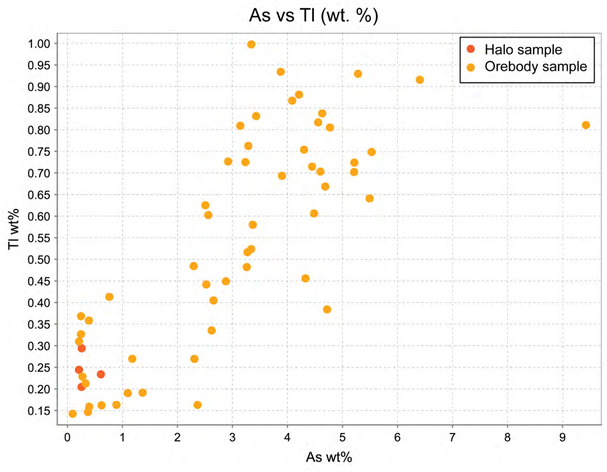

- Tl appears to depend on the presence of As, with a positive correlation (0.79) noted (Fig. 4b).

Figure 4b (left). As vs Tl concentrations in orebody and halo pyrite.

5. Pyrite trace element variation: Intra-grain scale

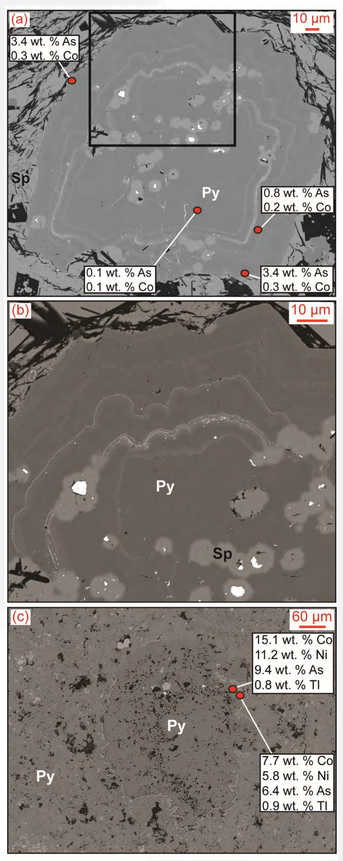

- Pyrite mineral chemistry **can record the hydrothermal evolution of a mineralizing system.**
- Island Pod pyrite preserves oscillatory zoning (Fig. 5a-b), indicating episodic flow of hydrothermal fluids.
- Intra-grain and other small scale (<250 µm) variation suggests a continuously evolving mineralizing system, which received fresh pulses of trace element-bearing fluids (Fig. 5a-c).
- Commonly, As and Co concentrations systematically increase from pyrite cores to rims. Changes in As from one band to another of up to 3 wt. % are characteristic of precipitation from distinct pulses (Caruso et al., 2018).

Figure 5a. Pyrite oscillatory zones. As and Co concentrations consistently increase from core to rim. **Figure 5b.** Detail of the box outlined in Fig. 5a, showing growth bands in more detail.

Figure 5c. A thin (<5 µm) Fe-sulfide band surrounded by pyrite. This band revealed the highest concentrations of Co, As and Tl from all Fe-sulphides analysed.

6. Applications: Exploration and Sustainable Development Goals

Exploration applications

- Pyrites offer a useful tool for understanding the genesis of ore deposits, with a single grain potentially recording the entire fluid history of a system.
- Pyrite trace element differences between the Island Pod orebody and its sub-economic halo suggest a potential application of pyrite mineral chemistry as a vector towards mineralization.

Sustainable Development Goals (SDGs) applications

- Zn has a role to play in several of the SDGs (Fig. 6). From its use as a fertiliser in agriculture (SDGs 2, 3) to its potential use in long term energy storage (SDGs 7, 11, 12, 13), Zn demand will increase with sustainable development.
- Ireland has an opportunity to be a world leader in Zn production, and significantly contribute towards achieving several of the SDGs.

Figure 6. Some of the SDGs in which Zn may play a role.

References:

Caruso et al. (2018). Precambrian Research, v. 317. p 211 – 229.
Doran et al. (submitted). Economic Geology.
Kyne et al. (2019). Economic Geology, v. 114, p. 93-116.
Torremans et al. (2018). Economic Geology, v. 113, p. 1455-1477.
Wilkinson et al. (2005). Economic Geology, v. 100, p. 63-86.

This publication has emanated from research supported in part by a research grant from Science Foundation Ireland (SFI) under Grant Number 13/RC/2092 and co-funded under the European Regional Development Fund and by iCRAG industry partners.

Aggregate Potential of Irish South Coast Offshore Palaeovalleys (AggrePOP): Preliminary Results

O'MAHONY, E.[1,2,3], WHEELER, A. [1,2,3] and PETERS, J. [1,2,4]

[1] School of Biological, Earth and Environmental Science, University College Cork; [2]Environmental Research Institute, University College Cork; [3]Irish Centre for Research in Applied Geosciences (iCRAG);

[4]Marine and Renewable Energy Ireland, MaREI Centre.

INTRODUCTION

- New construction and development projects are a vital aspect of improving social wellbeing and sand and gravel are often required for such projects (1).
- Known shortage of angular sands vital for concrete production could be strained even further by predicted enlargement of Cork City by c.100,000 new residents in the near future (2).
- From an ecological and socioeconomic perspective, marine mining aggregates can both cause significantly less permanent habitat modification and increase job prospects in the Irish South Coast (3,1).
- The AggrePOP aims to quantify resource quality in order provide these critical and potentially more environmentally-responsible resources, with the end goal of delimiting resource presence.

METHODOLGY

- Data obtained was predominantly collected on board the *RV Celtic Voyager* cruise no: CV18034 – A joint venture between the AggrePOP and Eirwind projects.
- This was done via the use of a combination of multiple data acquisition systems such as; EM2040 Bathymetric surveying (Fig. 1), Shipek grab sampling and Vibrocoring (Fig. 2) accumulating to help better quantify the South coast seabed substrate.
- Post in-situ sediment extraction, particle size analysis is completed via the use of a Malvern Mastersizer 3000 optical system that uses laser diffraction to measure particle size distribution (PSD) of a given sediment ranging from 0.1 to 1500 µm

Fig. 1 Map of CV18034 cruise area. The white, arrowed line shows multibeam survey track line and direction. Labelled, yellow dots mark the areas targeted for coring activities.

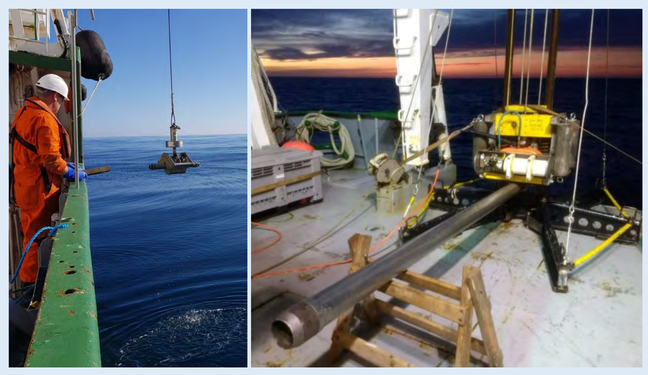

Fig. 2 (Left): (Action shot) Shipek grab sampler in use off the South-West coast of Cork. (Right): Vibrocorer stored safely ready for use during the AggreWind research cruise (CV18034). Barrel length 3 m; diameter 11 cm.

RESOURCE IDENTIFICATION

- The south coast of Ireland sports a jagged coastline, the seabed is quite similar in nature. ArcGIS is used to compile physical sediment data with remotely sensed data in order to quantify the seabed.
- Bathymetry and Backscatter collected from both research cruises and INFOMAR projects.

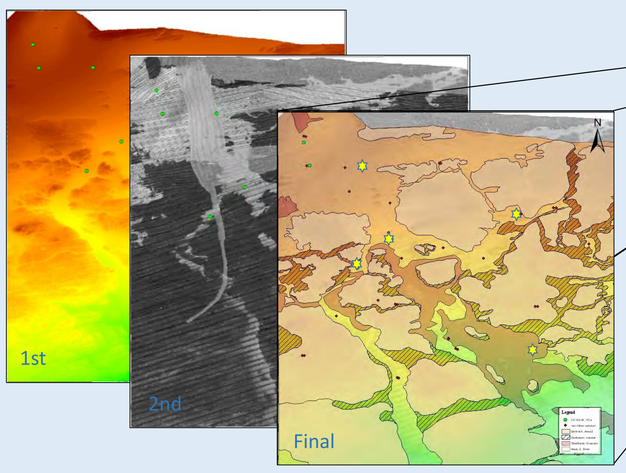

Fig. 4 Left to right: Bathymetry – Backscatter – Combined to distinguish Bedrock from sediment and sediment veneer.

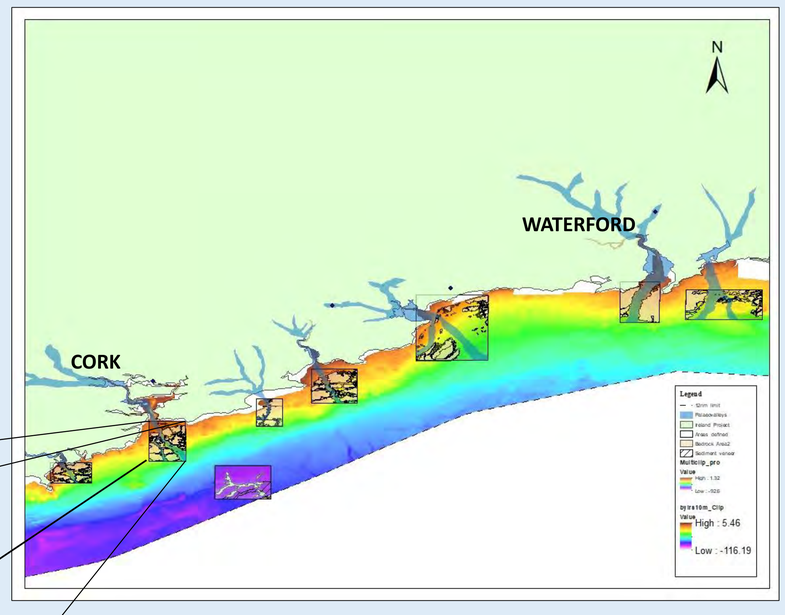

Fig. 3 Regional display of both remote and physical data used in the AggrePOP specific areas of research, inc: Multibeam, Vibrocore and Shipek grab sample data. Note, the data has been condensed and clipped to increase resolution.

- 5 Vibrocores from the area 2 (Fig. 4), show initial signs of sand to gravel sized grains. A positive result for preliminary sediment analysis (ANNOTATED BY YELLOW STAR).

ENVIRONMENTAL BENEFITS OF MARINE AGGREGATES

- Marine aggregates (MA) have some benefits over their terrestrial counterparts. From an industry standpoint, MA are typically cleaner and less prone to pyritization with improved calcium carbonate contents (4).
- Studies of a mixed seabed substrate (sandy to pebbly) under low dredging intensity has shown full natural recovery of the seabed within a short 10-year period (5).
- 1 typical aggregate ship delivers around 250 lorry loads of product, largely reducing carbon emissions and infrastructure damage due to extensive truck-based transport.

RESOURCE QUALITY -

- PSD Malvern laser diffraction and sieve stack analysis will be performed on the 36 cores and 32 grab samples to assess and quantify particle size distribution across the South Coast; (below is an initial size fraction classification of Grab (black) and Vibrocore (green) samples taken, displayed on a FOLK 7 ternary plot)

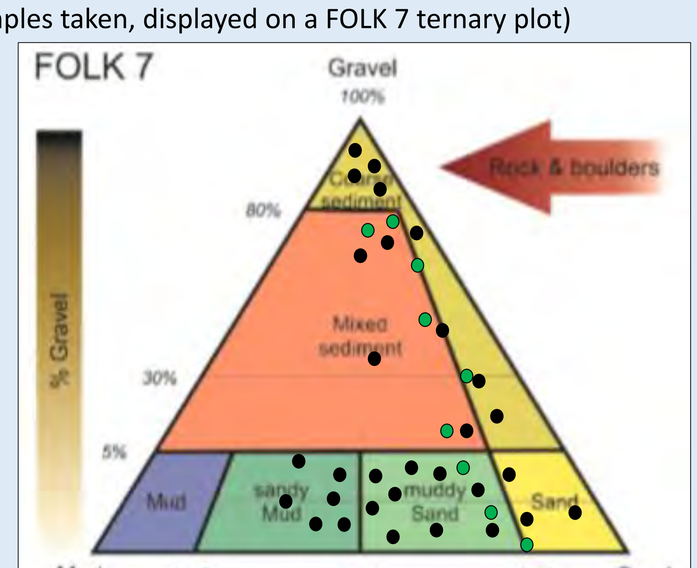

Fig. 5 Folk 7 Ternary plot template taken from Kaskela *et* al., (2019)

FUTURE PLANS AND ACKNOWLEDGEMENTS

- Probable comparative particle size analysis study against quantified known terrestrially quarried aggregates located on the upstream areas of the studied palaeovalleys.
- Carbonate content to be included in particle size analysis to assess the lithic fraction versus the carbonate fraction of South Coast sediment samples.
- The authors would like to commend the Marine Institute, the MaREI Centre and the INFOMAR project for access to workspace and invaluable research data.

SCAN ME

Scan QR to visit AggrePOP webpage

REFERENCES

[1] Sutton, G. (2008). Irish Sea Marine Aggregate Initiative (IMAGIN) Project Synthesis Report Including: Geological Assessment, Environmental Assessment, Morpho dynamic Modelling Web-based GIS system, Cost benefit Analysis, Aggregate Resources and Market-Wales. *Marine Environment and Health Series*, No. 36.

[2] Morgenroth, E. (2018). Prospects for Irish regions and counties: scenarios and implications. *ESRI Research Series Number 70*. The Economic and Social Research Institute Whitaker Square, Sir Rogerson's Quay, Dublin 2.

[3] Deprez, M. (2000). Physical and biological impact of marine aggregate extraction along the French coast of the Eastern English Channel: short and long-term post-dredging restoration. ICES Journal of Marine Science, 57, 1435.

[4] Prentice, J. E. (1990). *Geology of construction materials* (Vol. 4). Springer Science & Business Media.

[5] Le Bot, S., Lafite, R., Fournier, M., Baltzer, A., Desprez, M. (2010). Morphological and sedimentary impacts and recovery on a mixed sandy to pebbly seabed exposed to marine aggregate extraction (Eastern English Channel, France). Estuarine, Coastal and Shelf Science, 89, 232.

This publication has emanated from research supported in part by a research grant from Science Foundation Ireland (SFI) under Grant Number 13/RC/2092 and co-funded under the European Regional Development Fund and iCRAG industry partners.

Fingerprinting Volcanic Ash of the Irish Midlands

Hilde A. Koch[1,2] (hilde.koch@icrag-centre.org), Michael E. Philcox[2], Balz Kamber[3] ,David Chew[1,2]
[1]iCRAG, [2] Trinity College Dublin, [3]Queensland University of Technology

INTRODUCTION

The Lower Carboniferous limestones in Ireland host the Irish Zn-Pb orebodies, one of the most significant sources of Zn in the world but stratigraphic correlations are difficult, relying on incomplete biostratigraphy. The main goal of this study to develop a chemostratigraphic reference framework for the volcanic ash layers to support exploration for the carbonate zinc-lead deposits of Ireland.

The conventional practice in most tephra correlation is to analyse the elemental chemistry of volcanogenic glass (e.g. Lowe, 2011 [1]). The studied tuffs were deposited into Mississippian age carbonates of the Irish Midlands Basin and are largely diagenetically altered to bentonite clay bands which coincides with the devitrification of glass. But despite alteration, some bentonites contain resistant phenocrysts like zircon and apatite. Therefore, this study introduces a multi-proxy tool using **high-precision trace element bulk-rock geochemistry, apatite characterisation as well as U-Pb zircon geochronology**.

SAMPLE DESCRIPTION

Three different tuff horizons were sampled from two drillcores (3470/15; 3471/4) in the Slieve Dart area in the north-west of Ireland. Individual tuff horizons are shown in different colours. Tuff 1 is the stratigraphically highest tuff in the drill-cores, liing in the Oakport Limestone formation, followed by Tuffs 2 and 3, which occur in the Kilbryan Limestone.

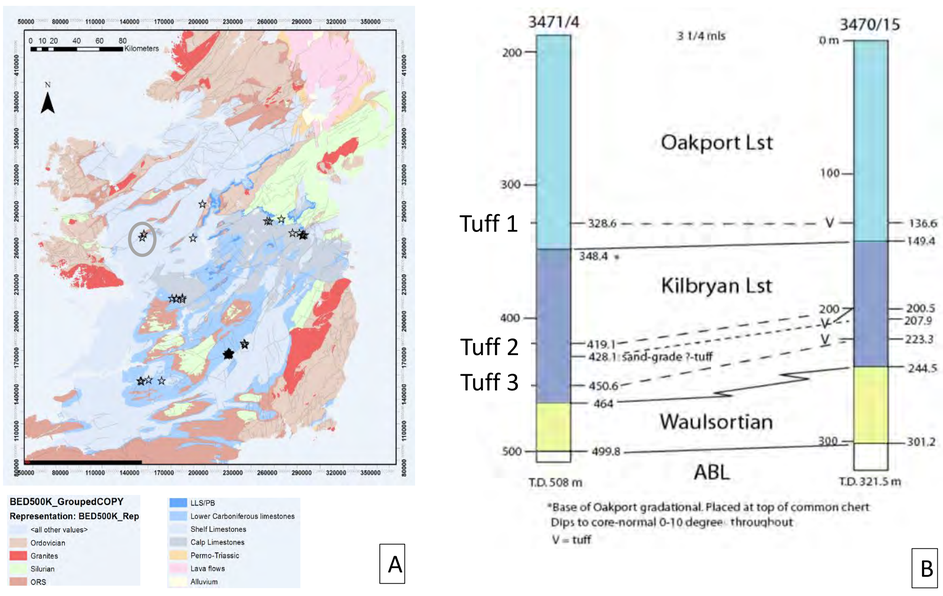

A) Simplified geological map of Ireland, showing the locations of available samples (black stars). This poster shows the results for the highlighted area. B) Stratigraphic columns for the two sampled boreholes from Slieve Dart.

U-Pb ZIRCON DATING

The used method was laser ablation inductively coupled mass spectrometry (LA ICP-MS). Tuff 1 in both drill cores did not yield any zircons. Zircons from the four other samples are plotted on U-Pb zircon Wetherill concordias. Samples yield concordant analyses as well as discordant analyses which are interpreted as older inherited grains, common Pb bearing grains and grains which suffered Pb loss (C, D, E, F). The concordant ages for the 2nd tuffs are 345.4 and 347.6 Ma, whereas the ages for the 3rd tuffs are both around 358.5 Ma

RESULT

U-Pb zircon dating reveals that Tuff 2 and Tuff 3 car be differentiated. Tuff 2 is roughly 12 Ma younger than Tuff 3.

SEM-CL imaging of the zircons shows the zoning and the average sizes of the occuring zircons (G).

drillcore 3471/4

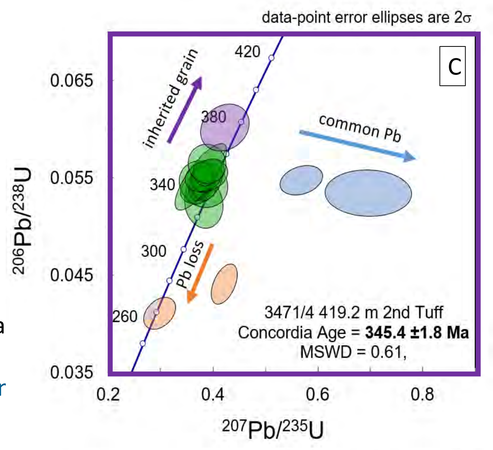

drillcore 3470/15

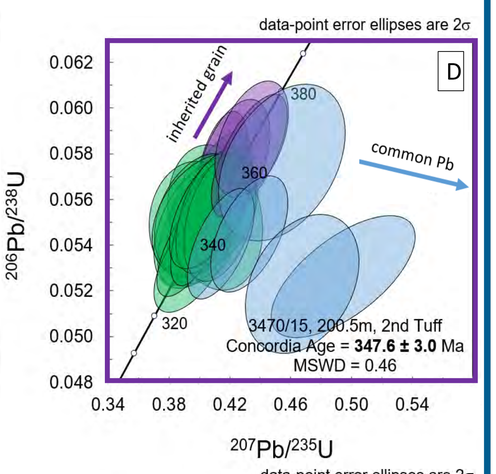

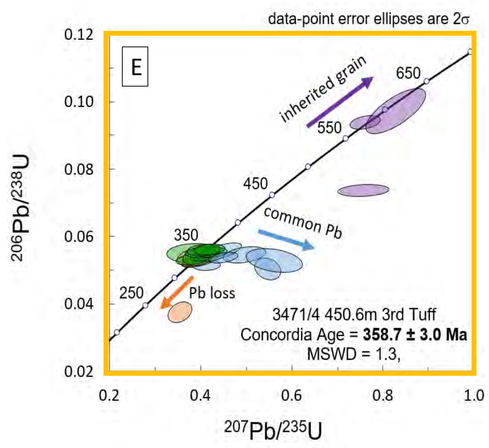

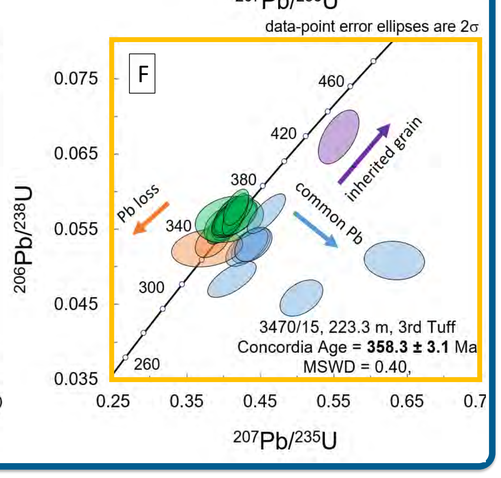

HIGH-PRECISION TRACE ELEMENT BULK GEOCHEMISTRY

Volcanic ashes in general are not a one-to-one geochemical image of their source. Their bulk-rock geochemistry may be influenced by alteration, phenocrysts, aeolian fractionation, dilution with matrix sediments,… . To minimise the influence of these secondary effects on the tuffs, the focus is on aluminium, titanium, niobium, tantalum , rare earth elements (REEs) [2]. Used method is a refined high-precision solution ICP - MS trace element analysis [3], [4] using low-P hotplate HF-HNO_3 digestions. REE/Al ratios were first normalised to MUQ before they were vertically translocated to comparable levels in the diagram (H). Negative europium anomalies, like observed in all three tuff layers, are characteristic of silicic igneous rocks. They also indicate highly evolved, sub-alkaline magma sources [5]. Marker Tuffs from a different area (Tara Deep) are shown for comparison.

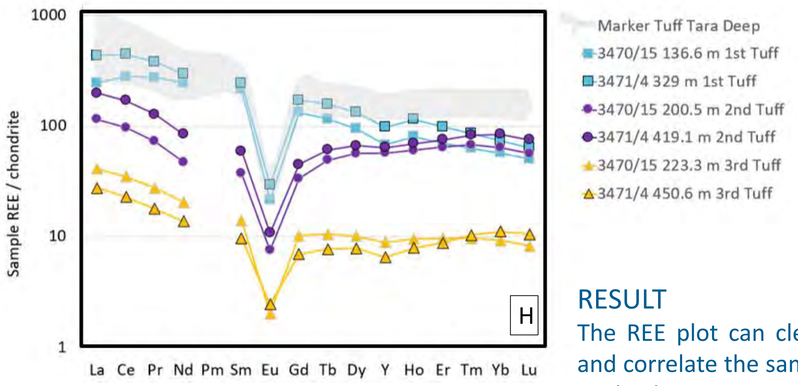

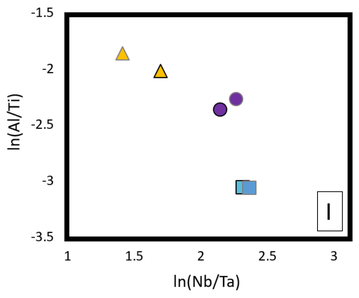

RESULT

The REE plot can clearly distinguish three tuff horizons and correlate the same horizon across cores indicating an evolved magma source. Binary plots also separates the three different tuff layers (I).

MATCHOGRAM

Modified method after Marx et al., 2005 [6] compares the relative concentrations of the least mobile elements of two samples with each other. First step is to divide all elements from sample A with the corresponding element in sample B. A perfect match would be unity. To correct for asymmetry and bias, the concentration of sample A serves once as the numerator and once as the denominator. Results are summed up and divided by two to receive the symmetrical ratio. Step two corrects for dilution effects. Finally, the reference point is set to zero. Therefore, a perfect match would result in the sum of absolute deviates (Σ_D) of zero. The closer the samples' Σ_D is to zero, the more likely they share the same origin. The following element list was used: Al, Ti, Y, Nb, Sn, Ta, La, Pr, Nd, Sm, Gd, Dy, Er, Yb

	TUFF 1 3471/4	TUFF 1 3470/15	TUFF 2 3471/4	TUFF 2 3470/15	TUFF 3 3471/4	TUFF 3 3470/15
TUFF 1 3471/4	0					
TUFF 1 3470/15	0.4	0				
TUFF 2 3471/4	5.0	5.8	0			
TUFF 2 3470/15	3.2	4.1	0.7	0		
TUFF 3 3471/4	5.9	6.3	5.7	5.1	0	
TUFF 3 3470/15	7.9	8.4	4.7	4.2	0.4	0

RESULT

The three different tuff horizons can be distinguished.

APATITE CHARACTERISATION

Apatite ages are less precise than Zircon ages. But as the trace element chemistry of apatite can provide an effective link to the parent igneous rock type of the tuffs, apatite dating will only be used to rapidly characterise sample age populations before analysing them for trace elements. Apatite dating as well as trace element data were gained using LA ICP-MS. Only both tuff 3 yield enough apatites to date them. Apatite U-Pb ages for sample 3471/4 and 3470/15 all lie on Tera-Wasserburg discordias (J, K), yielding lower intercept ages 379 ± 28 Ma and 368 ± 35 Ma, respectively. The initial Pb composition was anchored using an initial $^{207}Pb/^{206}Pb$ composition derived from the Stacey and Kramers model with a conservative uncertainty of 0.02, as otherwise they exhibit a relatively poor constrained intercept age due to the small spread in U-Pb ratios.

The Sr/Y vs ΣLREE biplot introduced by O'Sullivan et al., 2019, in review discriminates Tuff 3 apatites as felsic granitoid apatites (L). Tuff 1 falls into the alkali-rich igneous apatite and Tuff two into the mafic granitoids to mafic igneous apatite field.

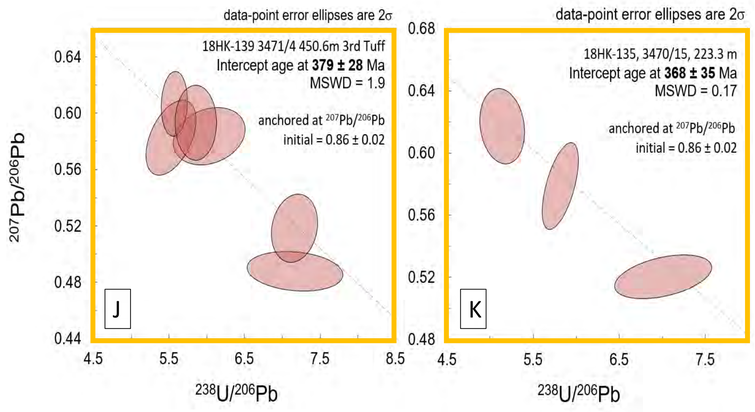

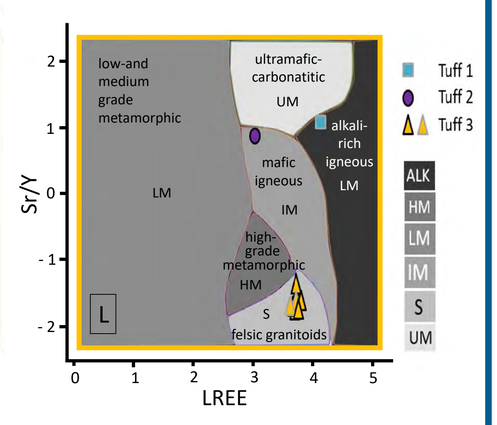

The rare earth elements of apatite phenocrysts were normalised to chondrite. The REE pattern of both tuff 3 layers are notably different from those of the stratigraphically higher beds (M).

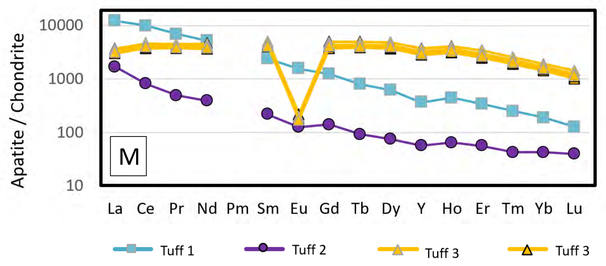

RESULT

The apatite ages for both Tuff 3 samples are in accordance with the zircon ages. The principal component analysis links both tuff 3 samples to a felsic parental magma composition which is already indicated by the whole-rock chemistry. The REE patterns from tuff 3 are also distinguishable from tuff 1 and tuff 2. Thus, the combined approach is able to reveal different ash beds and can be used for a big dataset to develop an Irish chemostratigraphic framework.

REFERENCES

[1] Lowe (2011) *Quaternary Geochronology* **6**, 107-153
[2] Kiipli et al. (2017) *Sedimentary Geology* **347**, 148-159
[3] Eggins et al. (1997) *Chemical Geology* **134**, 311-326
[4] Babechuk et al. (2010) *Geochimica Et Cosmochimica Acta* **74(4)**, 1448-1470
[5] Rollinson (1993) Using geochemical data: evaluation, Singapore. Ongman
[6] Marx et al. (2005) Earth Surface Processes and Landform **30**, 699-716

SITE VISIT, 2nd December 2019
iCRAG

This publication has emanated from research supported in part by a research grant from Science Foundation Ireland (SFI) under Grant Number 13/RC/2092 and co-funded under the European Regional Development Fund and by iCRAG industry partners.

Vein-hosted Copper Deposits and Hydrothermal Processes of SW Ireland

J. Lang[1], P. Meere[1], R. Unitt[1], S. Johnson[2]

[1]Irish Centre for Research in Applied Geosciences (iCRAG), School of Biological, Earth and Environmental Sciences, University College Cork, Ireland
[2]Irish Centre for Research in Applied Geosciences (iCRAG), University College Dublin, Ireland

ALLIHIES

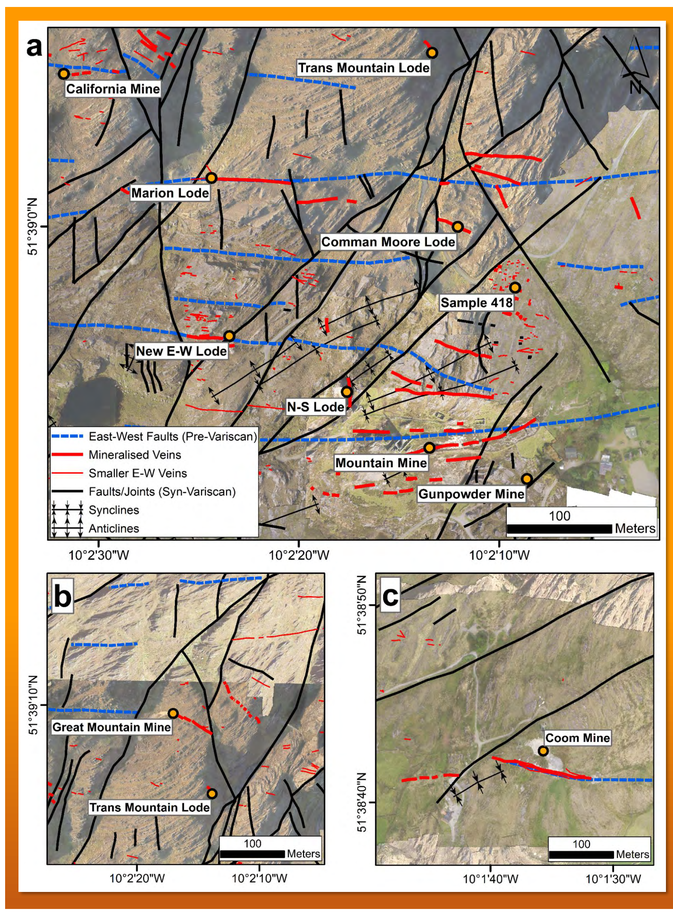

Fig. 2) Structural Map of the historic copper mines at Allihies, Beara Peninsula.
Pre-Variscan, extensional faults and mineralised veins (striking mainly E-W) are affected by syn-Variscan, SW-NE striking structures (drone maps and Bing™ Satellite Maps (2016), including field analysis and modifications from Reilly (1986)).

a) Major lodes of the Mountain Mine Area with pre- and syn-deformation structures.
b) Sinistral faulted lode of Great Mountain Mine (NW of Mountain Mine Area).
c) Sinistral faulting of Coom Lode (ESE of Mountain Mine).
d) Historic sample of mineralised quartz vein with molybdenite and minor chalcopyrite from National History Museum London (NHM, Russell collection, 1918)

➔ Re-Os chronometry on molybdenite for Mountain Mine revealed an age of 366.4 ± 1.9 Ma

d)

366.4 ± 1.9 Ma

INTRODUCTION

This study focusses on the historically mined vein-hosted copper deposits in southwest Ireland. Central to this is determining the role of Upper Palaeozoic Munster and South Munster Basin structural architecture on the nature and timing of mineralisation. Aerial image interpretation and field studies revealed large scale, basin related E-W to SW-NE striking extensional faults (Fig. 1). These extensional faults are associated with copper bearing quartz veins and large N-S striking (transfer?) faults. Mineralised sediment beds follow the Variscan strike (SW-NE). They occur in proximal distance to E-W striking faults and mineralised quartz veins.

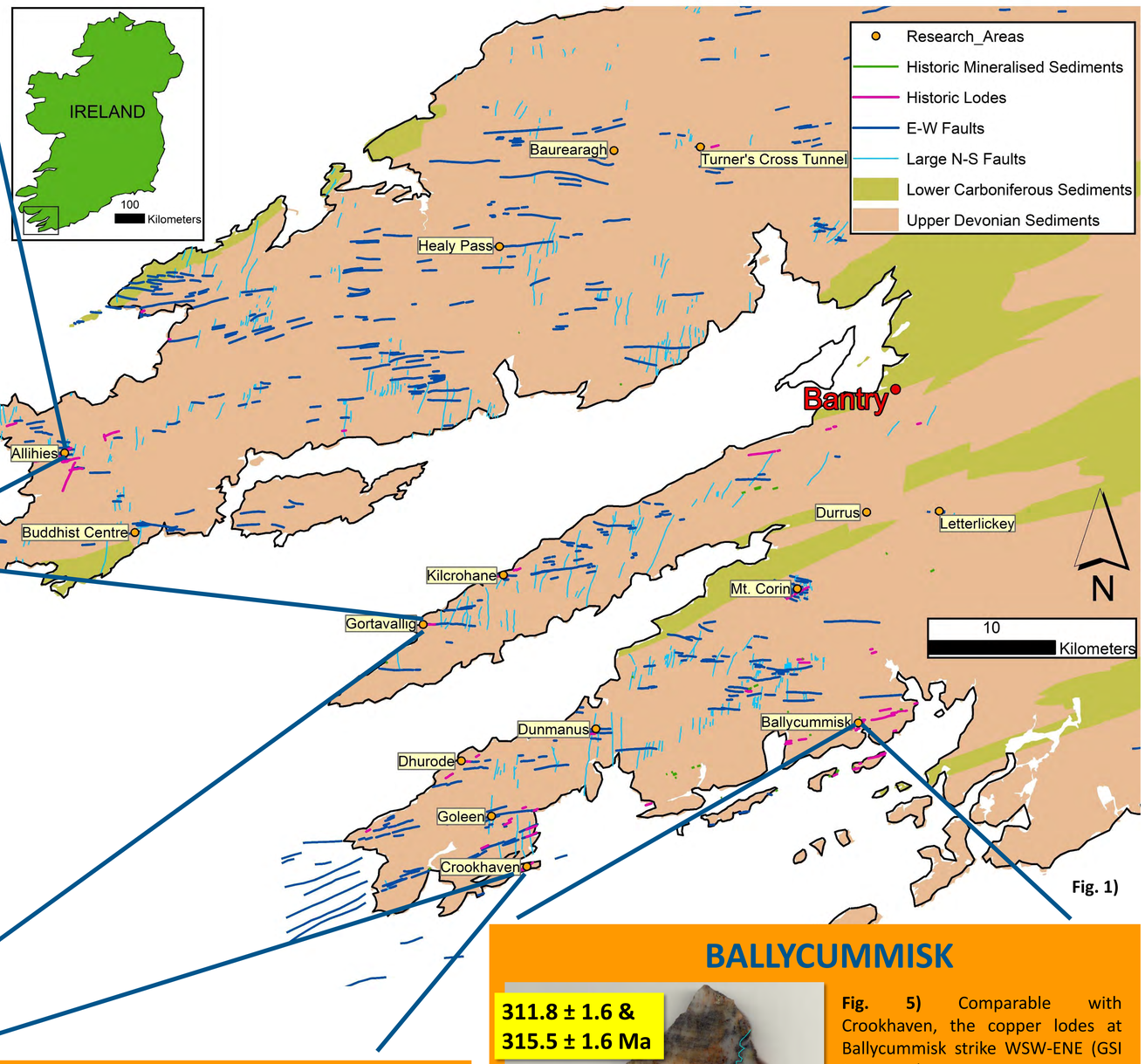

Fig. 1)

GORTAVALLIG

Fig. 3) Map of the historic copper mines at Gortavallig, Sheep's Head (including high resolution drone imagery and ArcGIS® BaseMap, 2019).
The copper bearing quartz veins follow E-W striking extensional faults. The major extensional fault shows a sinistral offset (110 m) caused by a high angle, syn-Variscan reverse fault (SW-NE striking).

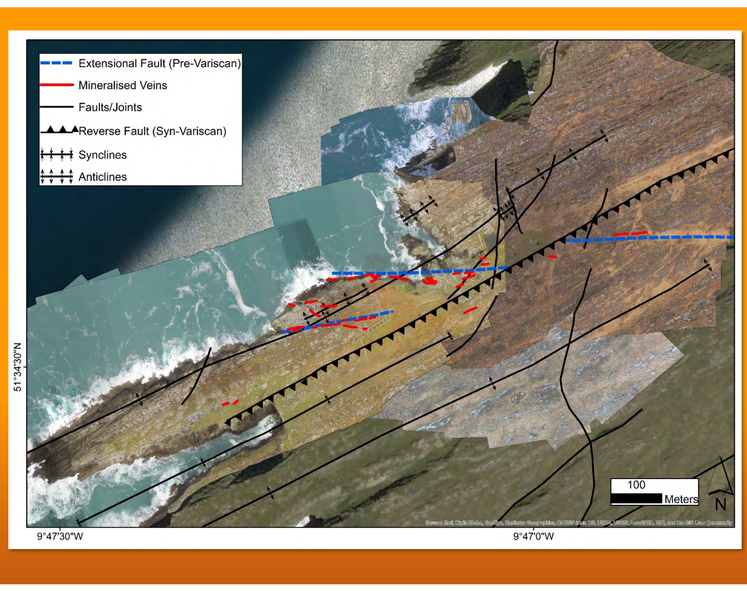

BALLYCUMMISK

311.8 ± 1.6 &
315.5 ± 1.6 Ma

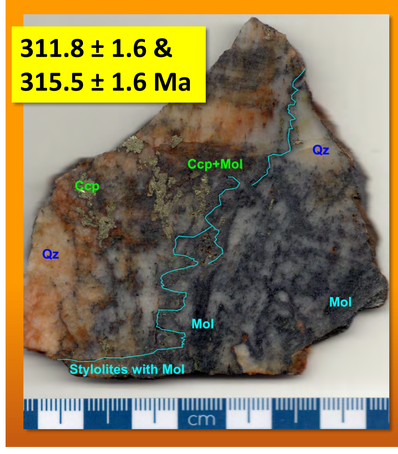

Fig. 5) Comparable with Crookhaven, the copper lodes at Ballycummisk strike WSW-ENE (GSI Jetstream).
A historic molybdenite sample from NHM (Russell collection, 1907) and a recent finding from the Ballycummisk dumps show Re-Os ages of 311.8 ± 1.6 Ma and 315.5 ± 1.6 Ma.
Molybdenite covered stylolites within the mineralised quartz vein sample indicate a post-mineralisation (Variscan) compressional event.

CROOKHAVEN

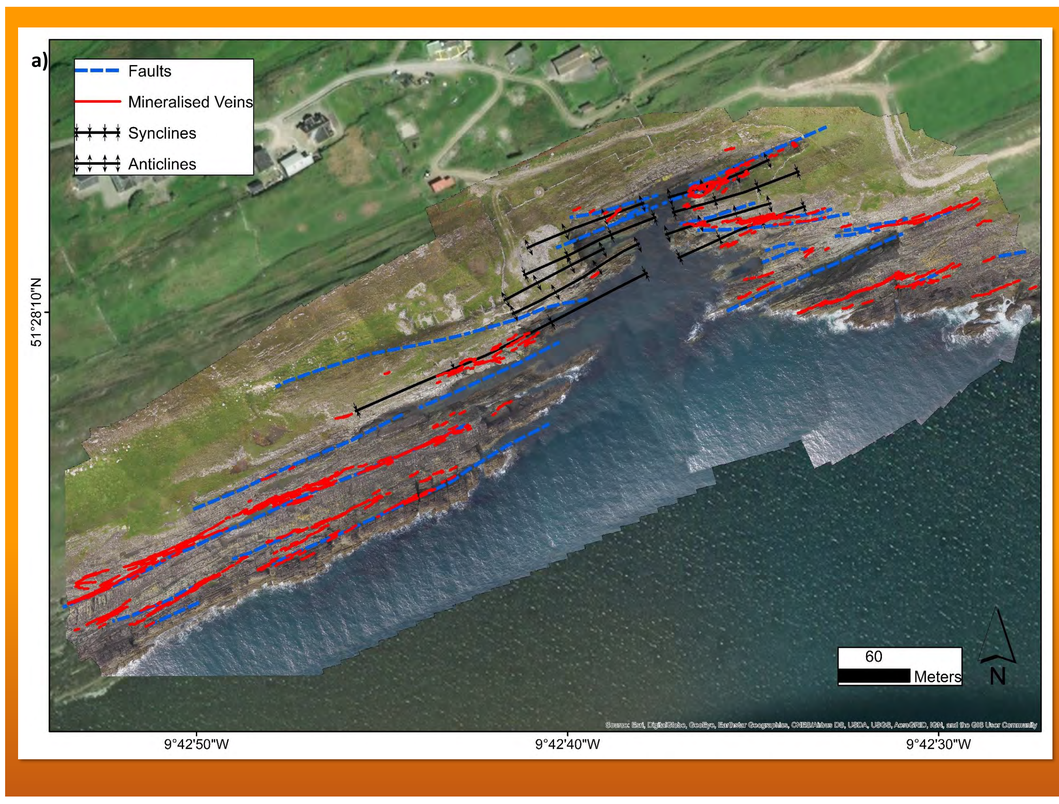

Fig. 4) The copper mines of Crookhaven are located on the southern coast of Mizen Head.

a) Drone imaging (including ArcGIS® BaseMap, 2019) and field data show a WSW-ENE strike of the pre-Variscan extensional faults and the associated mineralised quartz veins. This pre-Variscan strike is parallel to the syn-Variscan structures (folds and faults).
b) A set of smaller mineralised (chalcopyrite) quartz veins occur sub-horizontal within altered siltstone. Variscan compression from SE-NW caused small-scale folding and cleavage.

b)

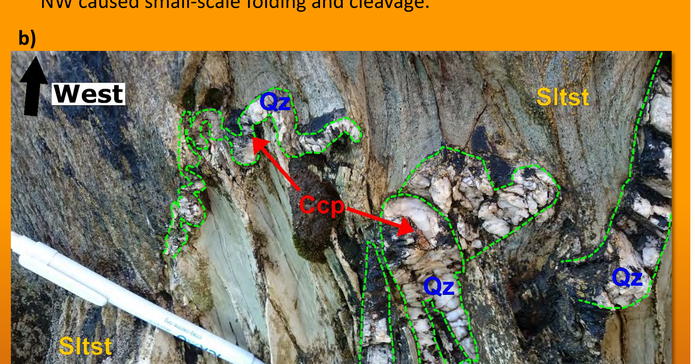

Fig. 6) Copper is an essential product for sustainable, environmental friendly and modern techniques. Several hundred kilograms of copper wire is needed for the construction of one e-car.
Copper has a high electrical conductivity and is therefore used in almost every electrical device (smartphones, computers, flat screens).
The key components of wind turbines are large copper coils which produce sustainable electrical energy.

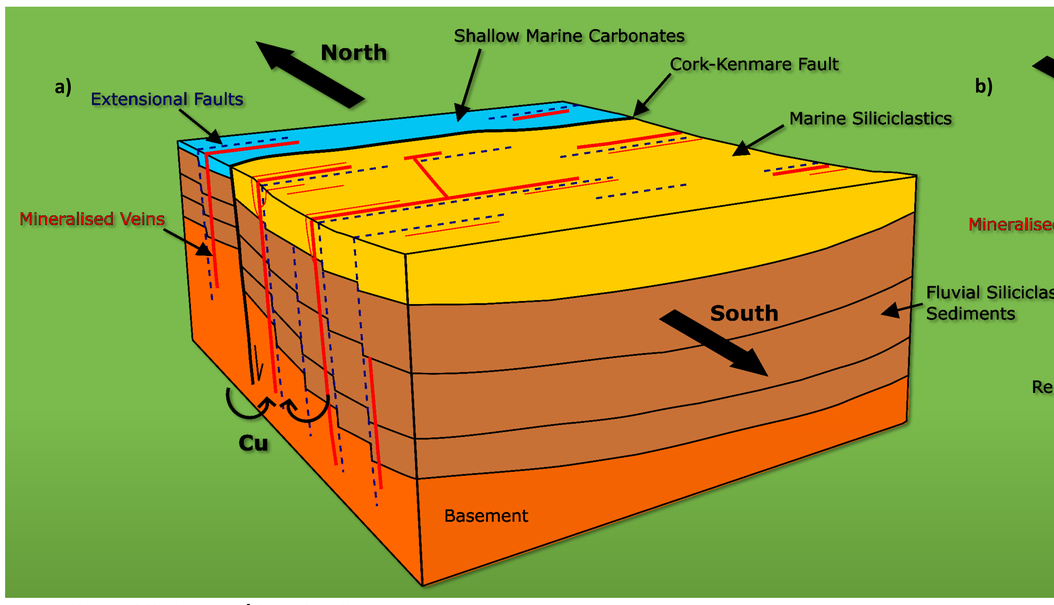

Fig. 7) Results/Hypothesis
The North-South extension during the development of the Munster and the South Munster Basins caused large scale E-W striking extensional faults which provided a deep sourcing fluid pathway for medium to high saline copper rich fluids (Fig. 7a). These fluids formed the mineralised, mainly E-W striking and steep dipping quartz veins.
The end Carboniferous Variscan Orogeny deformed, faulted and folded the basin structures as well as the mineralised veins and remobilised silica-rich fluids which precipitated quartz veins into tension gashes (saddle reefs, en echelon veins, sub-horizontal veinlets) (Fig. 7b).

ACKNOWLEDGEMENTS/REFERENCES

We would like to thank the team from the Allihies Copper Mine Museum for giving us the access to the amazing underground cavities of Mountain Mine. Many thanks to the mineral curators from the National History Museum London for providing sample material for the Re-Os dating. Thanks a lot to David Selby (Durham University, UK) for the Re-Os dating.
Reilly, T.A. 1986. A review of vein mineralization in SW County Cork, Ireland. In: Andrew, C.J., Crowe, R.W.A., et al. (eds) Geology and Genesis of Mineral Deposits in Ireland. Irish Association for Economic Geology, Dublin, 513-544.
Figure 1 (Historic Lodes and Historic Sediments) contains Irish Public Sector Data (Geological Survey) licensed under a Creative Commons Attribution 4.0 International (CC BY 4.0) licence (jetstream.gsi.ie, accessed February/March 2019). Figures 1-4 were created using ArcGIS® software by Esri (including BaseMap) and Microsoft® Bing™ Satellite Maps, 2016-2019. ArcGIS and ArcMap™ are the intellectual property of Esri and are used herein under license. Copyright © Esri. All rights reserved.

This publication has emanated from research supported in part by a research grant from Science Foundation Ireland (SFI) under Grant Number 13/RC/2092 and co-funded under the European Regional Development Fund and by iCRAG industry partners.

Geochemical halos as a tool for exploration of Irish-type Zn-Pb deposits

Lola Yesares[1], Julian Menuge[1], Drew Drummond[2], Adrian J. Boyce[2], John Ashton[3] and Robert Blakeman[3]

[1]iCRAG and School of Earth Sciences, University College Dublin, Belfield, Dublin 4, Ireland (lola.yesares@icrag-centre.org); [2]Scottish Universities Environmental Research Centre, East Kilbride, Glasgow G75 0QF, UK; [3]Boliden Tara Mines DAC, Navan, Co. Meath, Ireland

INTRODUCCTION

Tara Deep is a recently discovered Irish-type deposit, satellite to the Navan orebody, with an inferred mineral resource of 10 Mt @ 8.5% Zn and 1.8% Pb. It is mainly comprised of sphalerite- and galena-rich stratabound lenses hosted by the Courceyan Pale Beds. The Tara Deep deposit is overlain by the Arundian Upper Dark Limestone (UDL) [1] which includes towards the footwall the Thin-Bedded Unit (TBU). The TBU is formed by alternating sequences of dark mudstones, siltstones and calcarenites. Here, seafloor exhalative sulfide deposition has been linked to Pale Beds mineralization [2].

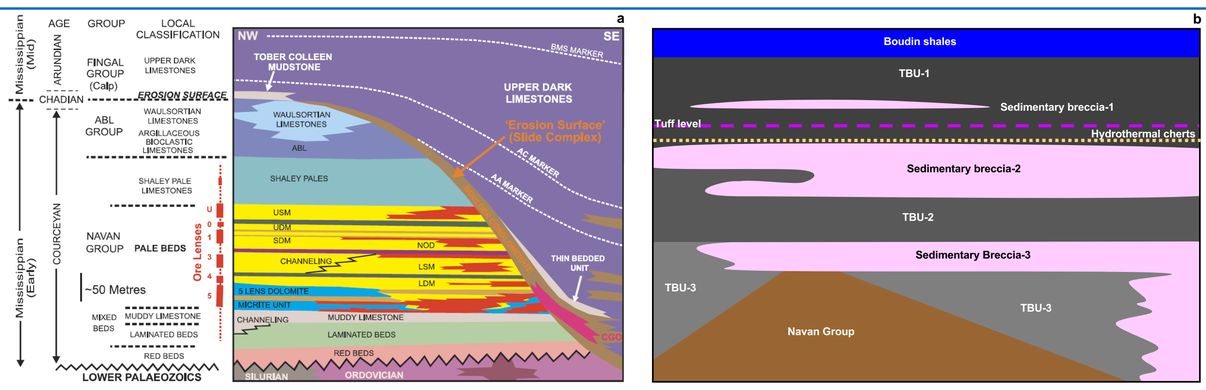

Fig. 1. Geological sketches of the Tara Deep Deposit and the overlying Upper Dark Limestones. (a) Schematic stratigraphy of the Navan area [1]; and (b) Schematic cross section of the Thin-Bedded Unit (TBU).

MINERALOGY vs S ISOTOPE COMPOSITION

In-situ laser S isotope analysis has been performed on petrographically well-characterized samples of TBU-hosted mineralization. Four mineral assemblages have been identified:

(1) Laminated pyrite (Fig. 2):

It is the major assemblage and is mostly composed of 0.5-15 cm thick bedding-parallel layers of framboidal pyrite and subordinate interstitial sphalerite. It is widely distributed in the TBU, progressively decreasing upwards and closely associated with organic matter-rich mudstones. Sulphides have mean δ34S value of -23‰.

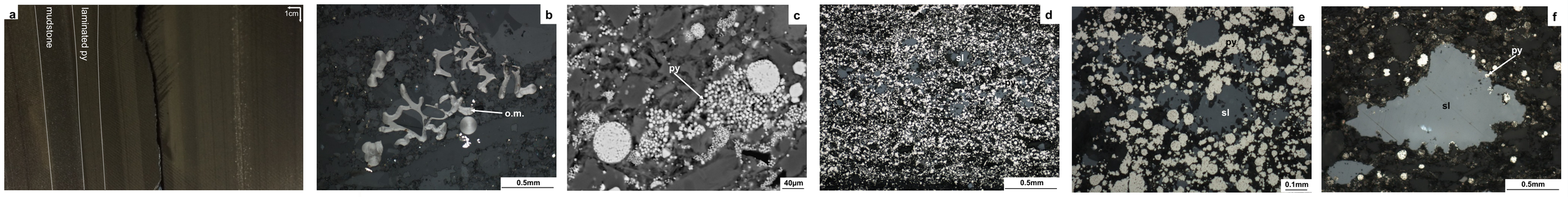

Fig. 2. Hand specimen, reflected light and back scattered electron images of the laminated pyrite assemblage from TBU overlying the Tara Deep deposit. (a) Mudstone replaced by ~1 cm alternating layers of fine-grained pyrite parallel to the bedding; (b) Relicts of organic matter (o.m.) included in mudstone; (c) Framboidal and fine aggregates of pyrite microcrystals filling open space in the mudstone; (d), (e) Interstitial sphalerite (sl) included in framboidal pyrite; and (f) Detail of interstitial sphalerite embedding pyrite framboids.

(2) Pyritized calcarenite (Fig. 3):

It is widely distributed throughout the TBU and occurs mainly in calcarenites. Textural patterns include filling of open spaces and fossil replacement by pyrite with mean δ34S of -13‰.

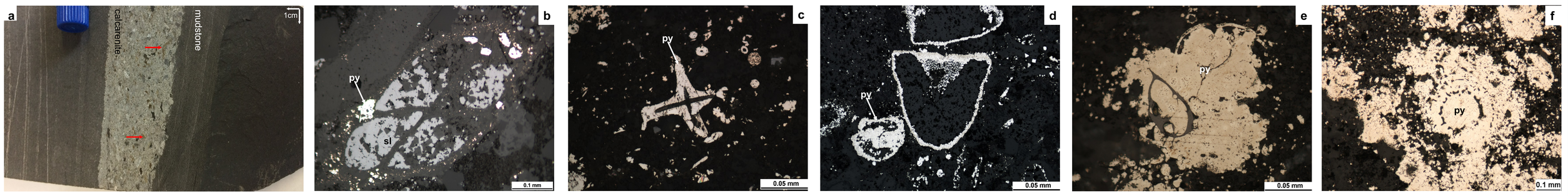

Fig. 3. Hand specimen, reflected light and back scattered electron images of the pyritized calcarenites from TBU overlying the Tara Deep deposit. (a) calcarenite with high degree of pyritization; (b) Microforaminifera internal mould filling by sphalerite (sl) and external mould by pyrite and calcite; (c), (d) External mold of microforaminifera replaced by pyrite (py); (e), (f) Microforaminifera and radiolaria replaced by pyrite (py).

(3) Replacive assemblage (Fig. 4):

It is pervasively distributed throughout the TBU and occurs as late remobilizations both crosscutting, and parallel to, the bedding overprinting the early laminated pyrite. It comprises mostly marcasite, with minor pyrite, sphalerite, chalcopyrite, galena, stibnite, arsenopyrite and pentlandite, with mean δ34S of +10‰.

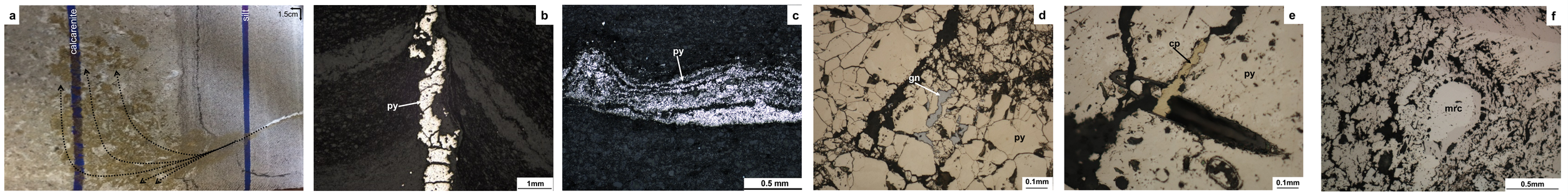

Fig. 4. Hand specimen, reflected light and back scattered electron images of the replacive assemblage from TBU overlying the Tara Deep deposit. (a), (b), (c) Marcasite and pyrite filling fractures and interstices in both silts and calcarenite; (d), (e) Interstitial galena (gn) and chalcopyrite (cp) in pyrite; and (f) Skeletal marcasite (mrc) replacing radiolaria in calcarenite.

(4) Hydrothermal cherts (Fig. 5):

Mainly comprises 0.5-2 cm thick microcrystalline quartz bands rimmed by euhedral coarse Mn-rich dolomite associated with bird's eye marcasite, fine euhedral aggregates of pyrite, sphalerite, chalcopyrite, and galena which includes very fine exsolved Ni-sulfosalts and stibnite. It is found systematically at higher stratigraphic levels in the TBU and a heterogeneous horizontal distribution suggests fault or fracture control. Sulphides have mean δ34S value of +16‰.

Fig. 5. Hand specimen, reflected light and back scattered electron images of the hydrothermal cherts from TBU overlying the Tara Deep deposit. (a), (b) Centimetre scale hydrothermal cherts included in mudstone which shows a reddish Mn-alteration; (c) Sulfide rim formed by marcasite (mrc) bird's eye texture associated with pyrite (py); (d) Sulfide rim comprises chalcopyrite (cp), galena (gn) and sphalerite (sl); (f) Detail of galena forming the rim showing fine inclusions of stibnite (stb), siegenite (sie) and Ni-Sb sulfosalts.

Hydrothermal chert

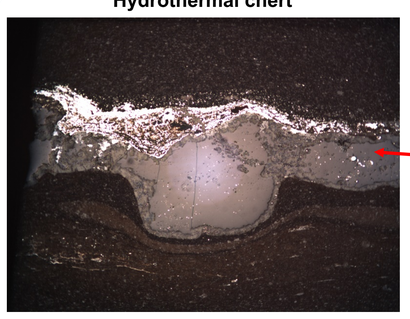

Replacive association

Fig. 6. S isotope analyses from the mineralized TBU and its related mineralogy.

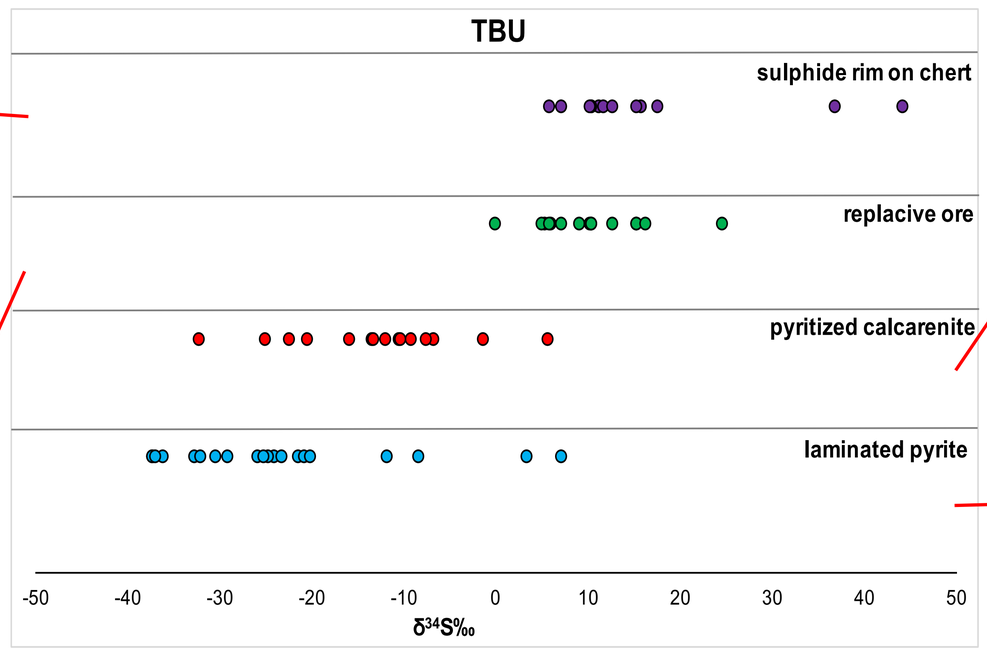

calcarenite

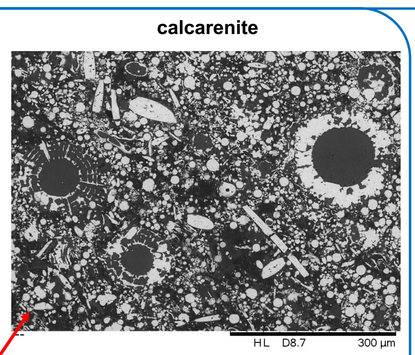

Laminated pyrite

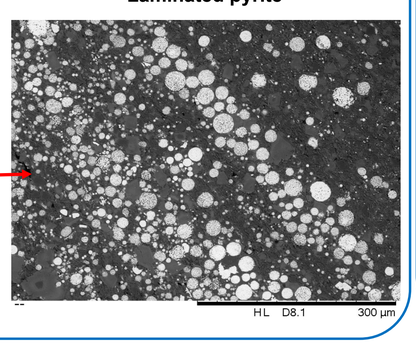

CONCLUSIONS

Detailed petrographic and S isotope analyses indicate overlapping diagenetic and multi-phase hydrothermal sulphide mineralization in the TBU. First, light $\delta^{34}S$ in both laminated pyrite and pyritized calcarenites suggests a bacterial origin within sediments during early diagenesis. Later, anomalous values of chalcophile elements, linked to hydrothermal chert and replacive (heavy $\delta^{34}S$), sulphides, suggest hydrothermal exhalation during early-mid diagenesis. Similarities in mineralogy and S isotope compositions suggest genetic links between the TBU mineralization and the underlying Tara Deep deposit. Hence, the TBU mineralization forms part of the geochemical halo to Tara Deep.

European Union
European Regional Development Fund
Ireland's European Structural and Investment Funds Programmes 2014-2020
Co-funded by the Irish Government and the European Union

This publication has emanated from research supported in part by a research grant from Science Foundation Ireland (SFI) under Grant Number 13/RC/2092 and co-funded under the European Regional Development Fund and by iCRAG industry partners.

The Distribution of Energy Critical and Precious Metals at the Scale of a Porphyry Copper Deposit

M. Brodbeck[1], S. McClenaghan[1], B.S. Kamber[2], P. Redmond[3]

[1]Department of Geology, Museum Building, Trinity College Dublin, Dublin 2, Ireland
[2]School of Earth and Environmental Sciences, The University of Queensland, St. Lucia, Austalia
[3]KoBold Metals, Berkeley, California, USA

brodbecm@tcd.ie

Introduction

- For fertile porphyry systems with large metal endowments, bulk concentrations of major commodities (Cu, Mo, and Au) are well constrained from assay data
- Energy critical elements (ECEs) and precious metals, relevant for energy production/conversion technologies can occur as trace constituents in copper ores
- These trace metals can be potentially be recovered as by-products, adding value to the primary targeted commodities.
- For example, 90 % of the global Te production is recovered from anode slimes during the Cu refinng process (USGS Mineral Commodity Summaries)
- Mineralogy and substitution mechanisms, responsible for the deportation of trace ECEs in Cu ores are not fully understood -> effective recovery limited!
- Insufficient knowledge on the mineral scale distribution of deleterious elements (i.e. As, Cd, Sn) that may result in refining penalties

-> Characterisation of trace metals signatures (penalty vs. credit) may add value to resources, improve recovery and help migitate environmental effects

-> By linking trace metal signatures and abundance of ore phases, zones of high trace metal potentials at the deposit scale can be identified

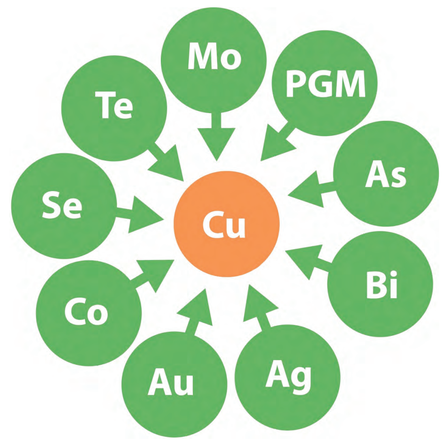

Cu and its potential by-products (Hageluken and Meskers, 2010)

Bingham Cu-Mo-Au Porphyry Deposit

- Bingham Canyon is a giant copper deposit, situated in northern Utah, USA
- Belongs to a belt of Eocene to Oligocene intrusions
- Deposit developed after a change from regional compression to extension
- Bingham stock: monzonite and a series of mineralisation related porphyry dikes
- Historical samples were taken from the high-grade (>1% Cu, >1g/t Au) zone
- At least five distinct crosscutting porphyry phases have been identified:
  1. Quartz monzonite porphyry (QMP)
  2. Latite porphyry (LP)
  3. Biotite porphyry (BP)
  4. Quartz latite porphyry breccia (QLPbx)
  5. Quartz latite porphyry (QLP)
- Each porphyry phase, at declining intensity, with associated sequence of quartz veins, copper-gold mineralisation and potassic alteration

Geological Maps and cross sections (Redmond and Einaudi, 2010)

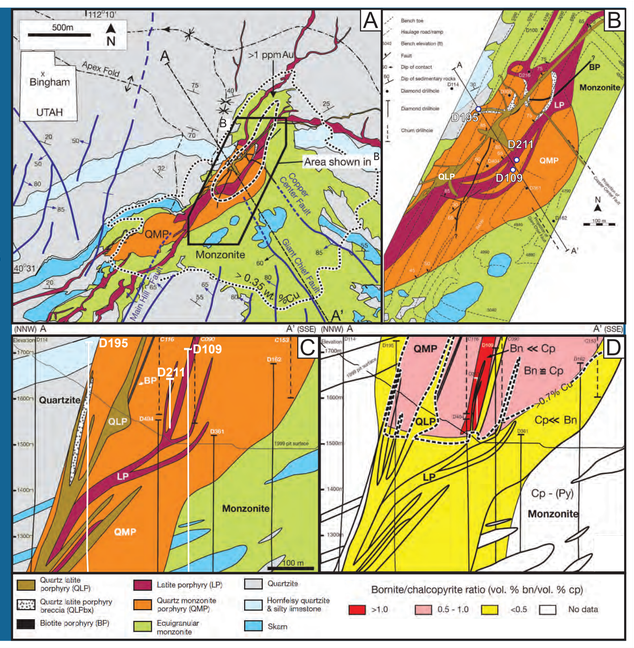

Results

1
- Vein hosted Cu-sulphides are bornite, chalcopyrite and digenite
- Abundace of all sulphides decreases over porphyry sequence
- Mineralisation decreased with time

2
- Bornite major host for Se, Sn and Bi -> conc. in QMP > LP, BP
- Chalcopyrite primary host of Co, Ga, Ge, As, Cd and In -> conc. QMP, LP > BP
- Digenite major host for Ag, Sb, Te and Au -> conc. in QMP
- Penalty elements: Cd and As commonly <10 ppm, Sn <30 ppm

3
- When digenite is associated with bornite (exsolution), digenite yields higher concentrations of Ag and Au, while Bornite hosts excess Bi

4
- Rare micron to nanoscale inclusions of telluride, electrum, native Au and wittichenite contain high concentrations of Te, Ag, Au, and Bi

1 Mineralogy

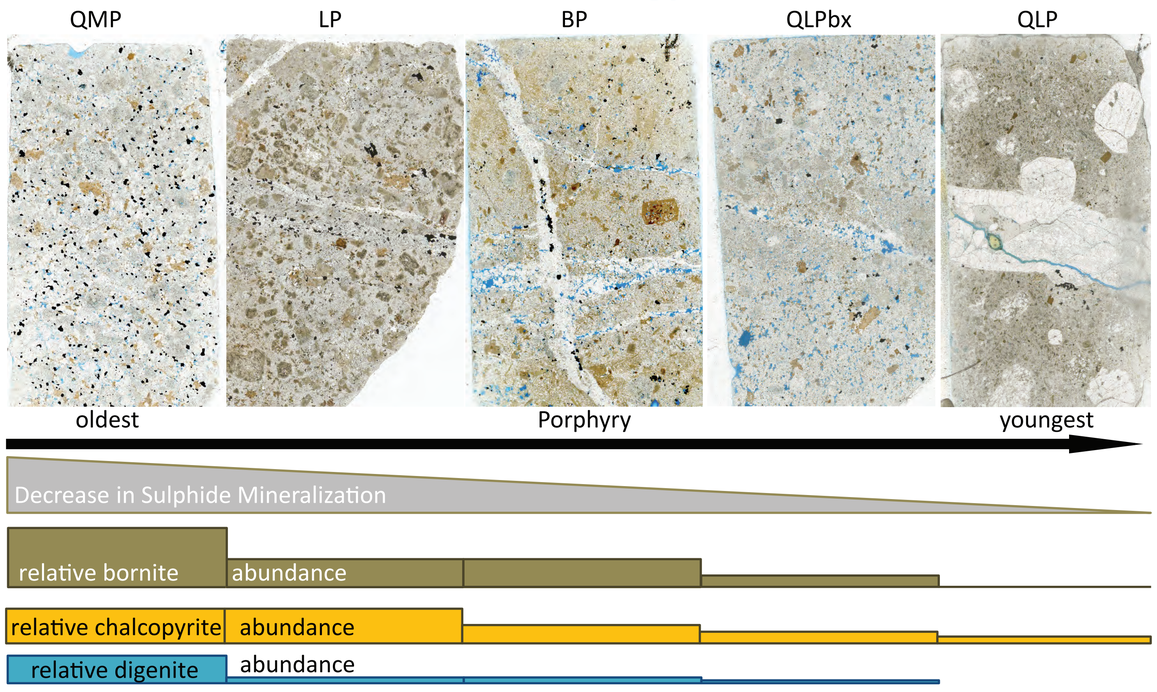

Representative thin section examples of the five porphyry dikes at Bingham Canyon ordered from oldest to youngest intrusion, simplified mineralisation intensity (locally mineralisation intensity might be different) and relative abundances of Cu- (Fe-) sulphides over the porphyry sequence.

2 Trace Element Contents of Cu- (Fe-) Sulphides

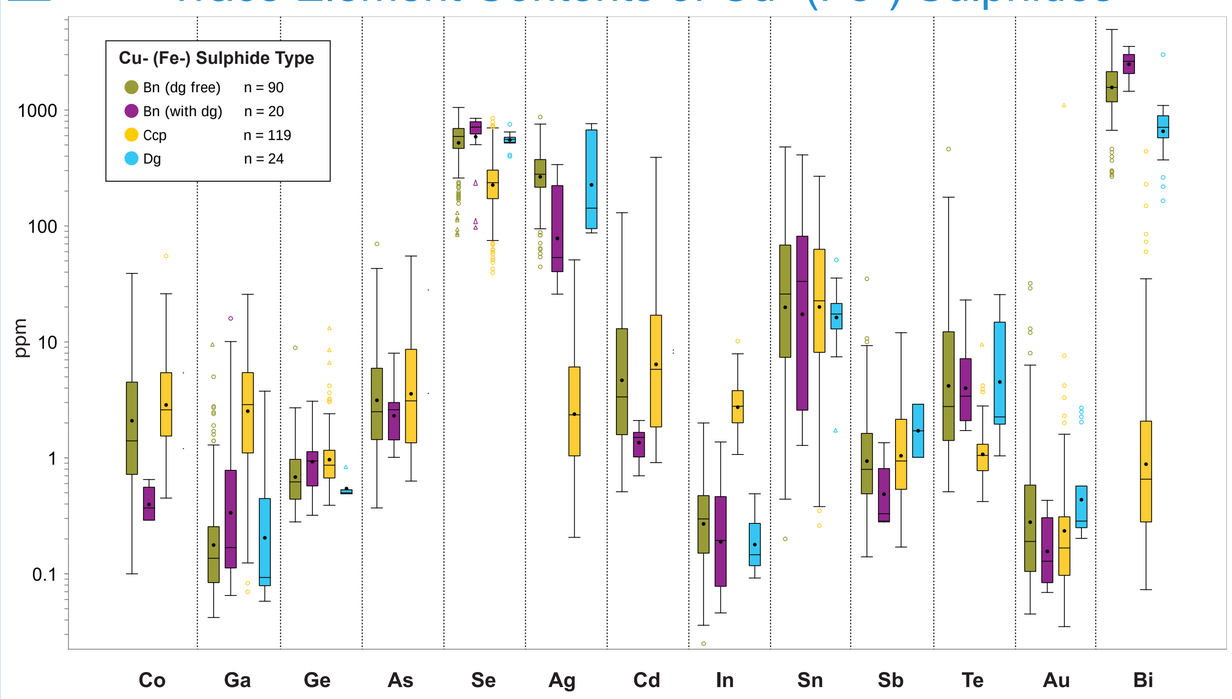

Trace element box and whisker plots of Cu-(Fe-) sulphides. Bn (bornite), Ccp (chalcopyrite), Dg (digenite). Boxes are bordered by the 25 and 75 percentiles. Lines in the boxes indicate the medians, circles represent geometric means. Circular outliers are defined by being 1.5 times the interquartile range from the boxes. Triangular outliers are defined by being three times the interquartile range from the boxes. Whiskers are extreme values that are not defined as outliers. Each box represents a minimum of 5 samples.

3 LA-ICP-MS Trace Element Maps

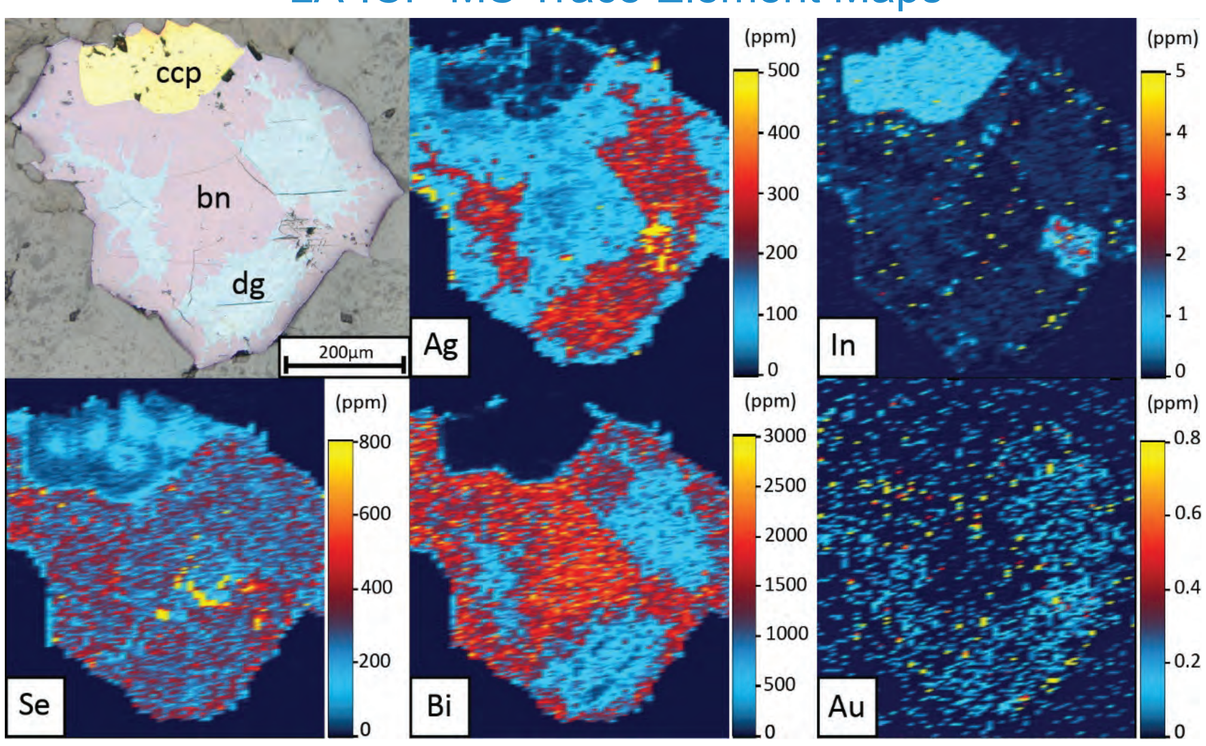

LA-ICP-MS trace element distribution maps of a bornite (bn), digenite (dg) and chalcopyrite (ccp) composite crystal

4 Trace Metal Inclusions

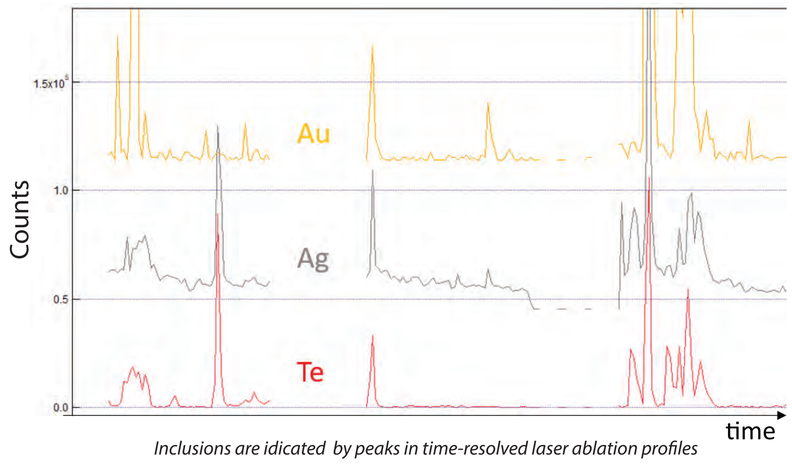

Inclusions are idicated by peaks in time-resolved laser ablation profiles

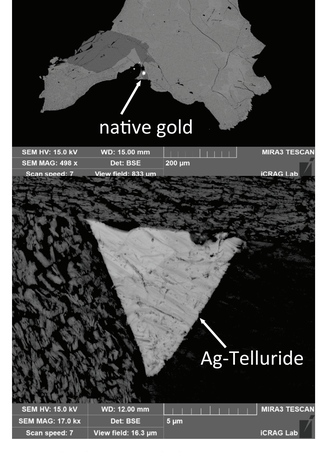

Backscattered electron images

Methods

- Reflected light microscopy -> Mineral characterisation
- SEM-EDS -> Major element chemistry of sulphides, BSE imaging
- Spot laser ablation inductively coupled mass spectrometry (LA-ICP-MS)

-> Trace element chemistry of sulphides

- LA-ICP-MS mapping -> Visualisation of trace metal distributions

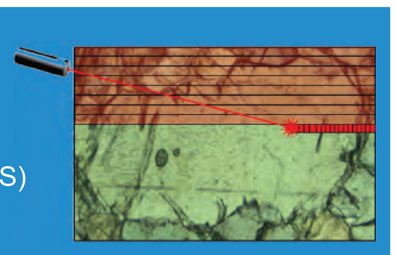

Laser spot raster -> Map

This publication has emanated from research supported in part by a research grant from Science Foundation Ireland (SFI) under Grant Number 13/RC/2092 and co-funded under the European Regional Development Fund and by iCRAG industry partners.

Tackling Sustainable Development Goal 13 via Dawsonite Precipitation

Niamh Faulkner[1], Juan Diego Rodríguez-Blanco[1]
1) Department of Geology, Museum Building, Trinity College Dublin

13 CLIMATE ACTION

SDG13
- "Take urgent action to combat climate change and its impact".
- Limit atmospheric CO_2 levels to 450 ppm by 2100

CCS
- May 2019 saw the highest recorded atmospheric CO_2 levels on record: 414.7 ppm.
- Basaltic CCS theoretically has the potential to store 5000 Gt of carbon (Gislason *et al.* 2014).

DAWSONITE
- $NaAlCO_3(OH)_2$ (Orthorhombic)
- Dawsonite precipitates as a dominant CO_2 bearing phase in aluminosilicate mineral rich reservoirs.

1)BACKGROUND

- The aim of the Paris Agreement (UNFCCC, 2015) is to limit the increase in the global average temperature to well below 2°C above pre-industrial levels and pursuing efforts to limit the temperature increase to 1.5°C above pre-industrial levels".
- A minimum of 15-20% of global CO_2 emission reduction will need to result from Carbon Capture and Storage (CCS).
- An estimated 6000 Mt CO_2 yr^{-1} will need to be sequestered (International Energy Agency, 2013).

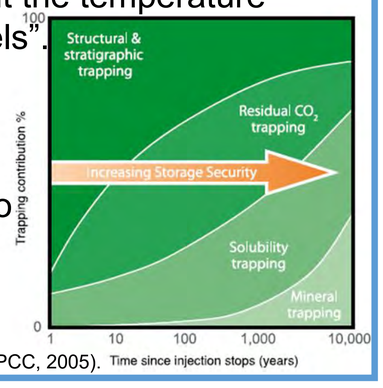

Figure 1: Types of *in situ* geological CCS (IPCC, 2005).

2)KNOWLEDGE GAP

- Despite the high content of Al^{3+}, Na^+ and K^+ in basalts, no methods to target the crystallization and stabilization of dawsonite have been tested during the carbonation of basaltic rocks.
- There are discrepancies between field data, modelling and experimental about the conditions that dawsonite forms in e.g. pH and pressure.
- More knowledge on the kinetics of the Al-Carbonate system;
  - Feldspars typically are replaced by dawsonite in high pressure CO_2 systems. However, a lack of dawsonite in natural CO_2 accumulations suggests that is only stable in a narrow chemical window & easily transforms to clays.

3)BASALTIC CCS

- Compared to conventional CCS, in sedimentary reservoirs, basalt is highly reactive to CO2, resulting in rapid carbonation.
- Basaltic rocks are considered as a great potential repository for CCS because of their Ca^{2+}, Al^{3+}, Na^+, Mg^+ and Fe^{2+} content, and their abundance on the Earth's surface (~10%).
- The CarbFix project has shown that solubility trapping occurs immediately & carbonation is rapid, >95% mineralized within 1 year (Matter *et al.*).
- Basaltic reservoirs don't require a cap rock, as the dissolved CO_2 isn't buoyant & doesn't migrate back to the surface.
- It has been estimated that the active rift zone in Iceland could store over 400 Gt CO_2 (CarbFix, 2019).

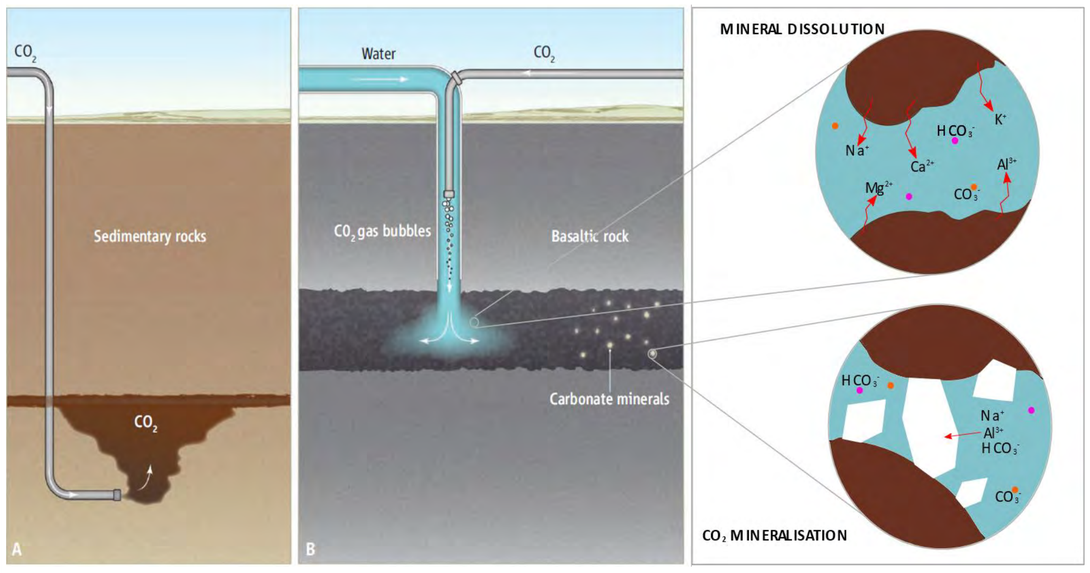

Figure 2: Carbon storage in sedimentary basins versus basaltic rock. Based on Gislason & Oelkers (2014)

4)METHODS

- There are two methods used to synthesize dawsonite:
  - Solutions mixing.
  - Mineral- aqueous solution interaction (Figure 3).
- Solutions mixing involves adding an Al bearing solution, e.g. $Al(NO_3)_3$, to a CO_3- bearing solution, e.g. HCO_3-.
- Mineral- aqueous solution interaction involves adding e.g. gibbsite (Al(OH)3) to a Na-(H)CO3- solution under hydrothermal conditions. The aim is for dawsonite to fully replace the gibbsite.
- Boehmite, AlO(OH), precipitation is an issue with both methods, but can apparently be countered by increasing the Na:Al ratio.

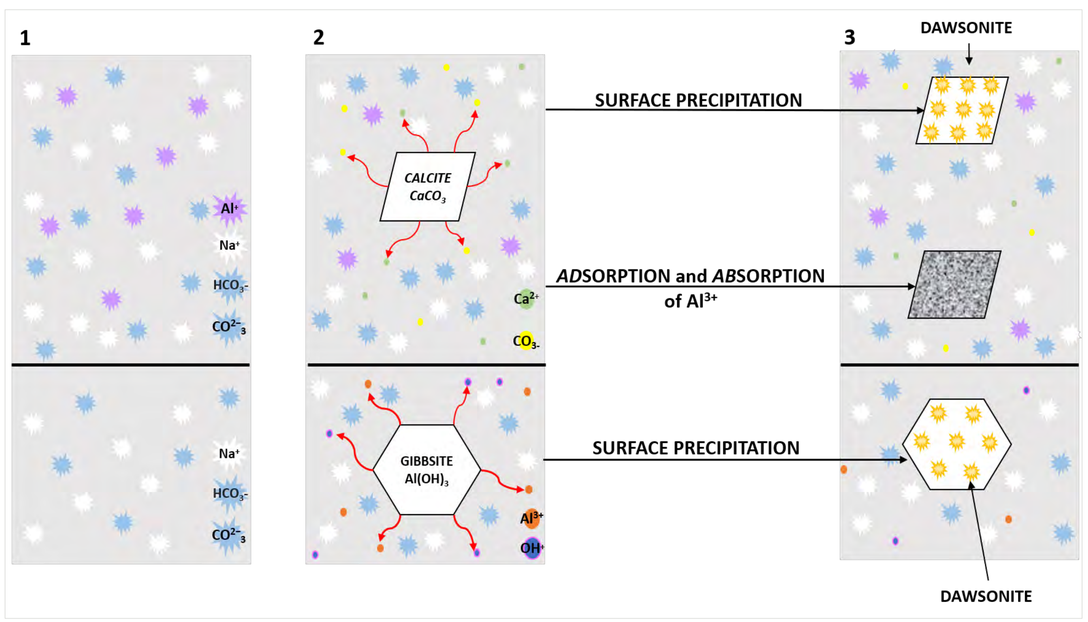

Figure 3: Dawsonite synthesis via mineral- aqueous solution interaction of calcite and gibbsite. Dawsonite precipitates on the surface of the calcite and gibbsite.

This publication has emanated from research supported in part by a research grant from Science Foundation Ireland (SFI) under Grant Number 13/RC/2092 and co-funded under the European Regional Development Fund..

Ireland's European Structural and Investment Funds Programmes 2014-2020
Co-funded by the Irish Government and the European Union
European Union
European Regional Development Fund
Science Foundation Ireland For what's next
Geological Survey Suirbhéireacht Gheolaíochta Ireland | Éireann

iCRAG
IRISH CENTRE FOR RESEARCH IN APPLIED GEOSCIENCES

Siobhán Burke (1,3)*

Andrew Wheeler (1,3)

Oisin McManus(4)

David Chew (2,3)

[1] School of Biological, Earth and Environmental Sciences, University College Cork (UCC)

[2] School of Natural Sciences, Trinity College Dublin (TCD)

[3] Irish Centre for Research in Applied Geosciences (iCRAG)

[4] INFOMAR, Marine Institute, Rinville, Oranmore

*siobhan.burke@icrag-centre.org

UCC University College Cork, Ireland Coláiste na hOllscoile Corcaigh

Trinity College Dublin The University of Dublin

Irish offshore heavy mineral placer development and mineralogy

1. INTRODUCTION

Ireland has not yet fully explored the potential for secure and sustainable offshore mineral deposits. Heavy mineral rich sands have been identified in Ireland bearing lucrative Ti-rich minerals e.g. ilmenite, rutile and titanite but could also possess other economically important minerals i.e. rare earth elements (REEs) and platinum group elements (PGEs), amongst others. Their distribution and accumulation are controlled by source, hydrodynamics and a tendency to sort by individual mineral densities therefore understanding sediment transport pathways is imperative in identifying priority targets and assessing economic viability.

2. STUDY AREAS

- Blacksod Bay
- Achill Island
- Clew Bay

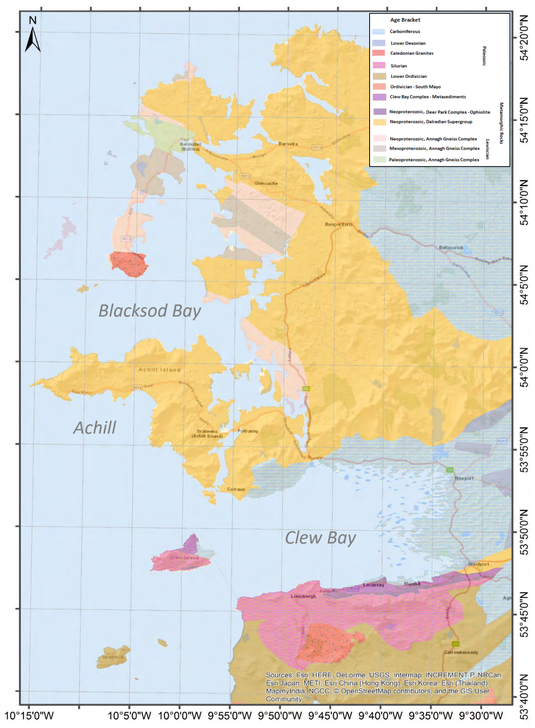

Fig 1. Geologic map of study area displaying high grade metamorphic terrane and offshore study areas.

3. APPROACH

- Offshore research surveys – identify key offshore sites to study.
- Collection of seabed mapping and shallow seismics to help understand concentration processes and quantify.
- Geochemical characterisation of mineral sands.
- Source identification

4. SAMPLE COLLECTION

Marine research survey QuIMPeR I 2017:

Acquisition of:

- 213km of high resolution shallow seimics
- 213 km of high resolution multibeam bathymetry
- 19 vibrocores
- 86 offshore grab samples

5. SEM-EDS (PHASE ANALYSIS)

Fig 2. Location of sample S_33 off Achill Head

MINERAL CHARACTERISATION

- Following heavy liquid separation using 2.9g/cm3 methylene iodide, 1g of heavy mineral concentrate from offshore placer sand was mounted using epoxy resin for analysis under SEM-EDS (Fig 2 – bottom left).
- Two grain size fractions (63-125 um and 125 – 250 um) are analysed in order to identify all HM assemblages within the placer.
- Multiple fields of view are mapped and collected for elemental composition using EDS and stitched together into a montaged image (Fig.3).
- This allows us to quantify and identify major phases in the sample

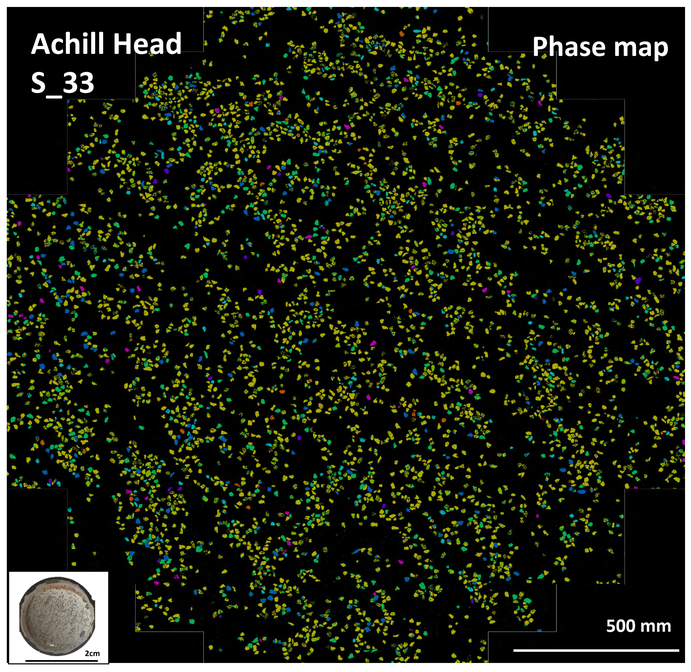

Fig 3. EDS Phase map displaying concentration of minerals phases in sample.

6. PLACER MINERALOGY - preliminary

Achill Head - sample S_33

Mineral assemblages show mostly

- Exsolved Fe-Ti oxide mostly dominate the Achill Head sample.
- Ti bearing minerals (rutile) abundant but concentrated in Quartz. Grade yield up to 55% wt% Ti.
- Abundant amphibole and zircon phases
- Minor amounts of garnet (almandine), Cr-spinel, apatite, rutile and titanite.

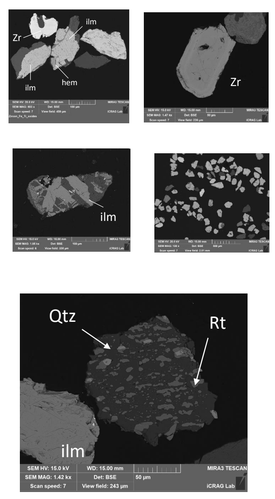

7. MINERAL CONCENTRATION %

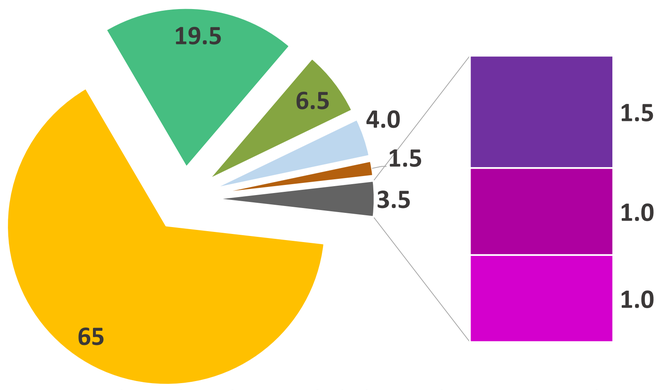

Fig 6: Minor phases have been excluded using this mapping tool – further work is needed in order to capture full spectrum of mineralogy and improve results.

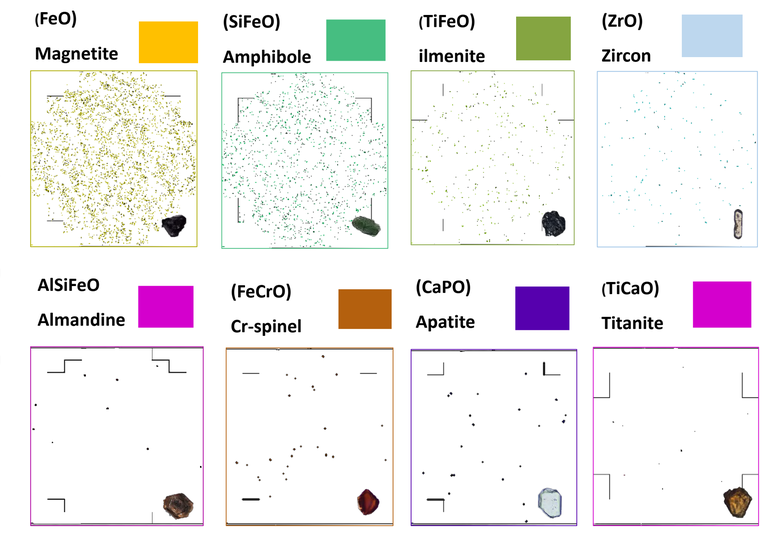

8. CONCENTRATION MECHANISMS

Settling velocity (Critical Current Velocity Depositional Threshold) for each sample in Blacksod Bay was calculated by using the mode grainsize of each sample.

Soulsby (1997) defines the formula to calculate the critical current velocity depositional threshold from particle size distributions as:

$$\mathcal{U}_{setl} = \frac{v}{d}\left[\left(10.36^2 + 1.049D_{*3}\right)^{\frac{1}{2}} - 10.36\right],$$

Where,

v = kinematic viscosity of water = 1.4313 x 10^{-6} m^2/s (8°C and 35.1 ppt)

d = grain diameter = mode of sample grain size curve

D* = D_* = dimensionless grain size = $\left[\frac{g(\rho_s-\rho)}{\rho v^2}\right]^{\frac{1}{3}} d$

ρ = water density = 1027.4 kg / m^3

ρ_s = grain density = 2650 kg / m^3 (quartz)

Results:

Results show display that with grainsize settling velocity increases. In samples where placers are highly concentrated we see a lower grainsize and settling velocity figure. Grainsize fractions 63-250um are more concentrated in heavy minerals in comparison to samples above this grain size fraction. (See Fig 7)

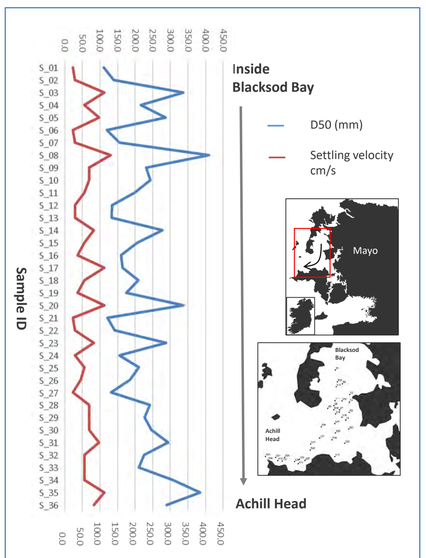

Fig 7: Map displaying grainsize vs settling velocity. Placer sample S_33 has a lower grainsize and settling velocity.

9. PLACER TRAPS - CLEW BAY SPARKER TRANSECTS

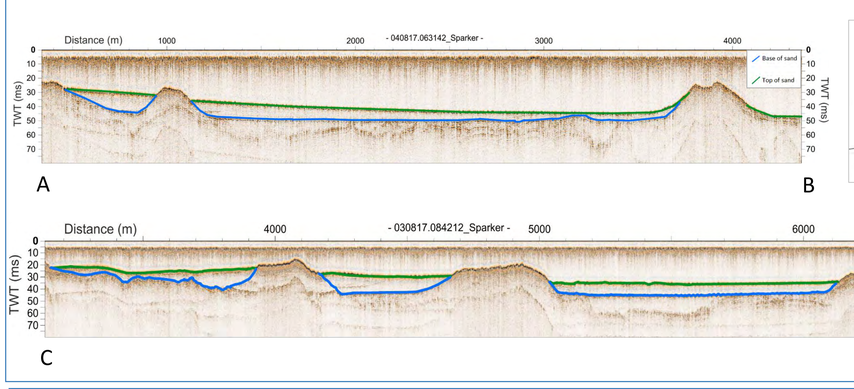

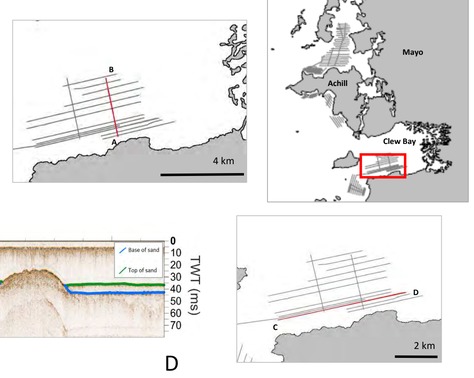

Fig.8. High-resolution single channel seismic profiles collected in Clew Bay using the Sparker. The top and base of each sand horizon was picked using IHS Kingdom suite in order to calculate spatial thickness of the sand body. The seismoacoutic data reveals laminar layering of sand buried and sub-buried drumlins within Clew Bay.

10. ISOPACH MAPS – SAND CONCENTRATION

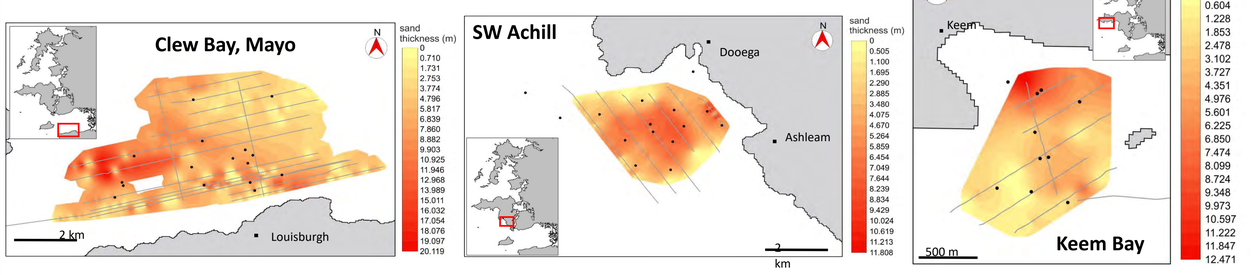

Fig 9. The thickness of sand was calculated using IHS Kingdom suite. At Clew bay it appears that sand thickness increases moving offshore however, Keem displays an increase with thickness moving into the bay. SW Achill is mostly homogenous.

RESULTS

- **Clew Bay** displays sand thickness **up to 20 meters**. Concentrations are focused mostly between glacial bed forms.
- SW Achill displays no particular trend but uniform depth distribution. Sand thickness **up to 11 meters** in depth.
- **Keem** shows a denser thickness of sand moving onshore towards the bay with sediment thickness **up to 12 meters.**

11. SOURCE

The study area is located in NW Co. Mayo, Ireland. The geology of the area comprises mostly of high grade metamorphic terrane gneisses, schists with granite, metabasite and pematitic intrusions.

- Future work will utilise detrital U-Pb geochronology to fingerprint the source region of the heavy mineral placer sands.
- Key Indicator minerals titanite, zircon, rutile and garnet will help distinguish source terraces and in combination with trace element analyses to provide insight into potential source rocks.

12. MBES MAPPING – Clew Bay

QUiMPeR II marine survey successfully mapped the extent of Clew Bay to a 1m resolution. The data will be utilised to create a sea bed classification for the area and identify areas of placer formation

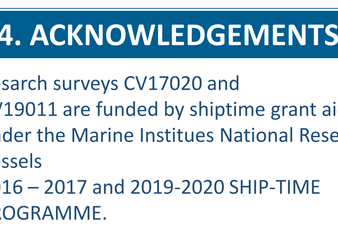

Fig 10. Tracklines and grab sampling

Fig 11 . Acoustic Backscatter

Fig 12 . Clew Bay 2m shaded relief

13. CONCLUSIONS

- Placer mineralogy for Achill Head is mostly dominated by Fe-Ti oxides (Fig. 5)
- Phase mapping is useful for estimating the % of mineral present but not useful for minor phases (Fig. 6).
- Settling velocity (concentration) is controlled by grain size and density. In placer samples we see a correlation of grainsize and settling velocity (Fig.7).
- In Clew Bay – placer development may be controlled by seabed morphology i.e. buried drumlins and could be a reason why sand is concentration (baffling effect) (Fig.8)
- Sediment thickness in NW Mayo is associated with coastlines that have sheltered bays and inlets but in the case of Ashleam (SW Achill) where there is no apparent trend in sedimentation, it is likely that rock falls and landslides are responsible for sand accumulation and concentration close to shore. This is supported by existing backscatter available from INFOMAR.

14. ACKNOWLEDGEMENTS

Resarch surveys CV17020 and CV19011 are funded by shiptime grant aid under the Marine Institues National Research Vessels 2016 – 2017 and 2019-2020 SHIP-TIME PROGRAMME.

This publication has emanated from research supported in part by a research grant from Science Foundation Ireland (SFI) under Grant Number 13/RC/2092 and co-funded under the European Regional Development Fund and by iCRAG industry partners.

Ireland's European Structural and Investment Funds Programmes 2014-2020 Co-funded by the Irish Government and the European Union

European Union European Regional Development Fund

Science Foundation Ireland sfi For what's next

PIP Petroleum Infrastructure Programme

GEOSCIENCE IRELAND Exploring Developing Sustaining

lundin mining

Trevali MINING CORPORATION

Teck

Geological Survey Suirbhéireacht Gheolaíochta Ireland | Éireann

Tellus Understanding Underground

INFOMAR Integrated Mapping for the Sustainable Development of Ireland's Marine Resource

Foras na Mara Marine Institute

The application of machine learning methods to aggregate geochemistry predicts quarry source location: a case study from the Irish aggregate industry.

Coláiste na Tríonóide, Baile Átha Cliath
Trinity College Dublin
Ollscoil Átha Cliath | The University of Dublin

*[a]Dornan, Tadhg — *tadhg.dornan@icrag-centre.org, dornant@tcd.ie
[a]O'Sullivan, Gary
[c]O'Riain, Neal
[b]Stüeken, Eva
[a]Goodhue, Robbie

[a]Trinity College Dublin (TCD), Department of Geology, Museum building, College Green, Dublin 2, Ireland/ Irish Centre for Research in Applied Geosciences (iCRAG), O'Brien Centre for Science (East), University College Dublin, Belfield, Dublin 4, Ireland

[b]School of Earth and Environmental Sciences, University of St Andrews, St Andrews, Scotland, UK.

[c]Unafiiliated

1. Background

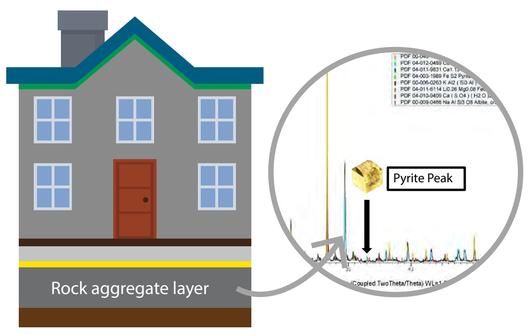

Pyrite is often found in the sub-floor, rock aggregate layer of Irish houses.

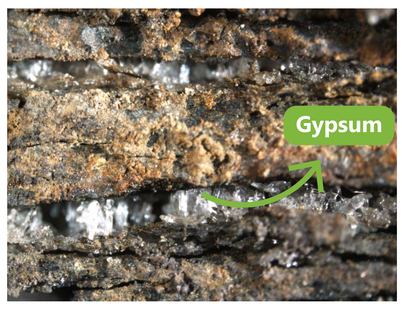

Oxidation of pyrite forms H_2SO_4. This reacts with limestone aggregate and results in gypsum formation. Gypsum crystallisation causes delamination and expansion of aggregate material.

Pyrite families 'left in limbo' as plan rejected over cost to Government

More generous remedial scheme rejected under Dáil rules

Mon, Jun 19, 2017, 13:35 | Updated: Mon, Jun 19, 2017, 13:37

Mark Hilliard

Pyrite damage: residents campaigning in 2011. By January this year the Pyrite Resolution Board had approved 1,277 applications for remediation, with repairs completed in 526 cases. Photograph: Cyril Byrne

12,500 thought to be affected. €50,000 to remediate each home. Overall cost to Irish Government: **€562,500,000.**

Study area

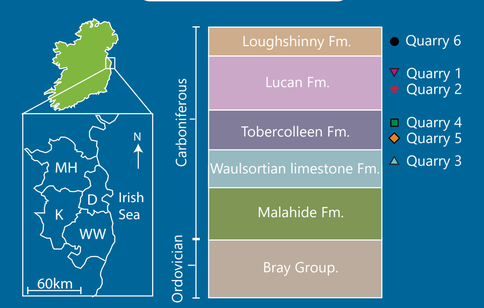

Pyrite to be analysed from 8 different quarry sources (A-H), located in east of Ireland in counties Meath (MH), Dublin (D), Kildare (K) and Wicklow (WW).

2. Analytical techniques

SEM - EDS

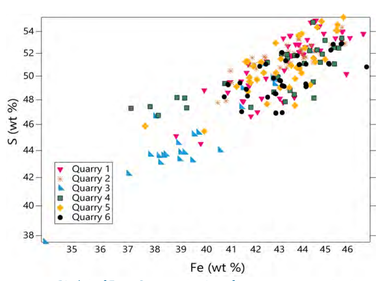

Bi plot of Fe vs S concentrations for quarry sources 1 – 6

In-situ major element analysis of the pyrite crystals was undertaken using a Tescan MIRA XMU field emission scanning electron microscope (FE-SEM) equipped with an Oxford X-max 80mm2 Energy Dispersive Spectrometer at the Centre for Microscopy and Analysis (CMA)/iCRAG Lab in Trinity College Dublin.

All analyses were carried out using a working distance of 18.5 mm, an acceleration voltage of 20 kV, with a 0.2 nA beam current to maintain a detector dead time around 30 per cent, and a counting time of 30 seconds using both natural pyrite (Fe, S) and pure metal standards (Co, Ni, As, In).

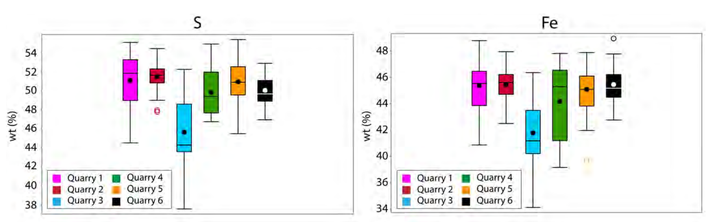

Box and whisker plot of SEM - EDS analysis of bulk rock aggregate from quarry sources

IRMS

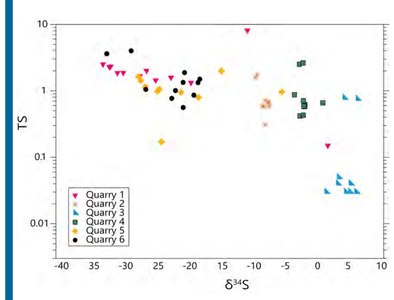

Bi plot of TS vs $\delta^{34}S$ concentrations for quarry sources 1 – 6

Isotope analyses were carried out at the University of St. Andrews with an EA Isolink coupled to a MAT253 IRMS via a Conflo IV. Decarbonated rock powders were weighed into 8 x 5 mm tin capsules and combusted at 1020°C under a constant He stream with a 5-second pulse of O2 gas (flow rate of 250 ml/min) to convert all sulphide to SO_2 gas.

Analytical accuracy was monitored with IAEA-S1, which agreed with internationally recognized values to within < 0.5‰. Peak areas were calibrated for abundance measurements with of a series of sulphanilamide standards. The isotopic data are expressed in standard delta notation relative to VCDT

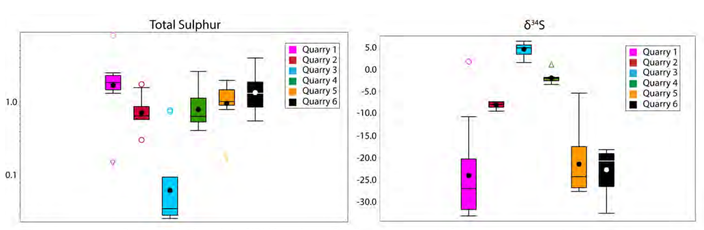

Box and whisker plot of IRMS analysis of bulk rock aggregate from quarry sources 1 – 6.

LA - Q - ICPMS

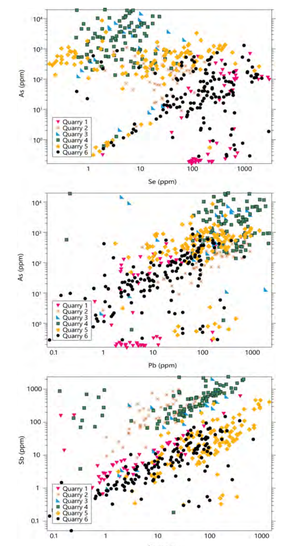

Bi plot of trace element concentrations for quarry sources 1 – 6.

LA-Q-ICPMS analysis was carried out at in the iCRAG Raw Materials Characterisation Laboratory in Trinity College Dublin, using a 193 nm Teledyne CETAC Analyte G2 ArF excimer laser coupled to a Thermo Fisher Scientific iCAP-Qc mass spectrometer.

Elements such as Au, V, In and Tl were all included in the early analysis stages, however, Au, V and In were all found to be below the detection limits of the instrument, while Tl and Ni were found to have mass interferences with ^{208}Pb and ^{58}Fe respectively. As a result, none of the elements were included in later analyses.

Regular ablations of the carbonate matrix were also conducted to verify that no contamination of the pyrite trace element content was occurring due to contribution from carbonate matrix.

Box and whisker plot of LA - Q - ICPMS analysis of pyrite from quarry sources 1 – 6

3. Principle Component Analysis

PCA is an unsupervised statistical method that rotates and shears a data matrix of n-dimensions along axes (components) of greatest variability.

For PCA, if the ppm values of the various trace, minor and major elements are examined in isolation, and not in the context of the entire ablated volume, misleading determinations may result.

As a result, the data used in PCA has been transformed using centred log ratio (CLR) transformation, including a residual value ((v) or "stoichiometry) representing non-analysed elements to sum to unity (i.e. 1 million ppm).

CLR is calculated as the log of the individual measurement divided by the geometric mean of that element across the entire dataset. CLR can be calculated using ioGAS, CoDaPack or "R".

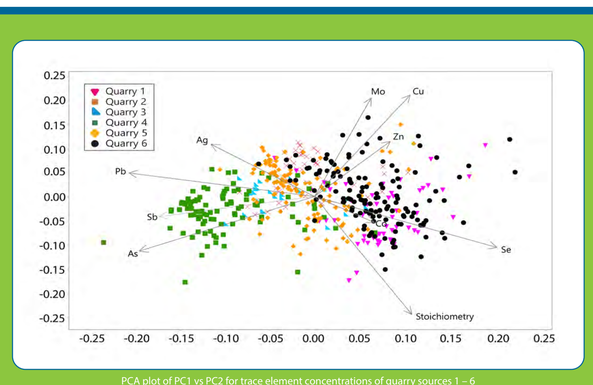

PCA plot of PC1 vs PC2 for trace element concentrations of quarry sources 1 – 6

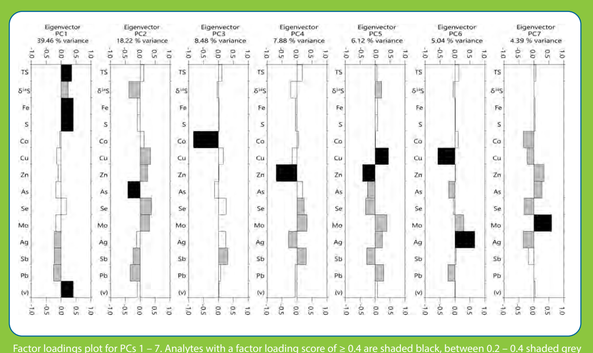

Factor loadings plot for PCs 1 – 7. Analytes with a factor loading score of ≥ 0.4 are shaded black, between 0.2 – 0.4 shaded grey and ≤ 0.2 are shaded white. (v) represents stoichiometry, the residual value needed for CLR transformation.

4. Machine learning

Machine learning methods employ computational algorithms that attempt to emulate the process of human intelligence and neural networks by learning from data fed into the system. Machine learning methods may be useful to our understanding when applied to any kind of data, and are increasingly applied to large geochemical datasets.

Two main types of machine learning software were used in this investigation; the Aggregate Quarry Classification Model (AQCM) and Waikato Environment for Knowledge Analysis software (WEKA).

Both pieces of software use Logistic regression and random forest learning models in order to classify and predict the quarry sources of aggregate fill based on their geochemical composition. Two different pieces of software were used in order to compare the results of the AQCM with that of a freely available piece of software.

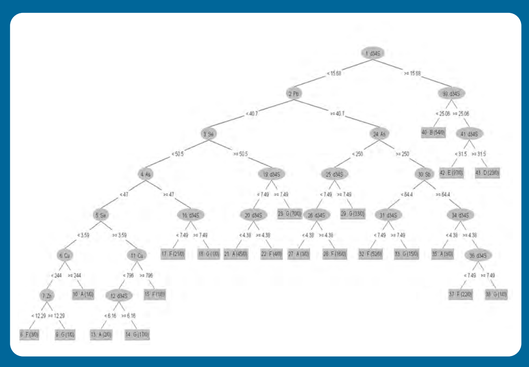

Example of decision tree used as part of the random forest classification of quarry sources 1 - 6 using WEKA software

Elements	AQCM		WEKA	
	Logistic regression		Logistic regression	
	Raw	PCA	Raw	PCA
Majors	31.44%	61.75%	31.75%	24.81%
Traces	63.10%	65.70%	74.02%	74.95%
S isotopes	54.52%	29.70%	69.85%	38.09%
Majors traces	84.57%	85.98%	99.79%	95.24%
Majors S isotopes	90.74%	81.38%	99.64%	100%
S isotopes traces	95.49%	89.09%	99.38%	99.18%
Majors traces S isotopes	98.15%	94.76%	99.59%	98.34%

Elements	AQCM		WEKA	
	Random forest		Random forest	
	Raw	PCA	Raw	PCA
Majors	62.37%	51.26%	61.31%	58.03%
Traces	57.95%	50.62%	77.32%	78.88%
S isotopes	62.56%	43.43%	63.49%	47.62%
Majors traces	95.47%	67.27%	100%	90.68%
Majors S isotopes	100%	98.24%	100%	99.64%
S isotopes traces	96.61%	57.69%	100%	90.92%
Majors traces S isotopes	100%	77.92%	100%	93.79%

Results for the classification of quarry sources 1 – 6 by AQCM and WEKA using random forest classification and logistic regression models.

Conclusions

- Using machine learning models, such as logistic regression and random forest, it is possible to generate an accurate source identification mechanism for aggregate quarry sources based on their bulk rock and pyrite geochemistry. Depending on the dataset used, these models can range in accuracy from 31 % to 100 %.
- The accuracy of these models is enhanced using median concentration values when combining datasets. These median values are applied as the composition of the pyrites analysed by SEM – EDS and LA – Q- ICPMS follow a non – normal distribution. Were this classification mechanism used as part of an actual quarry classification system, mean values taken from a near normally distributed dataset would need to be established in order to accurately represent the quarry composition.
- Although PCA was used as part of this investigation, it proved detrimental to the performance of the machine learning models, causing the performance of the logistic regression and random forest models to drop by 25 % and 19 % respectively. PCA transformation reduced the dimensionality of the dataset and caused the variables to appear monotonous to the machine learning models leading to a reduction in model performance.
- Machine learning models from both the AQCM and WEKA reached classification accuracies of 100 %. However, both models offer their own set of advantages in the classification process. For instance, WEKA can create visualisations of the classification process, while also offering a slightly improved performance when compared to the AQCM, especially when using single variable datasets. The advantages of the AQCM lies in the code as it is entirely open source and customisable to fit the needs of any classification system.

Aggregate Quarry Classification Model (AQCM)

The AQCM is a bespoke piece of machine learning software, tailored to the data generated through the geochemical analysis of bulk rock aggregate and pyrite. This software has been made open source and can be used for the classification of any geochemical database. Further information regarding how to operate the AQCM and its potential uses can be found usingthe QR code attached to this poster.

SCAN ME

Waikato Environment for Knowledge Analysis software (WEKA).

WEKA is a free to download collection of machine learning algorithms. It contains tools for data preparation, classification, regression, clustering, association rules mining, and visualization . This software is coded in the Java programming language and allows users to harness machine learning models without any prior computer programming knowledge

Published Work

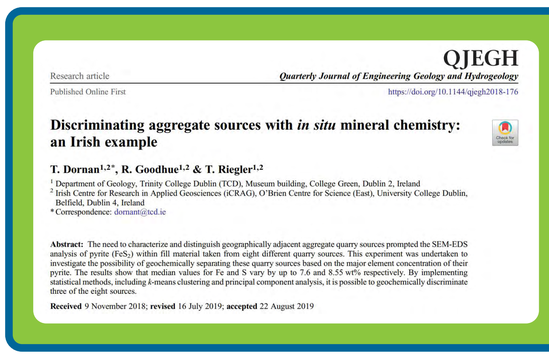

QJEGH

Research article — *Quarterly Journal of Engineering Geology and Hydrogeology*

Published Online First — https://doi.org/10.1144/qjegh2018-176

Discriminating aggregate sources with *in situ* mineral chemistry: an Irish example

T. Dornan[1,2]*, R. Goodhue[1,2] & T. Riegler[1,2]

[1] Department of Geology, Trinity College Dublin (TCD), Museum building, College Green, Dublin 2, Ireland
[2] Irish Centre for Research in Applied Geosciences (iCRAG), O'Brien Centre for Science (East), University College Dublin, Belfield, Dublin 4, Ireland
* Correspondence: dornant@tcd.ie

Abstract: The need to characterize and distinguish geographically adjacent aggregate quarry sources prompted the SEM-EDS analysis of pyrite (FeS_2) within fill material taken from eight different quarry sources. This experiment was undertaken to investigate the possibility of geochemically separating these quarry sources based on the major element concentration of their pyrite. The results show that median values for Fe and S vary by up to 7.6 and 8.55 wt% respectively. By implementing statistical methods, including *k*-means clustering and principal component analysis, it is possible to geochemically discriminate three of the eight sources.

Received 9 November 2018; **revised** 16 July 2019; **accepted** 22 August 2019

Published in the Quaterly Journal of Engineering Geology and Hydrogeology, this paper illustrated that a clear geochemical variation exists between pyrites from 8 different aggregate quarry sources located in eastern Ireland.

The results from this paper indicated that further research into the geochemistry of pyrite was needed in order to discover which technique provided the clearest compositional variation between the quarry sources.

This publication has emanated from research supported in part by a research grant from Science Foundation Ireland (SFI) under Grant Number 13/RC/2092 and co-funded under the European Regional Development Fund and by iCRAG industry partners

Ireland's European Structural and Investment Funds Programmes 2014-2020
Co-funded by the Irish Government and the European Union

European Union
European Regional Development Fund

Science Foundation Ireland sfi For what's next

PIP Petroleum Infrastructure Programme
HomeBond
TII Bonneagar Iompair Eireann Transport Infrastructure Ireland
GEOSCIENCE IRELAND Exploring Developing Sustaining

The Re-Os Isotope System: Introduction, Applications, and Development

Danny Hnatyshin, Murray Hitzman, and Sean Johnson

IRISH CENTRE FOR RESEARCH IN APPLIED GEOSCIENCES

UCD DUBLIN

1 Introduction to Rhenium (Re) and Osmium (Os)

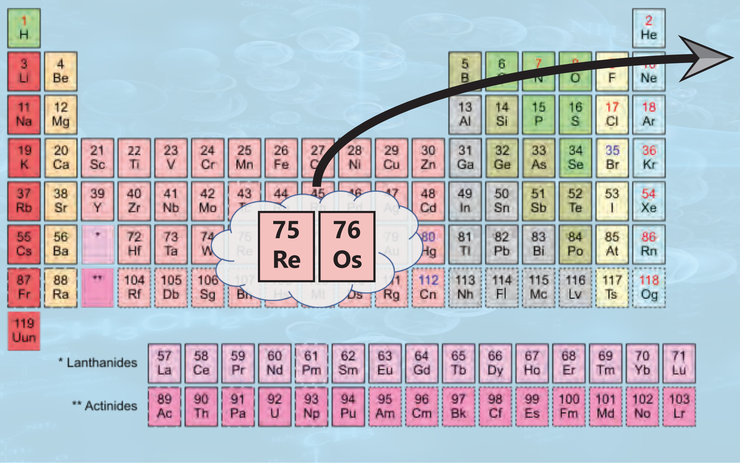

★ **Both Rhenium and Osmium are Platinum Group Elements with interesting geochemical behavior.**

Chalcophile/Siderophile

Organophile

★ **Re and Os accumulate in certain minerals and substances (sulfides, metals, organics).**

★ **Re and Os are often devoid in the minerals/rocks that make up the majority of the crust.**

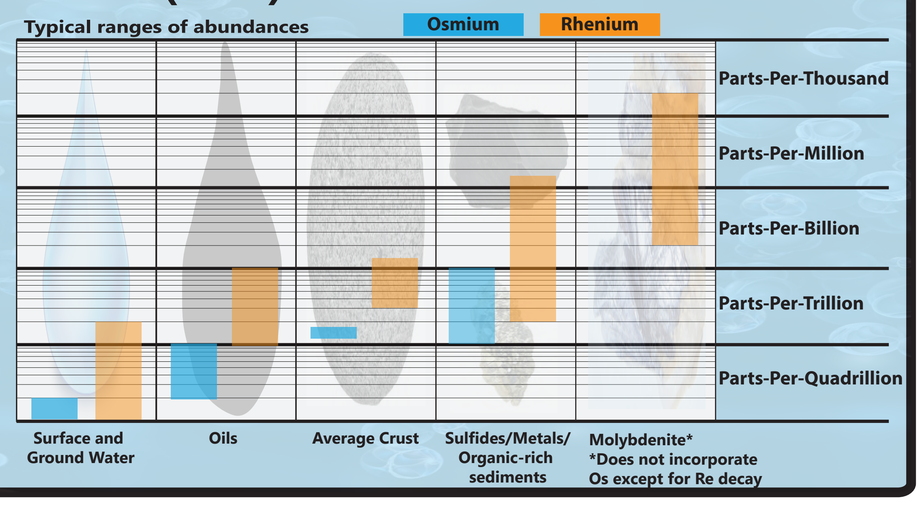

2 Applications of the Re-Os system

Isotope Dating

★ **The isotope ^{187}Re is radioactive and decays into ^{187}Os. The older the rock or mineral becomes the more Re converts into Os. Through measuring the relative abundances of these elements we can determine how old a rock or mineral is.**

^{187}Re → **Half-Life** → **42 Billion Years** → ^{187}Os

★ **Due to the unique geochemical behavior of Re (i.e. chalcophile/siderophile/organophile) compared to other radioactive elements (e.g. uranium, rubidium) this isotope system can date rocks that would typically be impossible, such as sulfide minerals (ECONOMIC GEOLOGY) and organic-rich sediments/rocks (PETROLEUM GEOLOGY, CHRONOSTRATIGRAPHY).**

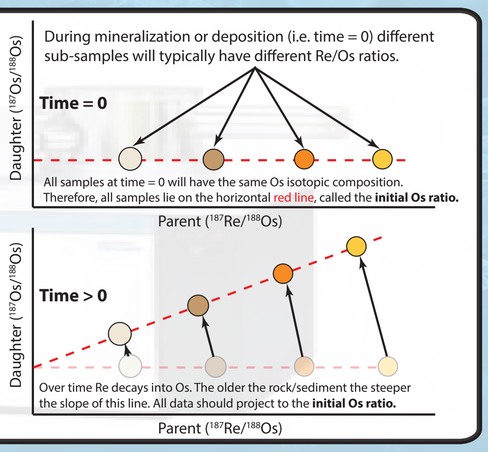

Geochemical Tracing

★ **Different systems can be defined by their different $^{187}Os/^{188}Os$ isotopic compositions.**

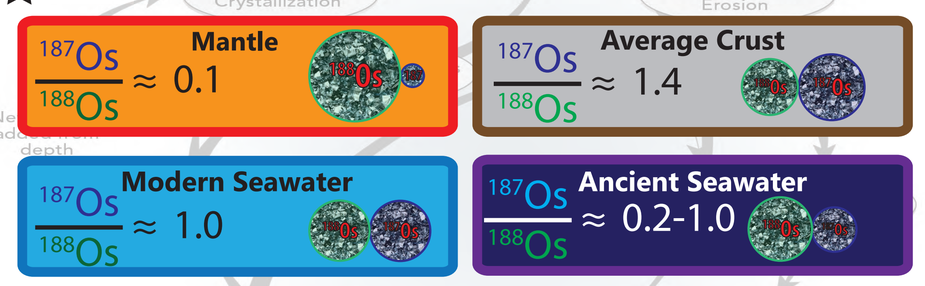

★ **In ore systems the Os composition can be used to find the source of fluids (e.g. magmatic vs crustal fluids).**

★ **Os isotope stratigraphy can be used to monitor the relative inputs of magmatic, cosmic and crustal sources found in sediments. Can be useful as a weathering proxy.**

★ **Anthropogenic contamination can be monitored using Os isotopes because the abundance and isotopic composition of anthropogenic sources is often distinctive**

3 Real World Research Examples

Pyrite Re-Os Geochronology

Re-Os dating of pyrite confirms an early diagenetic onset and extended duration of mineralization in the Irish Zn-Pb ore field
Danny Hnatyshin, Robert A. Creaser, Jamie J. Wilkinson, and Sarah A. Gleeson
GEOLOGY, February 2015; v. 43; no. 2; p. 143–146; Data Repository item 2015055 doi:10.1130/G36296.1

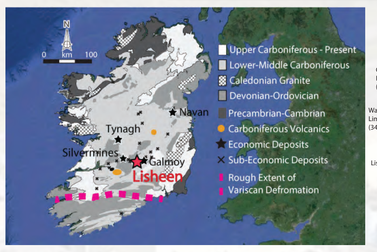

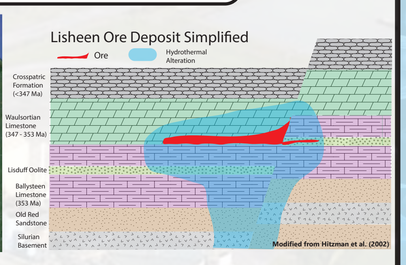

★ **Proper geochronology of Lisheen was important in determining what genetic models are possible for Lisheen (e.g. diagenetic vs. epigenetic)**

★ **The mineralogy of Lisheen precluded many dating techniques (e.g. U-Pb) and some other methods proved problematic (e.g. paleomagnetism)**

★ **Pyrite Re-Os geochronology is known to be a robust system that isn't typically disturbed by secondary events.**

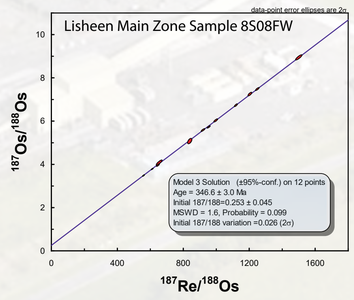

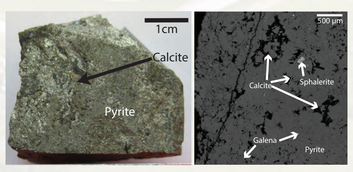

★ **The precise nature of this date (347 +/- 3.0 Ma) is consistant with a early diagentic mineralization event for Lisheen.**

Osmium Isotope Tracing

Cretaceous oceanic anoxic event 2 triggered by a massive magmatic episode
Steven C. Turgeon & Robert A. Creaser nature Vol 454 17 July 2008 doi:10.1038/nature07076

★ **Ocean anoxic events (OAE) can be found throughout geologic history, however their cause is often poorly understood. During these events a large amount of organic material is often preserved and is often marked by an excursion in carbon isotope space.**

★ **One possible mechanism that can trigger widespread anoxia is the emplacement of large igneous provinces.**

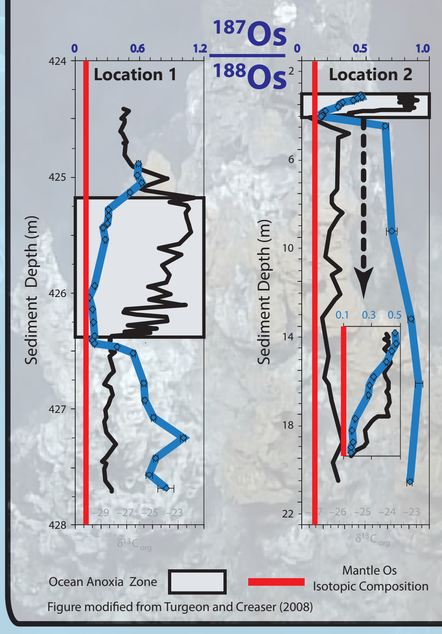

Figure modified from Turgeon and Creaser (2008)

★ **Turgeon & Creaser (2008) proposed a way to test if large-scale magmatic activity coincided with ocean anoxia in the Cretaceous.**

★ **An increase of magmatic activity should lower the $^{187}Os/^{188}Os$ of seawater and associated sediments.**

★ **In organic-rich sediment deposited during ocean anoxia they observed a sharp decline in the $^{187}Os/^{188}Os$.**

★ **In organic-rich sediment deposited around the time of ocean anoxia they observed a sharp decline in the $^{187}Os/^{188}Os$.**

★ **Mass balance calculations suggested that Os input from magmatic sources increased by 30-50x. Suggesting a strong link between magmatism and the OAE**

Environmental/Anthropogenic Tracing

Rhenium-Osmium isotope systematics of surface, shallow and deep groundwater from the Western Canada Sedimentary Basin (WCSB)
Danny Hnatyshin, Ben Rostron, Robert A. Creaser Unpublished PhD Thesis, November 2018

★ **This study focused on defining the Re and Os composition of groundwater from the Western Canada Sedimentary Basin.**

★ **Water/oil samples were collected from water source wells and oil wells.**

★ **During collection there were suspected signs of sample contamination.**

★ **Due to the extremely low concentrations of Re and Os in groundwater mixing with secondary sources can possibly be easily recognized**

A Mixing Formation Waters

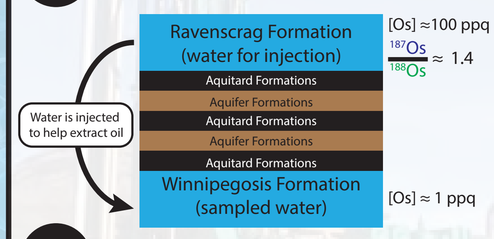

Measured Composition
[Os] ≈20 ppq $\frac{^{187}Os}{^{188}Os} \approx 1.4$

Suggests mixing of ~20% Ravenscrag water and ~80% Winnepgosis water

Consistant with estimates given using oxygen and hydrogen isotopes

B Contamination in Oil

Belly River Formation Oil Resevoir

Sample 1	Sample 2	Sample 3
$\frac{^{187}Os}{^{188}Os} \approx 2.1$	$\frac{^{187}Os}{^{188}Os} \approx 3.3$	$\frac{^{187}Os}{^{188}Os} \approx 0.2$
[Os] ≈ 1800 ppq	[Os] ≈ 600 ppq	[Os] ≈ 50000 ppq

★ **Samples 1 and 2 are typical values for Oil (radiogenic Os signature)**

★ **Sample 3 has a mantle signature (unlikely in the WCSB!). Simplest explanation is that the Os is sourced from metal associated with the well.**

4 Re-Os at UCD

Goals/Philosophy for the UCD Re-Os Laboratory

★ **UCD's Re-Os group is relatively new (<5 years) and is interested in developing the lab into a well-recognized research facility.**

★ **Approach the analytical capabilities of world-class Re-Os labs (e.g. University of Alberta, Durham University, Colorado State University).**

★ **Provide opportunities for students, researchers, and industry to acquire high-precision and accurate Re-Os ages and isotopic ratio's.**

★ **Working towards these goals requires collaboration with established research labs and experts in the appropriate fields.**

Research Capabilities

★ Short-term Capbilities ★ Potential Future Development

★ **Isotopic analysis of non-radiogenic sulfides (e.g. pyrite)**

★ **Isotopic analysis of organic-rich sediments (e.g. black shales)**

★ **Isotopic analysis of petroleum (e.g. crude oil)**

★ **Abundance analysis of water** ★ **Isotopic analysis of water**

★ **Isotopic analysis of highly radiogenic sulfides (e.g. molybdenite)**

Workflow Considerations

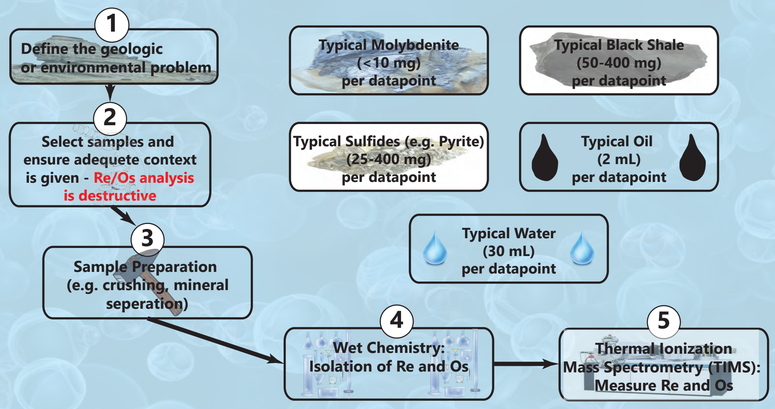

This publication has emanated from research supported in part by a research grant from Science Foundation Ireland (SFI) under grant number 13/RC/2092 and 16/SP/4319, and is co-funded under the European Regional Development Fund and by iCRAG industry partners.

Ireland's European Structural and Investment Funds Programmes 2014-2020
Co-funded by the Irish Government and the European Union

European Union
European Regional Development Fund

Science Foundation Ireland SFI For what's next

Characterising Hydrothermal Alteration along the Rathdowney Trend, Ireland

N.A Vafeas*[1]; M. Hitzman[1]; S. Johnson[1] and J. Güven[1]

[1]*Irish centre for Research in Applied Geosciences (iCRAG), University College Dublin.*

**Corresponding Author: nick.vafeas@icrag-centre.org*

Abstract

The hydrothermal dolomite and associated Black Matrix Breccia (BMB) at Lisheen mine are indicated to be the result of infiltration of deep-sourced hydrothermal fluids along normal fault conduits. These fluids have resulted in the dissolution of the surrounding Waulsortian dolomite and the reprecipitation of black hydrothermal dolomite i.e. (BMB) and the emplacement of phyllosilicates within the dolomitic matrix. Spatial characterisation of these fluid-derived phases may potentially reveal geochemical vectors towards future Irish type Pb-Zn deposits.

Aims

- Define hydrothermal alteration using petrographic and geochemical characterisation of the hydrothermal dolomite at Lisheen mine as well as the greater Rathdowney Trend.
- Potentially identify geochemical vectors for future sulphide exploration in Ireland
- Zinc and lead form a vital constituent in technologies for low-carbon energy. Future development of ore deposits in Ireland will directly contribute toward achieving UN sustainable development goals.

Geological Setting

Lead and zinc sulphide mineralisation at Lisheen is hosted within the lower Carboniferous rocks of the Rathdowney Trend and is intimately associated with hydrothermally-derived, replacive dolomite, commonly referred to as “Black Matrix Breccia”. Lisheen mine (Fig. 1) is a historically superb example of hydrothermal mineralisation and a prime testing locality for sulphide geochemical vectoring.

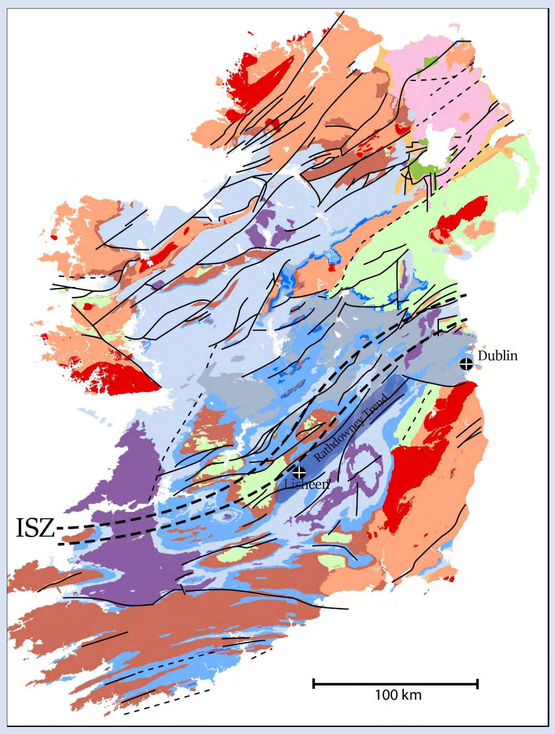

Fig. 1. Location of Lisheen mine along the Rathdowney Trend, Ireland

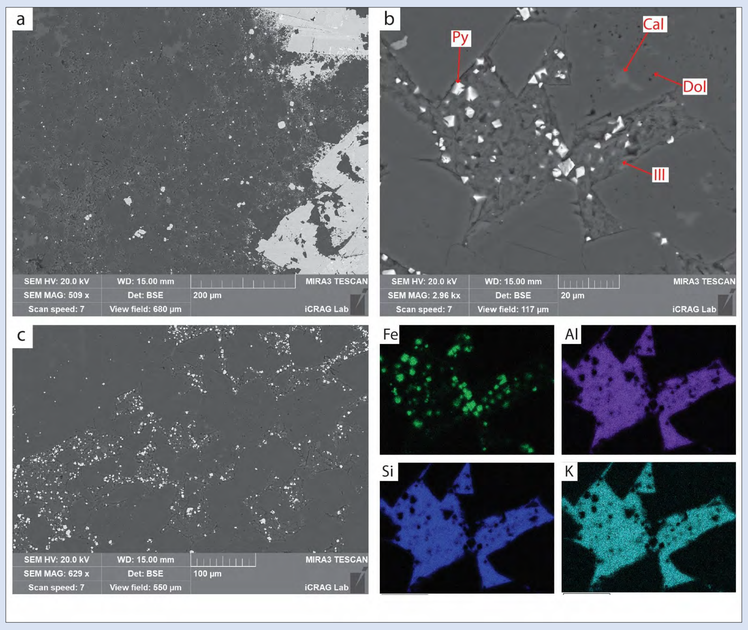

Fig. 4. a, b, c. Back-scatter electron images of the Black Matrix Breccia. D. Electron dispersive image of the elemental distribution within a phyllosilicate.

Geochemistry

Scanning electron microscopy analyses of BMB reveals an intricate mosaic of fine dolomite crystals, sulphide precipitates and phyllosilicates (Fig. 4). Sourced from underlying shales and mudstones, these phyllosilicates were mobilised by hot upwelling fluids. They are ubiquitous throughout the BMB and occur almost exclusively within fractures and inter-crystal pore spaces.

Sampling

Metal-bearing hydrothermal fluids infiltrated the carbonate stratigraphy of the Waulsortian Fm., resulting in rapid dissolution and replacement of regional dolomite by black hydrothermal dolomite.

The resulting rock is a dark, sulphide-bearing matrix with pale-grey Waulsortian Fm. clasts (Fig. 2).

Fig. 2. Example of classic matrix hosted BMB

Fig. 3. Sample of hydrothermal dolomite exhibiting settling textures over Waulsortian dolomite clasts.

Fluid-filled cavities form a prime environment for solution-based dolomite precipitation.

As indicated in Figure 3, hydrothermal dolomite precipitated out of a super-saturated fluid and settled on the cavity floor. Fragments of host dolomite fell into the settled precipitate, flexing around settled black dolomite laminae (Fig.3).

Microscopy

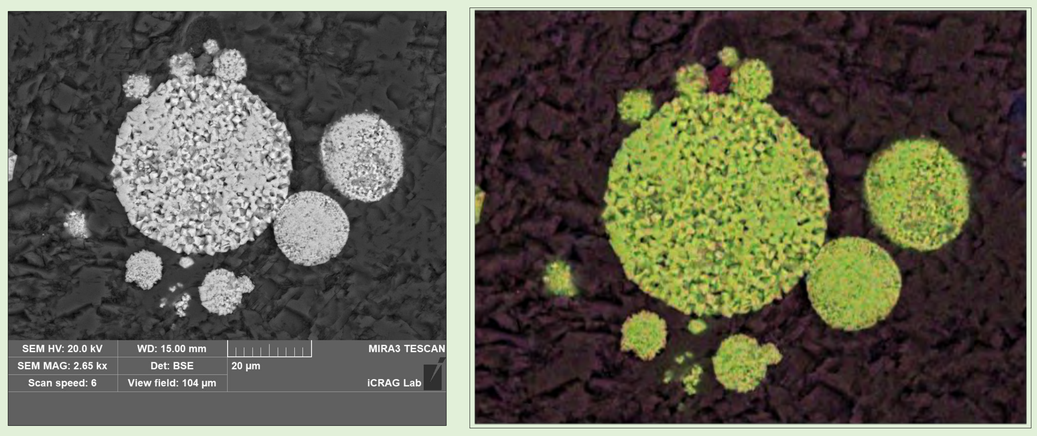

Fig. 5. Framboidal pyrite emplaced within the hydrothermal dolomite as well as a false-colour layered element map.

Spherical masses of framboidal pyrite within the hydrothermal dolomite (Fig. 5) reveal a temporal relationship between dolomite precipitation and sulphide development

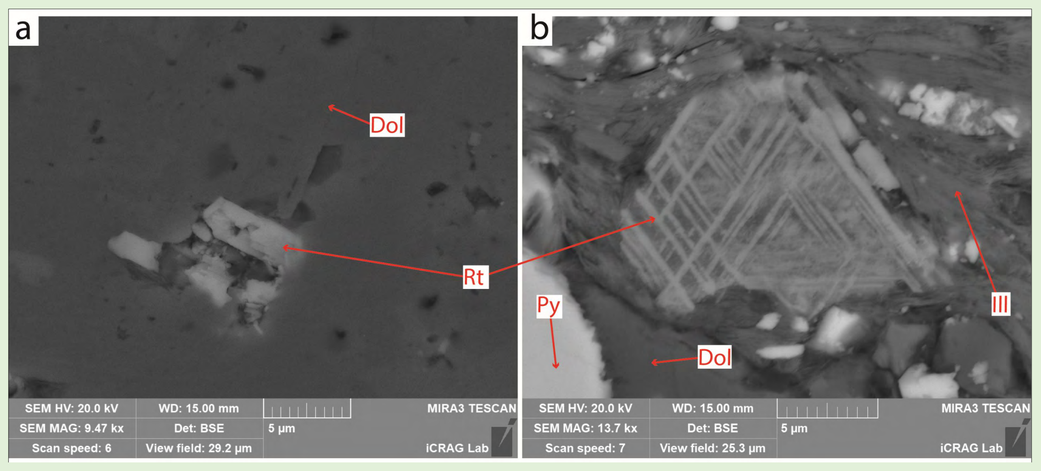

Fig. 6. Back-scatter electron images of detrital rutile in the Black Matrix Breccia.

Past studies have shown the hydrothermal fluids to be derived from a deep source, but how deep? The occurrence of tiny grains of detrital rutile (a high temperature Ti mineral) may provide further insight into this question (Fig. 6.).

This publication has emanated from research supported in part by a research grant from Science Foundation Ireland (SFI) under Grant Number 13/RC/2092 and 16/SP/4319 and co-funded under the European Regional Development Fund and by iCRAG industry partners.

Ireland’s European Structural and Investment Funds Programmes 2014-2020
Co-funded by the Irish Government and the European Union

European Union
European Regional Development Fund

Science Foundation Ireland sfi For what’s next

iCRAG 2019

Resources for a Sustainable Future

SECURE AND PROTECT GROUNDWATER RESOURCES

Visualisation of flow and contaminant transport in karst aquifers

Lea Duran, Laurence Gill

iCRAG IRISH CENTRE FOR RESEARCH IN APPLIED GEOSCIENCES

Trinity College Dublin, The University of Dublin

Project context and aims

Carboniferous limestone is the primary aquifer rock in Ireland, coinciding with the most productive agricultural land, areas of most economic activity and major centres of population. Much of this carboniferous limestone is karstified and as such, the aquifer is at greater risk of contamination and flooding issues due to the rapid transit of water, to the direct infiltration through swallow holes, the lowland nature of much Irish karst and the thin layer of soil cover which typically overlays them. It is thus of great importance to increase the often poor understanding of these complex systems. .

The primary aim of the project was to develop a **modelling approach** in order to simulate the **groundwater flow and contaminant transport** through **karst aquifers ,** using **visual 3D models**

Methods

Fieldwork and times series analysis are first used to build a conceptual model and a geological model using MOVE. This model is exported to **Leapfrog** in order to build a Modflow compatible grid and for visualisation purposes. This grid is exported to be used in **Modflow- USG with CLN** (from the USGS) and the GUI **Groundwater Vistas 7** (Figure 1).

The flow and contaminant transport simulations are carried out. Results are analysed and visualised in GWV7 and Leapfrog.
All the steps are checked against the current conceptual model of the studied site, but can be used to refine the conceptual model itself.

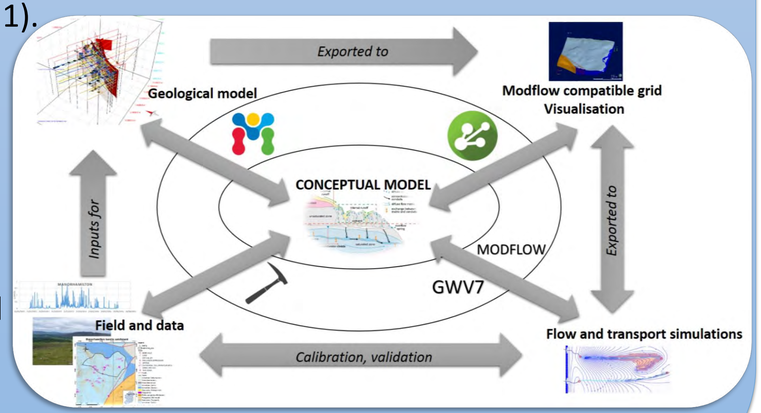

Fig. 1 : Workflow, steps for the groundwater modeling and software used

Study site

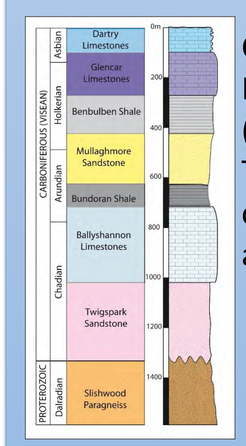

Fig. 2 : Stratigraphy

The first study site is a small **karst spring near Manorhamilton**, in County Leitrim. The karst network takes place in the Dartry Limestones formation (Fig. 2), covering the Glencar formation (with higher shale content).
Three tracer tests were carried out to check and redefine the catchment boundaries. Sinkholes and infiltration features were assessed through a field survey.

A water balance budget highlighted that the catchment was slightly bigger than expected. Time series analysis and signal analysis were used to characterise the hydrology of the catchment.

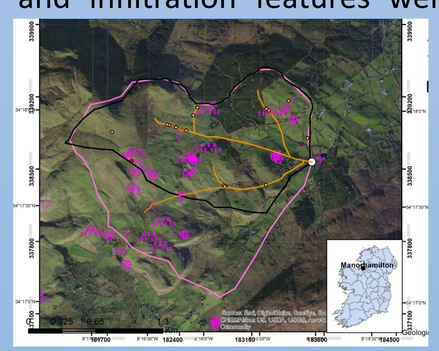

Fig. 3 : Catchment and conduits hypotheses

Flow model

The geological model built in MOVE was then exported to Leapfrog Geo where the hydrogeological module enables to assign the hydrological properties of each formation and to grid the model.

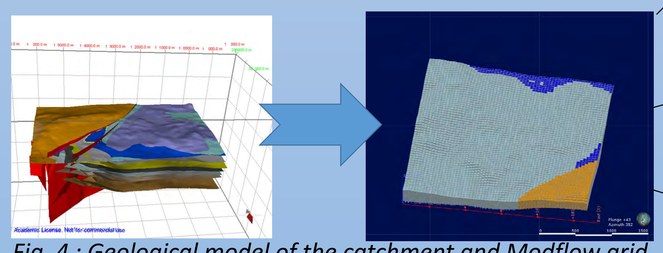

Fig. 4 : Geological model of the catchment and Modflow grid

The hydrogeological characteristics of the geological formations were based on existing literature (Gunn 1982, Misstear 2008, etc.), and the data collected in the field (tracer tests) for the karstified domain.

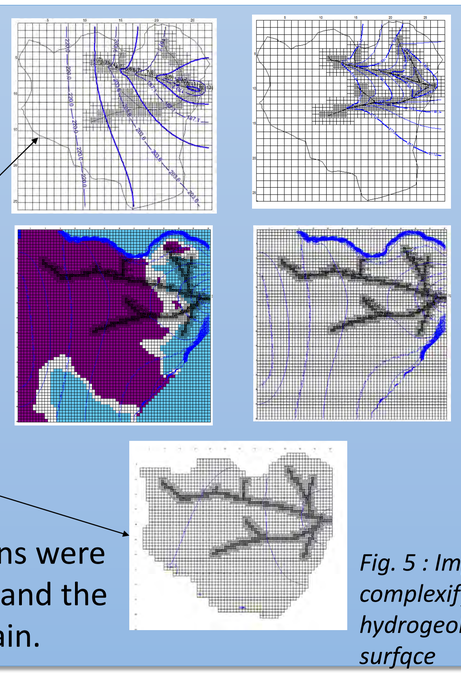

Fig. 5 : Impact of activating one or several conduits (up), of complexifying the geology (middle) and modifying hydrogeologigic parameters (bot.) on the portentiometric surfqce

Different boundary conditions were tested out (constant head, no flow cells, general head boundary, variable heads), and different geological set ups as well (permeability gradients in the « matrix domain », configuration of the karst network, …). Simulations were run in steady state and transient configurations and calibrated manually against observed data.

A sensivity analysis was carried out for the main parameters (impact of the hydraulic head and on the spring discharge).

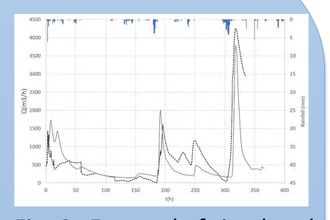

Fig. 6 : Exampel of simulated vs observed discharge at the spring for Oct.-Nov. 2017

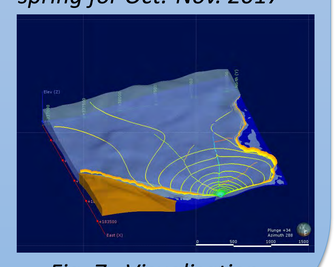

Fig. 7 : Visualisation in Leapfrog

Contaminant transport model

Once the flow model was calibrated, the transport modeling was done using the Block Centered Package (BCT). Different configurations were simulated (constant source located near the conduit network, punctual source in the fissured matrix domain) and the resulting impact of the contaminant transport depending on hydrogeological conditions assessed (fig. 8 and fig. 9).

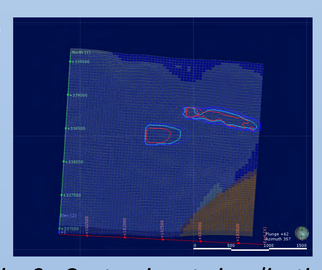

Fig. 9 : Contaminant visualisation

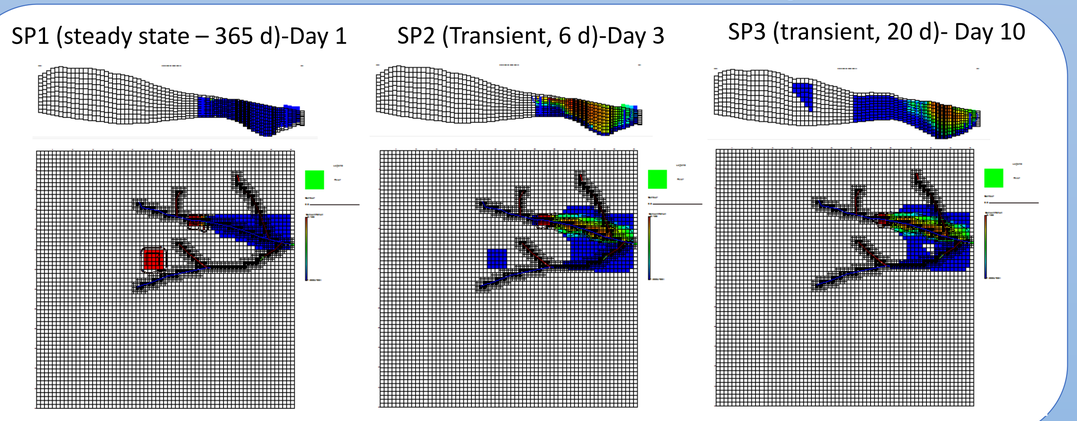

Fig. 8 : Contaminant transport in high flow conditions, effect of a major rain event and a recession

Conclusions and perspectives

After having built and validated the methodology on Manorhamilton catchment, a flow model was also built for a study site with more complex river interaction and surface-groundwater interaction processes : Ballindine catchment, county Mayo (Fig. 10 &11).

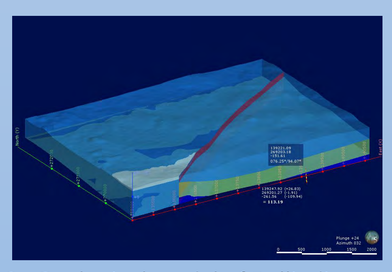

Fig. 10 : Geological model of Ballindine catchment

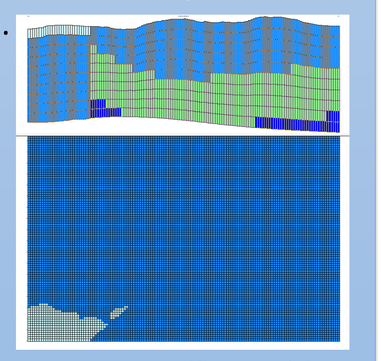

Fig. 11 : Modflow model

In conclusion, the combined use of flow and transport groundwater models and visualisation animations are useful tools to investigate the hydrogeological behaviour of karst aquifers. The models and their visualisation can help inform the management of water resources both quantitatively and qualitatively (climate change issues, contamination….)

This publication has emanated from research supported in part by a research grant from Science Foundation Ireland (SFI) under Grant Number 13/RC/2092 and co-funded under the European Regional Development Fund and by iCRAG industry partners.

Ireland's European Structural and Investment Funds Programmes 2014-2020 — Co-funded by the Irish Government and the European Union

European Union — European Regional Development Fund

Science Foundation Ireland — SFI For what's next

Geoserv · TII Bonneagar Iompair Éireann Transport Infrastructure Ireland · David Ball & Associates · TOBIN Consulting Engineers · GEOSCIENCE IRELAND Exploring Developing Sustaining · PIP Petroleum Infrastructure Programme

Spatiotemporal transients of water age determined with radium isotopes as a tool to assess the extent of vertical mixing in coastal systems.

Maxime Savatier, Carlos Rocha

Biogeochemistry Research Group, School of Natural Sciences, Museum Building, Trinity College Dublin, College Green, Dublin 2, Ireland. savatiem@tcd.ie

Water ages = The time it takes for any parcel of water to leave a system since it got into the system.
Water ages and Stratification play a key role for nutrient cycles and phytoplankton.

Why spatiotemporal changes of water ages in coastal area?

Fully and instantaneously mixed coastal systems do not exist.
Vertical mixing and ages patterns of estuaries continuously change depending on fresh water inputs, tides, wind…

Consequences?

- Water age, transit/residence time varies within system.
- Interplay between Phytoplankton, Nutrient and Water turnover time scales determine ecosystem function and response to change.
- -> Different parts of the system react in different ways to different stimulus

Aims

Illustrate the combined effect of stratification, spatiotemporal changes to water age and seasonal variability on elemental Nitrogen:Phosphorus (N:P) ratios in the water column.

Show consequences for the biogeochemical functioning of local ecosystems.

Develop an indicator of stratification based on Ra isotopes.

Study site

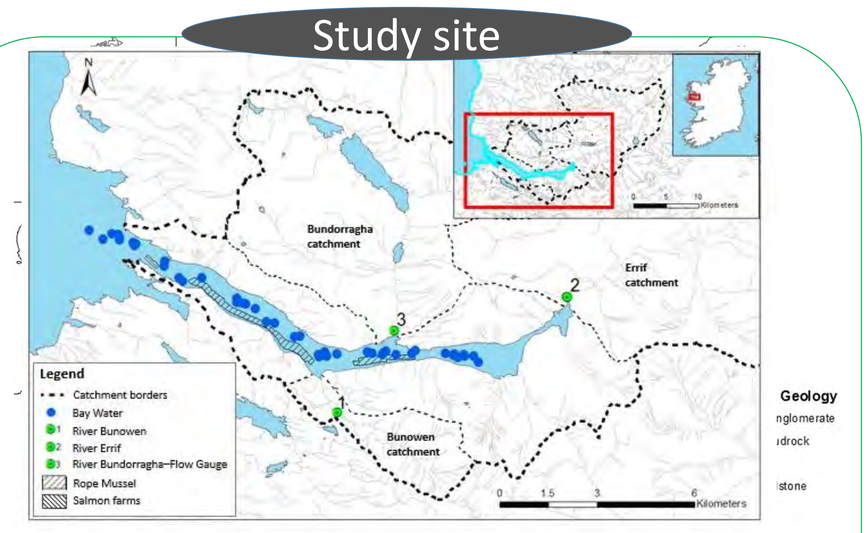

Killary Harbour: 105 Mm^3, Avg Depth 20 m, 700 m wide, 13 km long, 3.7m tidal range
River Discharge: 0.13 – 11.6 Mm3/d**,** 74% in the upper bay.

Results

Fieldwork

-Six successive detailed profiles of 224Ra/223Ra ages, nutrient and salinity in surface and deep waters.
-Sampling under different discharge conditions and during spring tide to estimate the minimum effect of river discharge for the system stratification.

Ra profiles in deep/surface waters

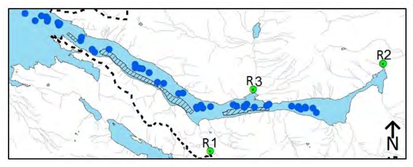

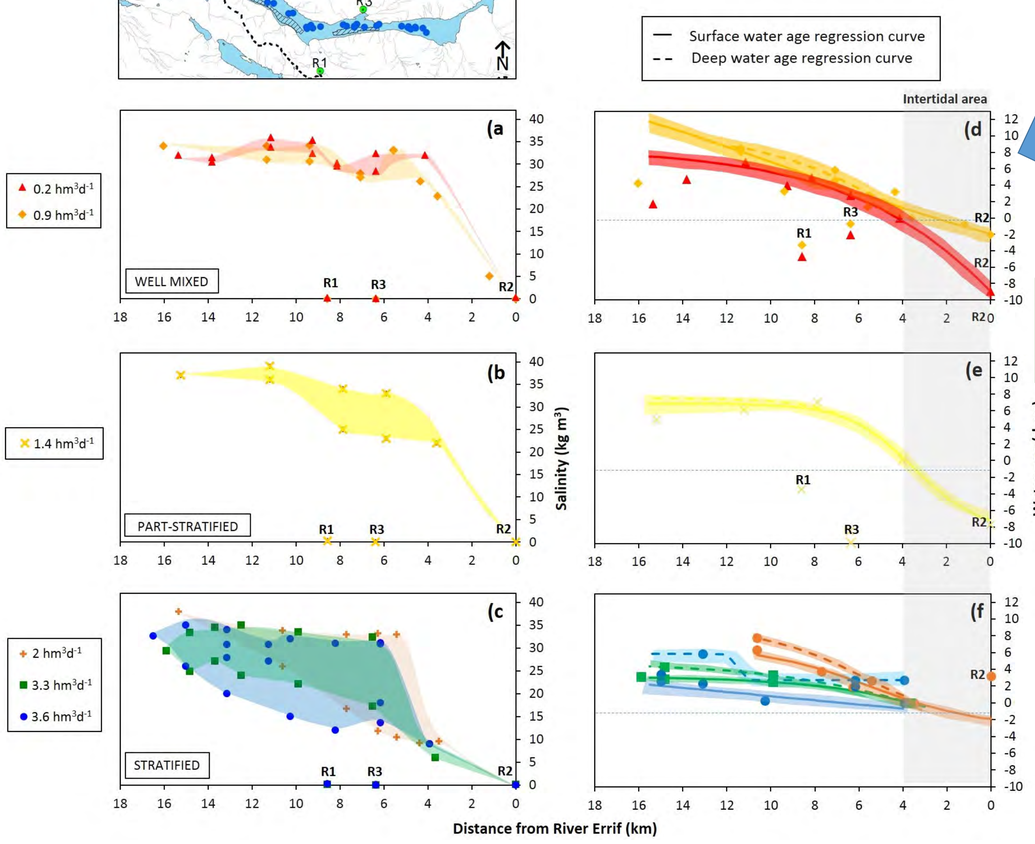

Discharge affect salinity (a,b,c) and ages (d,e,f) spatial variability. (coloured area show surface/deep salinity differences in a, b,c and RMSE of ages regression in d,e,f)

Repeat to derive temporal variability

Ra isotopes -> derive ages spatial variability (3.3hm3.d-1)

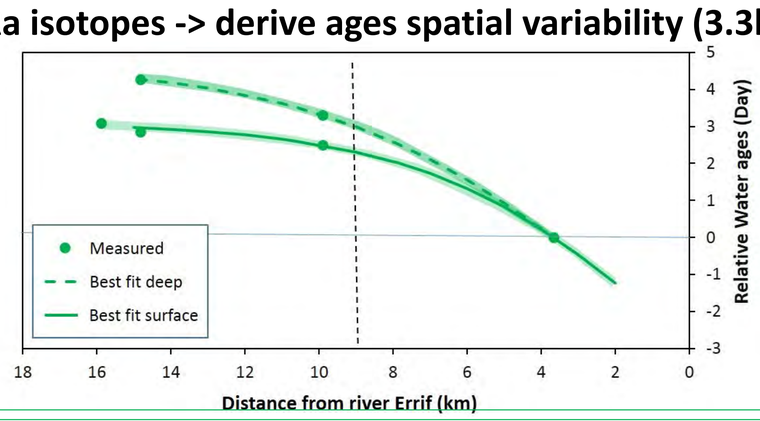

No effect of Ages on N:P ratio…

N:P ratio vs Ra derived water ages

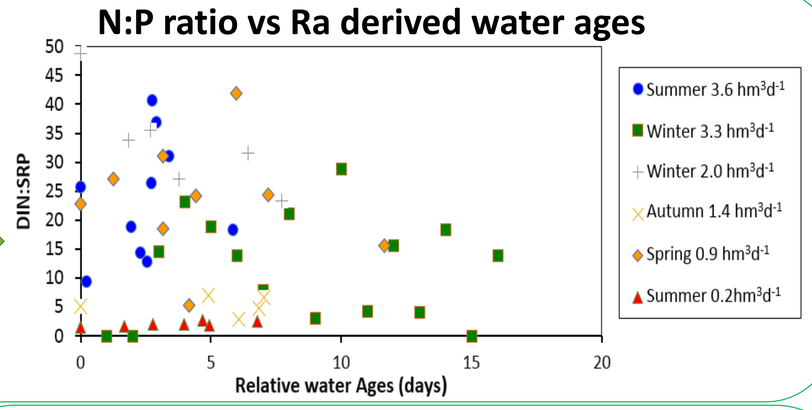

…but N,P cycles driven by discharge and stratification

Relative accumulation of SRP in deep water (b) when normalised age difference >0.2 (d) -> Higher N:P ratio (c)

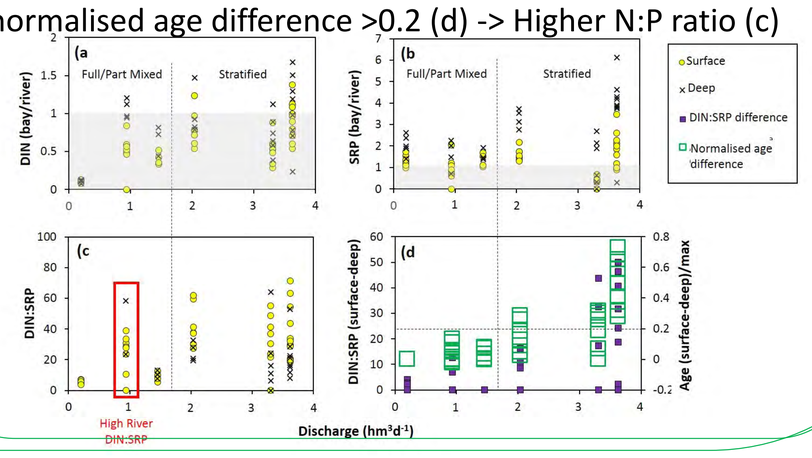

Results consequences for coastal systems

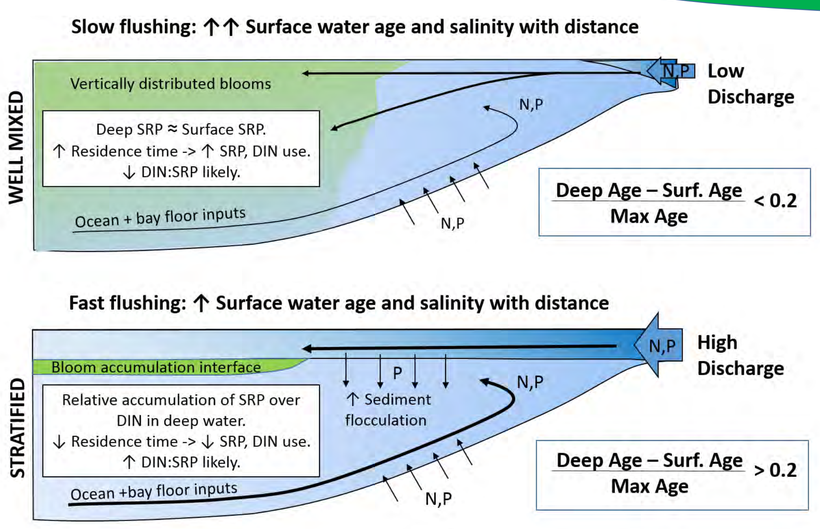

- Fully and instantaneously mixed coastal systems do not exist.
- Mixing is spatially and temporally variable.
- Benthic pelagic coupling and vertical exchanges plays a major role in nutrient dynamics.
- Thus:

➢System averaged transit time/residence time cannot predict system biogeochemistry.
➢Ra224/Ra223 allow to consider spatial and temporal variability of ageing profiles for surface and deep water, and estimate the magnitude of stratification for coastal systems.
➢Vertical mixing controls Benthic pelagic coupling, and hence N:P ratio in the water column. This is likely to affect the timing of Phytoplankton composition shift in estuaries.

This publication has emanated from research supported in part by a research grant from Science Foundation Ireland (SFI) under Grant Number 13/RC/2092 and co-funded under the European Regional Development Fund and by iCRAG industry partners.

Modelling diffuse groundwater recharge in Irish karst

Philip Schuler[1,2], Lea Duran[1,2], Paul Johnston[1], Laurence Gill[1,2]

[1]Trinity College Dublin; [2]Irish Centre for Research in Applied Geosciences (ICRAG)

Introduction

- Karst aquifers are vulnerable to contamination, yet, in Ireland and worldwide, they bare important groundwater resources for societies;
- Karstified aquifers are highly heterogeneous - triple porosity systems with different groundwater recharge, flow and discharge dynamics;
- Karst groundwater flow modelling is relevant but challening given the heterogeneity.

Objectives

1. Develop conceptual hydrogeological models of 3 study sites;
2. Quantify between slow (diffuse) and fast (concentrated) recharge and flow dynamics based on spring hydrographs;
3. Develop 3 numerical pipe network models accounting for the different dynamics.

Approaches

- Catchment delineation using water balances, tracer test and geological information;
- Characterise different recharge and flow components using recession, frequency and multi-resolution analysis using high-frequency long-term hydroclimatic time series;
- Establish most parsimonious models using InfoWorks ICM® (version 7.0.5., Innovyze Ltd., Wallingford, UK).

1. Identifying and modelling of recharge and flow components

Ballindine spring: low lying aquifer receiving major recharge from the losing stream Robe.

Manorhamilton spring: highly karstified conduit dominated upland-lowland aquifer.

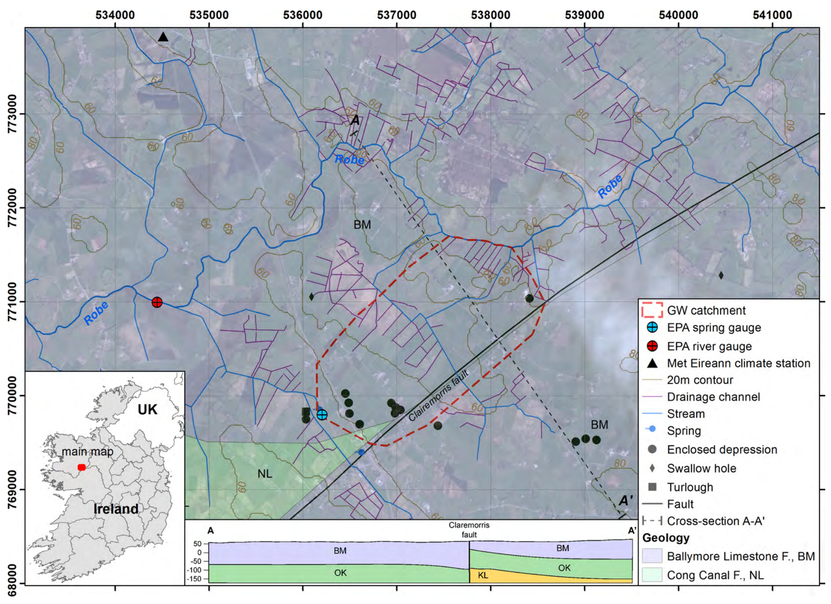

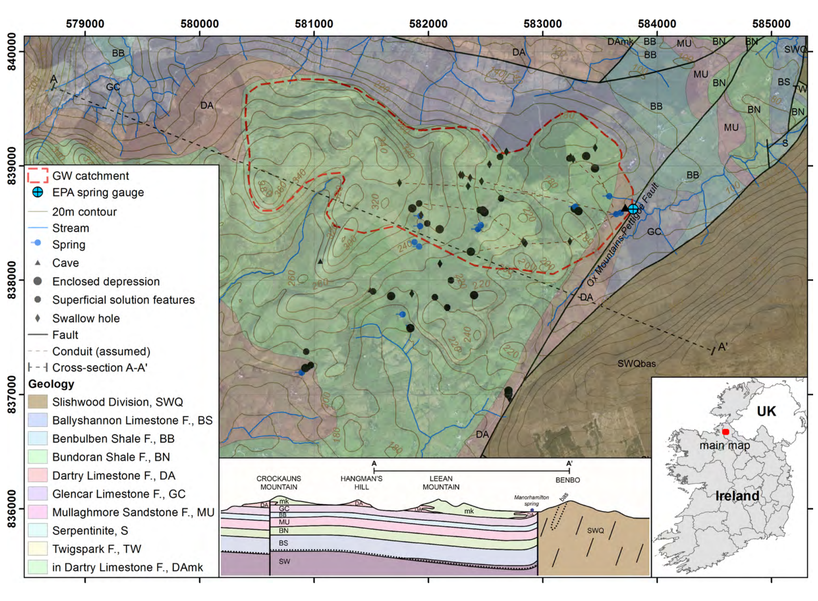

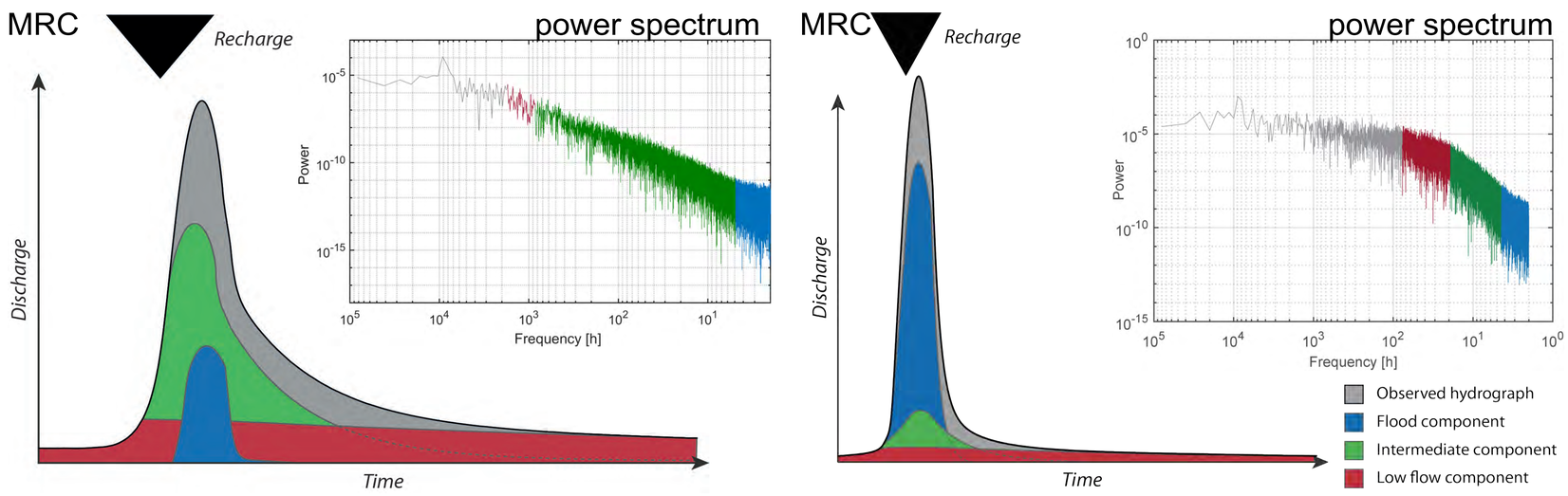

The power spectrum and the master recession curve (MRC) of both springs suggest the presence of three 'structured' components of low, intermediate and high frequency related to slow (diffuse), intermediate and quick (concentrated) recharge and flo .

2. Modelling

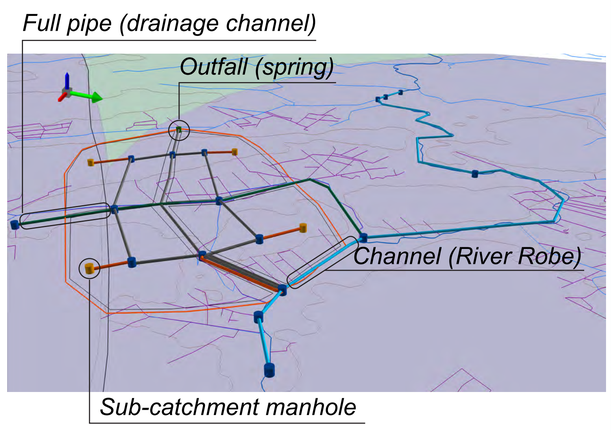

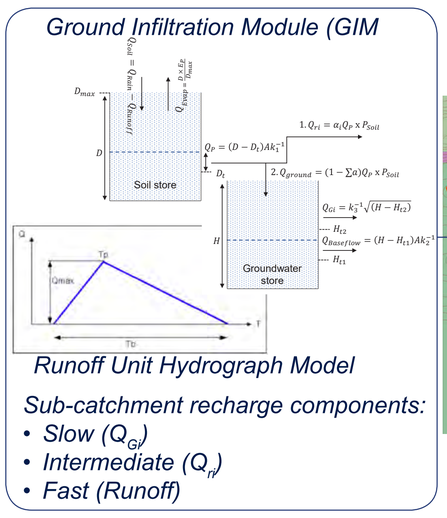

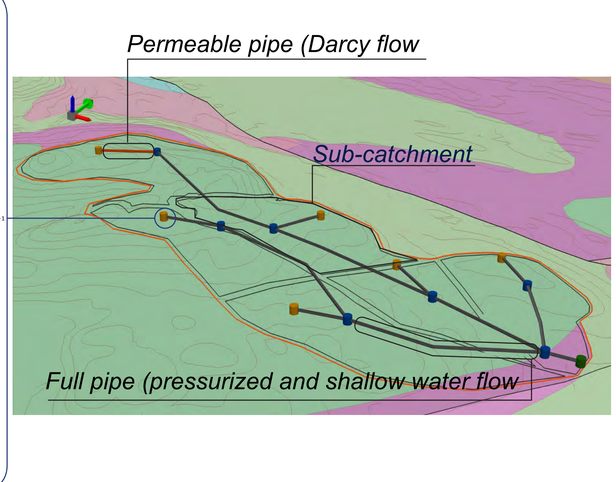

Sub-catchment recharge components:

- *Slow (Q_G)*
- *Intermediate (Q_r)*
- *Fast (Runoff)*

3. Results

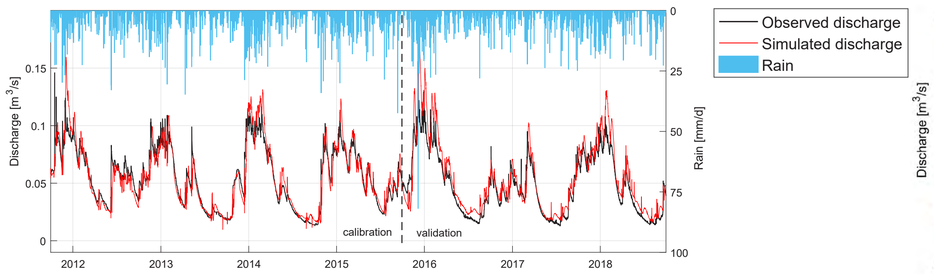

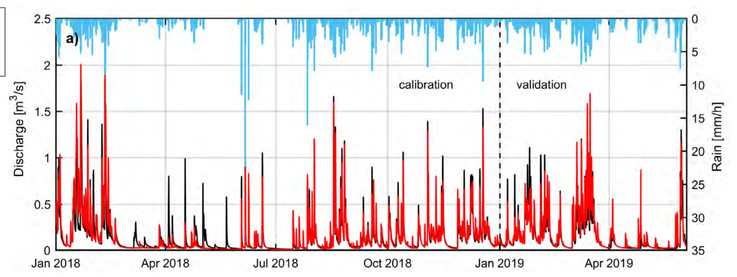

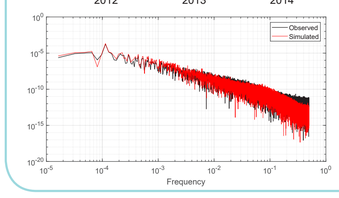

The simulated discharge and the power spectrum suggest that the overall discharge as well as recharge components are realistically represented by the model.

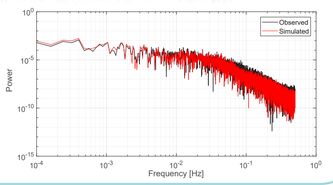

4. Application: Bell Harbour

Bell Harbour: coastal aquifer discharging via multiple submarine and intertidal springs from the Burren Plateau.

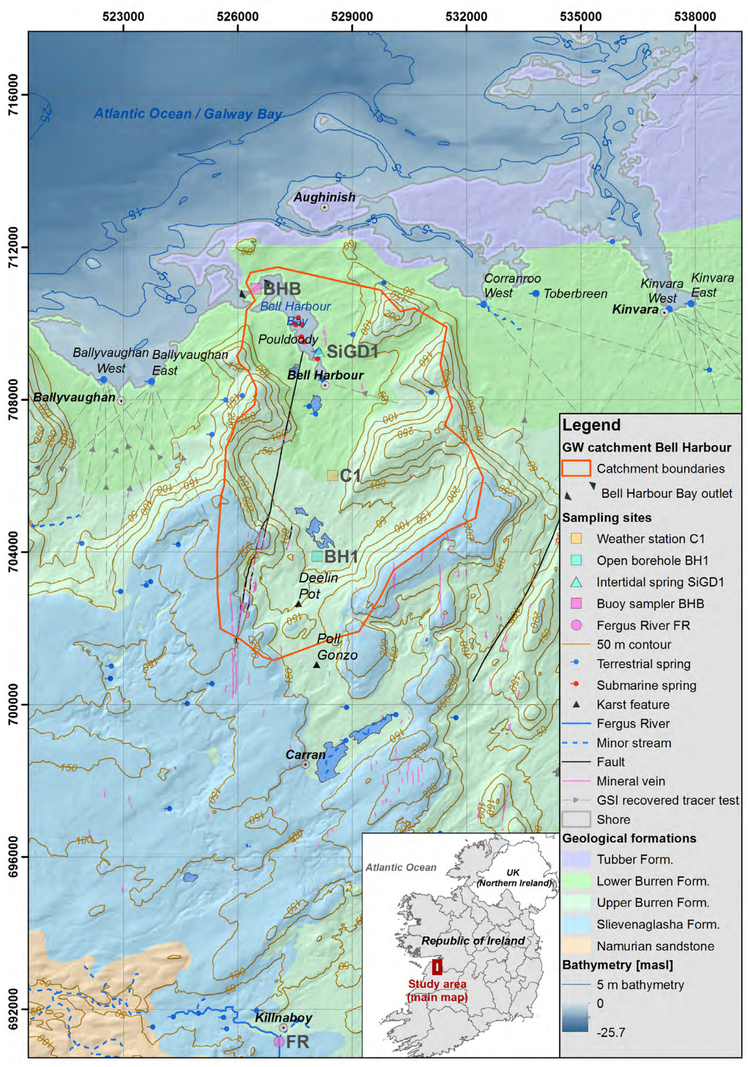

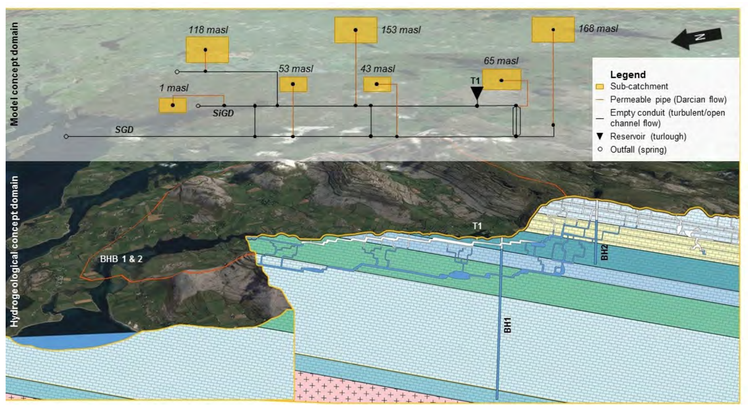

5. Results

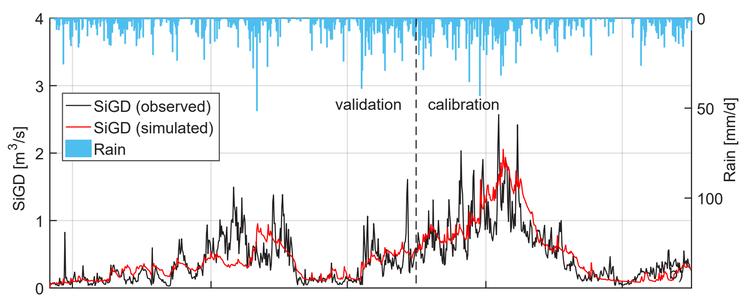

The developed modelling approach can represent a complex multi-level karst conduit aquifer with seasonally fluctuating shallow submarine and i - tertidal discharge.

6. Conclusions

- Time series analyses identified distinct recharge and flow components in the karst spring signals
- Pipe network models can simulate different karst recharge and flow dynamics and the overall spring discharges;
- Contaminant transport mechanisms may be realistically represented in such models.

October, 2019

This publication has emanated from research supported in part by a research grant from Science Foundation Ireland (SFI) under Grant Number 13/RC/2092 and co-funded under the European Regional Development Fund and by iCRAG industry partners.

Ireland's European Structural and Investment Funds Programmes 2014-2020
Co-funded by the Irish Government and the European Union

European Union
European Regional Development Fund

Science Foundation Ireland sfi For what's next

Geoserv · TII Bonneagar Iompair Éireann Transport Infrastructure Ireland · David Ball & Associates · TOBIN Consulting Engineers · GEOSCIENCE IRELAND Exploring Developing Sustaining · PIP Petroleum Infrastructure Programme

Principal Component Mapping of Geochemistry Data – An Example Using TELLUS Data from the Border Region

Seán Wheeler[1], Tiernan Henry[1], John Murray[1], Liam Morrison[1] and Frank McDermott[2]

E-mail: sean.wheeler@nuigalway.ie

[1]Earth and Ocean Science, NUI Galway & iCRAG
[2]Earth Science, UCD & iCRAG

Introduction:

TELLUS BORDER

National geophysical and geochemical data acquisition programme

2nd Phase (2011-13) = Border Region

Geochemistry data is from topsoil, stream sediment and stream water samples

Designed to avoid potential spurious correlation when using PCA on compositional data (e.g. geochemistry)

Compositional Data Analysis (CoDA)

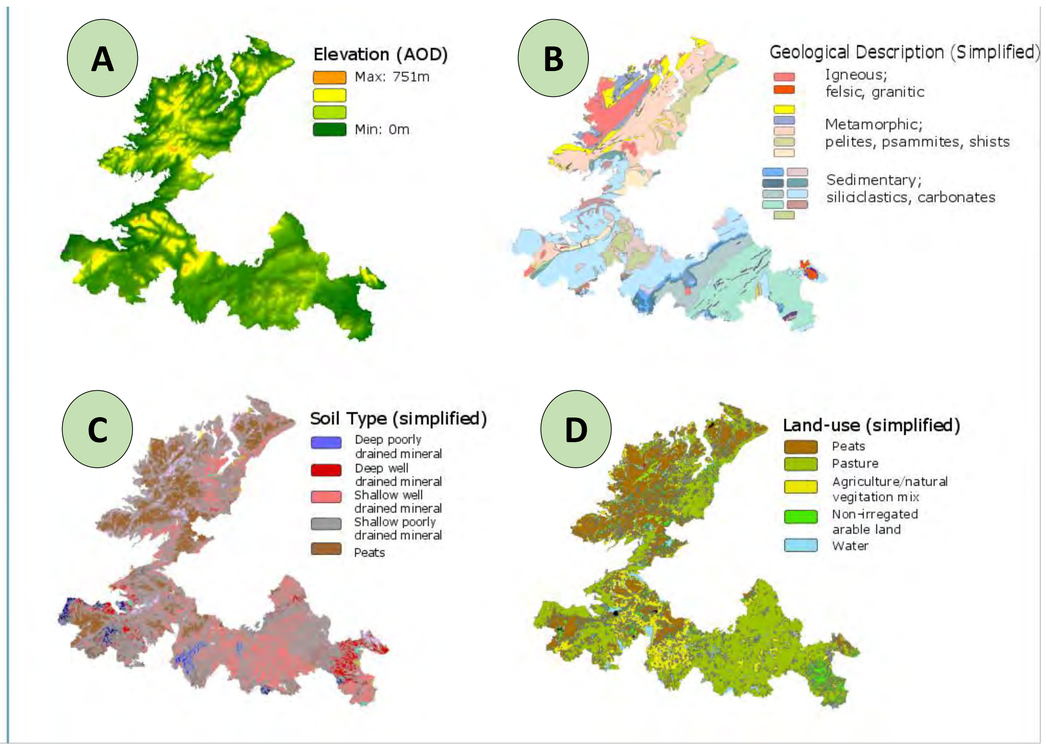

Figure 1: Environmental conditions in the study area
A. Elevation (source: ArcGIS), B. Geology (source: GSI), C. Soil type (source: Teagasc), D. Land-use (source: EPA)

Results:

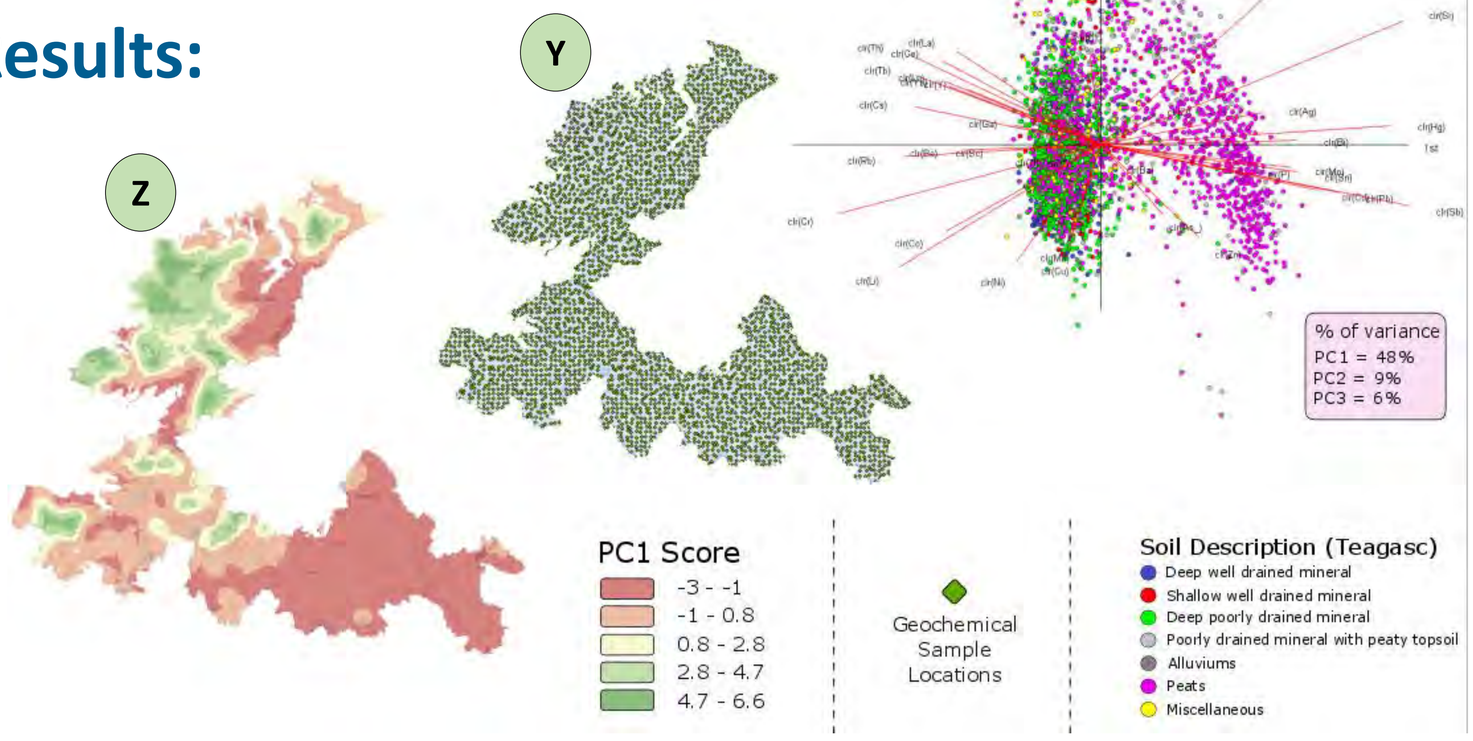

Figure 2: From CoDA to a PCA map (topsoil data)
X. Principal component compositional biplot, Y. Tellus topsoil sampling locations, Z. Interpolated (using kriging) principal component loading map

Method:

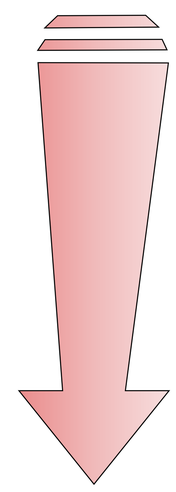

Raw data excel file

Data Preparation

Compositional Data Analysis

Principal component mapping in ArcGIS

X The Biplot…. (X Above ⬆)

Soil Type:	Relationships:	Explanation:
Peaty soils ● ● ● ●	Heavy metals (e.g. Pb, Cd, Sb and Hg)	Retention by organic matter (e.g. Zadrosny & Nicia, 2009, Borgulat et al., 2018)
Mineral soils ● ● ● ●	REEs (e.g. La, Ce, Tb, Lu, Yb, Sc, and Y)	Greater interaction with bedrock and niche flora (e.g. Tyler, 2004)

Z The Map…. (Z Above ⬆)

Biplot observation coordinates = PC loadings

⬇

Extract these and interpolate them geographically

Compare this map to the environmental conditions maps above especially the Teagasc soils map to demonstrate the accuracy of this process

Why though….?

Environmental Change

The CoDA method is an effective way of monitoring environmental change as it compares variations of numerous elements and compounds concurrently and is very sensitive to change. Detected changes can be viewed geographically using the PC mapping technique.

Mineral Exploration

On a smaller scale this method can be used to identify elemental associations that are indicators of economic mineral prospects. Mapping these associations as a pose to singular elemental mapping can help refine target locations.

Contaminant Tracking

Again on small scales, this process can be used to analyse the effects of contamination on the geochemistry of soils, sediments and waters. The geographical spread of the effect can be best monitored using principal component mapping.

This publication has emanated from research supported in part by a research grant from Science Foundation Ireland (SFI) under Grant Number 13/RC/2092 and co-funded under the European Regional Development Fund and by iCRAG industry partners.

Ireland's European Structural and Investment Funds Programmes 2014-2020
Co-funded by the Irish Government and the European Union

European Union
European Regional Development Fund

Science Foundation Ireland sfi For what's next

References:

1. BORGULAT, J., MĘTRAK, M., STASZEWSKI, T., WIŁKOMIRSKI, B., SUSKA-MALAWSKA, M. (2018). Heavy Metals Accumulation in Soil and Plants of Polish Peat Bogs. Pol. J. Environ. Stud., 27, 1-8.
2. ZADROZNY, P., NICIA P. (2009). Heavy metals in the peat soils of the Konecki County. Ecol. Chem. Eng. 16, 1205.
3. TYLER, G. (2004). Rare earth elements in soil and plant systems — A review. Plant and Soil, 267, 191-206.

Acknowledgements:
A massive thank you to the GSI particularly the Tellus project which provided the data for this study.

Bonneagar Iompair Éireann Transport Infrastructure Ireland
David Ball & Associates
TOBIN Consulting Engineers
PIP Petroleum Infrastructure Programme

Engineered silver nanoparticle (Ag-NP) behaviour in small scale treatment plants and in sewage sludge amended-soils

Viviana Bolaños-Benítez[1,3], Frank McDermott[1,3], Laurence Gill[2,3] and Jan Knappe[2]

[1]School of Earth Sciences, University College Dublin, Belfield, Dublin 4, Ireland
[2] Department of Civil, Structural and Environmental Engineering, Trinity College Dublin, The University of Dublin, Ireland
[3] Irish Centre for Applied Geosciences (iCRAG), University College Dublin

1. CONTEXT

1.1 Silver nanoparticles (Ag-NPs) are used widely as antimicrobial agents in consumer products and are released into sewage treatment systems

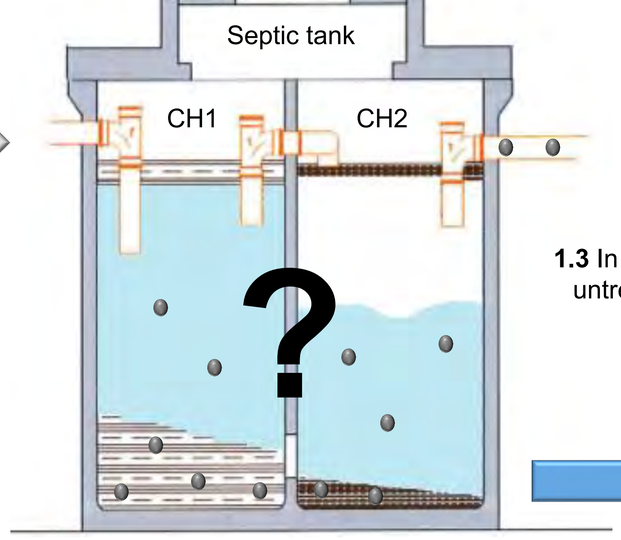

1.2 The wastewater contains a wide range of suspended particulate matter (SPM) with which NPs can interact

1.3 In countries like Ireland, untreated sludge can be land-spread

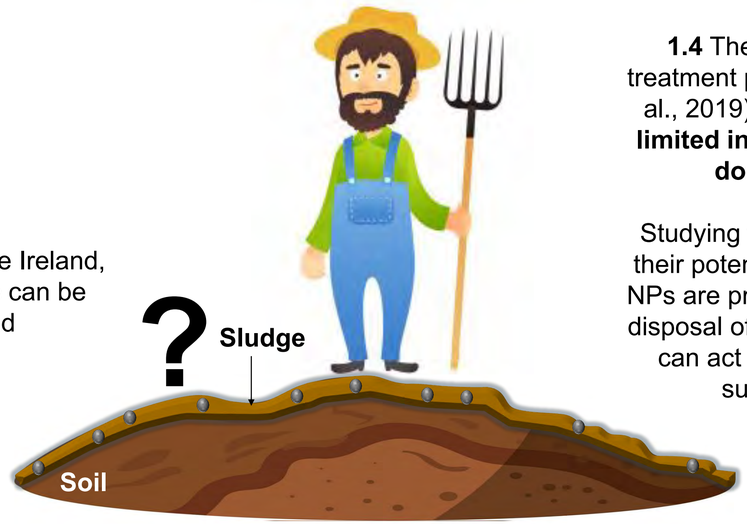

1.4 The fate of Ag-NPs in conventional wastewater treatment plants (WWTPs) (Kaegi et al., 2013; Fletcher et al., 2019) have been studied widely. However, **there is limited information on their behaviour in small scale domestic WWTPs such as septic tanks.**

Studying the fate of Ag-NPs in septic tanks is critical for their potential release into water bodies. Moreover, if Ag-NPs are preferentially sequestered into the sludge phase, disposal of the latter to landfill and/or its use as a fertilizer can act as a source of Ag-NPs through leaching and surface runoff under oxidising conditions.

2. EXPERIMENTAL METHODOLOGY

Four spiking experiments (EXP1, EXP2, EXP3 and EXP4) were performed to assess the aims of the study. For each experiment 20, 60 and 100 nm Ag-NPs were used.

Aims

This study focuses on:

- The partitioning of Ag-NPs in the wastewater/sludge system in septic tanks (EXP 1 and 2)
- The mobility of Ag-NPs in soils spread with untreated sludge (EXP 3 and 4)

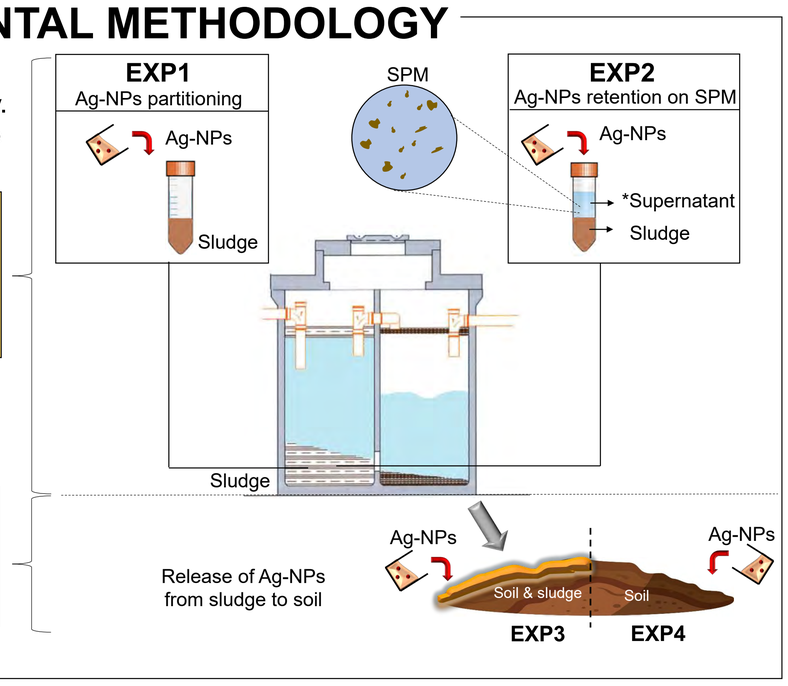

* Extracted after sludge centrifugation
SPM: Suspended particulate matter

3. ANALYTICAL TOOLS

Nanoparticle sizing and concentration measurement
Single Particle – ICP - MS

Flow rate: 0.36 mL/min

Dwell time: 5 ms

Transport efficiency: ~ 7% (60 nm Au-NPs)

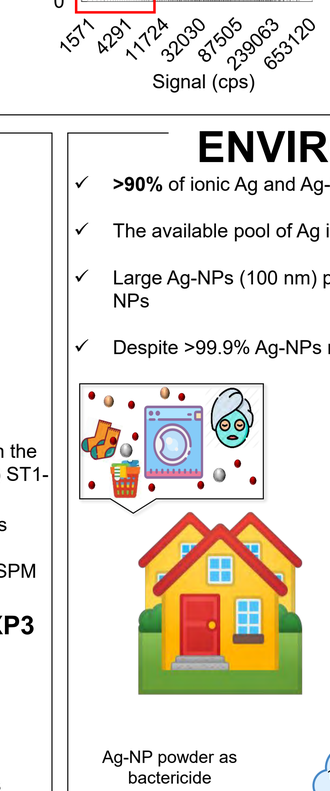

Ag-NPs imagining
TEM and SEM-EDX

TEM (nanoparticle standards)

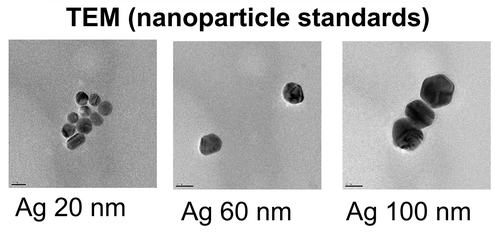

Ag 20 nm | Ag 60 nm | Ag 100 nm

Nanoparticle	Reported diameter (nm)	Measured diameter - TEM (nm)
Ag 20 nm	20 ± 4 nm	19 ± 4 nm
Ag 60 nm	60 ± 8 nm	61 ± 8 nm
Ag 100 nm	100 ± 8 nm	94 ± 16 nm
Au 60 nm	57 - 63	63 ± 6 nm

The measured diameter of Ag and Au-NPs by TEM is within the range reported by the manufacturer

4. RESULTS

4.1 Ag-NPs partitioning in the sludge's supernatant (EXP1)

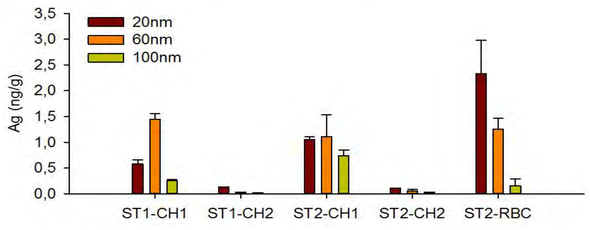

Fig 1 Total Ag and calculated corresponding number of nanoparticles in the supernatant of spiked sludge after 24 hrs

- ✓ Higher concentrations of smaller Ag-NPs (20 nm) are present in the supernatant, except for ST1-CH1
- ✓ **2%** of the Ag-NP added remained in the supernatant, while **98%** was retained in the solid phase of the sludge, mainly due to sulfidation

pH ~ 7, oxidating conditions (Eh - 178.6 and 64.8 mV) and HS^- concentration

52-83 µM | 62-94 µM

$$CH_4 + SO_4^{2-} \rightarrow HCO_3^- + HS^- + H_2O$$
$$HS^- \leftrightarrow H^+ + S^{2-}$$

Ag-NP sulfidation is thermodynamically favourable

- ✓ If a sulfidation rate of 11-14 nm of Ag converted to Ag_2S per day (Kent et al., 2014) is considered, 20, 60 and 100 nm Ag-NPs will be converted to Ag_2S in 2, 6 and 9 days, respectively.

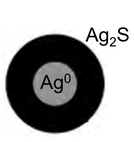

4.2 Ag-NPs retention on SPM (EXP2)

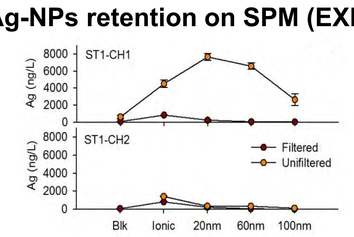

Fig 2 Total Ag in filtered (0.45 µm) (F) and unfiltered (UF) supernatant for (a) ST1-CH1 and ST1-CH2

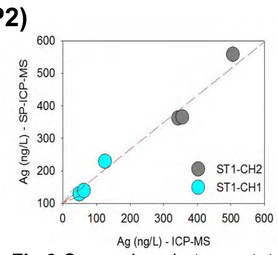

Fig 3 Comparison between total Ag concentration calculated by ICP-MS and SP-ICP-MS for 60 nm Ag-NP in the filtered solution

- ✓ In CH1, 80% more 100 nm Ag-NPs were found in the supernatant compared to CH2, as there are more particles < 0.45 µm and colloids available to retain the nanoparticles in suspension
- ✓ 60 nm Ag-NPs maintained their size in the supernatant and were more abundant in CH2 compared to CH1

4.2 Cont… Ag-NPs retention on SPM (EXP2)

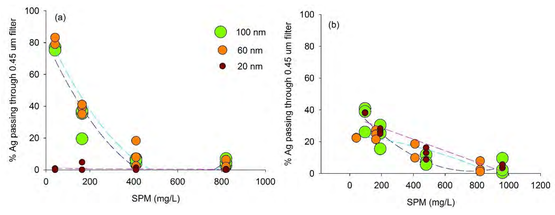

Fig 4 Average suspended particulate matter content (SPM) vs % of retained Ag in the 0.45 µm filter for different Ag-NP size for sludge of chambers (a) ST1- CH1 and (b) ST1-CH2

- ✓ The % of Ag passing through the 0.45 µm filter, decreases when SPM increases
- ✓ For CH1, the presence of 20 nm Ag-NP in the filtered solution is unaffected by SPM concentration

4.3 Retention and remobilization of Ag-NPs from soils (EXP3 and EXP4)

~ 99% Ag-NPs were retained

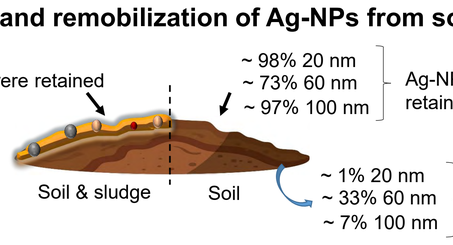

In the supernatant (liquid fraction)…

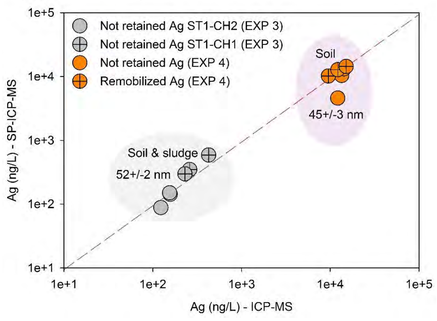

Fig 5 Correlation of Ag (60 nm Ag-NPs) concentration measured by SP-ICP-MS and ICP-MS in the supernatant

- ✓ The presence of sludge enhances the retention of Ag-NPs in the solid phase by >10 fold
- ✓ According to SP-ICP-MS results, the average Ag-NP size was higher in the presence of sludge, probably due to the increased of colloidal stability when humic acids adsorbed to Ag-NPs

ENVIRONMENTAL IMPLICATIONS

- ✓ **>90%** of ionic Ag and Ag-NPs is retained in the solid phase of the sludge
- ✓ The available pool of Ag is higher in the first chamber (ST-CH1)
- ✓ Large Ag-NPs (100 nm) preferentially sorb onto colloids and particles (> 0.45 µm) compared to smaller NPs
- ✓ Despite >99.9% Ag-NPs retention in the soil, the mobile 0.1% can be released into the water bodies

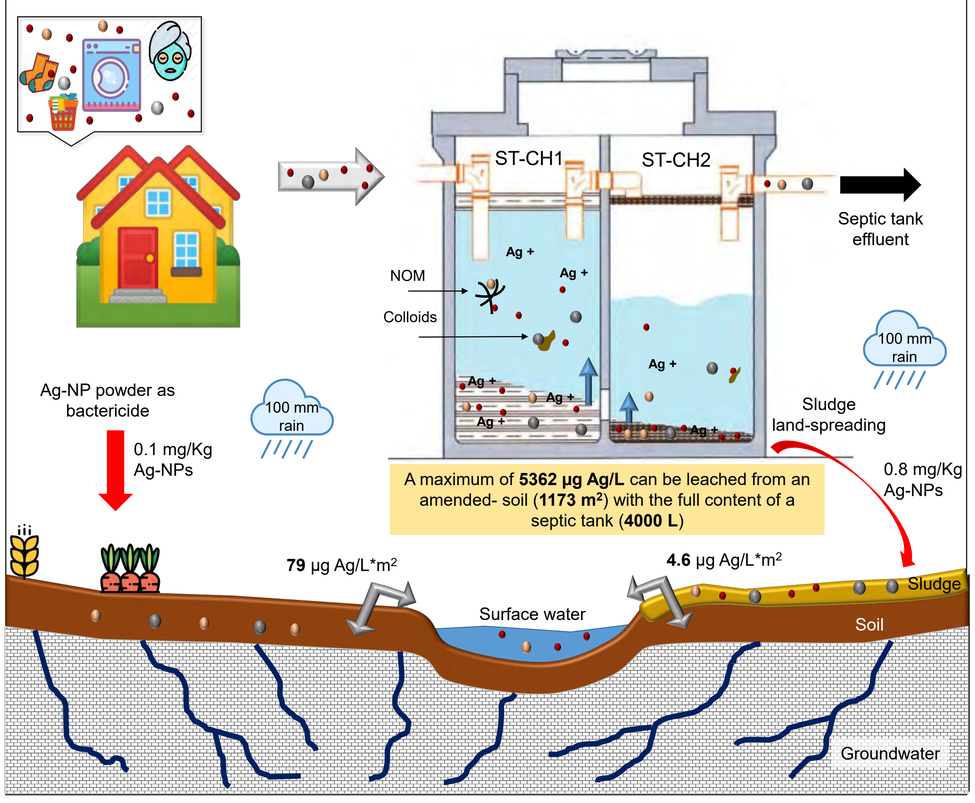

References

Batley, G.E., Kirby, J.K., McLaughlin, M.J., 2013. Fate and risks of nanomaterials in aquatic and terrestrial environments. Acc. Chem. Res. 46, 854–862
Fletcher, N.D., Lieb, H.C., Mullaugh, K.M., 2019. Stability of silver nanoparticle sulfidation products. Sci. Total Environ. 648, 854–860
Kaegi, R., Voegelin, A., Ort, C., Sinnet, B., Thalmann, B., Krismer, J., Hagendorfer, H., Elumelu, M., Mueller, E., 2013. Fate and transformation of silver nanoparticles in urban wastewater systems. Water Res. 47, 3866–3877
Kent, R.D., Oser, J.G., Vikesland, P.J., 2014. Controlled evaluation of silver nanoparticle sulfidation in a full-scale wastewater treatment plant. Environ. Sci. Technol. 48, 8564–8572.
Navarro, D.A., Kirby, J.K., McLaughlin, M.J., Waddington, L., Kookana, R.S., 2014. Remobilisation of silver and silver sulphide nanoparticles in soils. Environ. Pollut. 193, 102–110
Shafer, M.M., Overdier, J.T., Armstong, D.E., 1998. Removal, partitioning, and fate of silver and other metals in wastewater treatment plants and effluent-receiving streams. Environ. Toxicol. Chem. 17, 630–641

Acknowledgements

Special thanks to Dr. rer nat David Van Acken for his assistance and support for ICP-MS analysis at School of Earth Sciences (UCD)

This publication has emanated from research supported in part by a research grant from Science Foundation Ireland (SFI) under Grant Number 13/RC/2092 and co-funded under the European Regional Development Fund and by iCRAG industry partners.

The Dynamics of Carbon Cycling in Coastal Waters: Dublin Bay

Daniel Kerr[1], Aleksander Glaz[1], Anthony Grey[1], Margaret McCaul[1], Dermot Diamond[1], Xavier Monteys[2], Brian Kelleher[1]

[1]Dublin City University [2]Geological Survey Ireland

Introduction

The ocean is the main driver of the global carbon cycle, and easily contains the most carbon in its sediments and waters; of the carbon contained within the atmosphere, terrestrial biosphere and ocean, approximately 93% is located within the seas (1).

The carbon system in seawater can be described by four interconnected parameters:

- Total alkalinity (A_T),
- Dissolved Inorganic Carbon (C_T),
- Fugacity CO_2 (fCO_2)
- pH.

The values of the above parameters, in conjunction with CO2SYS software, can be used to produce an accurate description of the carbon system.

Dissolved Inorganic Carbon (DIC)

Dissolved inorganic Carbon is the total of all inorganic carbon species within a seawater sample, and can be expressed by the following equation:

$$C_T = [CO_2^*] + [HCO_{3-}] + [CO_3^{2-}]$$

As it is analytically difficult to discern between $[CO_2]_{aq}$ and $[H_2CO_3]_{aq}$, the sum of these species is defined as $[CO_2^*]$.

DIC is calculated using the formula:

$$C_T = \frac{N_S - b.t - a}{c} \cdot \frac{1}{V_S.\rho}$$

Where:

N_S = Coulometer reading for the sample (counts)
b = Background level of system (counts.min^{-1})
t = Time required to measure sample (min)
a = Acid blank (counts)
c = Coulometer calibration factor (counts.µmol^{-1})
V_S = Volume of sample at temperature of use (dm^3)
ρ = Density of sample (kg.m^3)

Sample Acquisition

- Carbon samples were collected from 15 locations (A-O) encompassing Dublin bay over a two day period.
- All samples were collected and stored in accordance with the Guide to Best Practices for Ocean CO_2 Measurements (2).
- Samples were subsequently transported to the National Oceanographic Centre, Southampton, U.K, for analysis.

Analysis Methods

Analysis was carried out using the VINDTA system (Versatile INstrument for the Determination of Total dissolved inorganic carbon and Alkalinity).

- Sample was acidified with 10% H_3PO_4
- Liberated CO_2 was purged with ultrapure carrier gas, N_2
- CO_2 trapped in absorbent containing ethanolamine
- Hydroxyethylcarbamic acid formed was then subsequently coulometrically titrated.
- Carbon Certified Reference Materials (CRM) (3) were used to produce a calibration factor for analysis of coulometer results.

Results

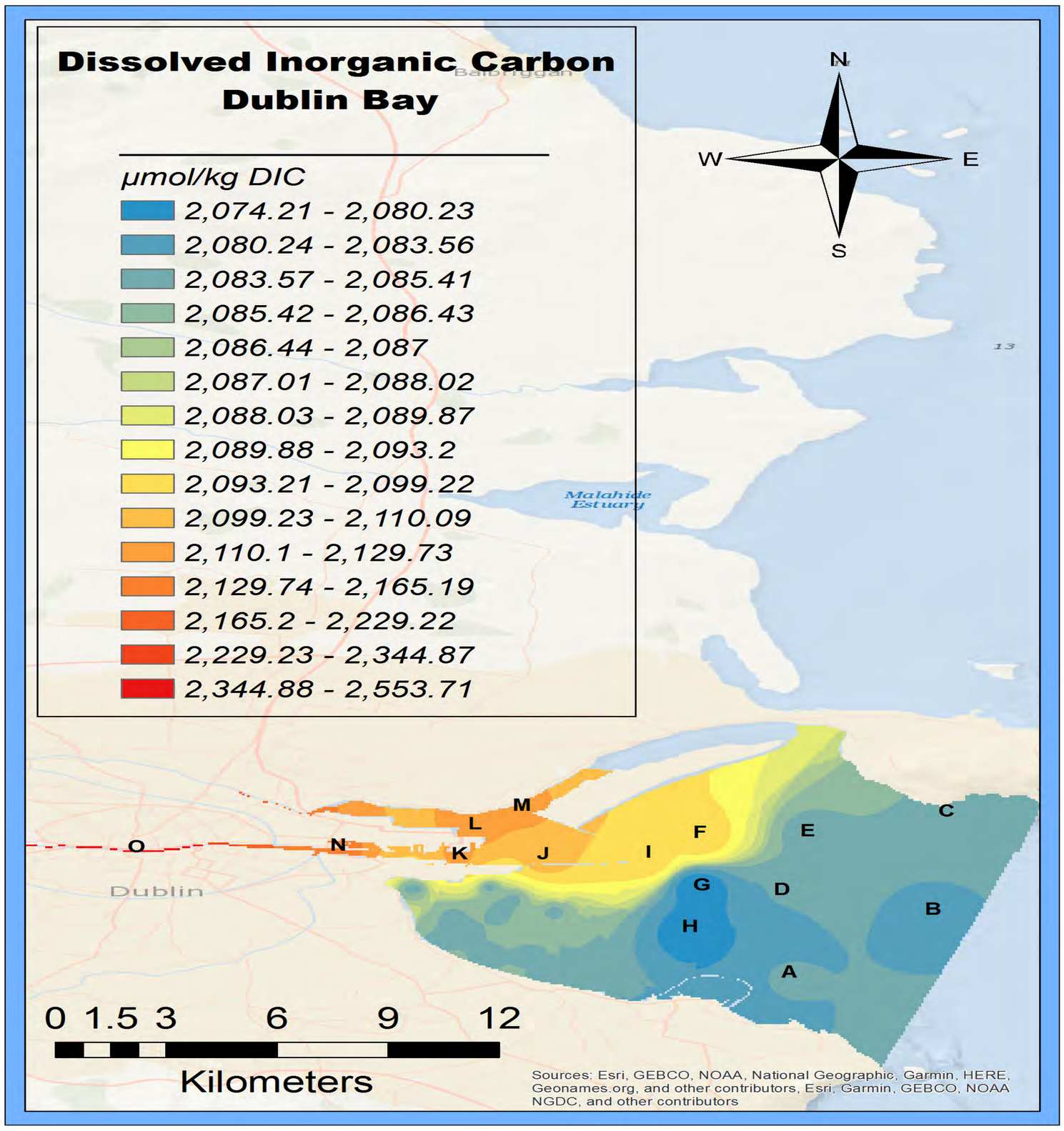

Figure 1: µmol.kg^{-1} DIC Sample Sites A to O. DIC output originating within the R. Liffey discharge area.

Discussion

- Trend of increasing µmol.kg^{-1} DIC values observed as sample sites became more river influenced.
- DIC values relatively constant within the bay and estuarial waters.
- Terrestrial carbonate weathering with subsequent DIC transport to ocean possible cause of observed increase within Liffey discharge area (4).
- Potential influence on bay carbon dynamics from Bull Island (5).

Next Steps

- **Continued sampling with the EPA**
- **Monthly sampling of two locations within Dublin Bay starting November 2019** – This will allow for the construction of temporal studies investigation carbon flux across seasonal cycles.
- **Transects of Dublin Bay –** Transects of Dublin Bay in order to obtain a suite of nutrient data will be used, along with EPA generated information, to compliment coastal carbon system dynamics investigations.
- **Role of CDOM in coastal carbon system -** Investigation into the role which CDOM plays in the coastal carbon cycle and its effects on the carbon system in coastal seawater.

Atlantic Ocean Climate Action Cruise

- Climate Linked Atlantic Sector Science (CLASS), Global Ocean Ship-based Hydrographic Investigations Program (GO-SHIP) and National Oceanography Centre (NOC) organised research cruise.
- RV James Cook will sail from Fort Lauderdale, USA, to Santa Cruz, Tenerife, Spain, along the 24° N in the Atlantic Ocean.
- Carbon system analysis will be conducted over a 42 day period.

References

(1) Feely, Sabine, & Wanninkhof, 2007, (2) Dickson, Sabine, & Christian, 2007, (3) Available from Dr. Andrew G. Dickson, Marine Physical Laboratory, Scripps Institution of Oceanography, University of California, San Diego (4) Hieronymus & Walin, 2013, (5) Cai, Wiebe, Wang, & Sheldon, 2000)

Contact Information

Daniel Kerr – Postgraduate Researcher
daniel.kerr7@mail.dcu.ie

This publication has emanated from research supported in part by a research grant from Science Foundation Ireland (SFI) under Grant Number 13/RC/2092 and co-funded under the European Regional Development Fund and by iCRAG industry partners.

iCRAG 2019

Resources for a Sustainable Future

SAFEGUARDING THE GEOMARINE ENVIRONMENT

Cold-Water Corals: Environmental Stressors and Sea Temperature Proxies

Erica Terese Krueger
Department of Geology, School of Natural Sciences, Trinity College Dublin, Dublin 2, Ireland

Background

- Cold-water corals are a key component of deep-sea ecosystems and are proxies for sea water temperature and environmental change.[1,2]
- Globally widespread, *Lophelia pertusa* is the most abundant cold-water coral and is found at depths ranging from 40 m to greater than 6000 m.[3,4]
- *L. pertusa* can tolerate a relatively wide range of temperature and salinity conditions and relies heavily on strong currents for food supply, sediment and waste removal.[4]
- These reef builders create biodiversity hot-spots, producing three-dimensional aragonitic structures that are used as habitat and shelter for fishes and invertebrates, and serve as an important carbon sink.[4,5]
- The comprehension of *L. pertusa* biology, ecology, and physiology is of utmost importance since they play such a vital ecological role in deep-sea environments.[3]

Image courtesy of Orejas et al., 2011. Long-term growth rates of four Mediterranean cold-water coral species maintained in aquaria. Mar Eco Prog Ser 429:57-65.

Broader Implications

- This research will aid in addressing pressing environmental challenges related to climate change and microplastic pollution.
- Negative consequences are predicted for cold-water corals if sub-optimal ocean conditions persist.
- If predictions are correct, increased ocean acidification will result in less carbon sequestration, decreased calcification rates, and a less robust skeleton, further resulting in a weaker defense against strong hydrodynamic currents.
- The impact of microplastics on cold-water corals is currently unknown.
- The demise of *L. pertusa* would be catastrophic to deep sea ecosystems, with a negative impact on marine biodiversity in general.
- A better understanding of how these oceanic parameters are affecting cold-water corals in terms of growth, structure, strength, and function is needed in order to determine how changes may influence these deep-sea ecosystem engineers in the future.

Research Objectives

- Developing novel geochemical proxies for seawater temperature
  - using multi-element statistics and clumped isotopes
- Determining the impact of microplastic ingestion on cold-water coral biomineralisation processes
  - in situ strength testing and electron backscatter diffraction fabric analysis

References

1. Chapron et al., 2018. Macro- and microplastics affect cold-water corals growth, feeding and behaviour. *Sci Rep,* 8**,** 15299.
2. Gaetani et al., 2011. Rayleigh-based multi-element coral thermometry: A biomineralization approach to developing climate proxies. *Geochim Cosmochim Ac*, 75, 1920-1932.
3. Gomez et al., 2018. Growth and feeding of deep-sea coral *Lophelia pertusa* from the California margin under simulated ocean acidification conditions. *PeerJ,* 6**,** e5671.
4. Mouchi et al., 2014. Potential seasonal calibration for palaeoenvironmental reconstruction using skeletal microstructures and strontium measurements from the cold-water coral *Lophelia pertusa*. *Journal of Quaternary Science,* 29**,** 803-814.
5. Mouchi et al., 2017. Multi-scale crystallographic ordering in the cold-water coral *Lophelia pertusa*. *Sci Rep,* 7**,** 8987.

Acknowledgements

- **Quentin Crowley,** Trinity Centre for the Environment; Trinity College Dublin
- **Andrew Wheeler,** School of Biological, Earth & Environmental Sciences; University College Cork
- **Elizabeth Tray,** Marine and Freshwater Research Centre; Galway-Mayo Institute of Technology
- **Paul F. Dennis,** Stable Isotope Laboratory; University of East Anglia
- **Furu Mienis,** NIOZ Royal Netherlands Institute for Sea Research

This publication has emanated from research supported in part by a research grant from Science Foundation Ireland (SFI) under Grant Number 13/RC/2092 and co-funded under the European Regional Development Fund and by iCRAG industry partners.

Ireland's European Structural and Investment Funds Programmes 2014-2020
Co-funded by the Irish Government and the European Union
European Union
European Regional Development Fund
Science Foundation Ireland sfi For what's next

Freshwater input magnitude and typology as a driver of Carbonate system variability in coastal seas

Maria Teresa Guerra*, Carlos Rocha

Biogeochemistry research group, School of Natural Science, Trinity College Dublin, College Green, Dublin 2, Ireland
*guerram@tcd.ie

Introduction: Contrasting study areas….why?

In recent years, there has been a growing awareness in the scientific community of the need to understand the drivers of carbonate chemistry on coastal seas. Land-ocean interaction could be of significant importance in predicting the future of aquaculture (**1**). Biogeochemical processes in coastal areas, i.e. the balance of photosynthesis, respiration, calcification, and CaCO3 dissolution can be different to those in the open ocean. Predicted pH values for the open ocean could be significantly different to those in coastal areas influenced by freshwater discharge, because the freshwater input, in the form of rivers and subterranean estuaries, are generally characterized by low pH values. Furthermore, several studies on subterranean estuaries underlined the importance of submarine groundwater discharge as a source of carbonate in the form of TA and DIC (**2,3,4,5**).

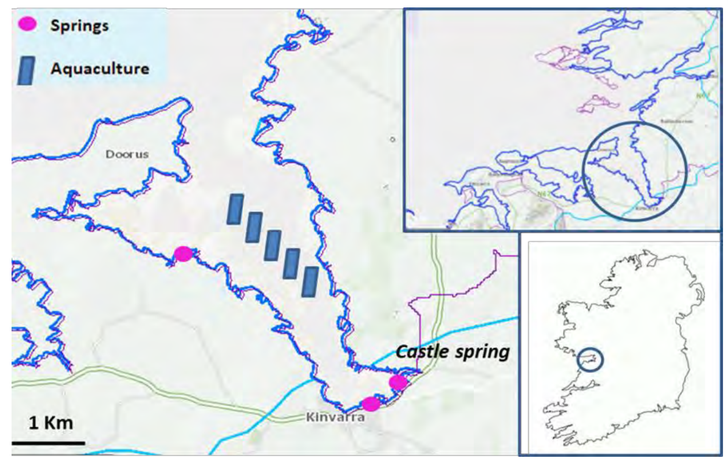

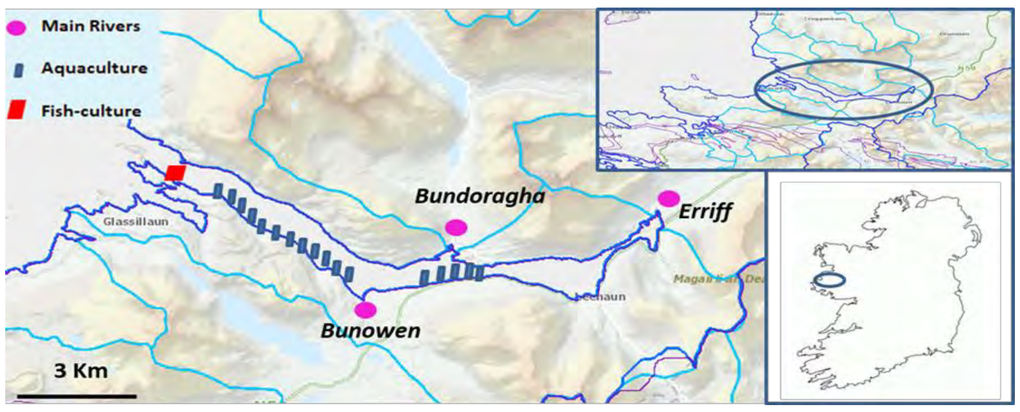

The aim of this study is to understand the effects of contrasting watershed inputs on coastal carbonate chemistry and ecosystem metabolism. Study sites are: Kinvara bay, underlain by limestone and fed from a karstic catchment where freshwater inputs are dominated by submarine groundwater discharge (SGD); and Killary harbour, characterized by shale, sandstone and conglomerates where freshwater input is via surface runoff in the form of rivers and several periodic streams. The two sources are characterised by contrasting TA compositions (high and low, respectively), but both have low pH.

Methodology

o Sampling strategies

The two areas were surveyed by seasonal sampling, with an aim to understand changes in carbonate system variability in response to freshwater magnitude. Spatial variations were addressed with sampling transects, from bay head to bay mouth with 6 sampling sites, plus a marine End Member (EM) sample and freshwater EM samples, in order to understand how the freshwater input affects the biogeochemistry on a long term time-scale.

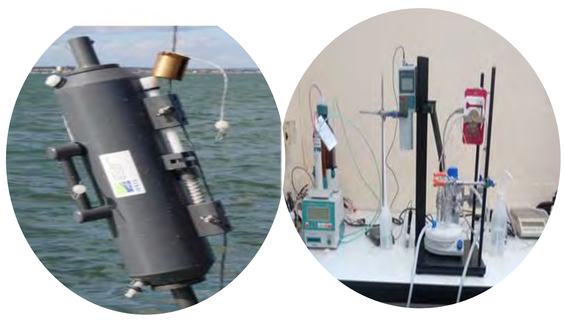

o Analysis

Three of the four parameters of the carbonate system, total alkalinity (TA), dissolved inorganic carbon (DIC) and pH, are analysed using open and close cell titration, following Dickson's(6) method and with his certified reference materials. A multi-parametric probe, the Aquaread Aquaprobe, is used to measure pH, temperature, salinity, and electrical conductivity at each station.

Results

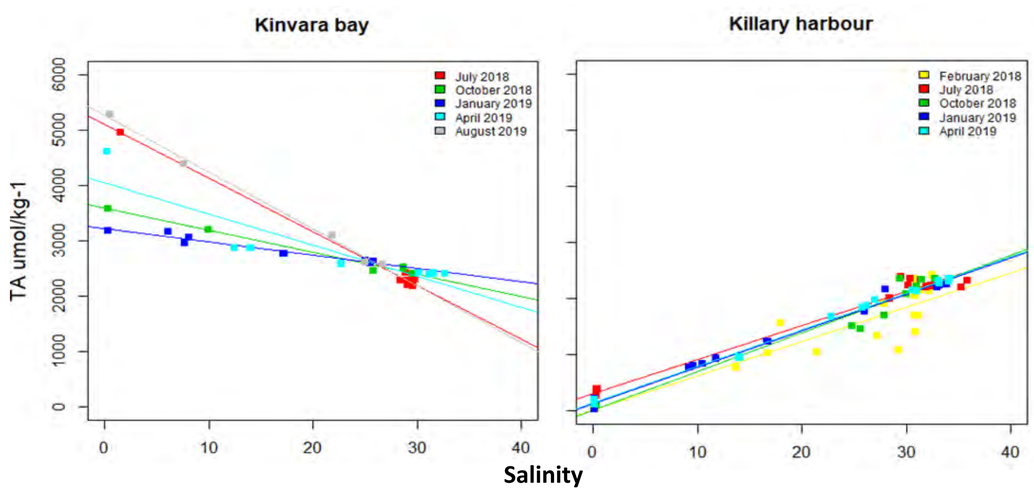

Spatial variability over the year was compared in the two selected study areas. The freshwater EMs are characterized by contrasting carbonate composition; therefore carbonate delivery to the coast varies in response to local geological features.

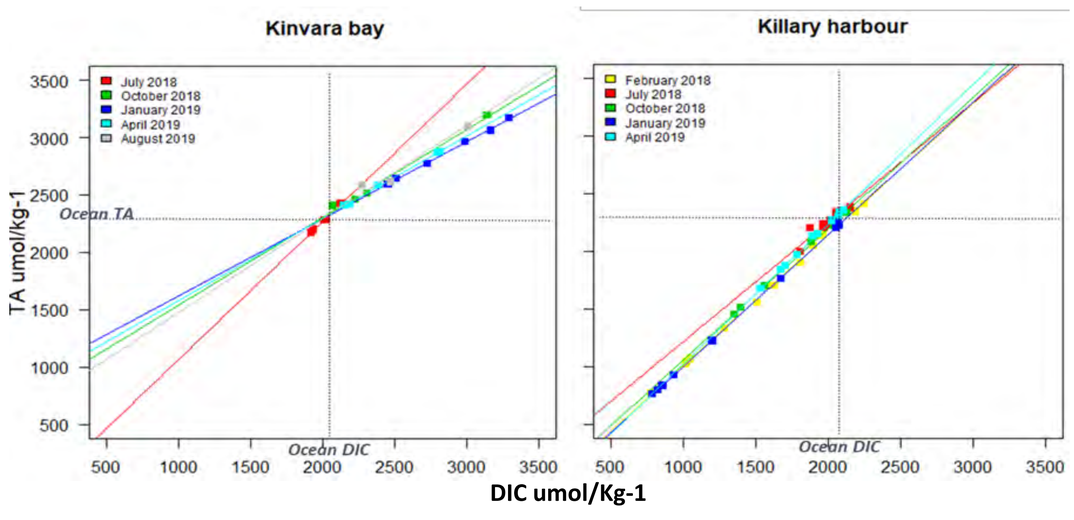

From TA and DIC plots, the TA:DIC relationship and slopes in the two selected study sites can be seen. Net community production (NCP) is calculated as relative percentage using the slope values obtained from TA and DIC measurements.

Conclusions

It is clear that freshwater input magnitude and composition act as important drivers of carbonate systems in coastal areas. In Killary Harbour, river TA is low, and the open ocean is the primary source of TA. Conversely, the primary source of TA in Kinvara bay is freshwater input from land, since the subterrenean estuaries in karstic areas are huge sources of TA. NCP scales with freshwater discharge in Kinvara, suggesting the freshwater magnitude is the main driver of autotrophic or heterotrophic conditions in the system. Freshwater magnitude and typology are determined to be important drivers of carbonate system metabolism, hence it will be possible to manage coastal seas, in relation to climate change predictions.

Bivalve aquaculture in Killary

References

(1) McGrath, T., McGovern, E., Gregory, C., & Cave, R. R. (2019). Local drivers of the seasonal carbonate cycle across four contrasting coastal systems. Regional Studies in Marine Science, 30, 100733. https://doi.org/10.1016/j.rsma.2019.100733
(2) De Weys, J., Santos, I. R., & Eyre, B. D. (2011). Linking groundwater discharge to severe estuarine acidification during a flood in a modified wetland. Environmental Science and Technology, 45(8), 3310–3316. https://doi.org/10.1021/es104071
(3) Santos, I. R., Bryan, K. R., Pilditch, C. A., & Tait, D. R. (2014). Influence of porewater exchange on nutrient dynamics in two New Zealand estuarine intertidal flats. Marine Chemistry, 167, 57–70. https://doi.org/10.1016/j.marchem.2014.04.006
(4) Cyronak, T., Santos, I. R., Erler, D. V., & Eyre, B. D. (2013). Groundwater and porewater as major sources of alkalinity to a fringing coral reef lagoon (Muri Lagoon, Cook Islands). Biogeosciences, 10(4), 2467–2480. https://doi.org/10.5194/bg-10-2467-2013
(5) McMahon, A., Santos, I. R., Cyronak, T., & Eyre, B. D. (2013). Hysteresis between coral reef calcification and the seawater aragonite saturation state. Geophysical Research Letters, 40(17), 4675–4679. https://doi.org/10.1002/grl.50802
(6) Dickson, a. G., & Goyet, C. (1994). Handbook of methods for the analysis of the various parameters of the carbon dioxide system in sea water. https://doi.org/10.2172/10107773

This publication has emanated from research supported in part by a research grant from Science Foundation Ireland (SFI) under Grant Number 13/RC/2092 and co-funded under the European Regional Development Fund and by PIPCO RSG and its member companies..

Ireland's European Structural and Investment Funds Programmes 2014-2020
Co-funded by the Irish Government and the European Union
European Union
European Regional Development Fund
Science Foundation Ireland sfi For what's next
PIP Petroleum Infrastructure Programme

Challenging the assumption of stability: *Assessing modes and variability of the AMOC during past warm climates*

Assessing the stability of the AMOC during past warm climates
Megan Murphy O' Connor & Audrey Morley
e-mail: megan.murphy-oconnor@icrag-centre.org

Motivation

The Atlantic Meridional Overturning Circulation (AMOC) plays a critical role in the climate system as it redistributes heat and energy around the globe[1]. Ireland is particularly sensitive to AMOC changes as it is situated along the path of the North Atlantic Current (fig.1). As a result of our short observational records however, the mechanisms controlling the strength of this circulation, and how it will respond to climate change are poorly understood[2]. Previously large disruptions of the AMOC were believed to be restricted to glacial boundary conditions[3]. However, recent observations and models show that we have over-estimated its stability during warm climates, with evidence that abrupt shifts of the AMOC have occurred during interglacial periods[4]. Here we propose to use climate proxies to investigate the response of the AMOC during warm climates under a range of different boundary conditions.

Figure 1: Simplified schematic of the AMOC.

Aims

1. **To identify triggers and thresholds that cause abrupt oceanographic changes under different boundary conditions.**
2. **To improve our understanding of the mechanisms linking the AMOC to climate.**

Planned work programme: A Multi-proxy Approach

o **Multi-proxy analysis of samples from high-resolution deep-sea sediment cores from the Feni Drift, Rockall Trough (fig.2) to determine the structure and response of the surface and deep branch of the AMOC during the selected past interglacial periods; MIS 1 (Holocene Thermal Maximum), MIS 5e, MIS 11 and MIS 19. These interglacials were characterised by distinct boundary conditions (greenhouse gas concentrations, orbital insolation, global temperatures etc.), but are all thought to be analogues for either pre-industrial conditions, or the climate of the natural near-future[5].**

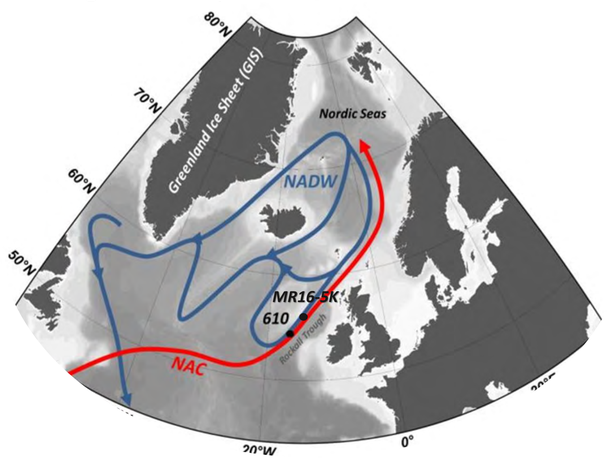

Figure 2: Core site DSDP 610 and MR16-5K.

1. Surface reconstruction

- Paired $\delta^{18}O$ and Mg/Ca measurements from planktic foraminifera (fig.3) will be used to determine surface temperature and salinity changes during our climate change intervals[6].
- Ice-drafted debris (IRD) counts per gram of sediment will also be used to constrain ice sheet variability during times of abrupt climate change.

2. Deep-flow reconstruction

- Grain size distributions of samples will be used to assess deep-water paleocurrent flow strength. End-Member Analysis (EMA) of the distributions will divide them into meaningful subpopulations depending on unique transport mechanisms and sources[7].
- The Nd isotope proxy ε_{Nd}, the ratio of $^{143}Nd/^{144}Nd$, will be used as a water mass tracer to establish the source of bottom-water for the AMOC deep return flow[8,9].
- Stable isotope analysis of benthic foraminifera ($\delta^{13}C$) (fig.4) will also be used to constrain deep water ventilation.

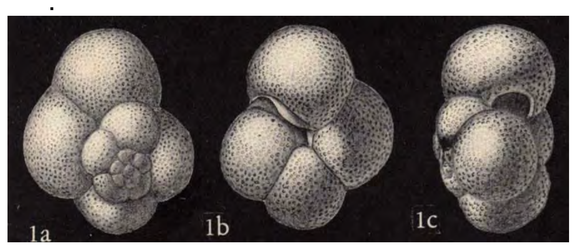

Figure 3,4 (top, bottom): Planktic, Benthic Foraminifera.

Progress To Date

- o Cores from DSDP 610B were XRF scanned at the MARUM IODP Bremen Core Repository to identify specific intervals for sampling (fig.5).
- o Samples from MIS 5e and MIS 19 were collected at 0.5 cm intervals to allow high resolution reconstructions of the AMOC during these periods (fig.5).
- o The samples collected from MARUM, along with suitable previously collected samples, were washed and prepared for analysis (fig.5).
- o Nd isotope analysis of 107 samples from the selected isotope stages is currently underway at Géosciences Université Paris-Sud (fig.5).

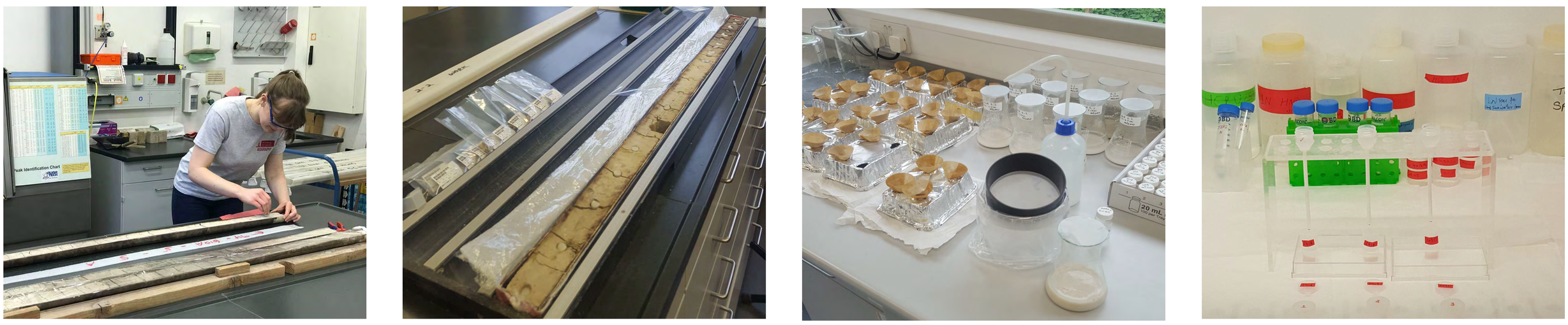

Figure 5 (left to right): Cores being prepared for XRF scanning at MARUM, sampling of cores, preparation of sediment for analysis, Nd isotope elution.

References

1. Sévellec, F. & Fedorov, A. (2016). 2. Zickfeld, K., Levermann, A., Morgan, M. G., Kuhlbrodt, T., Rahmstorf, S. & Keith, D. W. (2007). 3. McManus, J. F., Oppo, D. W. & Cullen, J. L. (1999). 4. Kleiven, H. F., Jansen, E., Curry, W. B., Hodell, D. A., & Venz, K. (2003). 5. Yin & Berger (2015). 6. Elderfield & Ganssen (2000). 7. Prins, M. A., Bouwer, L. M., Beets, C. J., Troelstra, S.R., Weltje, G.J., Kruk, R.W., Kuijpers, A. & Vroon, P. Z. (2002). 8. Lippold, J., Gutjahr, M., Blaser, P., Christner, E., de Carvalho Ferreira, M. L., Mulitza, S., Christl, M., Wombacher, F., Böhmb, E., Antz , B., Cartapanis , O., Vogel, H. & Jaccard, S. L. (2016). 9. Elmore, A. C., Piotrowski, A. M., Wright, J. D. & Scrivner, A. E. (2011). Figure 1: Srokosz, M., Baringer. M., Bryden, H., Cunningham, S., Delworth, T., Lozier, S., Marotzke, J. & Sutton, R. (2012). Figure 4: http://www.mikrotax.org/pforams/index.php?id=104177. Figure 5.: Gottschalk, J., N. Vázquez Riveiros, C. Waelbroeck, L.C. Skinner, E. Michel, J.-C. Duplessy, D. Hodell, and A. Mackensen (2016).

This publication has emanated from research supported in part by a research grant from Science Foundation Ireland (SFI) under Grant Number 13/RC/2092 and co-funded under the European Regional Development Fund.

Scan me

Synergies between the Sentinel Satellites and the use of Bio-optical and Flow cytometric measurements for tracing surface slicks along the Irish Western Shelf

Mullins, M.[1] and Croot. P.L[1]

1. *Earth and Ocean Sciences, School of Natural Sciences, National University of Ireland Galway*

Corresponding author: monica.mullins@icrag-centre.org

INTRODUCTION

- A challenge facing industry is the ability to distinguish maritime accidents from naturally occurring phenomena such as phytoplankton blooms and natural oil seeps [1].
- This project aims to link detection and monitoring of these natural and manmade surface slicks with satellite observations. Launch of the sentinel series of satellites provides opportunities for the fusion of *in situ* sampling with remote sensing. Products such as SAR roughness *(Sentinel 1) and* Ocean Colour *(Sentinel 3)* will be used.
- Sampling has been carried out across the western Irish coastal shelf on the *Celtic Explorer* last June (CE18009) and July (CE18010).

METHODS

- Conductivity Temperature and Depth (CTD) measurements are taken at sea *(Image 1).*
- Flow cytometry *(Image 2)* and microscopic enumeration methods are used to identify pico/nano and phytoplankton species. This includes identification of Harmful Algal Bloom species (HAB's).
- For chlorophyll concentrations, seawater was filtered through 25 mm GF/F filter. The filters were frozen and analysed back on land.
- Baseline optical measurements of CDOM, FDOM and nutrients will be taken from surface waters. Absorption is obtained using Ocean Optics Spectrometers *(Image 3).*
- Studies on the optical characteristics of CDOM formed from actively growing cultures of phytoplankton species such as *Emiliana huxleyi. (Image 4)*.

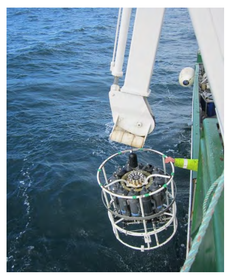

Image 1: Collecting seawater samples

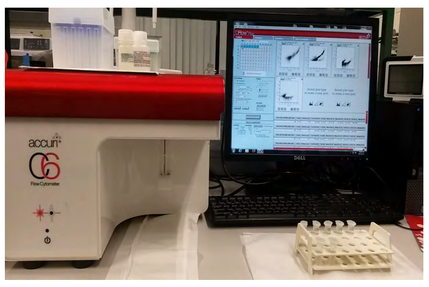

Image 2: Phytoplankton abundance via BD Biosciences Accuri C6 Flow Cytometer

Image 3 : Running CDOM samples on spectrometer

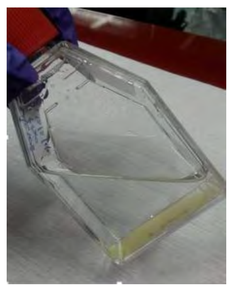

Image 4: Culturing Coccolithophores

PRELIMINARY RESULTS & DISCUSSION

Satellite observations:

- The warm dry summer experienced during *WESPAS 2018* provided an unprecedented number of clear sky days for obtaining good satellite images of the ocean colour distribution over the North West European shelf. *[5]*

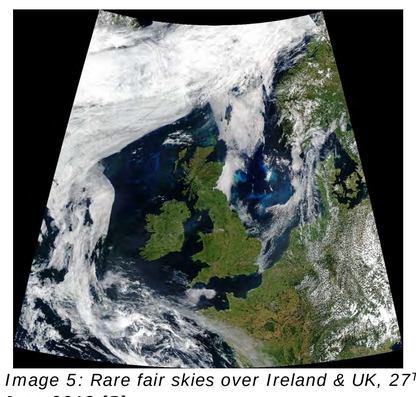

Image 5: Rare fair skies over Ireland & UK, 27TH June 2018 [5]

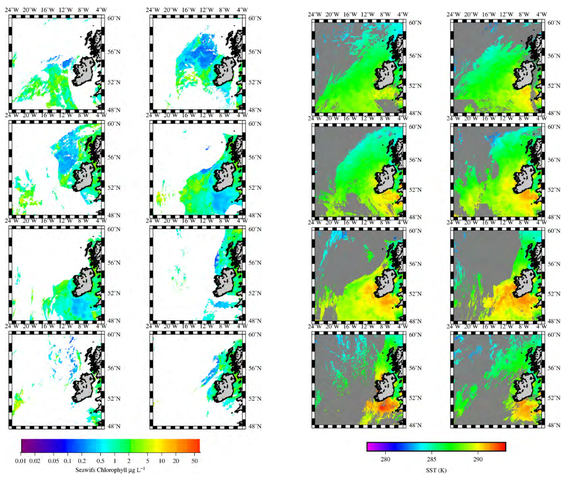

- The ocean colour images showed high chlorophyll levels along the shelf edge and porcupine mound with lower concentrations in the Celtic Sea. Below, an overview of the conditions during WESPAS, the satellite OC5Cl chlorophyll and SST from June 25 to July 2 (runs left to right, top to bottom). *[4]*

Bacteria, Pico and nanoplankton abundance:

- Unfiltered seawater samples collected directly from the CTD were run on an Accuri C6 flow cytometer while at sea according to (*Marie etal.,1997; Marie et al., 2014*) *[6]* Another sample is fixed with glutaraldehyde and then treated with the DNA Stain Syber Green to enumerate marine bacteria.
- Populations were determined using C6 software. *Synechoccus (P1), Picoeukaryotes (P2)* and *Nanoeukaryotes (P3).(As seen in Graph A03).* Bacterial cells were grouped along the curve. (*As seen in A05).*
- *Population counts were merged with CTD bottle data to create distribution maps in Ocean Data View.*

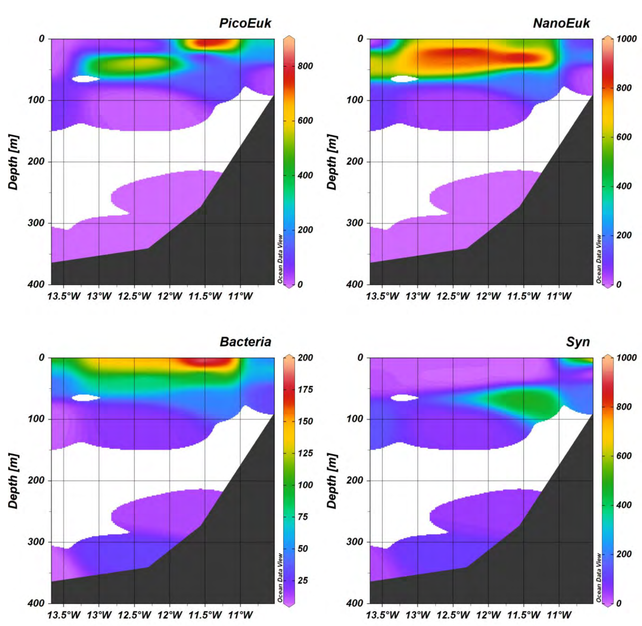

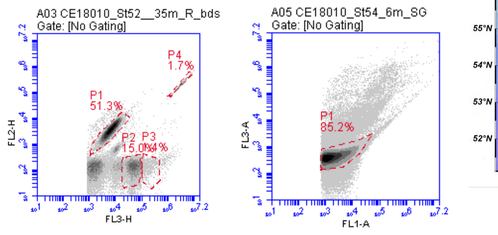

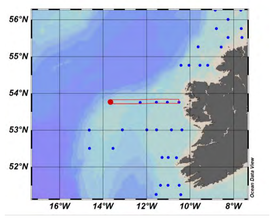

Sample area highlighted on the map in red. The numbers of Synechococcus (Syn), picoeukaryotes (PicoEuk), nanoeukaryotes (NanoEuk), and bacteria are shown in cellµL-1. In order to represent the bacterial populations they have been divided by 10^3.

For this transect (Syn) reached its peak abundance near shore and 35m depth and decreased towards open ocean. (PicoEuk), (NanoEuk), and bacterial populations reached their peaks at Station 53 increasing as they moved further from the coast and decreased again as they moved towards the shelf.

PRELIMINARY RESULTS & DISCUSSION

Chlorophyll concentration (5-6 m):

- The frozen filters were analysed in the laboratory for chlorophyll a (b & c) concentrations after extraction with 90% acetone using a Telfon grinder and subsequent measurement of the solution absorbance using an Ocean Optics Flame spectrophotometer with a low volume 10 cm pathlength cell and DT-mini light source. The concentration of chlorophyll a was calculated using the trichromatic equation of Jeffrey and Humphrey (1975). [2]
- Below: Near surface mixed layer chlorophyll measurements during *WESPAS*.

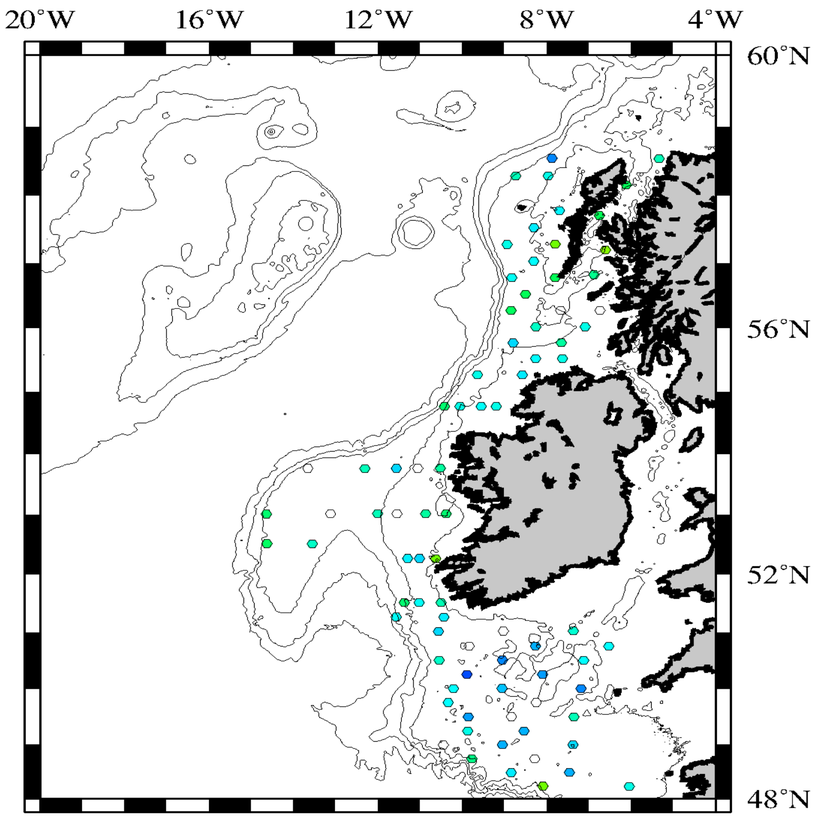

CDOM (5m - 424m):

- CDOM was collected from just below the surface waters, at regular intervals throughout the water column and just above the bottom. The first graph on the left represents the distribution of CDOM throughout the water column for Station 39, CE18009. This second graph to the left shows how CDOM concentration in surface waters decreases with distance from land in this transect. Stations marked in the map are corresponding to the graphs below.

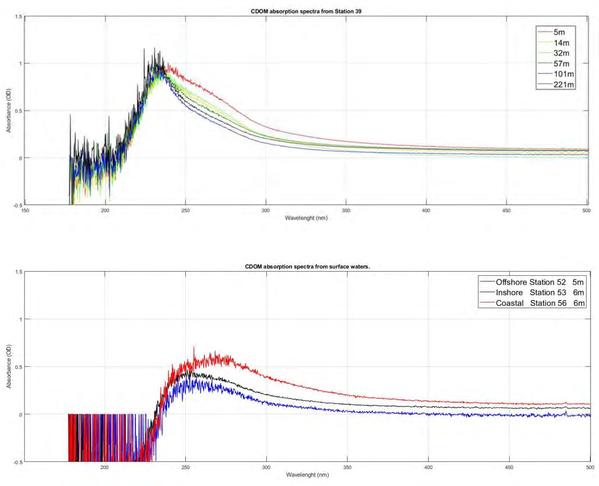

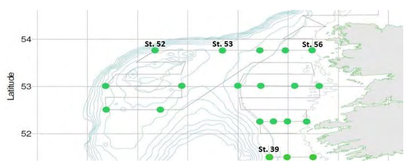

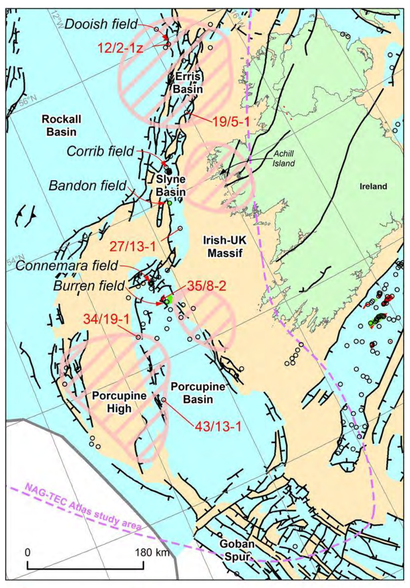

Above: Detailed map of the Irish Atlantic Margin, showing regional structural basins (Funck et al. 2014), and the areas where oil slicks have been observed (oil-slick data provided by CGG: GOSD 2014). [3]

FUTURE WORK

- Baseline studies of CDOM from phytoplankton and other natural sources along the west coast of Ireland.
- Concentrated sampling where oil slicks have been observed.[3]
- Satellite along with airborne hyperspectral observations of surface slicks along the Irish coast.
- Development of a Spectral library via 3D EEM fluorescence.

ACKNOWLEDGEMENTS

The authors would like to thank the staff of the Marine Institute's Fisheries Ecosystems Advisory Services for the opportunity to participate in *WESPAS 2018.* The Captain and crew of the *RV Celtic Explorer . The Chief scientists Ciaran O'Donnell and Michael O' Malley. Fellow scientists;* Catherine Jordan, Mark Dwyer, Kevin McGookin and John Phelan.

Tim McCarthy, Conor Cahalane, Daire Walsh and Aidan McGee at the National Centre for Geocomputation, Social Sciences Institute, National University of Maynooth, Ireland.

This work forms part of the Marine Geosciences spoke project 2.3 of iCRAG.

This publication has emanated from research supported in part by a research grant from Science Foundation Ireland (SFI) under Grant Number 13/RC/2092 and co-funded under the European Regional Development Fund and by PIPCO RSG and its member companies..

Ireland's European Structural and Investment Funds Programmes 2014-2020
Co-funded by the Irish Government and the European Union

European Union
European Regional Development Fund

Science Foundation Ireland sfi For what's next

PIP Petroleum Infrastructure Programme

REFERENCES

[1] Topouzelis, K., Karathanassi, V., Pavlakis, P. and Rokos, D. (2007). Detection and discrimination between oil spills and look– alike phenomena through neural networks. ISPRS Journal of Photogrammetry and Remote Sensing. Elsevier Volume 62, Issue 4, Pages 264 – 270

[2] S. W. JEFFREY and G. F. HUMPHREY, New Spectrophotometric Equations for determinations chlorophyll a, b, c1 and c2 in Higher Plants, Algae and Natural Phytoplankton. Biocbem. Pbysiol. Pflanzen (BPP), Bd. 167, S. 191-194 (1975)

[3] Geert-Jan Vis Geological Society, London, Special Publications 2017;447:443-455

[4] Data from Copernicus, the European Unions Earth Observation and Monitoring Programme

[5] NASA Earth Observatory images by Joshua Stevens, using VIIRS and MODIS data.

[6] Marie, D., Partensky, F., Jacquet, S. and Vaulot, D., 1997. Enumeration and Cell Cycle Analysis of Natural Populations of Marine Picoplankton by Flow Cytometry Using the Nucleic Acid Stain SYBR Green I. Applied and Environmental Microbiology. Marie, D., Rigaut-Jalabert, F. and Vaulot, D., 2014. An improved protocol for flow cytometry analysis of phytoplankton cultures and natural samples. Cytometry Part A, 85(11): 962-968.

iCRAG 2019

Resources for a Sustainable Future

ENERGY SECURITY

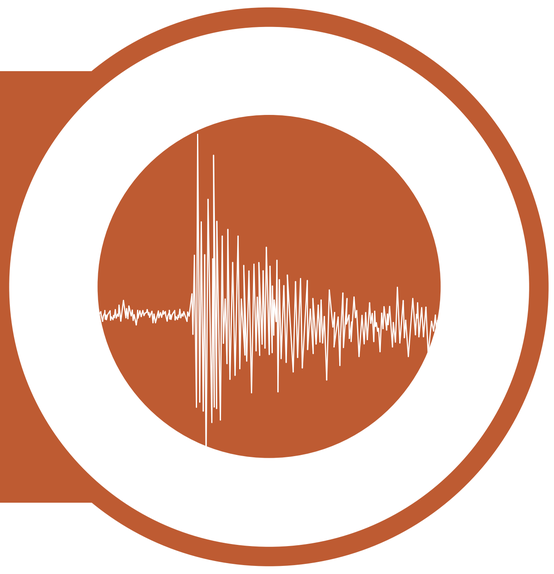

Apatite fission track analysis by laser ablation: A novel fast grain mapping approach using the map interrogation tool Monocle

C. Ansberque, D. Chew, K. Drost

Department of Geology, Museum Building, Trinity College Dublin, College Green, Dublin 2, Ireland
corresponding author: ansberqc@tcd.ie

1 LASER SPOT ANALYSIS ISSUES

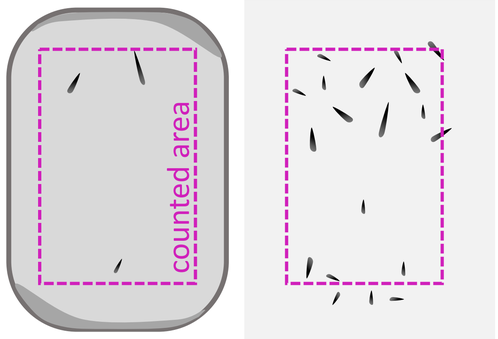

External Detector Method

- identical areas counted on apatite and mirror image in mica
- zonation and/or inclusion detected
- Spatial and depth-weighted U-heterogeneity taken into account or avoided (i.e. inclusions)

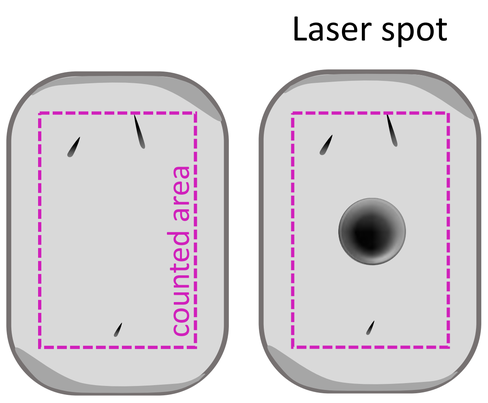

Laser spot analysis

- spot area ≠ counted area
- Hence U heterogeneity may not be accounted for
- U/Ca from spot may not be representative of that of the entire counted area

MAIN APPLICATION: Potential U-zoning cannot be detected by the spontaneous track density in young and/or low U apatites

2 MAPPING APPROACH

- Apatites are mounted in epoxy resin, ground, polished and etched to reveal spontaneous fission tracks. Fission tracks are counted under an Axio imager.Z1m (Zeiss) using TrackWorks (Autoscan).
- A Photon Machines Analyte Excite 193 nm ArF Excimer LA system coupled to an Agilent 7900 Q-ICPMS has been used to map the grains.
- Data are reduced in Iolite 2.5[1] using the Trace_Element_FTD and VisualAgeUcomPbine DRSs. Elemental regions of interest (i.e. counted areas) are drawn in Monocle[2]. Mean value of elements and ratios over the ROI are summarised in an exportable table from Monocle.

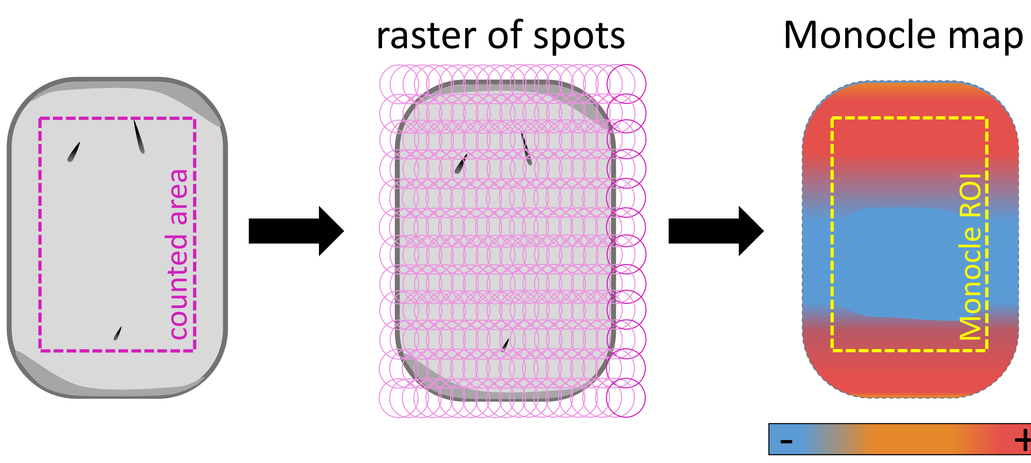

LA-Q-ICPMS settings:	
fluence	2.56 J.cm^{-2}
repetition rate	53 Hz
energy set point	2.7 mJ
scan speed	25 µm.s^{-1}
background	7 s
sampling mode	raster employing a 18 µm circle
raster depth	2 µm
isotopes analysed	^{43}Ca, ^{55}Mn, ^{88}Sr, ^{139}La, ^{140}Ce, ^{147}Sm, ^{153}Eu, ^{157}Gd, ^{175}Lu, $^{206, 207, 208}$Pb, ^{232}Th, ^{238}U
standards	NIST612, Durango (AFT), Madagascar (U-Pb)
apatite (used as unknowns)	McClure Mt (U-Pb); Durango, Fish Canyon Tuff, Paros, Sutlej (India) and Astor (Pakistan) valleys (AFT)

3 PRELIMINARY RESULTS

Durango (U-homogeneous; accepted age 31.4 ± 0.5 Ma[3])

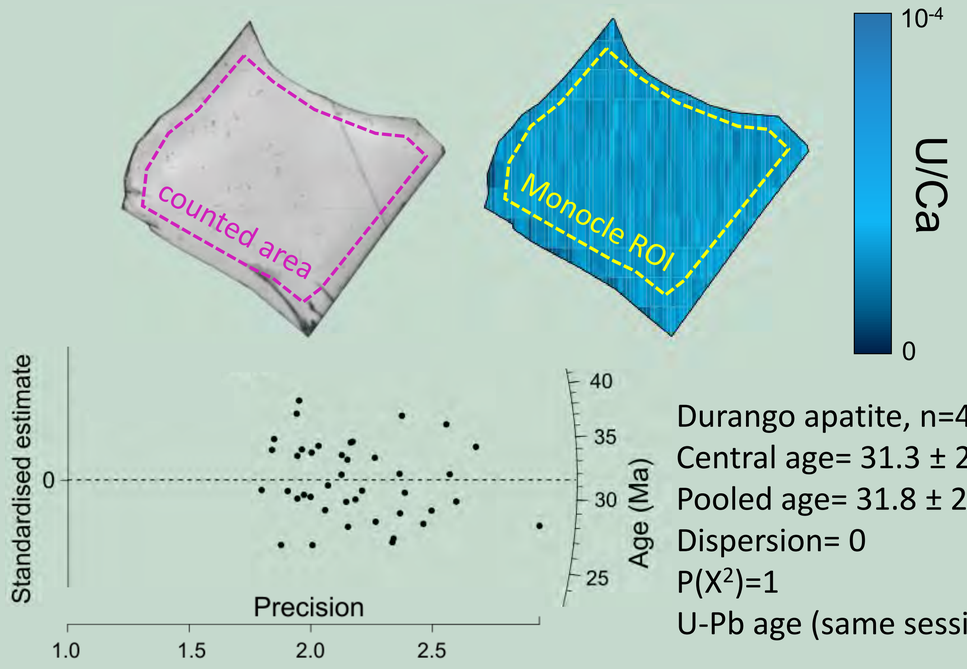

Durango apatite, n=41 shards
Central age= 31.3 ± 2 Ma
Pooled age= 31.8 ± 2 Ma
Dispersion= 0
P(X^2)=1
U-Pb age (same session) = 30.3 ± 1.7 Ma

Fish Canyon Tuff (U-heterogeneous; accepted age 27.8 ± 0.5 Ma[3])

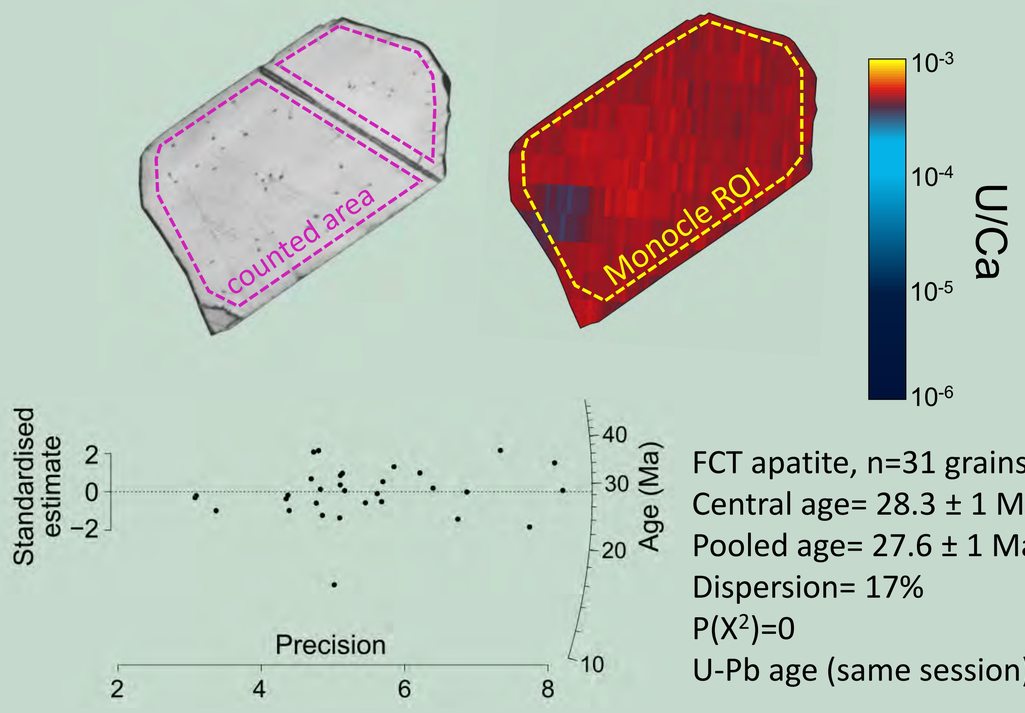

FCT apatite, n=31 grains
Central age= 28.3 ± 1 Ma
Pooled age= 27.6 ± 1 Ma
Dispersion= 17%
P(X^2)=0
U-Pb age (same session)= 30.9 ± 2.4 Ma

Paros (U-heterogeneous; accepted age 12.7 ± 2.8 – 10.5 ± 2.0 Ma[4])

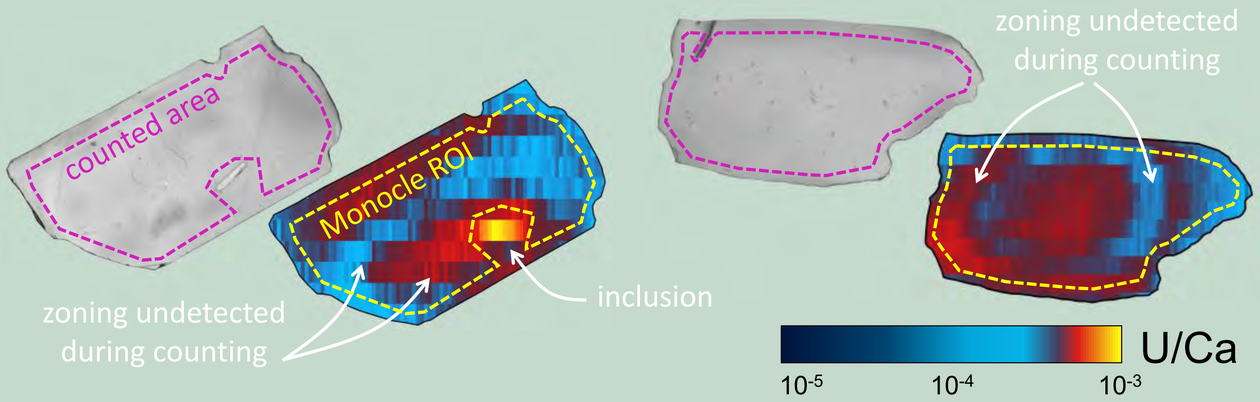

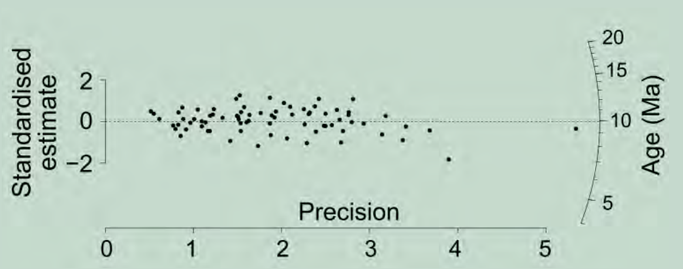

FCT apatite, n=76 grains
Central age= 9.9 ± 0.5 Ma
Pooled age= 10.4 ± 0.6 Ma
Dispersion= 0%
P(X^2)=1
U-Pb age (same session)= 12.0 ± 2.2 Ma

4 ADVANTAGES

- Irradiation free (!) and remove potential mismatches between FT-counted area and laser spot
- Method takes into account intra single-grain U-variation for a better representation of grain's heterogeneity, ideally suited for young and/or low U apatites
- Elemental region of interests can be easily defined using Monocle (i.e. to avoid inclusions, etc…)
- Combine multiple dating (AFT and U-Pb), and trace + REE analysis for provenance studies

[1] Paton, C. et al., (2011). *J. Anal. At. spectrum., v.26, p. 2508-2518*
[2] Petrus, J. et al., (2017). *Chemical Geology, v.463, p. 76-93*
[3] Hurford, A. J. (2018). *Fission-Track Thermochronology and its Application to Geology, chapitre 1, p. 3-23*
[4] Brichau, S. et al., (2006). *Earth and Planetary Science Letters, v. 241, p. 293-306*

Distribution and composition of a multi-layered salt-prone stratigraphy and its influence on rift basin development; The Slyne and Erris basins, offshore NW Ireland

Conor M. O'Sullivan [1, 2], Conrad J. Childs [1, 2], Muhammad M. Saqab [1, 2*], John J. Walsh [1, 2], Patrick M. Shannon [1]

[1] Irish Centre for Research in Applied Geoscience (iCRAG), University College Dublin, Belfield, Dublin 4, Ireland; [2] Fault Analysis Group, School of Earth Sciences, University College Dublin, Belfield, Dublin 4, Ireland; [*] Present Address: Norwegian Geotechnical Institute, 40 St. Georges Terrace, Perth, WA 6000, Australia.

Corresponding author email: **conor.osullivan@icrag-centre.org**

Rationale:

- Salt is proven throughout the Slyne and Erris basins and plays a crucial role in the petroleum system of these basins, acting both as an excellent sealing lithology and driver in the formation of hydrocarbon-bearing structural traps (e.g. Corrib gas field).
- To date very little work has been done to understand the controls on salt distribution both in these basins and across the greater Irish Atlantic margin.
- Salt will likely play a significant part in future gas discoveries in the greater Corrib area and understanding the timing and style of salt movement will be crucial to exploration success.
- The Slyne and Erris basins have the most numerous and data-rich well penetrations of both Permian and Triassic salt offshore Ireland.
- Salt bodies represent one of the best storage methods for sequestered CO_2 and understanding their composition and distribution aids in determining their suitability for future CC&S initiatives.

The Slyne and Erris Basins

- A pair of contiguous rift basins off the north-western coast of Ireland.
- Formed through a multiphase evolution involving Permian, Early Jurassic and Late Jurassic rifting, with periods of uplift during the end Middle Jurassic, Early Cretaceous and Cenozoic.
- Two layers of salt a present in these basins:
  - Upper Permian Zechstein Group
  - Upper Triassic Uilleann Halite Member (Currach Formation)
- The Zechstein Group is thickest and most salt-prone in the Slyne Basin and southern Erris Basin, with the salt content decreasing in the northern Erris Basin. This distribution is likely controlled by faults which were active during the Late Permian, such as the basin-bounding fault in the central and southern Slyne Basin, and the large faults to the east of Corrib.
- The Uilleann Halite is restricted to the northern Slyne and southern Erris basins, and represents a marine influence in that area during the Late Triassic, possibly sourced from the Rockall Basin to the northwest.

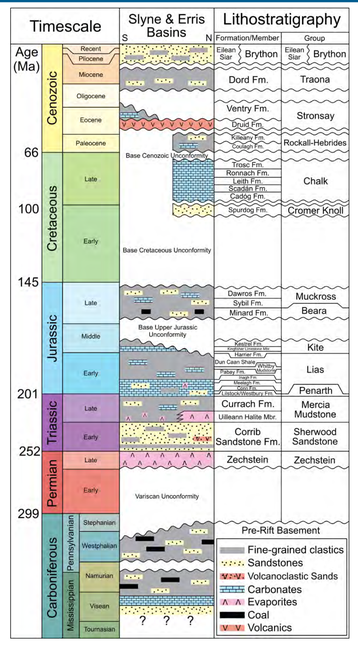

Figure 1: Slyne & Erris chronostratigraphic chart.

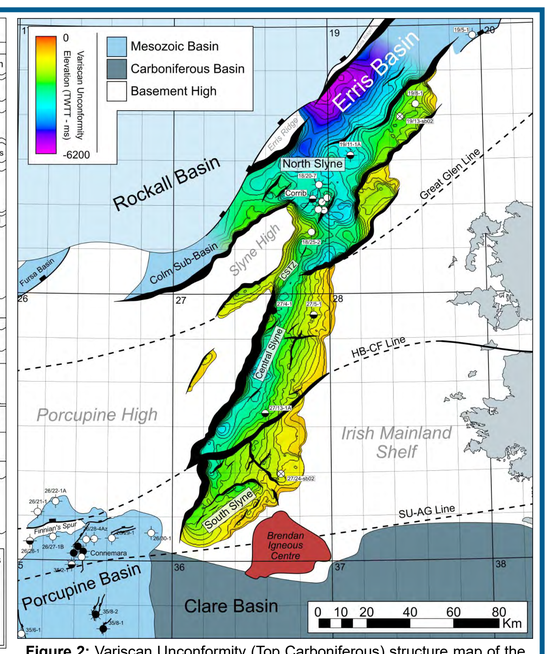

Figure 2: Variscan Unconformity (Top Carboniferous) structure map of the Slyne and southern Erris Basin

Salt composition:

- The Zechstein Group in the Slyne and southern Erris basin is composed of relatively clean salt (mostly halite and anhydrite) with minor interbedded mudstone and carbonate stringers.
- The Uilleann Halite Member composed of halite, with the proportion of halite increasing towards the base of the Upper Triassic section. This halite is interbedded with several mudstone stringers. When the member is not developed, the Currach Formation typically has infrequent metre to sub-metre stringers of halite and anhydrite at the base of the section.

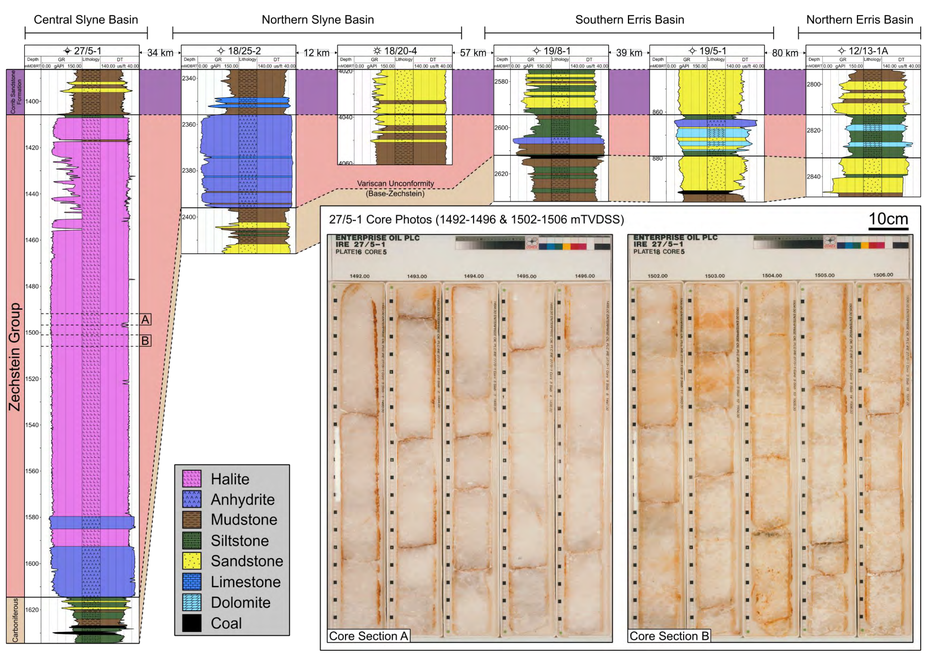

Figure 3: Lithological well correlation of the Zechstein Group through the Slyne and Erris basins. The Zechstein Group is more salt-prone in the Slyne Basin and southern Erris Basin, with the salt content decreasing in the northern Erris Basin (e.g. well 12/13-1A). The Zechstein Group in the southern Erris Basin appears more salt-prone on seismic sections (undrilled at present), with salt content decreasing towards the low-strain basin margins (e.g. wells 19/5-1 and 19/8-1).

Timing of salt movement:

- Salt movement is recorded during pre-rift, syn-rift and post-rift stages of basin development. These include:
  - Lower Jurassic growth sequences observed in a withdrawal syncline around Corrib (not shown).
  - Erosion of salt-cored structural highs at the Base-Upper Jurassic Unconformity (Figure 5).
  - Onlap on the flanks of rising salt-cored structures during the deposition of the Oxfordian Minard Formation (Figure 4).
  - Continued growth of salt-cored folds such as the Corrib structure during the Cretaceous and Cenozoic (Figure 7).
- Salt structures which form early often continue to develop e.g. the crest of the structure above the large salt roller in Figure 5, which has both a thinned Lower and Middle Jurassic section beneath the Base-Upper Jurassic Unconformity, and a thinned Upper Jurassic section beneath the Base-Cenozoic Unconformity.

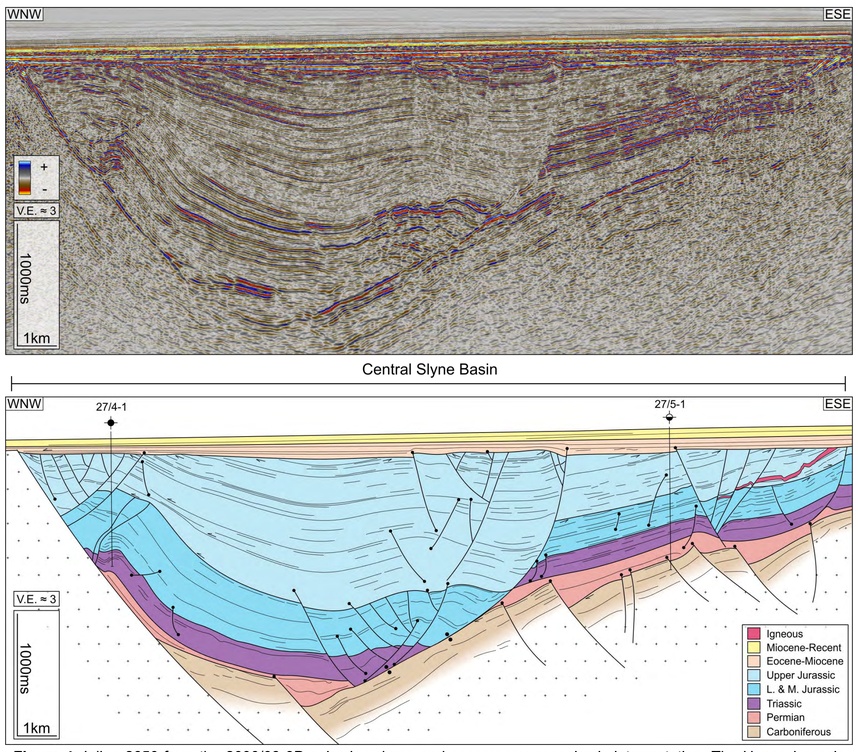

Figure 4: Inline 2650 from the 2000/08 3D seismic volume and accompany geoseismic interpretation. The Upper Jurassic section onlaps the steeply-dipping flanks of the structure targeted by the 27/4-1 well, with this Upper Jurassic section thickening into the hanging-wall of the large listric fault to the east. Growth of the structure was likely driven by a positive feedback mechanism of active salt and syn-tectonic sediment loading.

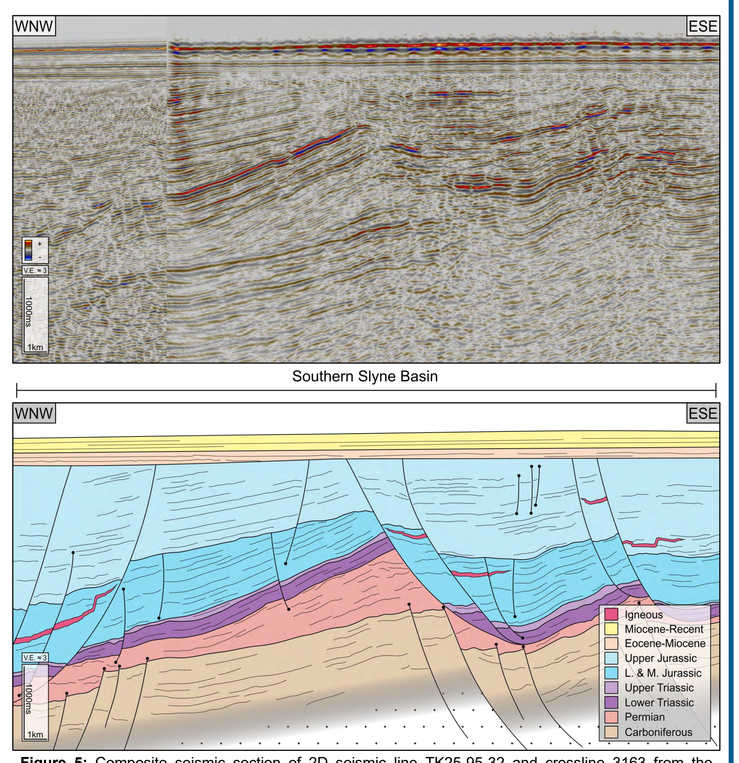

Figure 5: Composite seismic section of 2D seismic line TK25-95-32 and crossline 3163 from the 2010/01 (SL103D) 3D seismic volume, with accompanying geoseismic interpretation. The Middle and Lower Jurassic section is severely eroded on the crest of the fault block cored by the large salt roller, with a thicker section preserved in the hanging-wall of the fault bounding the structure.

Fault-style:

- The Zechstein Group acts as the main mechanical detachment in the Slyne and Erris basins, decoupling the pre-salt Palaeozoic basement from the Mesozoic post-salt section.
- The majority of post-salt faults are listric, soling out in the Zechstein Group. In the 2000/08 3D seismic volume, only 3 of 188 interpreted post-salt faults are hard-linked (~2%).

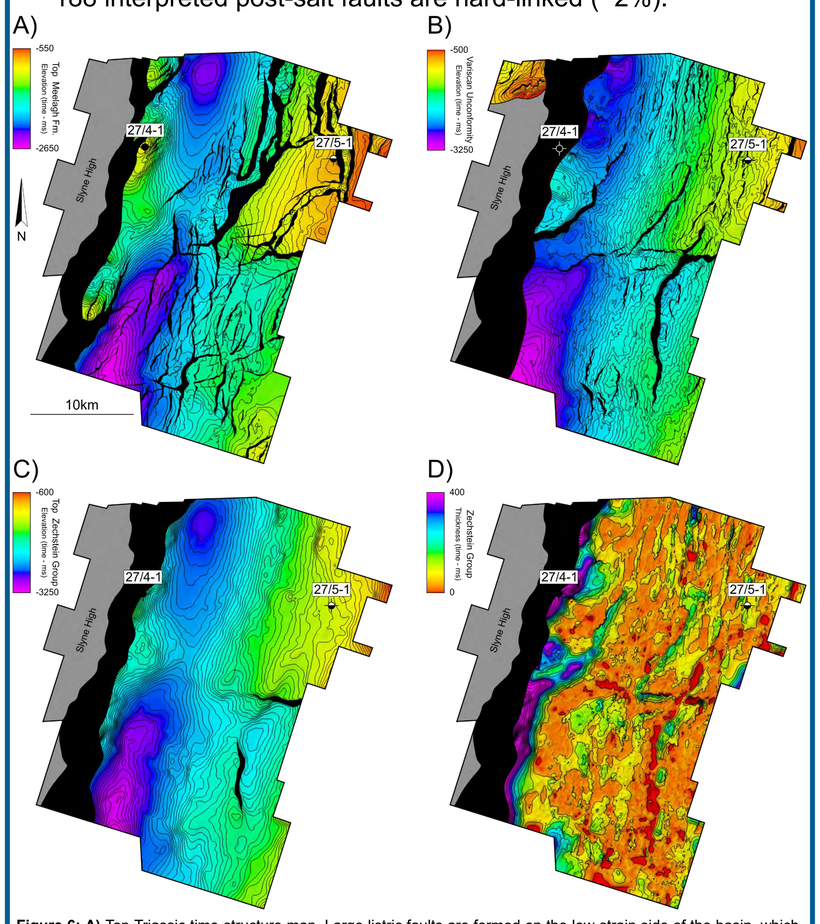

Figure 6: A) Top Triassic time-structure map. Large listric faults are formed on the low-strain side of the basin, which are slightly oblique to the main basin-bounding fault **B)** Variscan Unconformity time-structure map **C)** Top Zechstein Group [Top Salt] **D)** Zechstein Group thickness map (isochron). Several welds are formed across the survey, while the Zechstein Group is thickest adjacent to the basin-bounding fault.

Implications for future exploration:

- The presence of salt determines the style of faulting, with salt-prone areas experiencing thin-skinned, basement detached faulting during rifting
- Salt movement has taken place at multiple stages throughout the development of the Slyne and Erris basins. Understanding when and where is crucial to understand when traps form and how they change throughout basin development. Two examples of how this impacted hydrocarbon exploration are shown below:

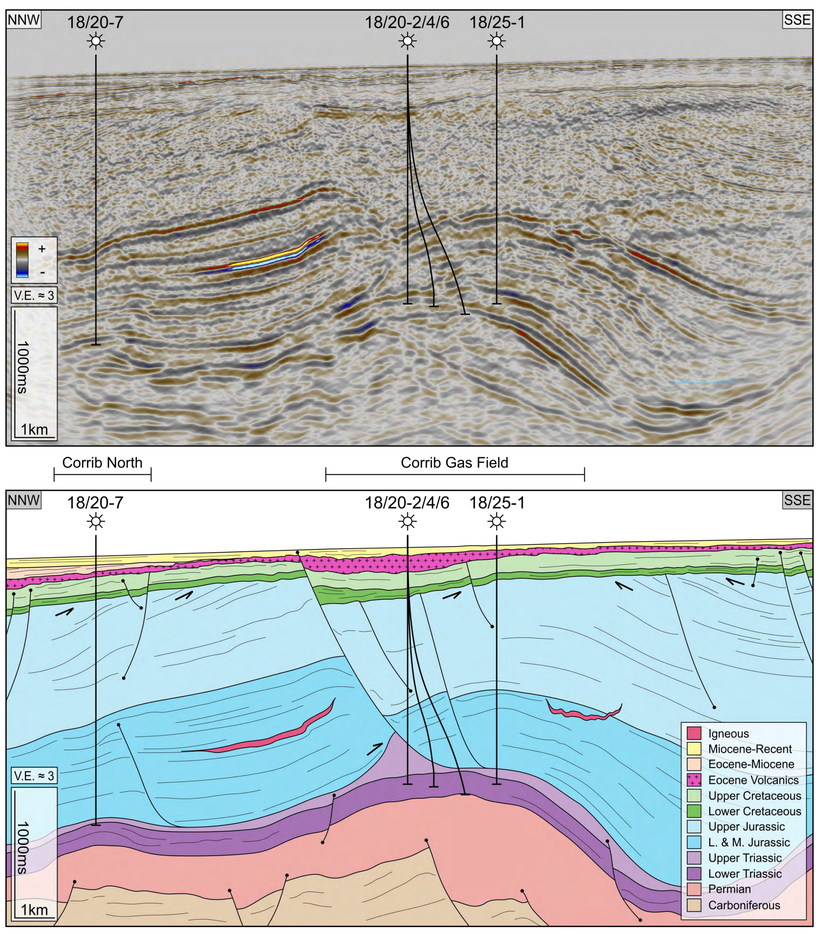

Figure 7: Arbitrary seismic section from the 2013/01 Corrib OBC seismic volume and accompanying geoseismic interpretation. The Corrib gas field is a salt-cored fold at Lower Triassic (reservoir) level, formed above a Zechstein salt pillow. A small diapir of Uilleann Halite has formed in the footwall of a major delamination fault in the Jurassic post-salt section, with a complex rollover geometry in the hanging-wall. The structural closure at the Corrib Sandstone Fm. Level is underfilled (~55% of total closure filled) due to further post-charge doming of the Zechstein during the Cretaceous and Cenozoic post-rift phases, likely driven by the development of the Rockall Basin to the northwest

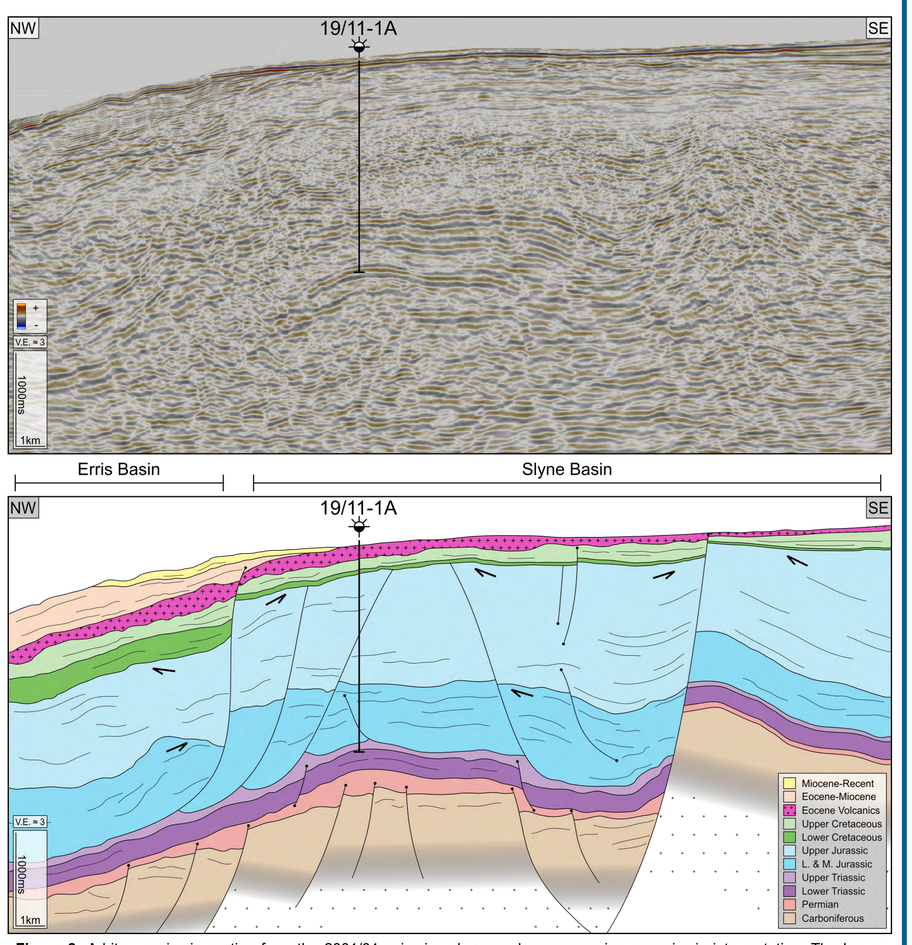

Figure 8: Arbitrary seismic section from the 2001/01 seismic volume and accompanying geoseismic interpretation. The Lower Triassic closure tested by the 19/11-1A well is identical at Mesozoic and Palaeozoic level to the Corrib structure, yet the Corrib Sandstone Fm. was water wet. The pressure regime encountered is similar to Corrib, suggesting the Uilleann Halite is providing an effective seal to a valid structural closure, while gas shows in the Lower Jurassic section indicate the presence of local charge. However the dip of the post-rift unconformity (i.e. Base-Cretaceous Unconformity) dips steeply westwards due to Cenozoic post-rift thermal subsidence in the Rockall Basin, indicating the western limb of the fold closed post-charge.

This publication has emanated from research supported in part by a research grant from Science Foundation Ireland (SFI) under Grant Number 13/RC/2092 and co-funded under the European Regional Development Fund and by PIPCO RSG and its member companies.

iCRAG funding bodies:

Ireland's European Structural and Investment Funds Programmes 2014-2020
Co-funded by the Irish Government and the European Union
European Union
European Regional Development Fund
Science Foundation Ireland Sfi For what's next
PIP Petroleum Infrastructure Programme

Software provided by:

Schlumberger
Petroleum Experts
Eliis

Data provided by:

Roinn Cumarsáide, Gníomhaithe ar son na hAeráide & Comhshaoil
Department of Communications, Climate Action & Environment
INFOMAR
EUROPA Oil & Gas
eni

Geometric and kinematic comparison of the Galicia Margin and the Porcupine Basin

Gaël Lymer[1,2] (*gael.lymer@ucd.ie*), M.M Saqab[3], C. Childs[1,2], T. Reston[4], J. Walsh[1,2]

[1]iCRAG (Irish Centre for Research in Applied Geosciences), School of Earth Sciences, University College Dublin, Belfield, Ireland
[2]Fault Analysis Group, School of Earth Sciences, University College Dublin, Belfield, Ireland
[3]Norwegian Geotechnical Institute, 40 St Georges Terrace, Perth WA, Australia ; [4]University of Birmingham, Geosystem Research Group, Birmingham, UK

Abstract

The Galicia Margin (West of Spain) and the Porcupine Basin (West of Ireland) are components of the Eastern North Atlantic rifted continental margins (**Figure 1**). We outline the structural architecture and kinematics of these basins from the seismic interpretation and fault analysis of multiple 2D and 3D seismic datasets. Our ongoing work suggests that many similarities between these basins arise from the operation of equivalent extensional processes from rift initiation through to hyperextension of the North Atlantic Ocean.

Shared structural features include: 1) Pronounced bathymetric V-shapes attributed to extension about a pole of rotation and/or a stepped variation in E-W extension facilitated by transfer faults, a fundamental characteristic of North Atlantic rifting. **2)** High beta-factors ($4<\beta<10$, Watremez et al., 2016) and hyper-extended continental crust, with similar associated fault geometries and orientations. **3)** Detachment faults, in both Galicia (the "S" reflector) and the Porcupine Basin (the "P" reflector, Reston et al., 2004), presumed to reflect the embrittlement of the continental crust before the break-up. **4)** Serpentinization arising from water circulation through the crust to the underlying mantle facilitated by crustal hyper-extension and the formation of low angle normal faults (<40°) and detachment faults. These and other constraints are helping to underpin the development of an integrated evolutionary model for hyper-extended basins.

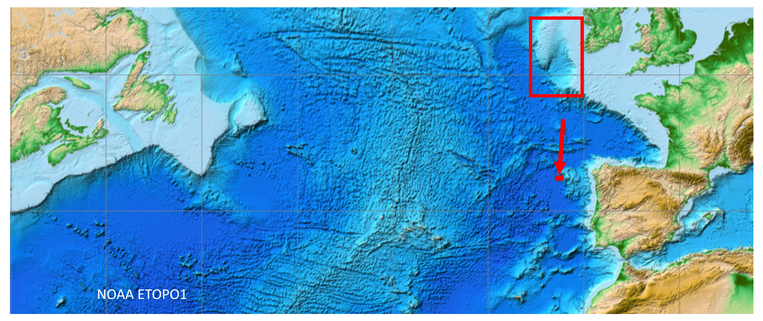

Figure 1: Southern North Atlantic Ocean and its rifted continental margins. The red arrow shows the location of the Galicia 3D volume west of Spain, and the red square shows the Porcupine Basin west of Ireland.

The Galicia margin

The structures of the Galicia Margin (Figure 1) have been defined recently using a new academic 3D seismic survey highlighting the architecture of the hyper-extended, distal, continental crust in unprecedented detail (**Figure 2**, **Lymer et al., 2019**).

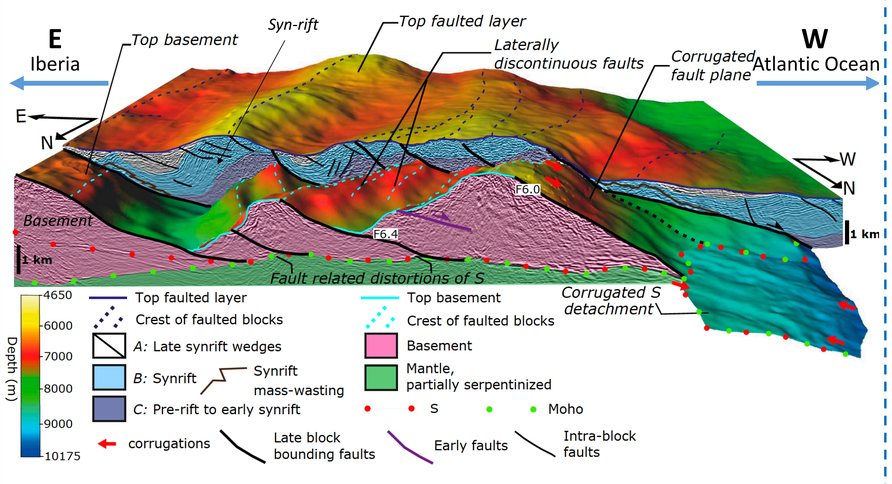

Figure 2: Perspective view from the north of the Galicia 3D volume showing the anatomy of the Galicia Margin with key structural and stratigraphic elements. Corrugated S detachment (Figure 3) is shown at the NW corner.

Kinematic implications of the 3D observations: CA change in direction of extension recorded by kinematic markers on the S detachment fault (**Figure 3**), northward decrease in fault heaves within the 3D volume (**Figure 4**), and associated higher thinning factors in the south (**Figure 5**), all suggest that extension of the Galicia Margin during rifting could be caused by a pole of rotation located 80 km north of the 3D volume (**Figure 6**).

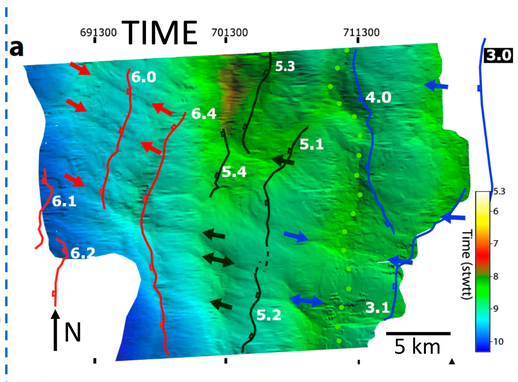

↑ *Figure 3: Time map of the S reflector displaying corrugations (arrows), orthogonal to their associated block-bounding faults rooting on S (numbered solid lines). The corrugations show an oceanward change in orientation from E-W in the East to ESE-WNW in the West. Green dotted line underlines where S meets the crust-mantle boundary.*

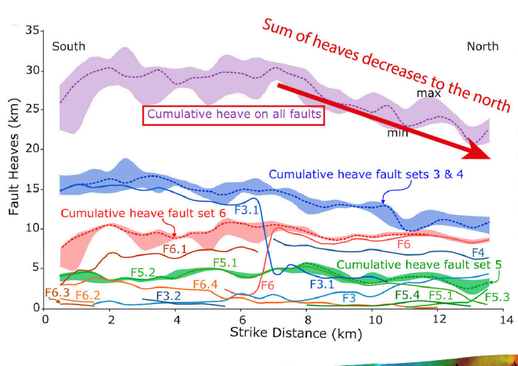

← *Figure 4: Fault heaves analysis (numbers are same than on fig. 3). The cumulative heave on all faults shows a decreasing of the extension toward the north of the 3D volume.*

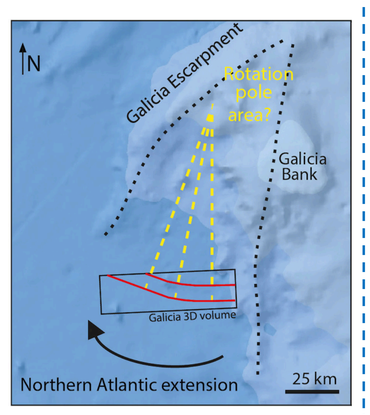

↑ *Figure 6: Bathymetric map of the distal Galicia Margin showing the location of a possible rotation pole defined by the intersection of the perpendiculars (dashed yellow lines) to the corrugations on S (red lines).*

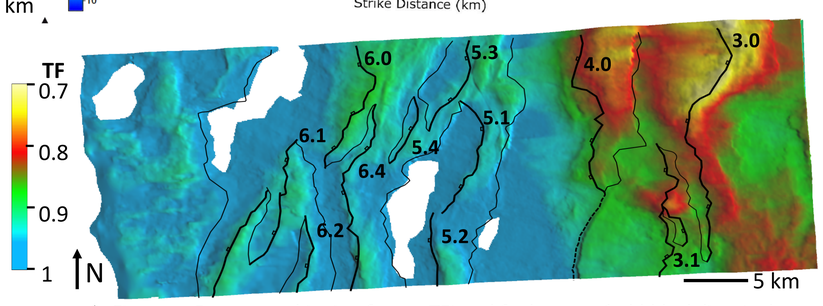

↑ *Figure 5: Basement thinning factor (TF) and faults map (bold black lines) where TF= 1-1/β and β = original thickness/measured (fault numbers are same than on fig. 3).*

Possible comparisons between the Galicia Margin and the Porcupine Basin

1) Kinematics

The geometries observed at the Galicia Margin and the Porcupine Basin (**Figure 7**) suggest similarities in terms of the kinematics of basin development.

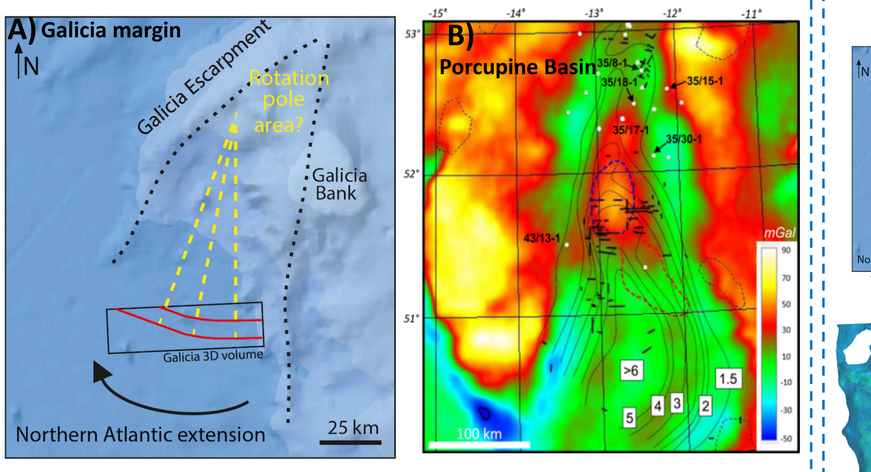

↑ *Figure 7: Regional geometrical comparison between the Galicia Margin (A, bathymetric map) and the Porcupine Basin (B, free air gravity anomaly map with numbers showing regional beta-factor variations (Gagnevin et al., 2017)).*

Our comparison of Galicia and Porcupine will permit testing of whether the basins developed by, for example, clockwise rotation of extension direction or by stepped variations in E-W extension facilitated by transfer faults.

2) Fault network geometry

Comparison of the architecture of the syn-rift structures (**Figure 8**) will allow to test the processes of fault networks development during rifting.

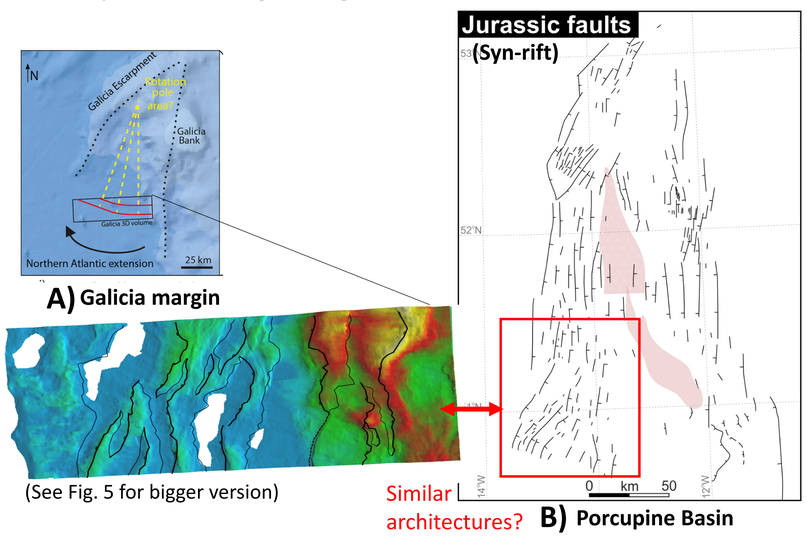

↑ *Figure 8: Fault network architecture of the Galicia Margin within the 3D volume (A) and of the Porcupine Basin (B). The southwest corner of Porcupine has geometrical similarities with the fault network at the southwest corner of the V-shape at the Galicia Margin.*

3) Detachment, β factor and low angle faults

Comparison of seismic sections from Galicia and Porcupine (**Figure 9**) reveals similar structures.

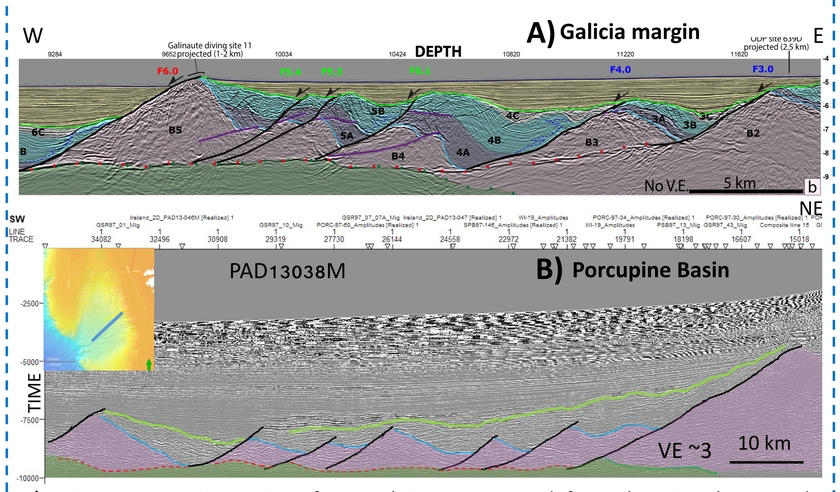

↑ *Figure 9: Seismic sections from Galicia (A, extracted from the 3D volume) and Porcupine (B). Green line: Top faulted layer; Blue line: Top basement; Red dashed line: Detachment faults; Green: Serpentinized mantle.*

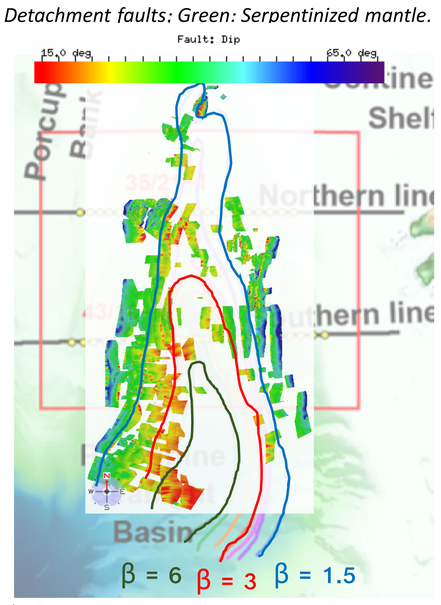

Clear correlation between high β factors and low angle faults for the Porcupine Basin **(Figure 10).** In both Porcupine and Galicia, fault dips of < 40° occur where β > 3 (crust < 10 km thick), with lowest fault dips where β > 5.

↑ *Figure 10: Fault dip map of the Porcupine, superimposed with β factor (Tate et al., 1993 & Watremez et al. 2016)*

Conclusions and future works

A preliminary comparison of the Galicia Margin and the Porcupine Basin permits definition of some of the processes of rift-related deformation, from detachment fault development and fault propagation through to simultaneous multiple fault activity.
Future work will address the kinematic processes of basin development controlling fault network geometry and continental break-up associated with rift propagation of the North Atlantic Ocean.

Our long-term aim is to develop an integrated model of offshore basin development and rift propagation that can be expanded to include other continental margins and associated rift basins.

References

- Gagnevin, D., Haughton, P. D. W., Whiting, L., & Saqab, M. M. (2017). Geological and geophysical evidence for a mafic igneous origin of the Porcupine Arch, offshore Ireland. Journal of the Geological Society, 175(2), 210–228.
- Lymer G., Cresswell D., Reston T.J, Bull J., Sawyer D., Morgan J.K., Stevenson C., Causer A., Minshull T.A., Shillington D.J. June 2019. 3D development of detachment faulting during continental breakup, Earth and Planetary Science Letters, 515, 90–99, https://doi.org/10.1016/j.epsl.2019.03.018
- Reston, T.J., Gaw, V., Pennell, J., Klaeschen, D., Stubenrauch, A. & Walker, I. 2004. Extreme crustal thinning in the south Porcupine Basin and the nature of the Porcupine Median High: implications for the formation of non-volcanic rifted margins. Journal of the Geological Society, London, 161, 783–798, http://doi.org/10.1144/0016-764903-036
- Tate, M.P., White, N. & Conroy, J.-J. 1993. Lithospheric extension and magmatism in the Porcupine Basin west of Ireland. Journal of Geophysical Research: Solid Earth, 98, 13,905–13,923, http://doi.org/10.1029/93JB00890
- Watremez, L., Prada, M., Minshull, T., O'Reilly, B., Chen, C., Reston, T., Shannon, P., Wagner, G., Gaw, V., Klaeschen, D., Edwards, R., Lebedev, S., 2016. Deep structure of the Porcupine Basin from wide-angle seismic data. In: Bowman, M. & Levell, B. (eds) Petroleum Geology of NW Europe: 50 Years of Learning – Proceedings of the 8th Petroleum Geology Conference, http://doi.org/10.1144/PGC8.26

This publication has emanated from research supported in part by a research grant from Science Foundation Ireland (SFI) under Grant Number 13/RC/2092 and co-funded under the European Regional Development Fund and by PIPCO RSG and its member companies.

Ireland's European Structural and Investment Funds Programmes 2014-2020
Co-funded by the Irish Government and the European Union
European Union
European Regional Development Fund
Science Foundation Ireland
sfi For what's next

Acknowledgements:
We thank the Petroleum Affairs Division of the Department of Communications, Climate Action and Environment for providing the seismic data from the Porcupine Basin used in this study.

PIP
Petroleum Infrastructure Programme

Full-waveform inversion and travel time tomography at Rockall Trough

Gaurav Tomar[1,2], and Chris Bean[1,2] and Satish C. Singh[3]

1. Dublin Institute of Advanced Studies

2. Irish Centre for Research in Applied Geosciences, Ireland

3. Institut de Physique du Globe de Paris, France

Introduction

Full waveform inversion (FWI) is a powerful technique for obtaining elastic properties of the sub-surface from the seismic data. FWI provides properties of the sub-surface at the scale of wavelength of the data set. The hyperextended Rockall Trough lies to the west of Ireland in NE Atlantic. It is under-explored, has complex geology and is known to be heavily intruded with volcanic sills. There, we have performed 2D elastic FWI on 10 km long streamer data set acquired from Rockall Basin in 2013-14. To reduce the computation time and the water layer's effect, we extrapolated the wavefield with a downward continuation and then performed refraction tomography to compute the starting velocity model for FWI. The velocity model obtained from refraction travel time tomography, indicates the velocity from 1.6-4 km/s for the sediments and we have also observed very high velocity ~ 6-7 km/s 3 km below the sea-floor. We have obtained preliminary results of FWI where, we have inverted the data in frequency range of 3-7 Hz. The velocity model shows some geological structures that can be seen in the migrated image. These high velocity structures could be lower crustal rocks in he area of study. FWI would also give us the exact velocity of the volcanic intrusions (sills).

Location of Rockall Trough and acquisition lines (in black)

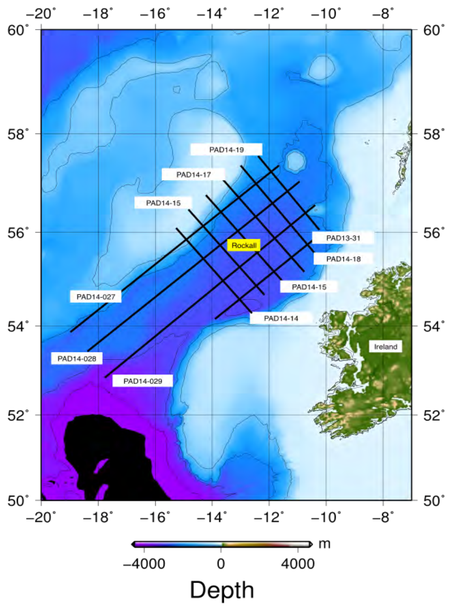

First arrival travel time tomography velocity model model

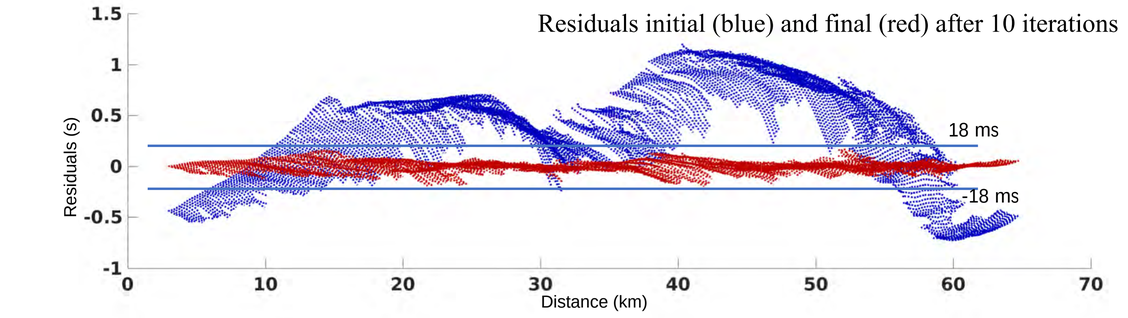

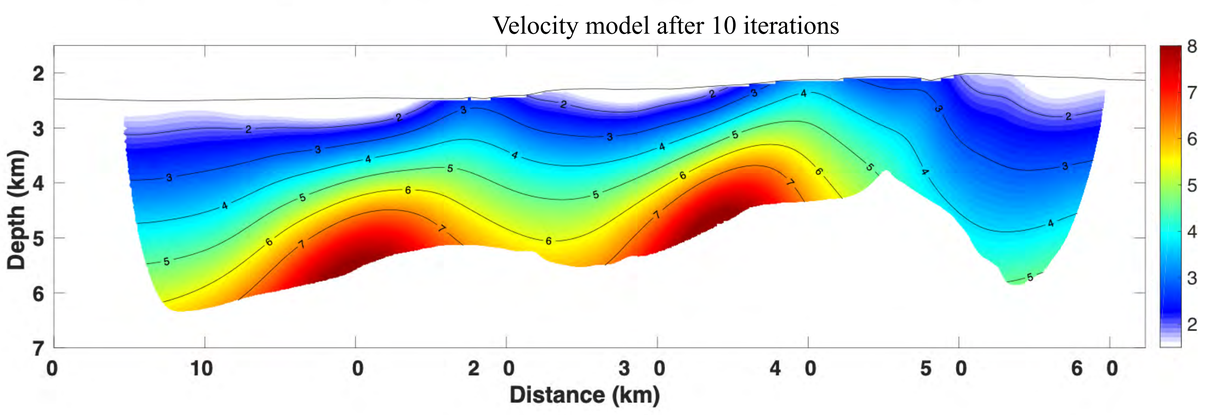

PSTM section of line PAD014-027 (shown in the map)

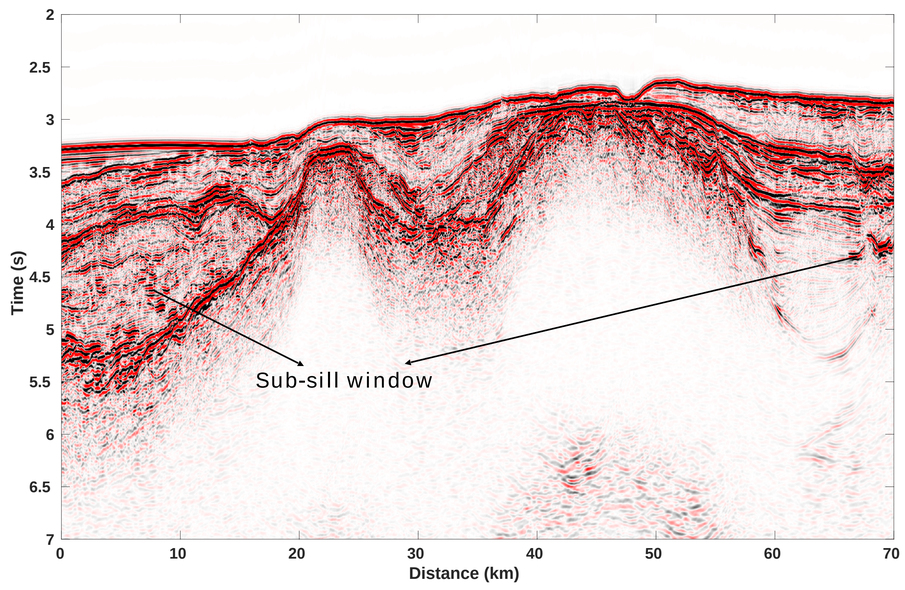

Full waveform inversion of refraction only (between 3-7 Hz)

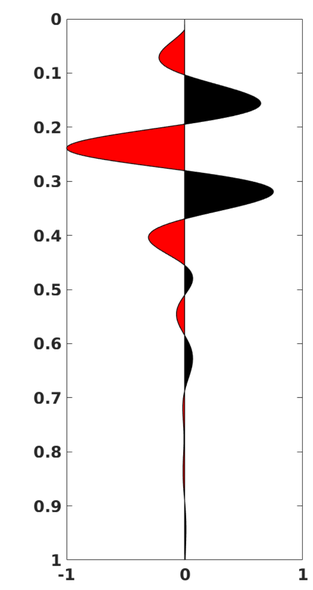

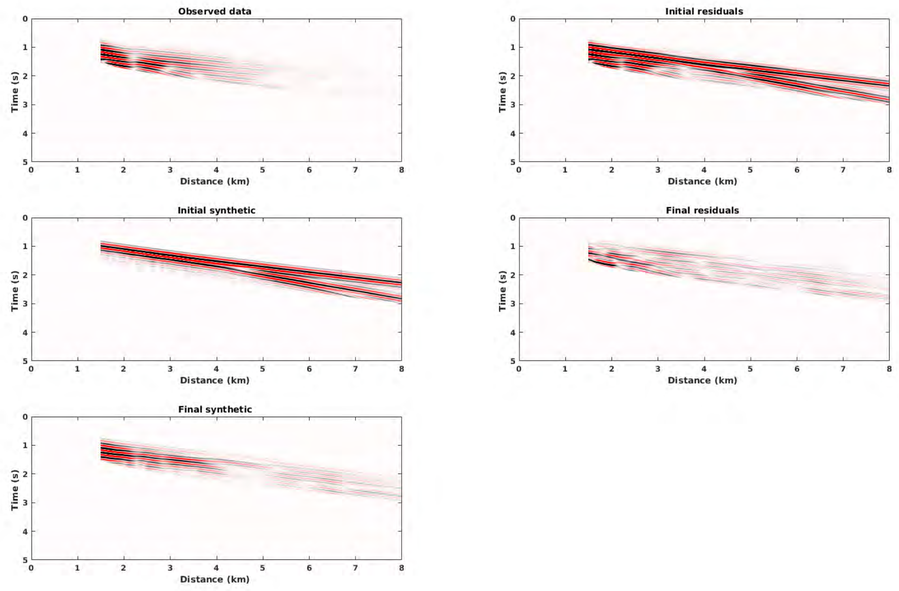

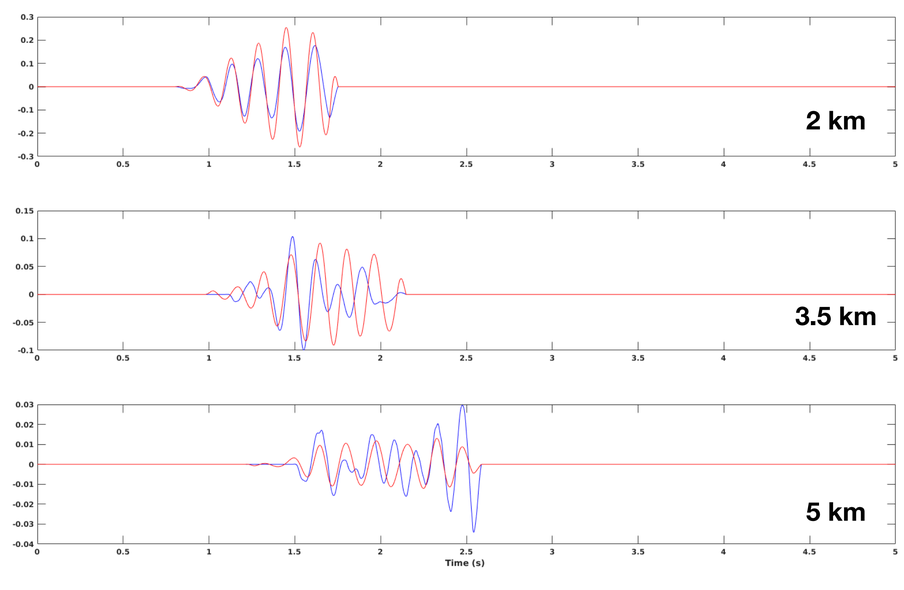

Full waveform inversion (FWI) method

The elastic FWI is iterative method that seeks to minimise a least-square misfit function S between observed d_{obs} and synthetic d_{syn} data (Shipp & Singh 2002).

$$S = \sum_{\text{shots}} \int_0^T \mathrm{d}t \sum_{\text{recs}} [d_{\text{syn}} - d_{\text{obs}}]^2,$$

Thus, the misfit is measured quantitatively by taking, sample by sample, the least squared difference between the two datasets (pressure recordings in our case) for every receiver in each of the shot gathers.

Then we use conjugate gradient method to solve the iterative inversion problem.

Preliminary results of FWI (Velocity model after 30 iterations)

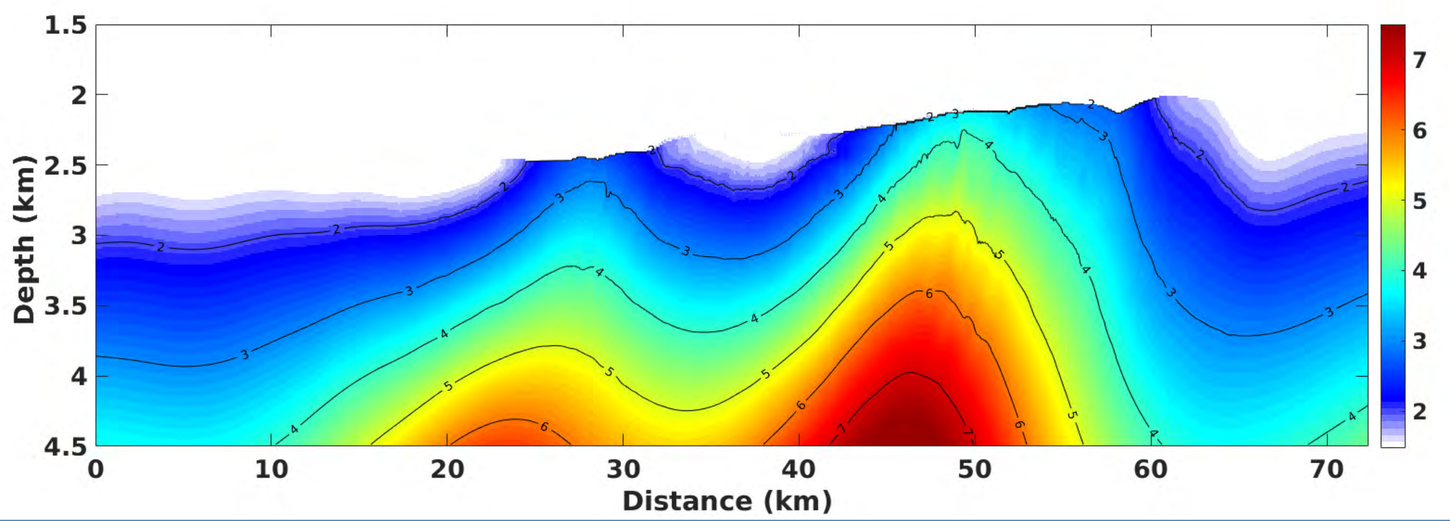

Conclusions and Perspectives

- First arrival travel time tomography was performed to obtain the initial velocity model for FWI. The velocity model was obtained with the uncertainty of 18 ms. We obtained very high velocity structures ~7 km/s just ~3 km below the sea-floor.
- FWI is performed on the downward continued data in the frequency range of 3-7 Hz, we have inverted the full wavefield of refractions of every 4th shot. The velocity model shows some structures that follows with the migrated image of seismic data.
- FWI will be carried out on the same profile for higher frequencies and then we will include the reflection in inversion.

This publication has emanated from research supported in part by a research grant from Science Foundation Ireland (SFI) under Grant Number 13/RC/2092 and co-funded under the European Regional Development Fund and by PIPCO RSG and its member companies.

Discrete numerical modelling of the evolution of fault systems in 3D

J. Aleksans[1,2], C. Childs[1,2], M.P.J. Schöpfer[3]

1: iCRAG (Irish Centre for Research in Applied Geosciences), School of Earth Sciences, University College Dublin, Belfield, Ireland

2: Fault Analysis Group, School of Earth Sciences, University College Dublin, Belfield, Ireland

3: Department for Geodynamics and Sedimentology, University of Vienna, Vienna, Austria

Abstract

The stages in the development of normal fault systems, from initiation through localisation to maturity, are well established from the study of ancient fault systems. However, there are many aspects of fault system evolution that are not yet understood and are not easily addressed using geological data alone. For example, there is significant current debate on the strains at which the lengths of faults are established. An approach that can improve the understanding of fault growth is appropriately scaled numerical modelling that complements geological data and analysis.

Methods

We use the Particle Flow Code in three dimensions which implements Distinct Element Method (DEM) for circular particles. Particles interact via a linear force-displacement law. Cohesion is modelled by adding linear elastic bonds to particle-particle contacts. These bonds break if either critical normal or shear strength is exceeded, thus creating a fracture surface within the rock volume.

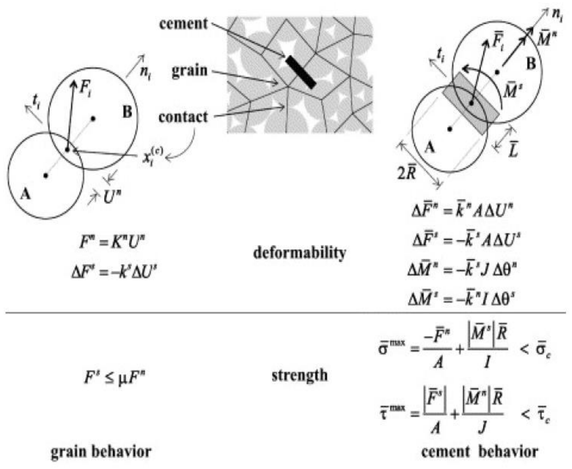

Figure 1.1. Force-displacement behaviour of grain-cement system (Potyondy and Cundall, 2004)

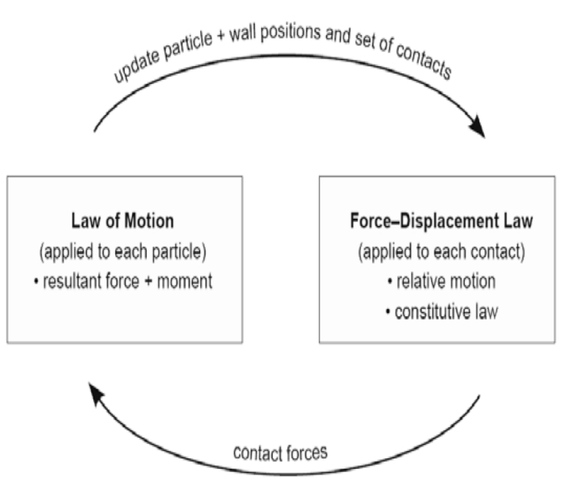

Figure 1.2. Calculation cycle in PFC 3D (Itasca, 2005).

Experimental Setup

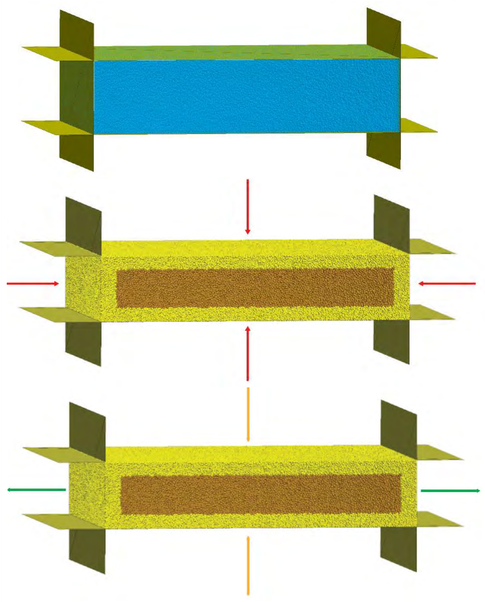

1) Generate space tightly packed by spherical particles.
* 1.6 million particles
* 4 rigid boundaries, 2 periodic boundaries

2) Divide particles in groups and assign mechanical properties
* Brown – hard, bonded; Yellow – soft (10% Young's modulus of hard layer), unbounded.
* Assign Young's modulus, Poisson ratio, tensile and shear strength, friction coefficient.

3) Confine the sample
* Sample is confined by slowly moving rigid walls inwards.
* Once confined, sample is relaxed, meaning all the particles come to a resting state.

4) Extend the sample
* Sample is extended by moving lateral walls apart
* Constant pressure is maintained from top and bottom

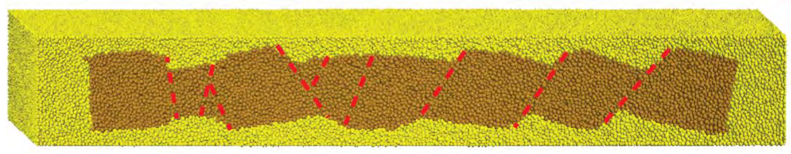

5) End result
* Presents faulted rock with rotational blocks

Evolution of the fault system

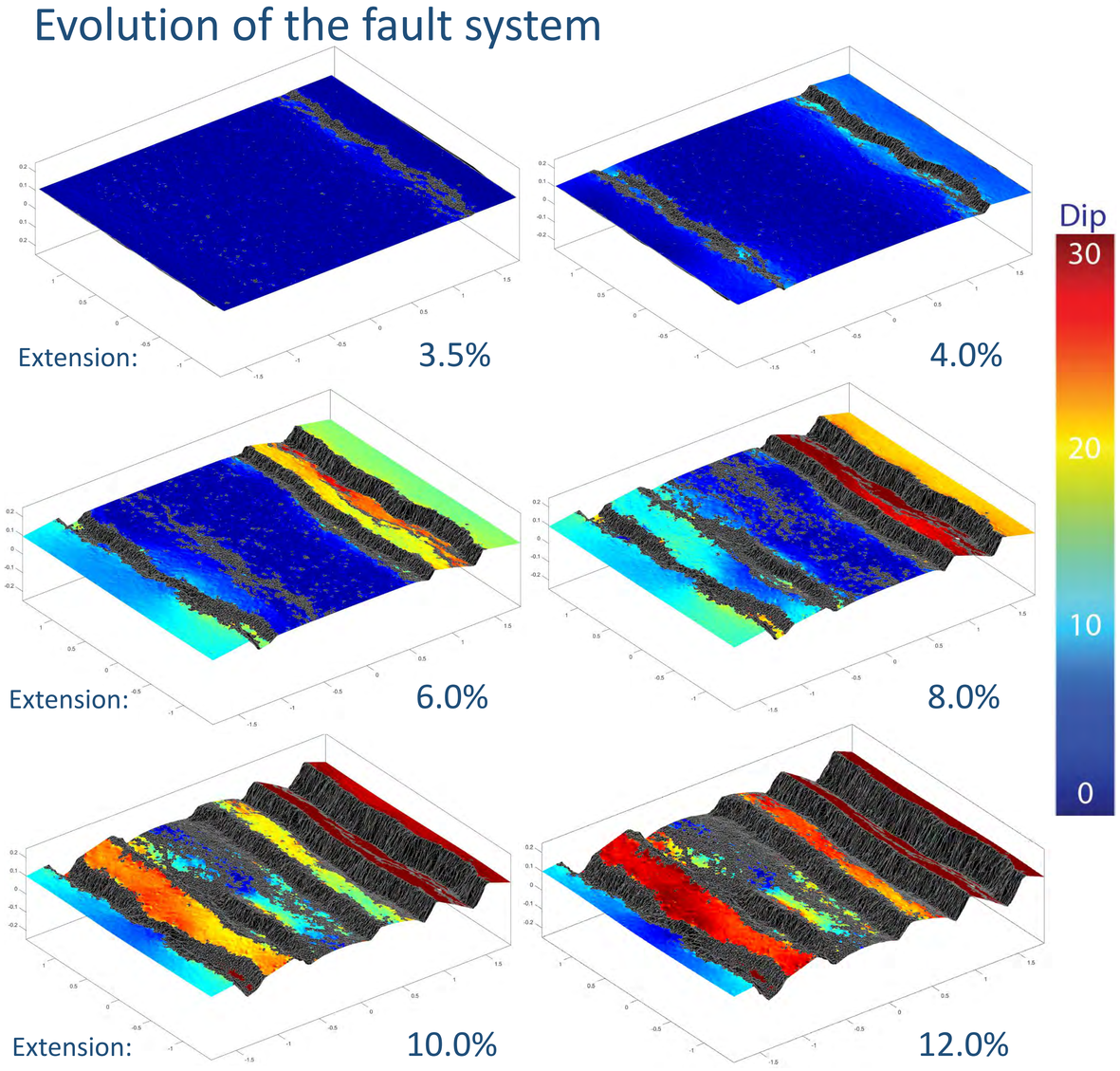

The developed model is capable of replicating evolution of the fault system in great detail. In these early stages of the development we can already observe features, which are common in natural systems, such as: horst-graben system, terraces, relays, conjugates. The data created can be exported into multiple formats which makes it easy to postprocess and analyse in various applications such as MatLab or Move. The current data set was created by

1) Export of data as point cloud coordinates from particle positions;

2) Data import into MatLab where it is post-processed to create polygons, which are intersecting a given plane;

3) Calculation of dip values from local variability of polygon endpoints, Lagrangian strain calculation from particle displacement values.

Parameter study of Young's Modulus variation

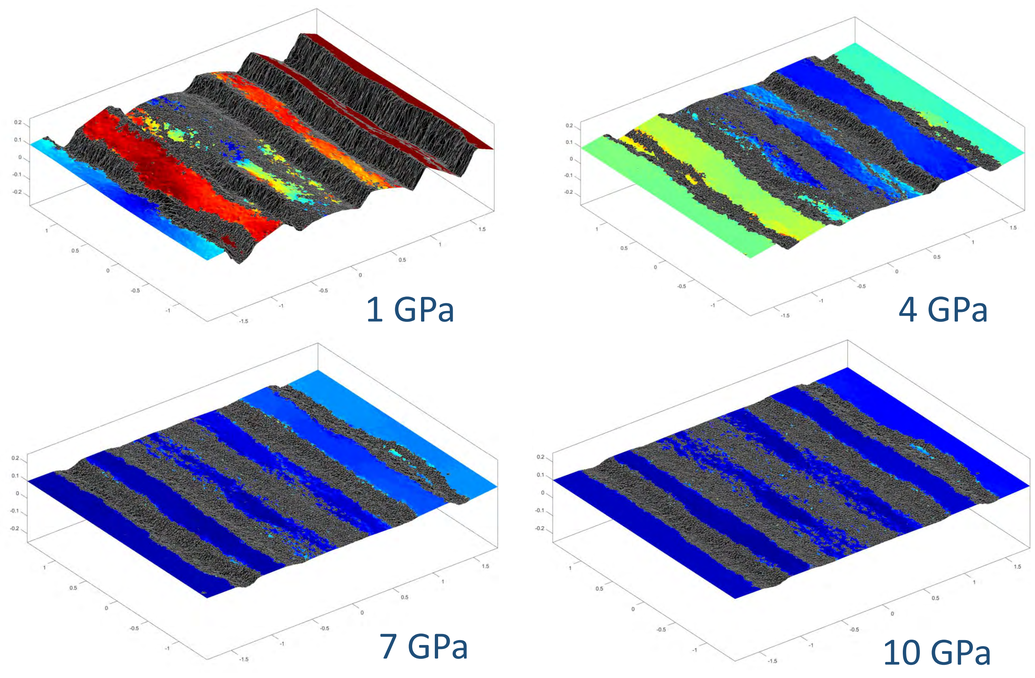

We have carried out parameter study where models with identical particle assemblage structures were assigned different Young's modulus values. The initial two prominent observations are: 1) switch from rotational fault system to boudinage; 2) reduction in fault sinuosity with increase in Young's modulus.

Sinuosity data and caption

Conclusions and future work

- In these early stages of the project the model has proven to be very versatile. Furthermore, adaptive data export options make it perfect for further data post-processing and analysis.
- Near future plans include looking more into modelled features of individual faults as well whole fault systems and comparing them with analogues from available geological data.
- The possibility of working in 3D makes it available to study fault geometry properties along the horizontal and vertical axis. To further explore the observed variability of fault sinuosity, which depends upon the change in Young's modulus it is planned to incorporate more detailed analysis, which would look into wavelength and amplitude of the fault sinuosity.

This publication has emanated from research supported in part by a research grant from Science Foundation Ireland (SFI) under Grant Number 13/RC/2092 and co-funded under the European Regional Development Fund and by iCRAG industry partners.

Ireland's European Structural and Investment Funds Programmes 2014-2020
Co-funded by the Irish Government and the European Union
European Union
European Regional Development Fund
Science Foundation Ireland sfi For what's next
Geological Survey Suirbhéireacht Gheolaíochta Ireland | Éireann

The Role of Tectonic Evolution, Crustal Structure and Multiphase Magmatism in the Evolution of the Hatton Rifted Continental Margin, Offshore Ireland, Using Seismic Reflection and Potential Field Methods

Laura Bérdi[*1,2,3], Manel Prada[1,2], Brian M. O'Reilly[1,2], Peter Haughton[2,3], Patrick M. Shannon[2,3] & Sara Martínez-Loriente[2,3]

1) Dublin Institute for Advanced Studies, Geophysics Section, 5 Merrion square, Dublin, Ireland, 2) Irish Centre for Research in Applied Geosciences (iCRAG), University College Dublin, Belfield, Dublin 4, Ireland, 3) School of Earth Sciences, University College Dublin, Belfield, Dublin 4, Ireland, 4) Institut de Ciencies del Mar, Barcelona, Spain, *laura.berdi@icrag-centre.org

1. INTRODUCTION

The Hatton Basin is located at the western European Atlantic Margin, approximately 600 km west of Scotland and Ireland (Fig. 1a). It is bounded by the Rockall Bank to the east and by the Hatton High to the west. The sediments in the Hatton Basin can be divided into eight main stratigraphic sequences (Fig. 2), spanning from Jurassic and/or older to Holocene on the basis of seismic reflection interpretation (this study, Fig. 1b), shallow borehole data (Hitchen, 2004 and DSDP data), seismic refraction studies (Jacob et al., 1995; Shannon et al., 1995; Vogt et al., 1998) and analogues from neighbouring offshore basins (e.g. McDonnell & Shannon, 2001). Due to the lack of deep borehole data in the study area, the Mesozoic evolution of the basin is not fully understood. On the basis of recent seismic reflection data interpretation, the project provides previously unkown seismic stratigraphic control on the presumed Mesozoic succession and sedimentary transport routes through time. Moreover, new constraints on the nature and timing of igneous processes and their influence on sedimentation are also recorded.

The results of this project will provide an in depth understanding of the nature and timing of geological processes in the area and thus, contribute to two main themes: **(1) Energy security** and **(2) Climate change.** Understanding the sedimentary and thermal evolution of the Hatton Basin plays a major role in defining whether there is a working petroleum system with possible hydrocarbon accumulations in the area **(1)**. Furthermore, the study of the igneous evolution of the basin could form the basis for further research on the effects of volcanic activity on the Paleocene-Eocene Thermal Maximum (PETM) global warming event **(2).**

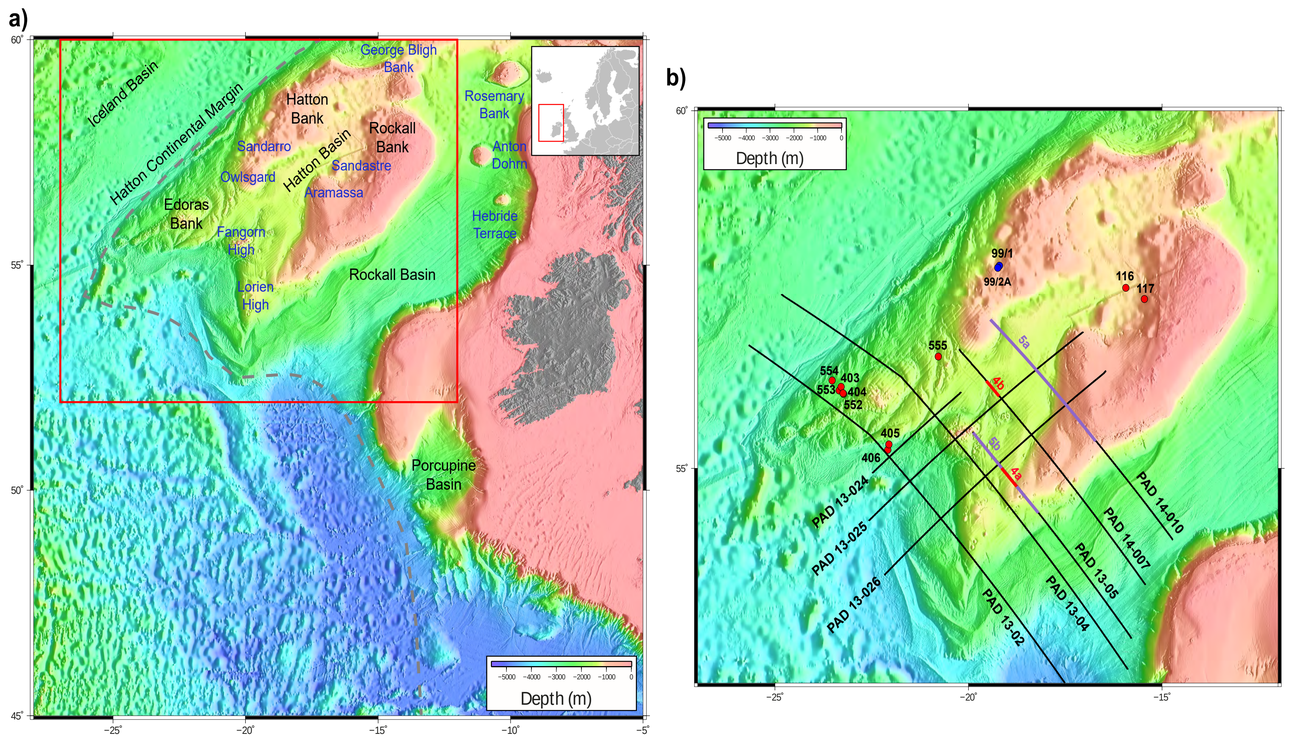

Figure 1. *a) Bathymetry map of the Hatton Basin showing the main tectonic structures (black) and igneous features (blue) in the area. The red rectangle highlights the study area. The well and seismic data used in this study are shown on fig. 1b). The red circles represent DSDP boreholes, the BGS boreholes are highlighted in blue and the ODP borehole is shown in green. The grey dashed line represents the continent-ocean boundary.*

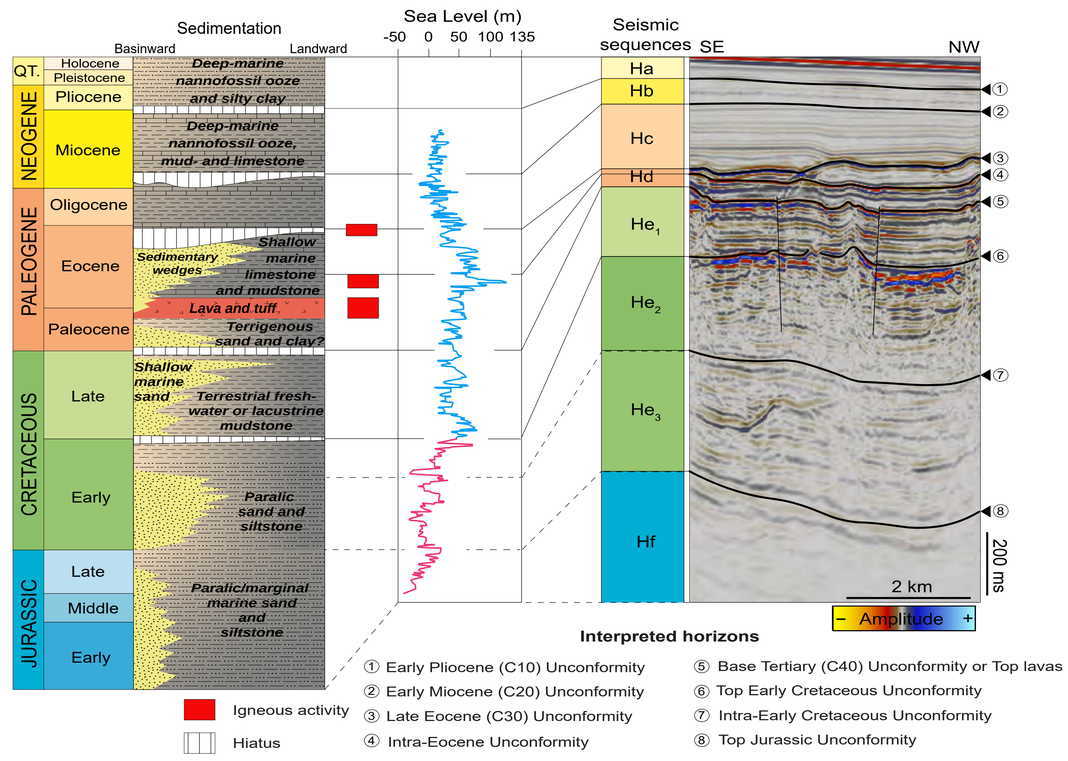

Figure 2. *General stratigraphic column of the Hatton Basin showing the mapped regional unconformities and sedimentary megasequences (after Laughton et al., 1972, Hitchen, 2004, Stoker et al., 2001) and the changes in sedimentation style and igenous activity during basin evolution (based on DSDP data, McDonnell & Shannon, 2001 and this study). Sea level curves are from Miller et al., 2005 (blue) and Sahagian & Jones, 1993 (pink).*

2. CORRELATION BETWEEN SEISMIC AND FIELD DATA

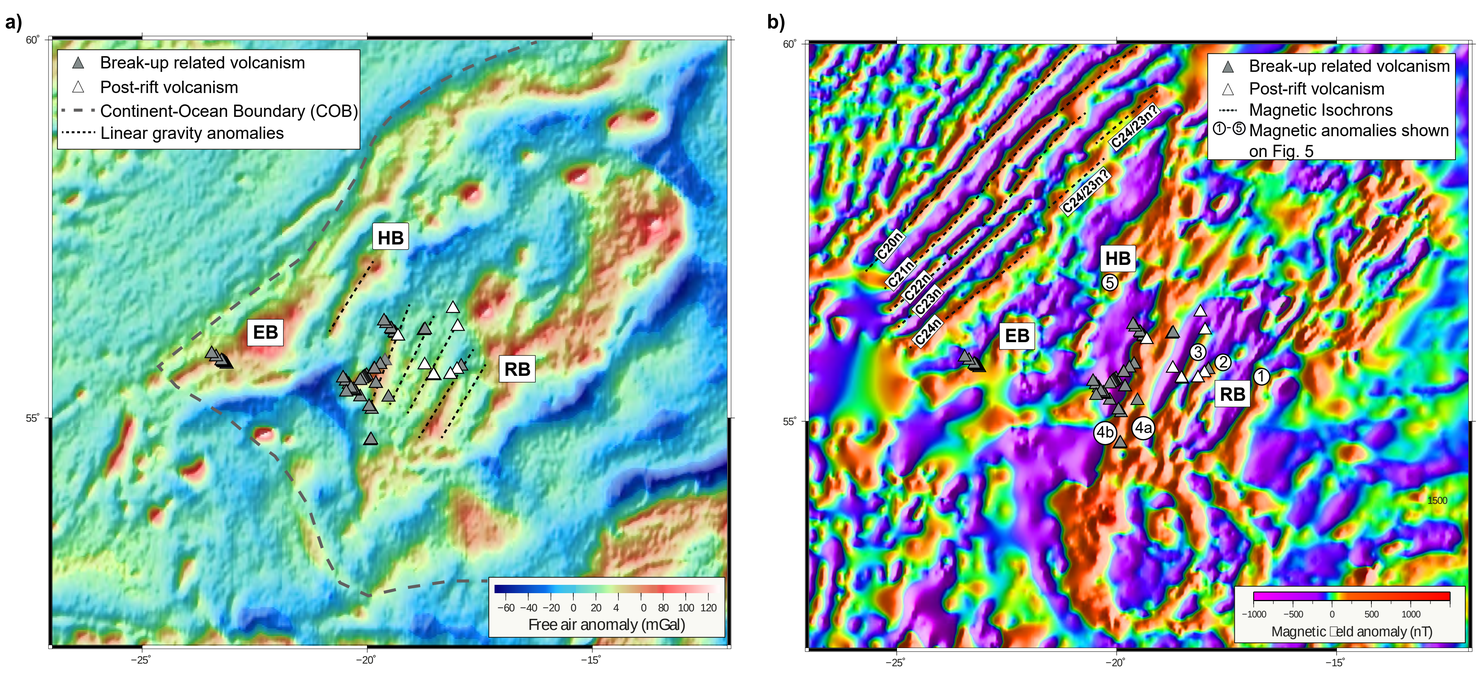

Figure 3. *Gravity (a) and magnetic map (b) of the Hatton Basin (Sandwell et al., 2014; Verhoef et al., 1996). The numbered, NNE-SSW oriented anomalies in the basin correlate to increases in the potential field (more pronounced in the magnetic field) when extracted in 2D view (see Fig. 5). Most of the paleo-volcanic cones in the basin are located along these anomalies, which indicates areas with inherited zones of weaknesses in the crust. Combined with results from geophysical modeling, magma is thought to have used these zones - interpreted as major normal faults - as pathways to enter the Hatton Basin through deep-seated dike intrusions. EB - Edoras Bank, HB - Hatton Bank, RB - Rockall Bank.*

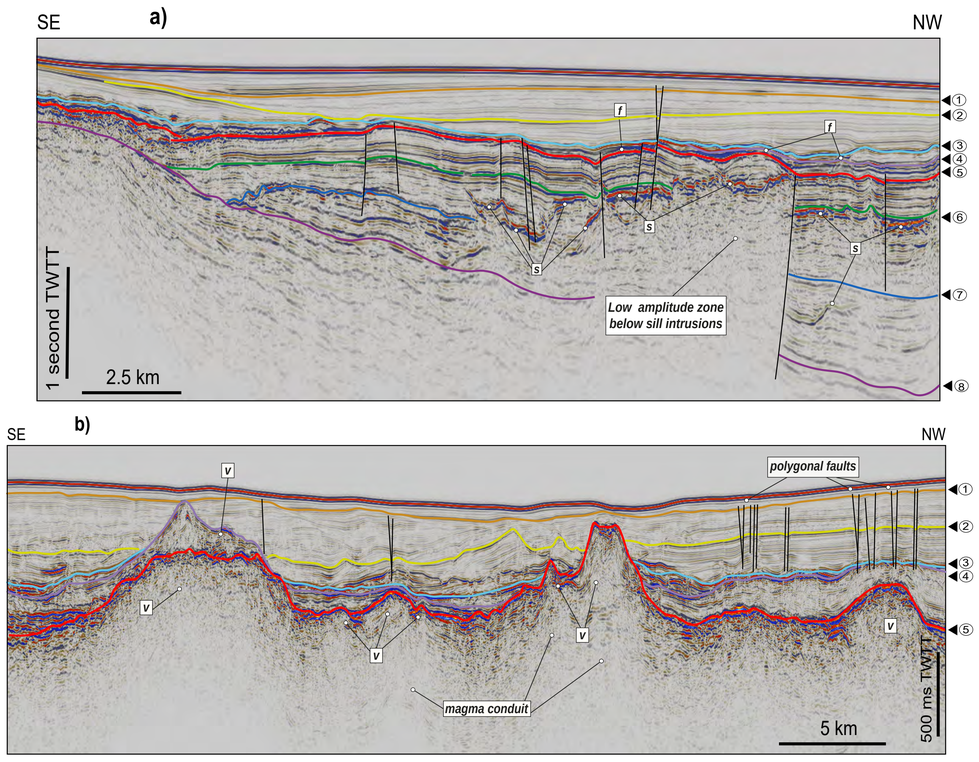

Figure 4. *Examples of high-resolution seismic data showing the sedimentary architecture of the Hatton Basin at the basin margin (a) and multiple phases of magmatism (b). The volcanoes shown of Fig. 4b formed during the regional Late Paleocene-Early Eocene magmatic period (around PETM time), while the volcanic cone on the southeastern end of the profile post-dates the breakup along the North Atlantic margin. Other magmatic products, such as sills and dykes are also observed in the dataset intruding host rocks. f - forced fold, s - sill, v - volcano. For horizon legend, refer to Fig. 2.*

3. GRAVITY AND MAGNETIC MODELING

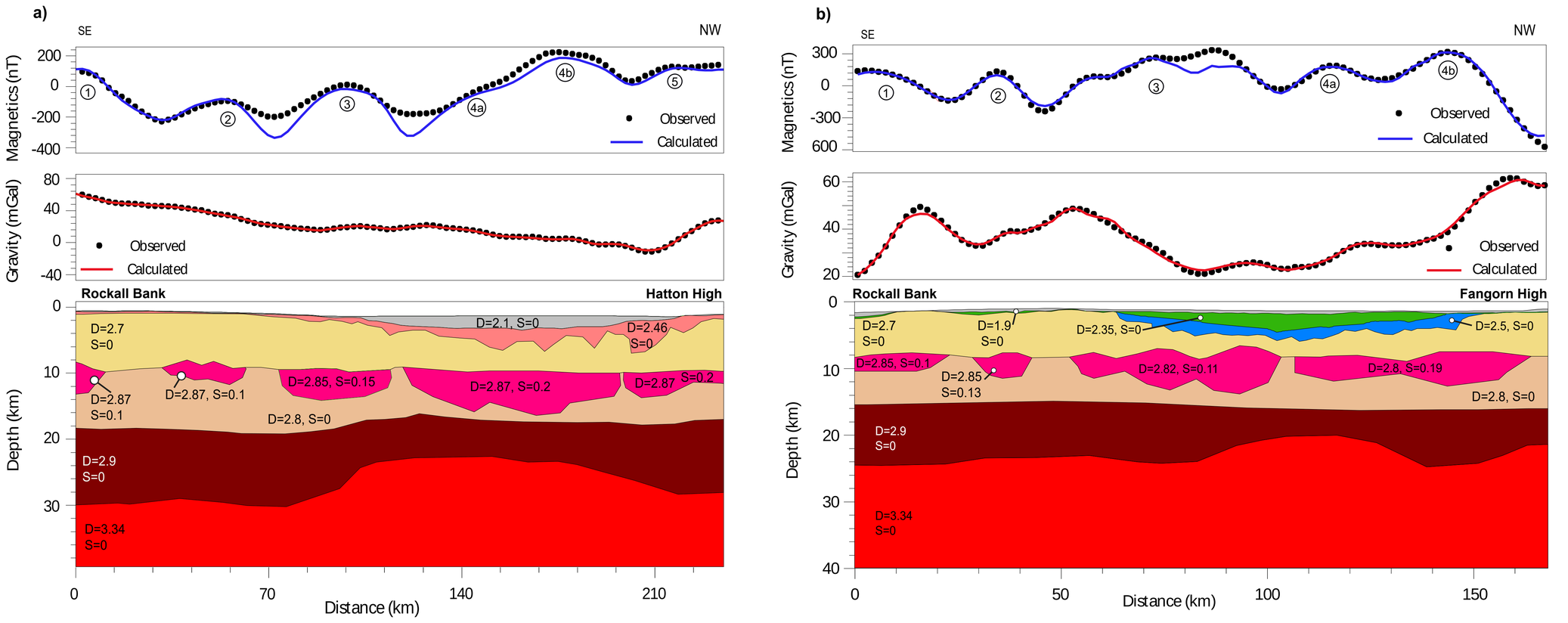

Figure 5. *Potential field models of PAD seismic profiles 14-010 (a) and 13-005 (b). The shape and extent of sedimentary blocks between the basement and seabed are based on seismic picks. The horizons were depth converted into the model and - with the exception of the top basement pick - were not modified during modeling. On Fig. 5a, the Paleocene block includes the Mesozoic and/or older sediments beneath (which could not be picked along the whole profile).The top basement was interpreted at the bottom of reflectivity on each seismic line and was then modified according to the gravity response during modeling. The models show a basement with highs, horsts and half grabens, accomodating the deposition of thick Mesozoic and/or older sediments. The magnetic anomalies represent igneous intrusions at the top of the middle crust/bottom of the upper crust, located in a parallel, linear pattern in 3D view (Fig. 3) with localised volcanism along them. These intrusions are likely to had reached the basin through reactivated basement faults. Gravity grid is from Sandwell et al. (2014), magnetic data is from Verhoef et al. (1996), modeling was performed in Geosoft.*

This publication has emanated from research supported in part by a research grant from Science Foundation Ireland (SFI) under Grant Number 13/RC/2092 and co-funded under the European Regional Development Fund and by PIPCO RSG and its member companies. Seismic data provided by the Petroleum Affairs Division of the Department of Communications, Climate Action & Environment.

Ireland's European Structural and Investment Funds Programmes 2014-2020 — Co-funded by the Irish Government and the European Union

Science Foundation Ireland sfi — For what's next

PIP Petroleum Infrastructure Programme

European Union — European Regional Development Fund

Hitchen, K. 2004. The geology of the UK Hatton-Rockall margin. Marine and Petroleum Geology, 21, 993-1012.
Jacob, A. W. B. , Shannon, P. M., Makris, J., Hauser, F., Vogt, U. & B. M. O'Reilly. 1995. An overview of the results of the RAPIDS seismic project, North Atlantic. Geological Society, London, Special Publications, 93, 429-431.
Laughton, A. S., Berggren, W. A., Benson, R., Davies T. A., Franz, U., Musich, L., Perch-Nielsen, K., Ruffman, A., van Hinte, J. E. And Whitmarsh, R. B. 1972. Initial reports of the Deep Sea Drilling Project, vol. 12. Technical report, U.S. Government printing Office, Washington D.C.
Miller, K. G. et al. 2005. The Phanerozoic Record of Global Sea-Level Change. Science, 310, 1293-1298.
Sahagian, D. & Jones, M. 1993. Quantified Middle Jurassic to Paleocene eustaic variations based on Russian Platform stratigraphy: Stage level resolution. Geol. Soc. of Am. Bull., 105, 1109-1118.
Sandwell, D.T., Müller, R.D., Smith, W.H.F., Garcia, E. & R. Francis. 2014. New global marine gravity model from CryoSat-2 and Jason-1 reveals buried tectonic structure. Science, 346, 65-67.
Shannon, P. M. , Jacob, A. W. B. , Makris, J. , O'Reilly, B. , Hauser, F. & U. Vogt. 1995. Basin development and petroleum prospectivity of the Rockall and Hatton region. Geological Society, London, Special Publications, 93, 435-457.
Stoker, M. S., van Weering, T. C. E., and Svaerdborg, T. (2001). A mid- to late Cenozoic tectonostratigraphic framework for the Rockall Trough. In P. M. Shannon, P. H. And Corcoran, D., editors, The Petroleum Exploration of Ireland's Offshore Basins, vol. 188, 411-438. Geological Society, London, Special Publications.
Verhoef, J., Roest, W.R., Macnab, R., Arkani-Hamed, J. (1996). Magnetic anomalies of the Arctic and North Atlantic Oceans and adjacent land areas; GSC Open File 3125, Parts a and b (CD-ROM and project report). Geological Survey of Canada, Dartmouth NS.
Vogt, U., Makris, J., O'Reilly, B.M., Hauser, F., Readman, P.W., Jacob, A.W.B. & P.M. Shannon. 1998. The Hatton Basin and continental margin: Crustal structure from wide-angle seismic and gravity data. Journal of Geophysical Research, 103, 12545–12566.

A hierarchical compression-based geomodelling workflow for Petrel

Marcus Carneiro[1,*] and Tom Manzocchi[1]

iCRAG and Fault Analysis Group, School of Earth Sciences, UCD

*mvcmartins@icrag-centre.org

Introduction

The compression-based modelling approach was developed to overcome the limitation of conventional object-, variogram- or MPS-based facies models in which geobody connectivity is an unconstrained model output determined primarily by the volume fraction of the geobodies.

The standalone vbFIFT package was developed to implement compression-based modelling in a hierarchical, object-based framework, and has proven the approach to be robust. It is, however, very difficult to use (Manzocchi et al 2007 and 2016).

The current project aims to make the approach more generally accessible to industry geomodellers, through its implementation as plugins and workflows accessible within the industry-standard Petrel Geomodelling software. This poster outputs the parts of the workflow under development.

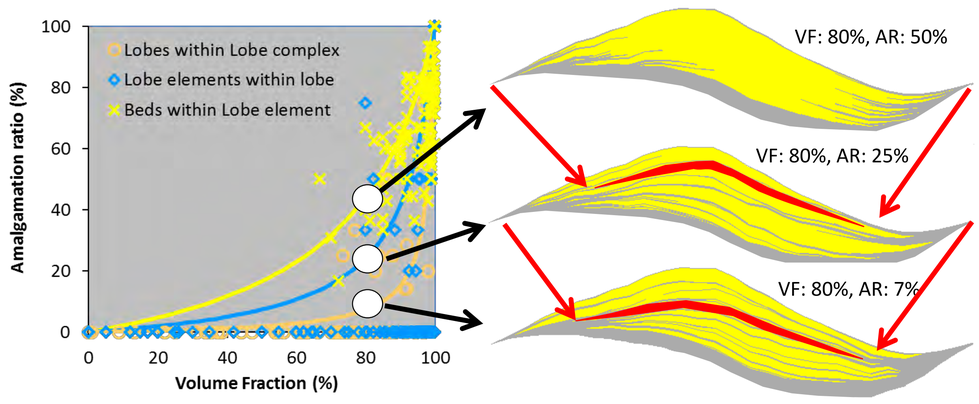

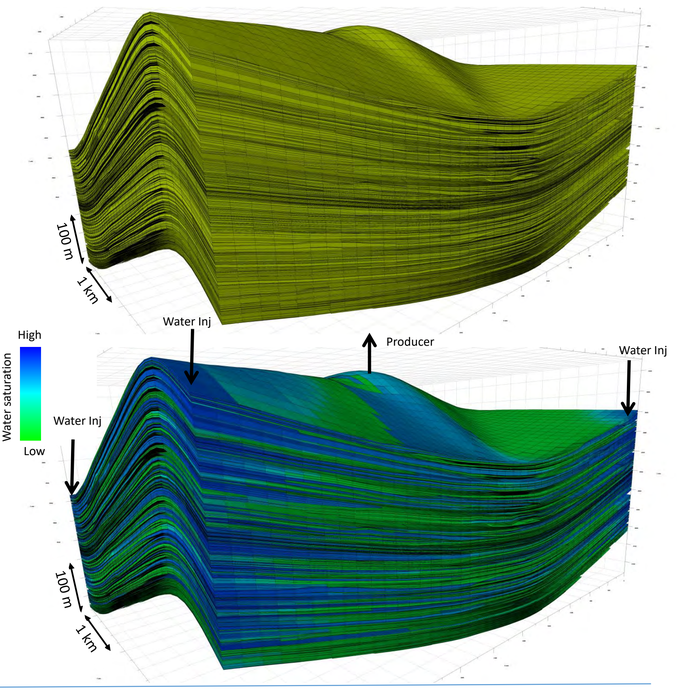

Above: Principal of the modelling approach applied to deep water deposits: Independent honouring of both amalgamation and net:gross ratios in compressed object-based models at each hierarchical level. Right: Hierarchical full-field scale (4.3 km *3 km *250m) but bed resolution (ca 15 cm) model of a deep-water lobe reservoir build and upscaled in vbFIFT, and flow-simulated in Eclipse. After Zhang (2015), Manzocchi et al. (2016).

The Workflow

Overview

This workflow aims to provide a platform where geomodellers are able to create models with unconstrained Amalgamation Ratio and Net:Gross. This platform should guide the user with parametrization through a series of modelling and grid operations through workflows of object-, variogram- or MPS-based facies models. A general approach of this workflow is outlined by the steps below.

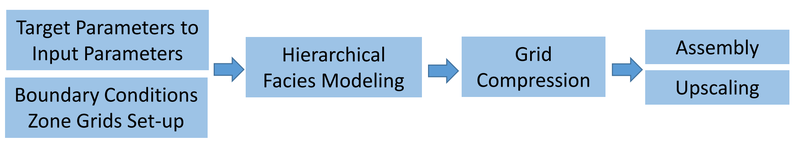

The designated steps can currently be achieved through the new plug-ins below:

1. Facies Designer

The Facies Designer plug-in allows the user to design plans for hierarchical modelling. A plan includes a hierarchical facies tree, and dimensional and target stacking parameters. Stacking parameters refer to Net:Gross and Amalgamation Ratio of the final model, and dimensional parameters to lengths, widths and thickness of the objects. The plug-in uses the appropriate compression model for the user-defined hierarchy to calculate the input parameters for facies modelling and compression step. The user can either use these parameters in Petrel facies modelling functions or in a simplified facies modeller implemented for the purpose of this workflow. The parameters are encapsulated within the workflow plan saveable in Petrel Workspace.

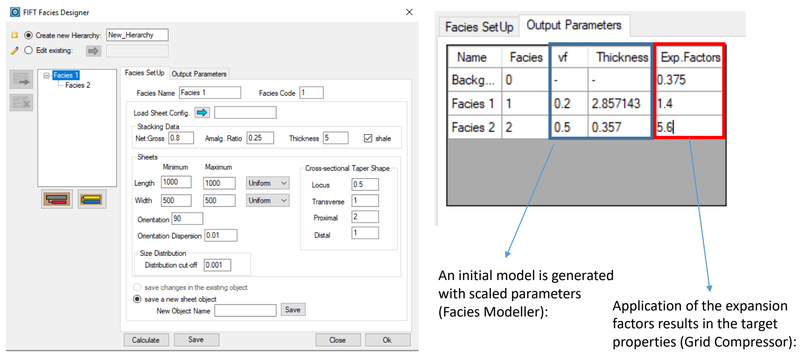

An initial model is generated with scaled parameters (Facies Modeller):

Application of the expansion factors results in the target properties (Grid Compressor):

Above: Input and output of parameters in the Facies Designer.

2. Model Creator

This plug-in sets up the boundary conditions, and zoning for surface-based models and rectangular models. In surface-based models, surfaces in point format define the top and base of every zone. In rectangular models, discretization, number of cells in x- and y- directions and thickness define zones with horizontal top and base. A single or multi-layered grid are output in the end for each user-defined zones for facies modelling using the FIFT facies modeller or Petrel facies modeling respectively.

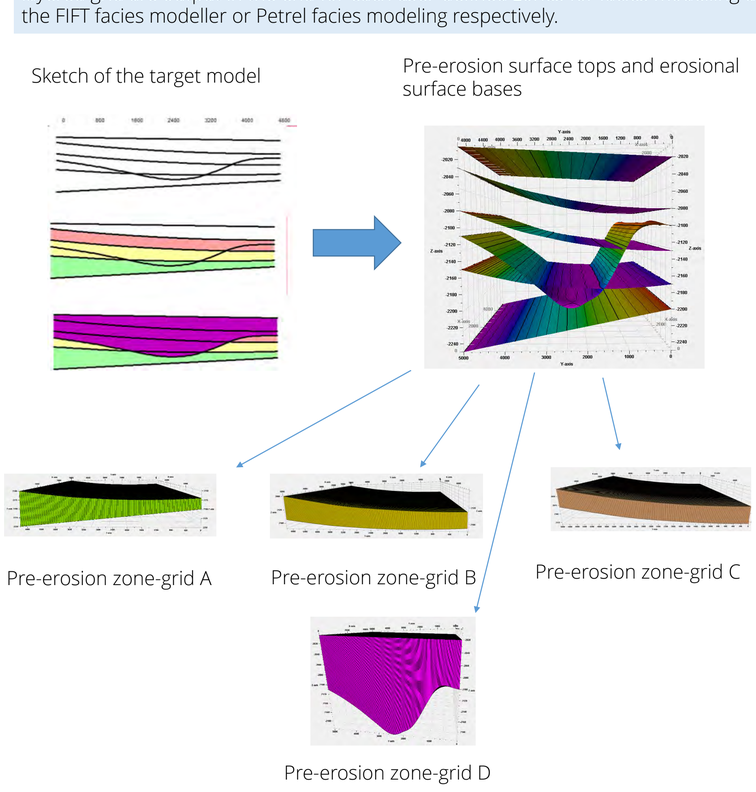

Above: Zone set-up using surfaces in the model creator. An independent grid is created for each zone to be performed separately in the modelling step.

3. Facies Modeler

A simple facies modeler was designed for the purpose of this workflow. This plug-in applies a workflow plan to a single layered zone grid. Based on stacking parameters (NTG, AR and thickness) of the workflow plan, it calculates a horizontal discretization (*dz*) and includes additional layers in the grid before modelling the facies. Next, the Facies Modeler distributes the facies in the grid where the objects of the top-level facies constitute the containers for the lower level facies. If a facies contains lower level objects, each object is mapped to a local grid in a pre-erosional state for further modelling. The local grids can be refined to allow smaller scale objects with thinner resolution.

In each level, objects are created up to the volume fraction in respect to that facies, and then the process is repeated for other facies of the same level. The amalgamation ratio is used as the input volume fraction. Objects are placed as such that younger beds erodes underlying beds. In the end, all the modelled grids are put together into a final grid.

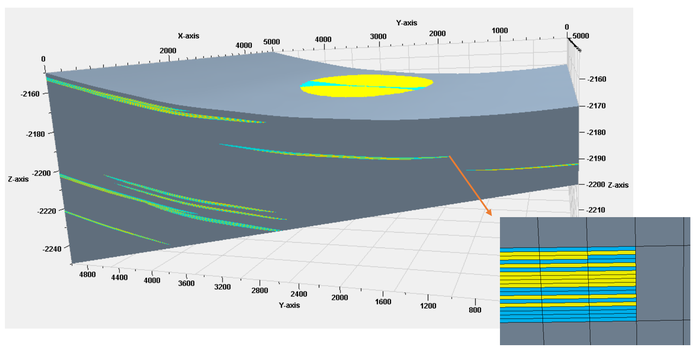

Above: Hierarchical facies model of Interbeds containing beds in a lobe element. The grid above has two distinct resolutions - one for the larger deterministic container and another for the stochastic interbeds containers.

4. Grid Compressor

In this step, the thicknesses of grid cells are modified to adjust the model to the target parameters. Once the model is generated with $v = AR$ to obtain the desired connectivity, the compressor plug-in increases the *NTG* by expanding sandstone cells and compressing shale cells, which leads to $AR < NTG$. The expansion factors depend on the number of hierarchical levels and the number of facies in each level. Nevertheless, it is a general rule that the expansion factors for shale and sandstone are $0 < E_{shale} < 1$ and $E_{sandstone} > 1$, respectively. Edges between sandstones and shale are compressed using the shale compression factor to reproduce more realistic geological structures.

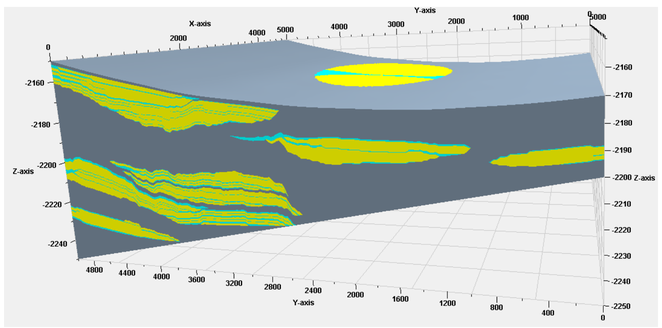

Above: Compressed model output from the Compressor Plug-in. In this model, both cells containing shale in grey and blue are compressed and the sand cells in yellow expanded.

5. Grid Upscaler (in Model Assembler)

The upscaler plug-in, which was a previous an independent software designed to decrease the grid size without affecting the overall connectivity, was turned into a functionality of the model assembler. The algorithm merges the grids cells with equivalent facies code vertically. The new Upscaling functionality at the Model Assembler allow users to select the facies in which grid cells must be upscaled before output the final model.

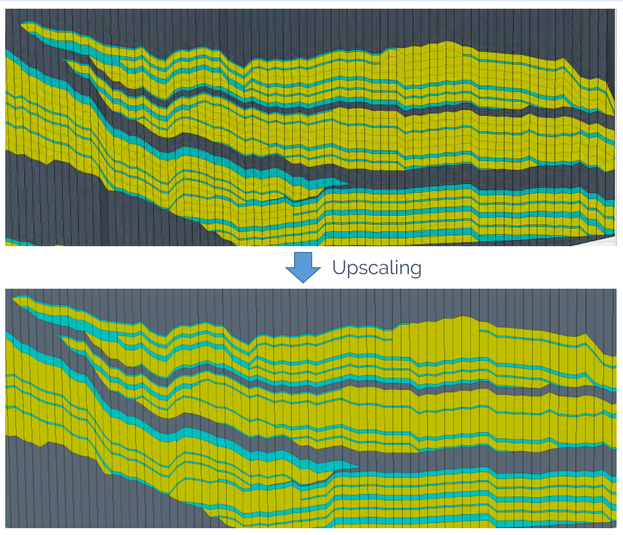

Above: Model output from the grid upscaler.

5. Model Assembler

Finally, the Model Assembler was created to merge all the zone models into one final model. In this step, zone grids are modified to conform with erosion rules. We consider that zones in shallower depths erode underlying zones and, if grid cells of different zones occupy the same location, the eroded cells are collapsed to accommodate the eroding cells. The example below shows that at some regions zone B was completely eroded and the cell stacks collapsed.

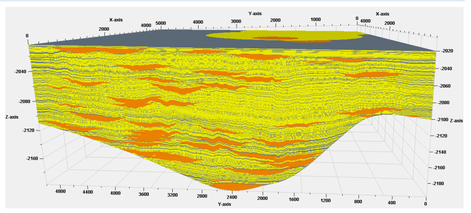

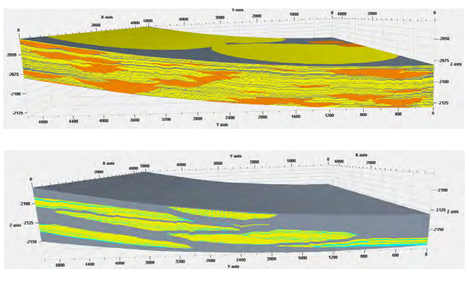

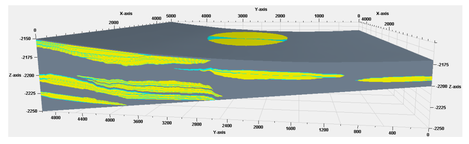

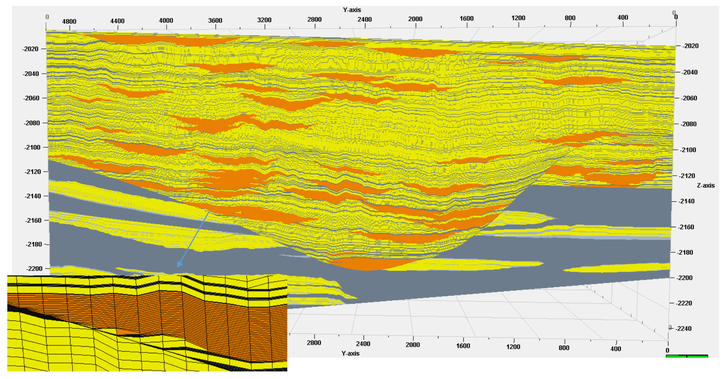

Above: The four zone models are merged into one final realisation.

Future Development Steps

1. Development of additional compression models for more general types of hierarchy.
2. Extension and improvement on the Facies Modeler Plug-in for more realistic geological realizations.
3. Development workflow worksteps equivalent to the Plug-ins.
4. Investigation of the impact that hierarchical compressed based model build using this workflow have in flow simulations.

References

1. Manzocchi, T., Walsh, J.J., Tomasso, M., Strand, J., Childs, C., & Haughton, P. 2007. *Static and dynamic connectivity in bed-scale models of faulted and unfaulted turbidites*. In: Structurally Complex Reservoirs. (Edited by Jolley, S.J., Barr, D., Walsh, J.J. & Knipe, R.J.). Geological Society of London, Special Publication 292, 309-336.

2. Manzocchi, T., Zhang L., Walsh D. A., Soni K. and Haughton P.D.W. (2016) New reservoir mdelling approaches for high net: gross, low amalgamation reservoir sequences. Presented at Atlantic Ireland 2016. Presentation available at: http://www.pip.ie/page/376.

3. Zhang, L.. *Quantitative characterisation and modelling of deep-water lobe deposits in a hierarchical context*. PhD thesis University College Dublin (2015).

This publication has emanated from research supported in part by a research grant from Science Foundation Ireland (SFI) under Grant Number 13/RC/2092 and co-funded under the European Regional Development Fund and by PIPCO RSG and its member companies.

Ireland's European Structural and Investment Funds Programmes 2014-2020
Co-funded by the Irish Government and the European Union

European Union
European Regional Development Fund

Science Foundation Ireland sfi For what's next

PIP Petroleum Infrastructure Programme

Provenance analysis of Irish Carboniferous sandstones:insights into sediment routing and palaeoclimate

iCRAG IRISH CENTRE FOR RESEARCH IN APPLIED GEOSCIENCES
Contact : martin.nauton@icrag-centre.org

NUI Galway OÉ Gaillimh

SORT sediment origins research team

Nauton-Fourteu, M.[1], Anders, B.[2],Tyrrell, S.[1], Morton, A. C.[3], Mark, C.[4], O'Sullivan, G. J.[5] and Chew, D. M.[5]

[1]Earth and Ocean Sciences, SORT, and Irish Centre for Research in Applied Geosciences (iCRAG), National University of Ireland Galway, Ireland
[2]Earth and Ocean Sciences and SORT, National University of Ireland Galway, Ireland
[3]HM Research Associates and CASP, University of Cambridge, UK
[4]UCD School of Geological Sciences, University College Dublin, Belfield, Dublin 4, Ireland
[5]Department of Geology and iCRAG, Trinity College Dublin, Ireland

Background and Rationale

In a sedimentary system, the sediment composition will be affected by multiple factors occurring at different stages (***right***). Labile phases such as feldspar can be removed through weathering, hence impacting hydrocarbon reservoir and aquifer reservoir quality. This results in sandstones with various compositions (e.g. quartz vs feldspathic arenites). Climate has a direct influence on the degree of weathering during transport, with for example, intense weathering conditions in hot and humid settings. Sediments can go through multiple sedimentary cycles, thus extending the exposure to weathering processes which complicates the understanding of palaeoclimate and changes in sediment composition. It is therefore essential to better constrain sediment routing. This can be done using a multi-proxy provenance approach, using minerals with different stabilities and resistance to weathering (***right***). Comparing the provenance of three Irish/UK Carboniferous basins can help towards answering some of these questions.

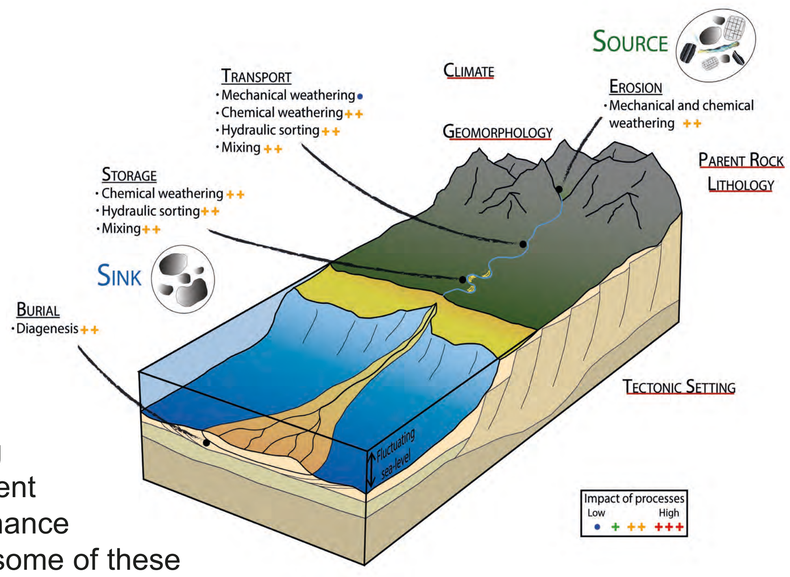

Multi-Proxy approach

Petrographic analysis

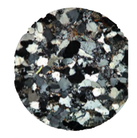

Information on sandstone composition

Zircon and Apatite U-Pb Geochronology

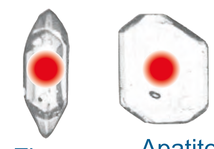

Zircon surviving recycling

Apatite weathered during transport
↳ first cycle?

Pb isotopes in K-feldspar

Labile phases
↳ most likely first cycle

Heavy mineral analysis

Information on recycling

NW Mayo — Mullaghmore Sandstone Formation ~340Ma

- Sub-feldspathic to feldspathic arenites
- Laurentian zircons and apatite populations
- Caledonian apatite population
- Most K-Feldspars with Laurentian affinity, some Caledonian grains.
  ↳ Sources from the North

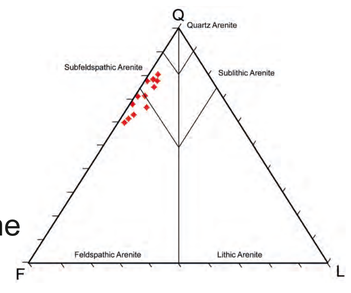

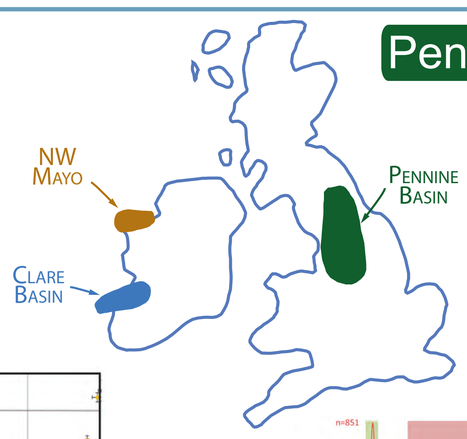

Zircon and apatite geochronology

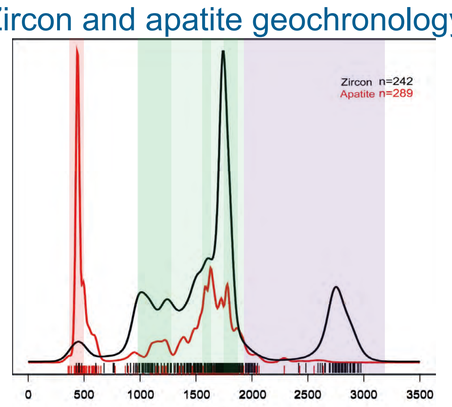

Pb in K-feldspar

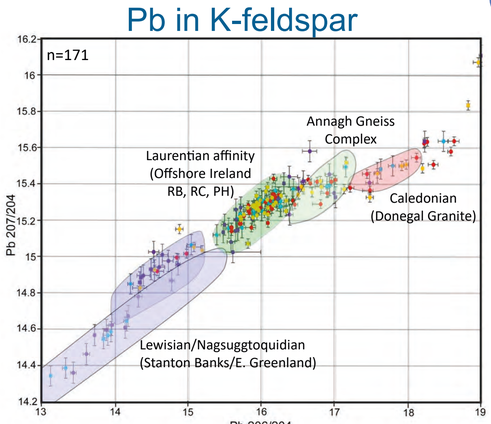

Pennine Basin — Millstone Grit - Namurian

- Sub-feldspathic arenites
- Laurentian and Caledonian zircon populations
- Two K-feldspar populations - at least two distinct sources
  ↳ Pennine delta flowing from the North

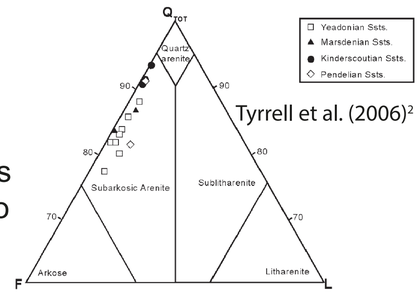

Zircon geochronology

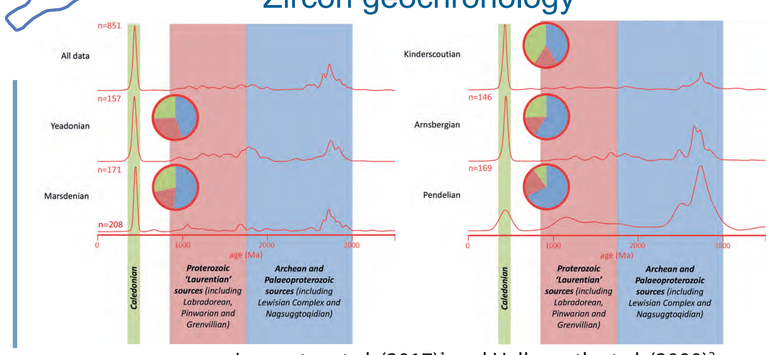

Lancaster et al. (2017)[1] and Hallsworth et al. (2000)[2]

Pb in K-feldspar

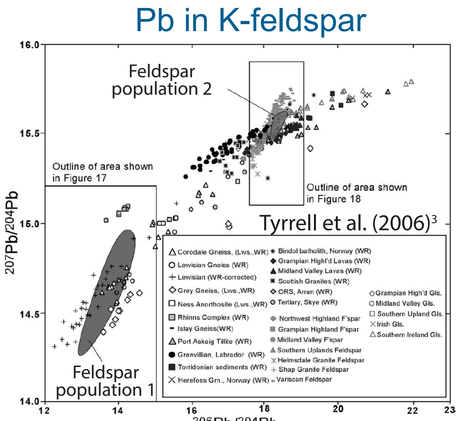

Clare Basin — Tullig Cyclothem - Namurian

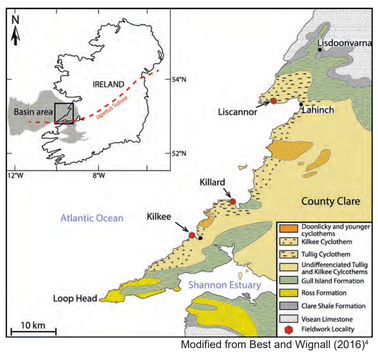

Modified from Best and Wignall (2016)[4]

- Petrographic analyses highlight quartz arenites (***below***).
- Heavy mineral assemblages show high zircon-tourmaline-rutile concentrations illustrating recycled sedimentary sources[5] (***below***).
- U-Pb geochronology data indicate detritus coming from both northern and southern sources. Comparing apatite and zircon data allows to identify the northerly derived zircon as recycled (***below***).
- Comparing these geochronology data with data from the Devonian Old Red Sandstone (ORS) on the Dingle Basin[6] (to the south), allows for further interpretation (***right***).
  ↳ These sandstones seem to be ultimately sourced from the south, with fresh input from southern terranes and recycling of sedimentary rocks from ORS basins.

Zircon and Apatite Geochronology

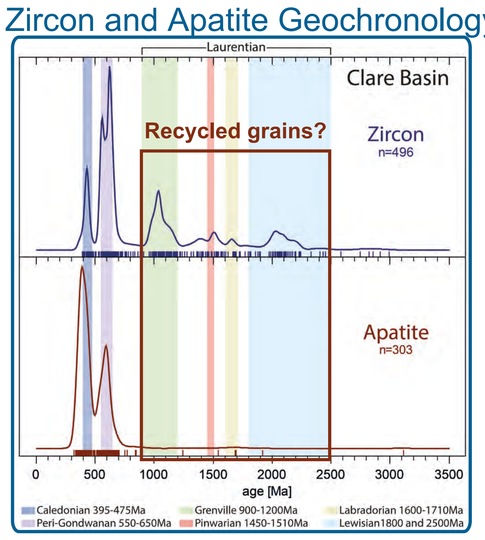

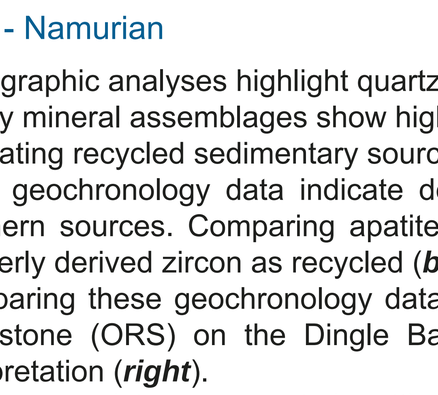

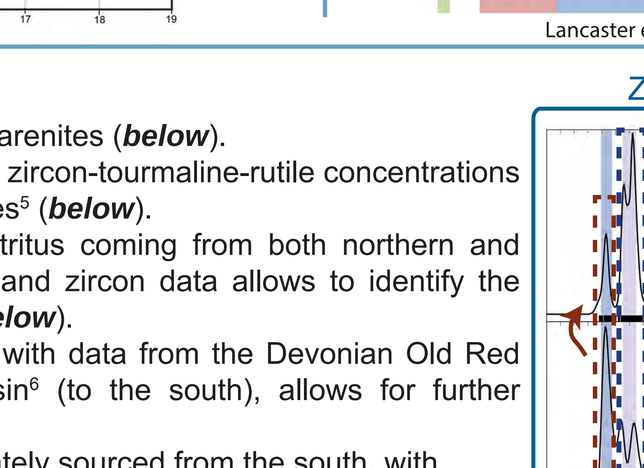

Zircon Clare vs. Dingle

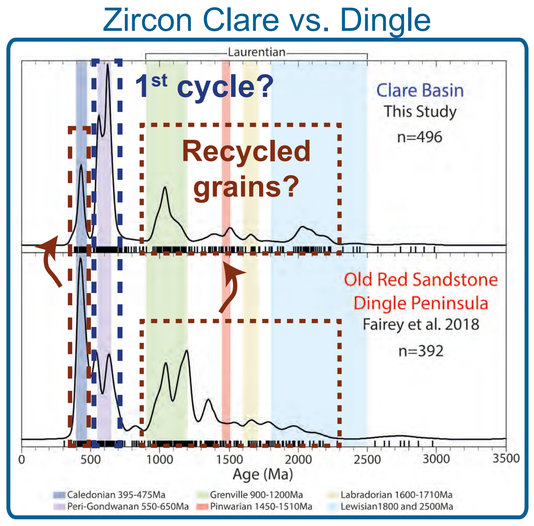

Apatite Clare vs. Dingle

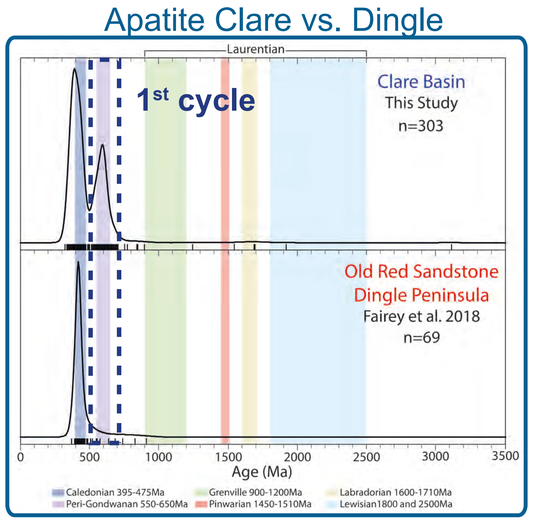

Comparison between basins

- Pennine and NW Mayo basins show immature sandstone compositions.
- Clare Basin sandstones are quartz arenites.
- Pennine and NW Mayo sandstones are most likely first cycle, with sources to the north (***right***).
- Clare Basin sandstones are derived from the south and have a more complex polycyclic origin with part of the sandstones being recycled from ORS basins and a part of fresh input from the south (***right***).

Conclusion

- Recycling is an important factor to take into account when investigating changes in sandstone composition as the sandstone maturity in the Clare Basin is due to recycling and not weathering during a first sedimentary cycle.
- A multi-proxy provenance approach can help distinguishing recycling, even in mature sandstones.
- Such work could help de-risking hydrocarbon exploration and helps towards a better understanding of palaeoclimate.

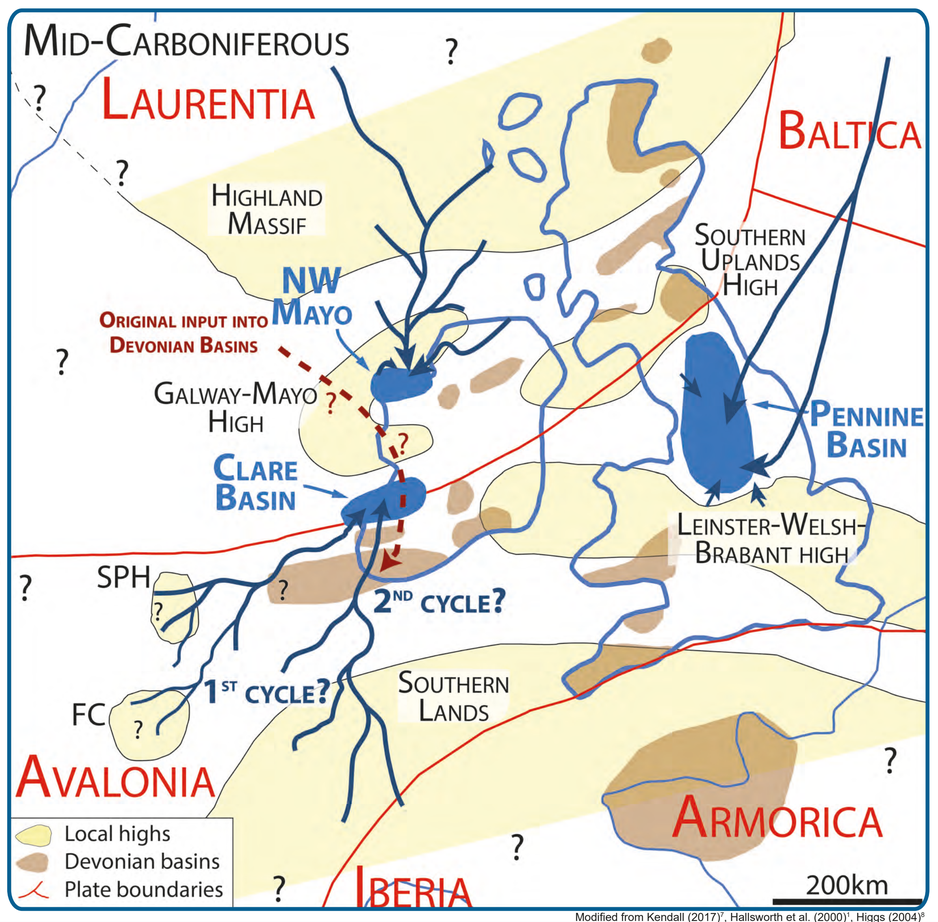

Modified from Kendall (2017)[7], Hallsworth et al. (2000)[1], Higgs (2004)[8]

Acknowledgments: Stephen Daly is acknowledged for the use of UCD crushing facilities.

This publication has emanated from research supported in part by a research grant from Science Foundaton Ireland (SFI) under Grant Number 13/RC/2092 and is co-funded under the European Regional Development Fund and by PIPCO RSG and its member companies.

Ireland's European Structural and Investment Funds Programmes 2014-2020
Co-funded by the Irish Government and the European Union

European Union
European Regional Development Fund

Science Foundation Ireland sfi For what's next

PIP Petroleum Infrastructure Programme

References:
[1]Lancaster et al., 2017, Interrogating the provenance of large river systems: multi-proxy in situ analyses in the Millstone Grit, Yorkshire.`
[2]Hallsworth et al., 2000, Carboniferous sand provenance in the Pennine Basin, UK: constraints from heavy mineral and detrital zircon age data.
[3]Tyrrell et al., 2006, The use of the common Pb isotope composition of detrital K-feldspar grains as a provenance tool and its application to upper Carboniferous paleodrainage, Northern England.
[4]Best and Wignall, 2016, A Field Guide to the Carboniferous Sediments of the Shannon Basin, Western Ireland.
[5]Hubert, 1962, A zircon-tourmaline-rutile maturity index and the interdependence of the composition of heavy mineral assemblages with the gross composition and texture of sandstones.
[6]Fairey et al., 2018, The provenance of the Devonian Old Red Sandstone of the Dingle Peninsula, SW Ireland; the earliest record of Laurentian and peri-Gondwanan sediment mixing in Ireland.
[7]Kendall, 2017, The Old Red Sandstone of Britain and Ireland — a review.
[8]Higgs, 2004, Ross and Bude Formations (Carboniferous, Ireland and England): reinterpreted as lake-shelf turbidites.

Provenance of Mesozoic sediments in the North Celtic Sea and St. Georges Channel Basin's: Exploring transition Fuels

Odhrán McCarthy([1,4]), Dr. Pat Meere([1,4]), Dr. Kieran Mulchrone([2,4]), Dr. David Chew([3,4]),
[1] School of Biological, Environmental and Earth Sciences, University College Cork. [2] School of Mathematics – NUI Cork. [3] Department of Geology, Trinity College Dublin. [4] iCRAG

Introduction

Establishing the provenance of sediments from source to sink is beneficial in gas exploration. The North Celtic Sea Basin (NCSB) and St. George's Channel Basin (SGCB), offshore of Irelands east coast, are proven economic prospects and the subject of this study (Fig 1. & 3.). This study will adopt a multidisciplinary approach including quantitative sedimentary petrology, detrital single grain geochronology and heavy mineral analysis (HMA) to elucidate the provenance and transport mechanisms of these Mesozoic Basins.

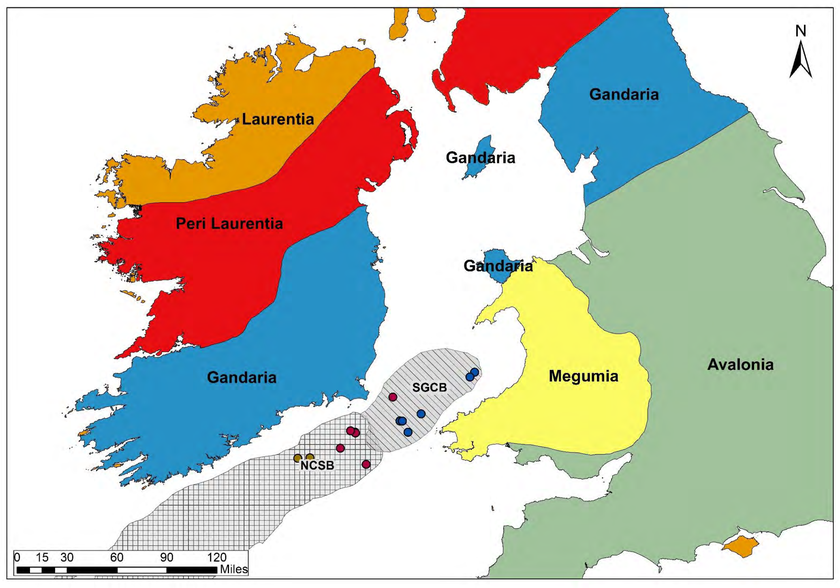

Interpreted Diagram of the Paleocontinents of Ireland and the UK. Paleocontinent's feed characteristic sediment allowing for the differentiation of source regions via HMA, Geochronology, sedimentary petrography.

Key Points

- Spatial and temporal variation in HMA suggesting limited basin connectivity
- Garnet identified as a key indicator mineral for the Jurassic with distinct source's in the Welsh basin and Wexford formation
- HMA & Apatite Geochronology can constrain the Triassic Budleighensis connection to Irish sea basin's from central UK basin
- New Pleinsbachian and Aalenian Zircon and Apatite age data has been collected and is being processed

Available Sediment Source regions Of the Mesozoic

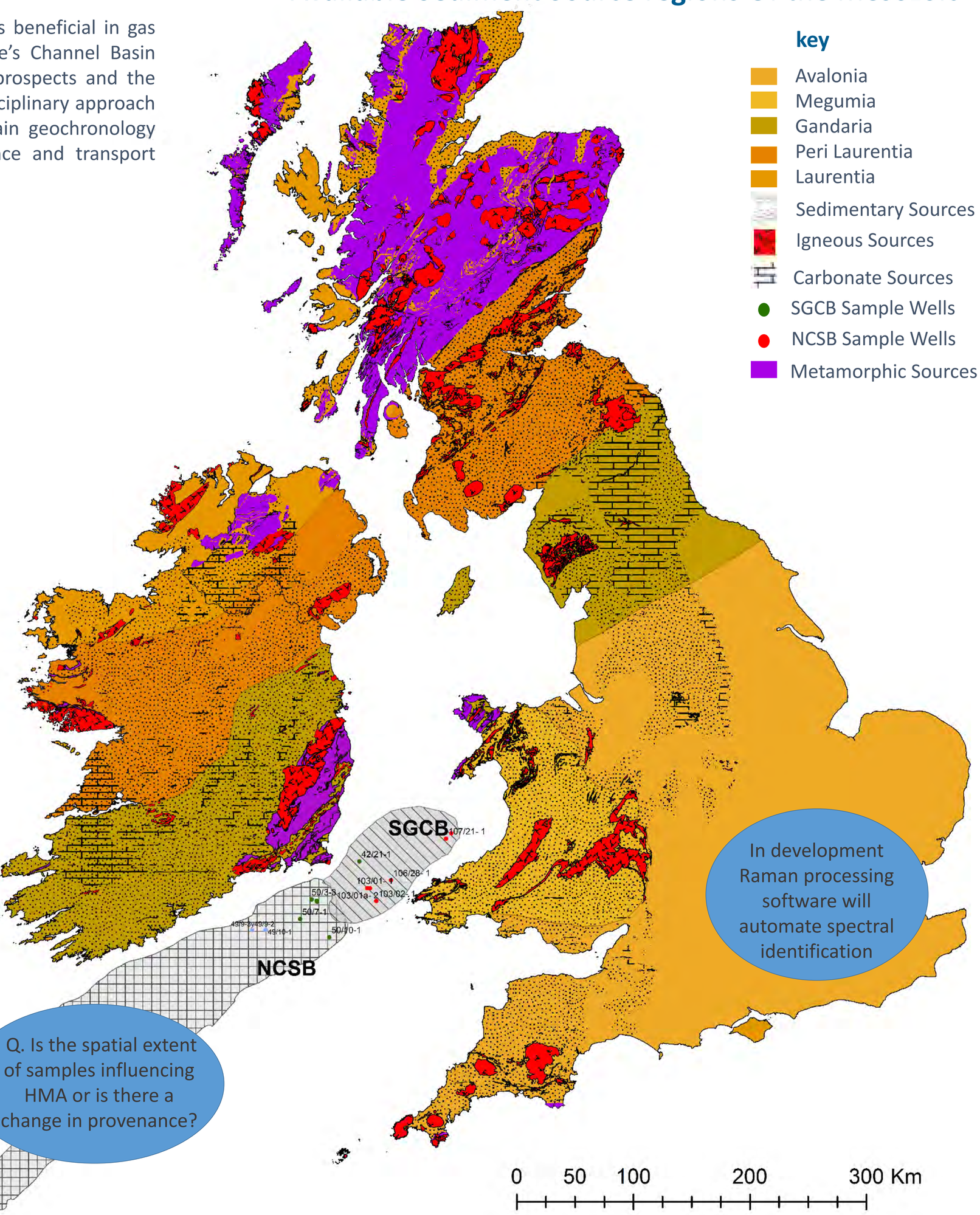

Heavy Mineral Analysis Results

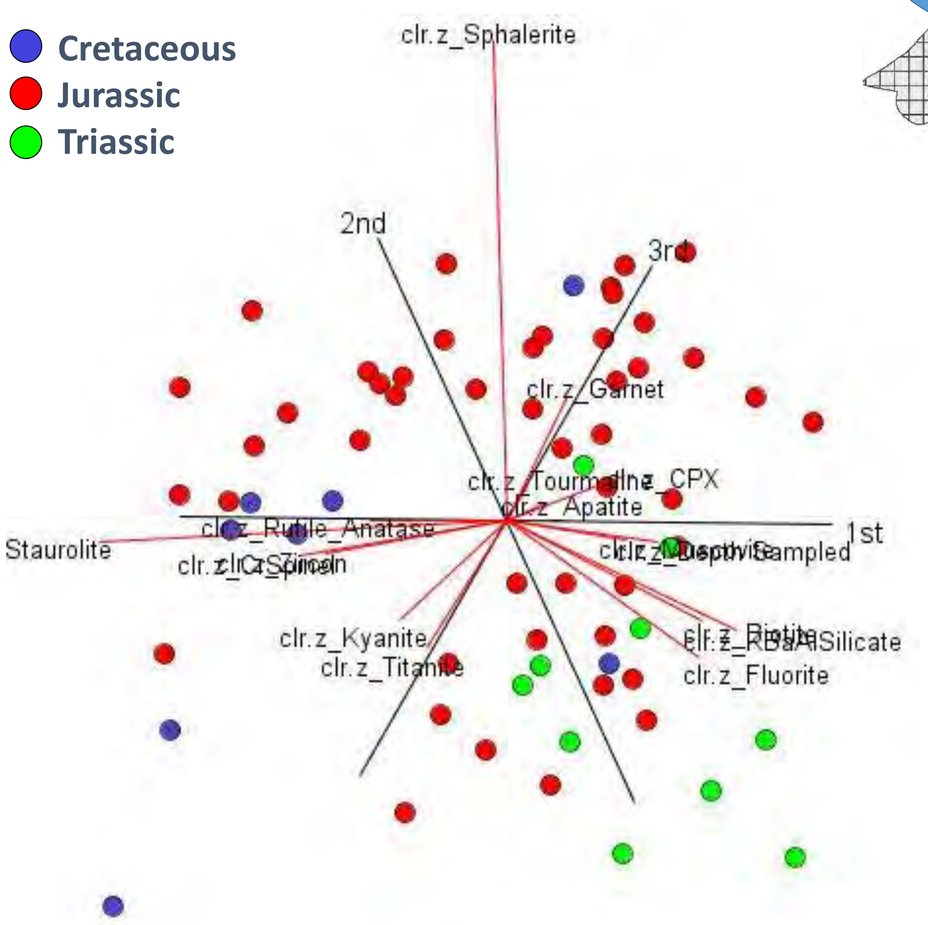

Principle Component analysis (PCA) biplot of heavy mineral ratios sampled throughout the NCSB and SGCB at different periods. Note the distinct temporal variance

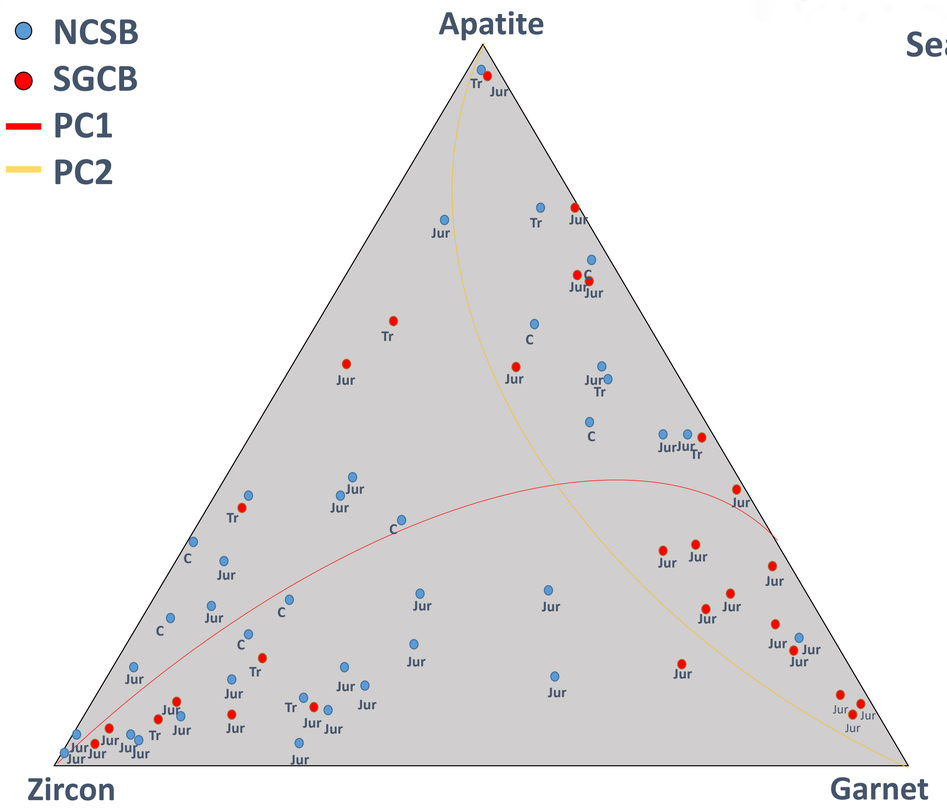

Centred ternary diagram of HMA PCA results highlighting the inter period and inter basin variation (T – Triassic, Jur- Jurasssic and C – Cretaceous samples)

Sea level Change through The Mesozoic

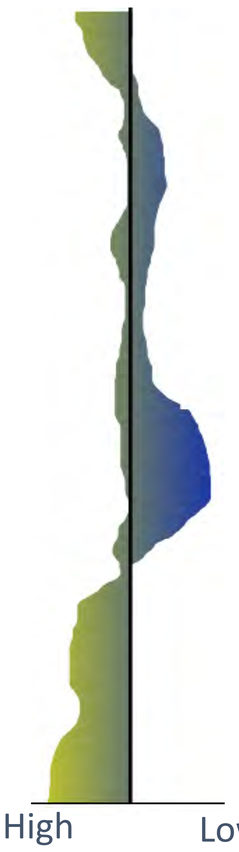

This publication has emanated from research supported in part by a research grant from Science Foundation Ireland (SFI) under Grant Number 13/RC/2092 and is co-funded under the European Regional Development Fund and by PIPCO RSG and its member companies.

Thermochronological & Geochronological Results from the Goban Spur, offshore Ireland

Rémi Rateau[1*], David Chew[1]

[1] Department of Geology, Trinity College Dublin - Irish Centre for Research in Applied Geosciences

* remi.rateau@icrag-centre.org

1. Introduction

Goban Spur geological context

- Starved passive margin
- Margin resulting from the opening of the southern North Atlantic from Jurassic times to now
- Conjugate margins: North Iberia Margin (NIM) & Flemish Cap (FC); a paleo-triple junction.
- Suspected presence of transitional crust = exhumed mantle

Samples

- 6 samples from Ifremer dredges:
  - 3 samples from **Granite Cliff 4000 (GC4)** 24, 25, 26
  - 2 samples from **Menez Bihan (MB)** 27, 28
  - 1 sample from **Mac Erca Castle (MEC)** 29

Granite Cliff 4000 (GC4) and Menez Bihan (MB)

- Tips of partially buried rotated fault block (see seicmic section below
- Located in the hyper-extended part of the margin

Mac Erca Castle (MEC

- Located east of the Pendragon Escarpement
- Seabed anomaly, probably tip of tilted fault-block

Seismic & Geosection

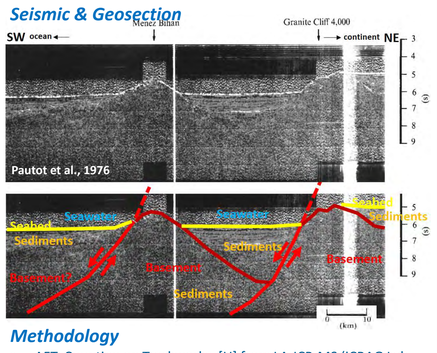

Methodology

- AFT: Counting on Trackworks, [U] from LA-ICP-MS (iCRAG Lab, Trinity College Dublin, Ireland)
- AHe: [U,-Th-Sm] solution ICP-MS; [He] EI-MS (UCL Geochemistry Lab, London, UK)
- U/Pb on zircon and apatites [U,Pb] from from LA-ICP-MS (iCRAG Lab, Trinity College Dublin, Ireland)
- *Data reduction*: Iolite 2.5, VizualAge, VizualAge UcomPbine, Isoplot 4.15
- *Interpretation and thermal modelling*: DensitPlotter, RadialPlotter, QTQt

Geodynamical Context

★ Study area = Goban Spur

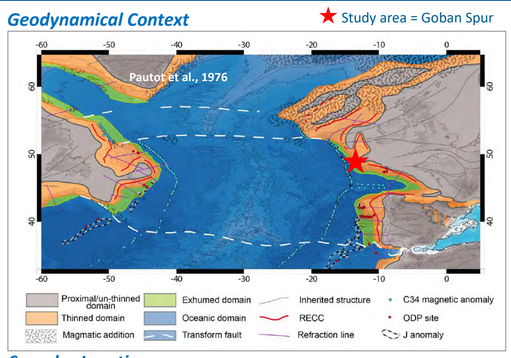

Samples Location

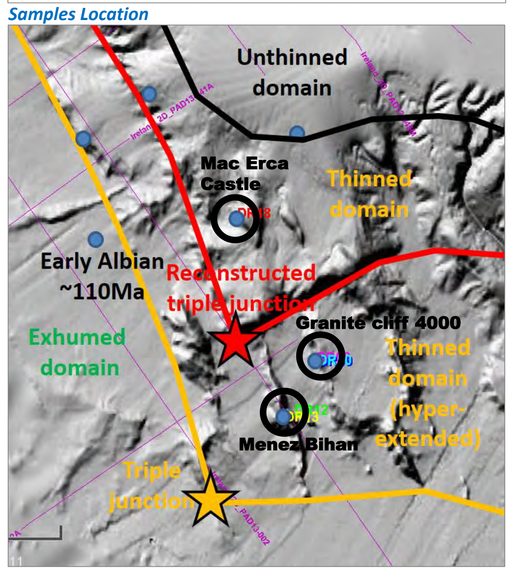

2. Goban Spur Samples Results

#	Lithology	Loc#	Zr U/Pb* Cores Ma	Zr U/Pb* Ma	Ap U/Pb* Ma	AFT** Ma	MTL µm	AHe*** Ma	[U] ppm	Cl %wg	Dpar µm
24	**Granite**	GC4	**406 ± 13** (1c) **563 ± 18** (1c)	**297 ± 1** (47c/56)	**302 ± 4** (40d/40)	**197 ± 11** (39/40x)	**12.0** (291)	88-**131**-**136**-220 (3/5/5)	**44**	**.26**	**2.0**
25	**TBC**	GC4	None	**~2700 Ma** (48d/49)	**1710 ± 16** (34d/40)	**42 ± 3** (40/40v)	**(13.6)** (6)	39-**39**-**56**-74 (4/5/6)	**20**	**.12**	**1.5**
26	**Granite**	GC4	**354 ± 21** (1c) **418 ± 9** (1c) **575 ± 9** (1c) **605 ± 9** (1c) **1767 ± 56** (1c)	**296 ± 2** (40c)	**298 ± 5** (40d/40)	**222 ± 11** (40/40x)	**13** (83)	63-**104**-**112**-281 (3/5/6)	**19**	**.11**	**1.6**
27	**Pyriclasite**	MB	**394 ± 16** (1c/17) **510 ± 19** (1c/17) **575 ± 8** (8c/17)	**294 ± 8** (7d/17) (vein or contamination?)	**447± 7** (40d/40) (478 ± 33) (5d/40)	**284 ± 9** (38/40v)	**12.9** (152)	No data	**21**	**.20**	**2.0**
28	**Granite**	MB	**360 ± 13** (1c) **389 ± 13** (1c) **429 ± 17** (1c) **556 ± 17** (1c) **612 ± 20** (1c) **1153 ± 42** (1c)	**289 ± 2** (42c)	**295 ± 4** (39d/40)	**143 ± 6** (40/40x)	**13.1** (101)	94-**94**-**101**-101 (4/4/6)	**20**	**.12**	**1.7**
29	**Sand**	MEC	No data	**Youngest: 280 ± 9** (1c/104) **Peaks: 421 ± 3** (15c/104) **463 ± 3** (19c/107) **567 ± 14** (15c/107) **1014 ± 19** (15c/107) **Oldest:** 2003 ± 67 (1c/104)	(460 ± 17) (6d/8) (535 ± 39) (2d/8)	**(126 ± 10)** (8/8v)	**(11.8)** (15)	No data	**31**	**.11**	**1.7**

 # GC4 = Granite Cliff 4000; MB = Menez Bihan; MEC = Mac Erca Castle

** U/Pb age = Age ± 2σ (number of grains included in age calculation/number of grains dated, c = age from concordant grains, d = age from discordia intercept)*

*** AFT age = central age ± 1σ (number of grains used in central age calculation/number of grains analysed, v = Chi test ok, x = failed chi-test)*

MTL = mean track length of TINCLEs (number of tracks used in MTL calculation)

**** AHe age = F_T-corrected ages: minimum age among all ages – minimum age among cluster of close ages – maximum age among cluster of close ages – maximum ages among cluster of all ages (number of grains in cluster, number of grains with meaningful ages, total number of grains analysed)*

Age colour code: Tertiary, Cadomian, Mesozoic, Proterozoic, Variscan, Archean, Caledonian

3. Thermochronological & geochronological Data from Granite Cliff 4000 & Menez Bihan

1) Late Variscan Granites

- All three granites have consistent zircon and apatites ages between 289-302 Ma, i.e. Late Variscan, similar to, and in the alignment of the Cornwall granites
- The granite samples seem to be associated with some positive magnetic anomalies that might represent the extent of the batholiths. They seem to be both on the edges of the batholiths

2) Sample 24 & 26 shared geological history

- Both dredges started and ended at the same water depth ~ 3200 to 4200mSS, cross each other at mid-slope and are separated at most by 1.3 km. Both recovered *'abundant large blocks of granitic rocks reaching up to 30cm; many of them appear clearly "in place", other only "possibly in place."' (Auffret et al., 1979)*
- Therefore, we conclude that both granite samples (#24 & #26) come from the same granite batholith and belong to same tectonic unit (a tilted fault block) and have most probably experienced the same tectonic and erosional (i.e. thermal history)
- One unknown is the location of these samples in the dredges: at most, these two samples might have a difference of bathymetry of 1000m (i.e. the difference the highest and lowest points of the dredges)

Method	#24	#26	#28	Source
U/Pb, zircon	297 ± 1	296 ± 2	289 ± 2	This study
U/Pb, apatite	302 ± 4	298 ± 5	295 ± 4	This study
Rb/Sr, whole rock	275 ± 3	270	251 ± 2	Auffret et al., 1979
Rb/Sr, biotite	281	N/A	N/A	Auffret et al., 1979
K/Ar, biotite	N/A	290	207 ± 2	Auffret et al., 1979

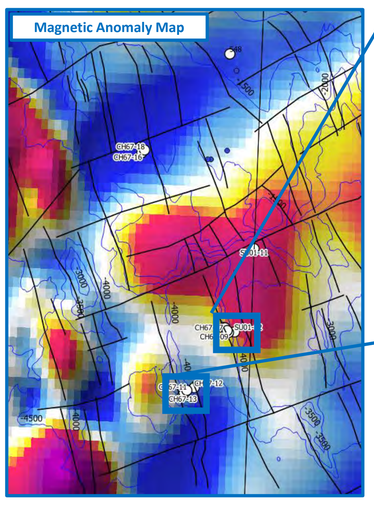

Fault-bend folding associated with normal faults in Porcupine Basin

Delogkos, E., Saqab, M.M., Walsh, J.J., Roche, V., Childs, C.

IRISH CENTRE FOR RESEARCH IN APPLIED GEOSCIENCES

UCD DUBLIN

1. Introduction

Normal faults in the Porcupine Basin often have associated hanging wall folding (Fig. 1) the origin of which is sometimes unclear, with interpretations ranging from inversion through to salt-related folding. This study investigates the development of these structures using a fault-bend folding model, in which folding is linked to irregular fault surface geometries arising from different processes including refraction and segmentation. The underpinning conceptual framework of this model is that a fault with an average dip and constant displacement on a large-scale, will have irregular geometries on smaller scales, the presence of which will generate fault-related folds. The purpose of the study is to provide a rationale for hanging wall fold development linked to fault geometry, without a requirement for additional complicating factors, such as inversion and halokinesis. Practical implications of this type of deformation include (i) definition of across-fault juxtaposition and sealing and (ii) the generation of hanging wall fault-related traps, both in terms of four-way and three-way dip closures.

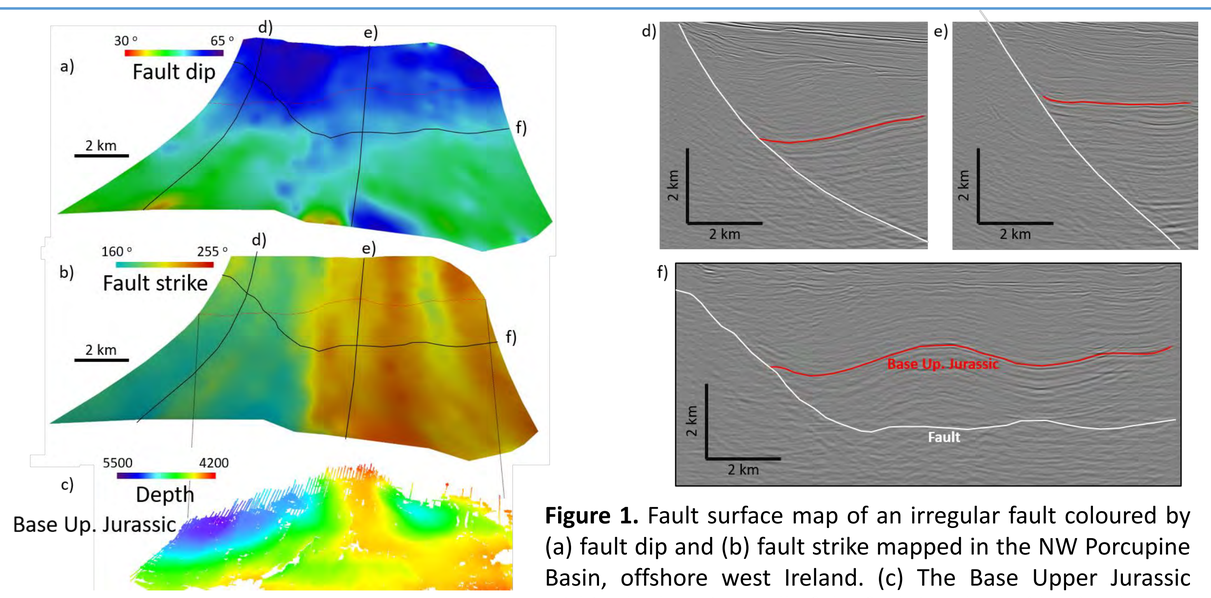

Figure 1. Fault surface map of an irregular fault coloured by (a) fault dip and (b) fault strike mapped in the NW Porcupine Basin, offshore west Ireland. (c) The Base Upper Jurassic within the hanging wall of the fault is coloured by depth.

2. A quantitative model of fault-bend folding and associated strain partitioning

A simple model is presented for the range of deformation arising from movement on fault surface irregularities, with fault-bend folding generating geometries reminiscent of both normal drag and reverse drag (Fig. 2). Our deformation algorithm assumes a constant discontinuous displacement (Dd) and total throw (Tt) boundary conditions accommodated by deformation which is neither constant bed length nor constant volume (e.g. Groshong et al., 2012). The hanging wall deformation is illustrated by assuming inclined simple shear with axial planes that have a dip equal and opposite to that of the fault surface (Groshong, 1989). This model highlights how along-fault displacements are partitioned between continuous (i.e. folding) and discontinuous (i.e. displacement) strain along fault bends characterised by the full range of fault dip changes (Figs. 2 and 3). The fault throw, the pre-eminent measure of the displacement on normal faults, can be subject to errors of +/- ca. 10% for realistic fault bend geometries (ca. 30°), even on sub-planar faults with constant displacement (Fig. 2).

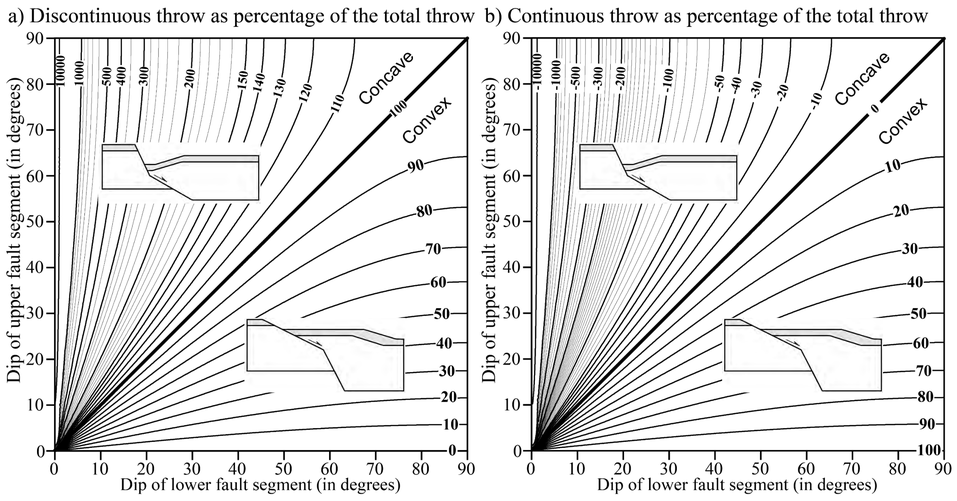

Figure 2. Graphs showing the relationship between (a) the discontinuous and (b) the continuous throw, as a proportion of the total throw, and the dips of the lower and upper fault segments of a sharp fault bend.

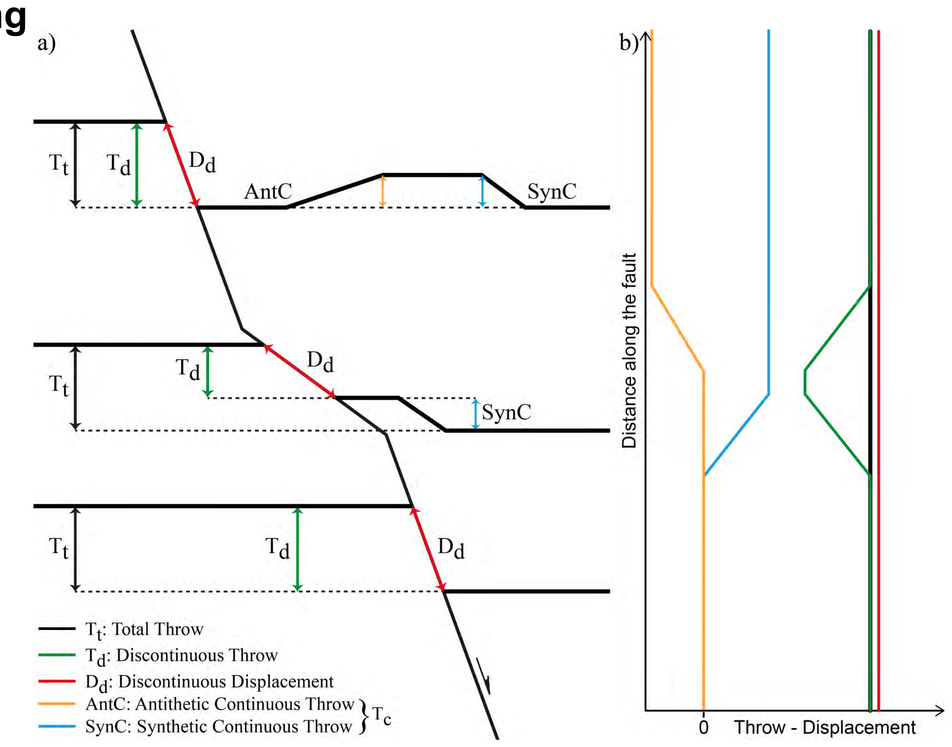

Figure 3. (a) Schematic diagram of a fault comprising three fault segments with intervening sharp convex and concave bends. The total throw (Tt) is partitioned into the discontinuous throw (Td) and the continuous throw (Tc); the latter comprises the antithetic continuous throw (AntC) and the synthetic continuous throw (SynC). (b) Throw-displacement profiles along the fault in (a) showing complementary variations of discontinuous and continuous throws in which the total throw and discontinuous displacement have constant gradients that are not affected by fault bends.

3. Geological case studies

Natural examples highlight the principal features of relatively simple normal faults displaying hanging wall deformation similar to those of our fault-bend folding model (Figs 2 and 3), and demonstrating the applicability of the associated strain partitioning. A recurring feature is that a proportion of the hanging wall deformation is accommodated by secondary faulting, that is synthetic and/or antithetic to the main fault. Whether hanging wall deformation is accommodated by folding and/or secondary faulting is a scale dependent issue, often reflecting the mechanical properties of faulted sequence and the amount of shear strain accommodated.

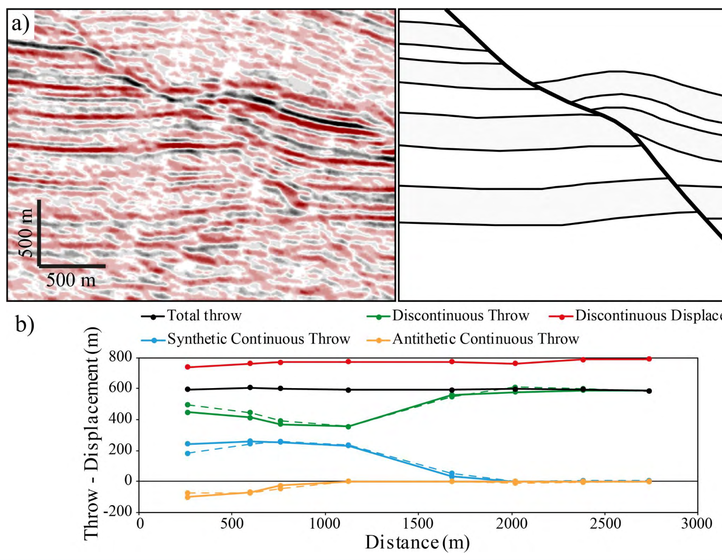

Figure 4. (a) Uninterpreted and interpreted seismic section of a non-planar fault and associated hanging wall deformation in the NW Porcupine Basin, offshore west Ireland (Saqab et al., 2016). (b) Throw-displacement profiles along the fault in (a) showing the complementary variations of the discontinuous and continuous throws and the unaffected distribution of both total throw and discontinuous displacement in the vicinity of fault bends.

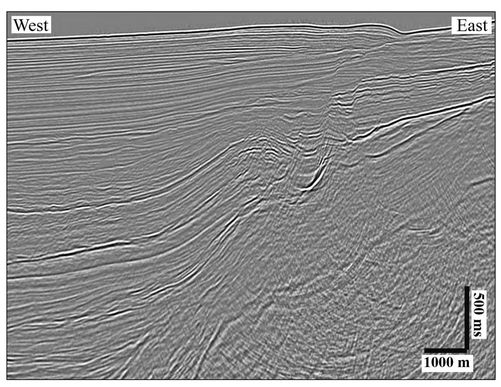

Figure 5. Seismic section illustrating hanging wall deformation associated with high shear strain accommodated along an irregular fault surface in the eastern Porcupine Basin, offshore west Ireland.

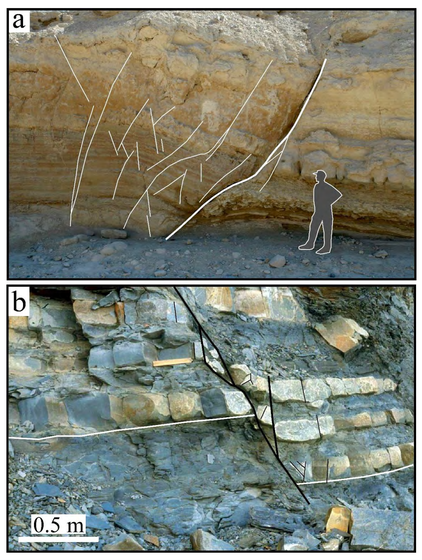

Figure 6. (a) Fault with a throw that exceeds the 4 m cliff height from Wadi Matulla, Sinai, Egypt showing a rollover anticline associated with a fault surface which has a sigmoidal shape (after Fossen 2016). (b) Fault with 0.5m throw contained within the Liassic limestone - shale sequence of Kilve, Somerset, UK, showing normal drag arising from a convex upward bend (and fault steepening).

4. Implications and future work

- An important implication of the proposed model is that the local throws measured along irregular normal fault surfaces will vary with values greater or less than the total throw.
- This model suggests that throw measurements that do not incorporate bend-related deformations will be subject to throw errors of +/- ca. 10%.
- The displacement partitioning into continuous rather than discontinuous deformation can affect across-fault juxtapositions, and can have a profound impact on fault seal assessments.
- The development of associated folding can also generate potential fault-related downside traps to natural resources.
- Future work will focus on understanding the role of the three-dimensional fault geometries (i.e. bends along both fault strike and dip; Fig. 1) on the development of hanging wall folding.

References

Fossen, H., 2016. Structural geology. Cambridge University Press.
Groshong Jr, R.H., 1989. Half-graben structures: Balanced models of extensional fault-bend folds. Geological Society of America Bulletin, 101(1), pp.96-105.
Groshong Jr, R.H., Withjack, M.O., Schlische, R.W. and Hidayah, T.N., 2012. Bed length does not remain constant during deformation: Recognition and why it matters. Journal of Structural Geology, 41, pp.86-97.
Saqab, M.M., Child, C., Walsh, J.J. and Delogkos, E., 2016. Multiphase deformation history of the Porcupine Basin, offshore west Ireland. In Atlantic Ireland Conference.

This publication has emanated from research supported in part by a research grant from Science Foundation Ireland (SFI) under Grant Number 13/RC/2092 and co-funded under the European Regional Development Fund and by PIPCO RSG and its member companies.

Ireland's European Structural and Investment Funds Programmes 2014-2020
Co-funded by the Irish Government and the European Union
European Union
European Regional Development Fund
Science Foundation Ireland sfi For what's next

Acknowledgements:
Seismic and well data were provided by the Petroleum Affairs Division of the Department of Communications, Climate Action and Environment. We thank them both for providing access to the data which underpins our study and we also thank the member companies of PIP, the industry partners for iCRAG's hydrocarbon research.

FAULT ANALYSIS GROUP
PIP Petroleum Infrastructure Programme

Sand detachment mechanisms on the modern seafloor: A review of processes and examples

John W. Counts, Lawrence A. Amy, Peter Haughton, Aggeliki Georgiopoulou

IRISH CENTRE FOR RESEARCH IN APPLIED GEOSCIENCES

UCD DUBLIN

Abstract

Sand bodies in deep marine environments can become isolated from their sources in a variety of ways, creating bed geometries that can act as stratigraphic traps after burial. Although stratigraphic trapping mechanisms have been well-studied in the subsurface and in outcrop, a comprehensive review of sand detachment in the modern deep sea has not previously been undertaken. Here, we reviewed data from over 200 publications in the form of sediment cores, seismic lines, and seafloor bathymetry and backscatter maps, in order to reveal the primary ways in which sands initially emplaced in deep-sea channels and canyons may become disconnected from the shelf.

- *Sand-filled channels may be destroyed or eroded through large-scale slope failures, cutting off deepwater lobes and the distal parts of turbidite systems.*
- *Slope failures can also generate isolated sands themselves, as they result in mass transport deposits that can transform into turbidity currents that partition sand into discrete beds.*
- *Within existing channels, turbidity currents can generate erosion at points where the flow becomes unconfined, creating a channel-lobe transition zone (CLTZ) characterized by scours and non-deposition of continuous sands.*
- *Meandering submarine channels on low-gradient slopes may create smaller isolated sand bodies through flow stripping and meander loop cutoff, becoming separated from their primary sources by abandoned channels and hemipelagic muds.*
- *Slope-parallel contour currents may form erosive moats at the bases of slopes and rework sands into deep-sea contourites.*

While many post-depositional and post-burial processes can also affect the connectivity of subsurface reservoirs, some of these syndepositional detachment mechanisms are known to result in effective isolation on their own, forming traps in productive hydrocarbon systems. By examining these processes in the modern marine environment where the geologic and oceanographic context is known, their controls and occurrence can be analyzed in a way not possible with other data sets. As such, this study provides a new perspective on an economically important aspect of sedimentary geology, and is meant to serve as a resource for those working on analogous deposits in the subsurface.

Sediment pathways to the deep sea

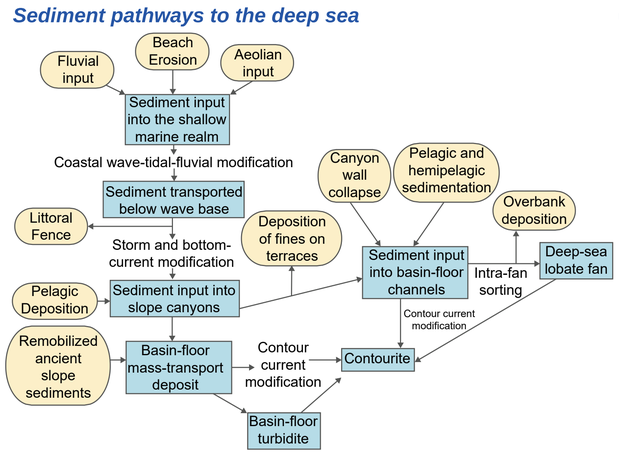

Clastic sand-dominated sediments in the marine realm are affected by numerous processes before reaching their point of final deposition in deepwater basins.

Because some detachment mechanisms are dependent upon the grain size and sorting of sediment, the complexity and combination of these pre-detachment processes decrease the predictability of the composition of end-point sediments, and therefore affect the ability to tie detachment to larger-scale oceanographic, geographic, and geologic parameters.

Observed detachment mechanisms

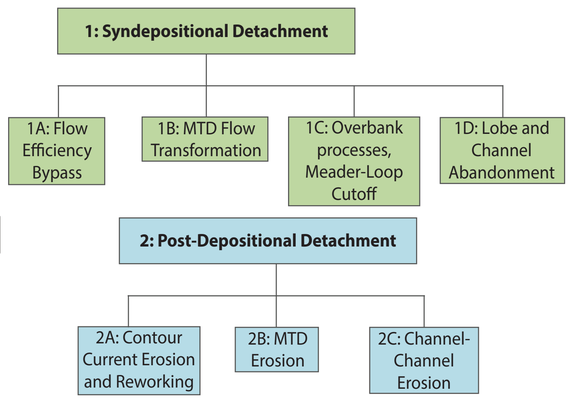

The detachment mechanisms described here have been classified according to both the timing of detachment and the detachment process. Syndepositional detachment occurs when pinchout formation is contemporaneous with deposition of the detached sandbody. Post-depositional detachment is the result of erosional truncation of an existing attached system. Each of these mechanisms is discussed in turn below, with examples from modern deepwater systems.

Selected occurrences of detached sands on the modern seafloor

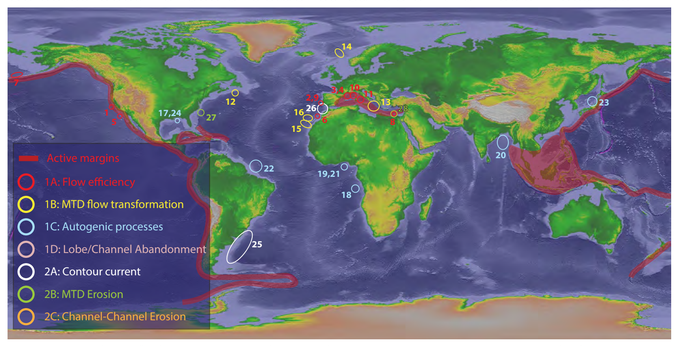

1: Monterey canyon and Fan (Paull et al., 2005; Fildani et al., 2006)
2: Lisbon/Cascais canyon (Wynn et al., 2002; Lastras et al., 2009)
3: Rhone fan (Wynn et al., 2002; Bonnel et al., 2005)
4: Valencia Fan (Palanques et al., 1995)
5: Navy Fan (Carvajal et al., 2017)
6: Agadir system (Ercilla et al., 1998; Stevenson et al., 2015)
7: Umnak/Pochnoi (Kenyon and Millington, 1995)
8: Rosetta (Migeon et al., 2010)
9: Setubal (Wynn et al., 2002; Lastras et al., 2009)
10: Var (Mas et al., 2010; Mulder et al., 1998)
11: Golo (Gervais et al., 2004; 2006)
12: Grand Banks (Piper and Aksu, 1987)
13: Augias (Heike and Werner, 2000)
14: Storegga (Haflidason et al., 2005; Bryn et al., 2005)
15: Sahara (Georgiopoulou et al., 2009b)
16: Agadir/Madeira (Talling et al., 2007)
17: GOM/Desoto Canyon (Posamentier and Kolla, 2003)
18: Congo (Babonneau et al., 2010)
19: Niger Delta (Hansen et al., 2017)
20: Bengal Fan (Emmel and Curray, 1983)
21: Benin Fan (Deptuck et al., 2007)
22: Amazon (Jegou et al., 2008)
23: Toyo (Nakajima et al., 1999)
24: Mississippi (Bentley et al., 2016)
25: Argentine Margin (Hernández-Molina et al., 2009)
26: Gulf of Cadiz (García et al., 2008)
27: Hatteras Transverse Canyon (Gardner 2016)
28: Rosetta Slide (Garziglia et al., 2008)

Global map of selected locations of detached sandbodies on the seafloor. The examples discussed here all occur on the modern or relatively recent seafloor, and ulilize core, backscatter, and/or bathymetric data to determine sedimentological properties of detached deposits. The modern seafloor allows these sediments to be put into a much more detailed geological and oceanographic context than their ancient counterparts.

Flow Efficiency and Bypass

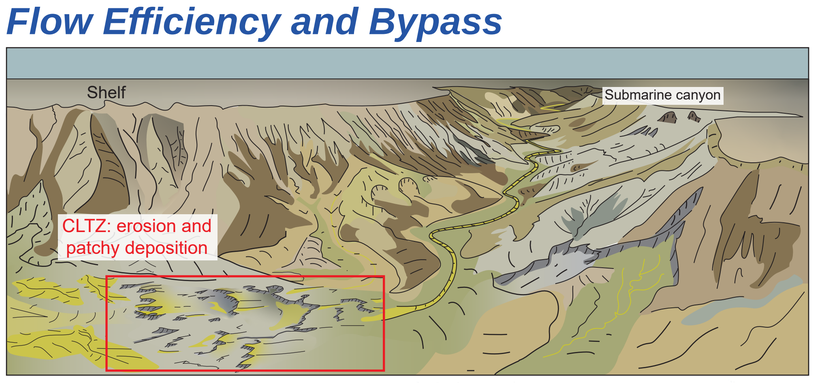

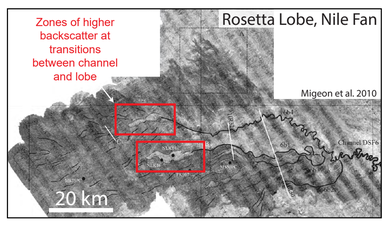

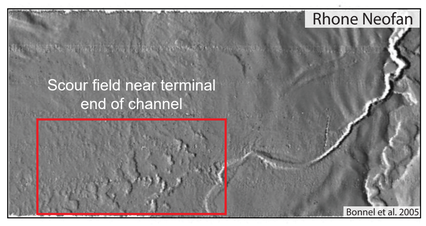

Turbidity currents may not deposit sediments continuously along their flow path, resulting in the bypass of certain areas of the seafloor, leaving zones of non-deposition or erosion in parts of the system. System bypass is also expressed through scouring, erosion, and/or nondeposition in the channel-lobe transition zone (CLTZ). This bypass process may result in the complete or partial detachment of distal parts of the system, including large-scale lobe deposits.

Flow Transformation

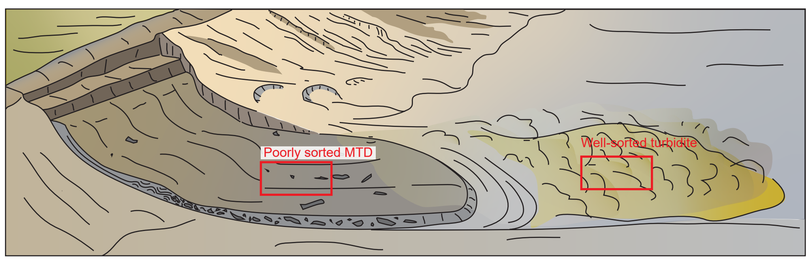

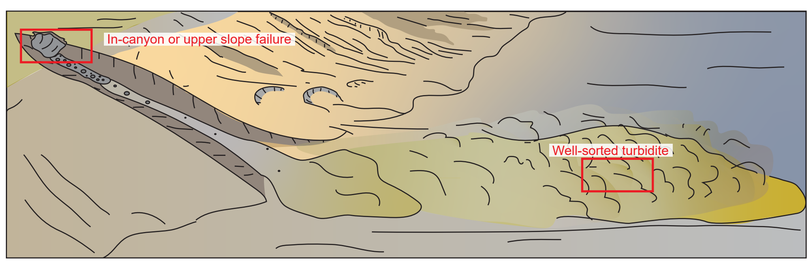

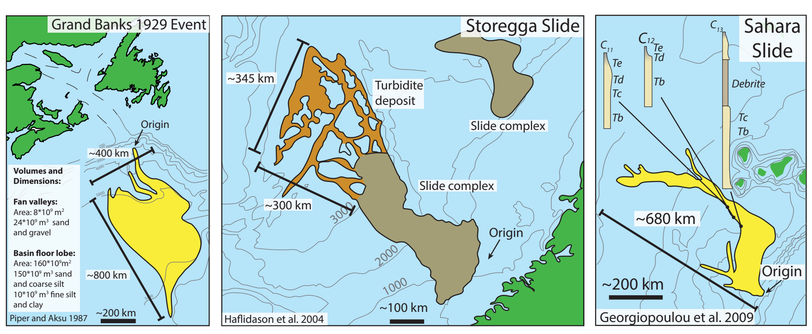

Slope failure deposits may quickly evolve into debris flows that travel for tens or hundreds of kilometres on the basin floor, forming extensive, poorly sorted, often mud-dominated deposits. Failure-generated debris flows, however, may further transform distally into turbidity currents, resulting in sand being partitioned into discrete massive or fining-upward beds of varying thickness. These slope failures are capable of producing extremely large-volume deposits that result in sandy, spatially extensive deposits on the seafloor.

Meander Cut-off

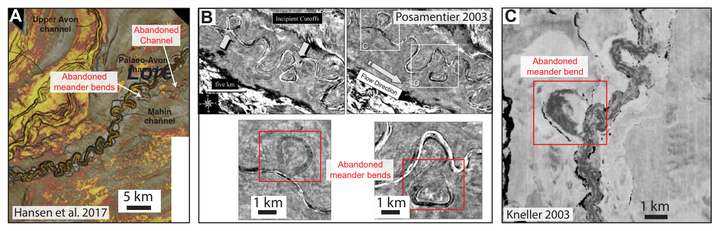

On a smaller scale, meander loops cutoff from the primary channel (formed through breaching of the meander neck) are present in some systems, creating C- or U-shaped bodies where thalweg sands a may be preserved.

Lobe Abandonment

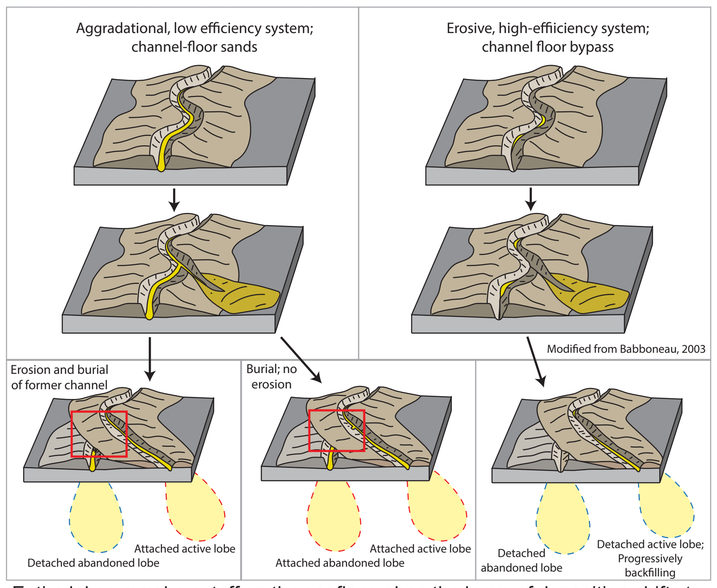

Entire lobes may be cutoff on the seafloor when the locus of deposition shifts to a new area. Detachment is dependent on: 1) the overall propensity for channels to be filled by sands, 2) the timing of channel filling, and 3) the effectiveness of the avulsion point at separating newly deposited channel-floor sands from those in the previous channel.

Channel-Channel Erosion

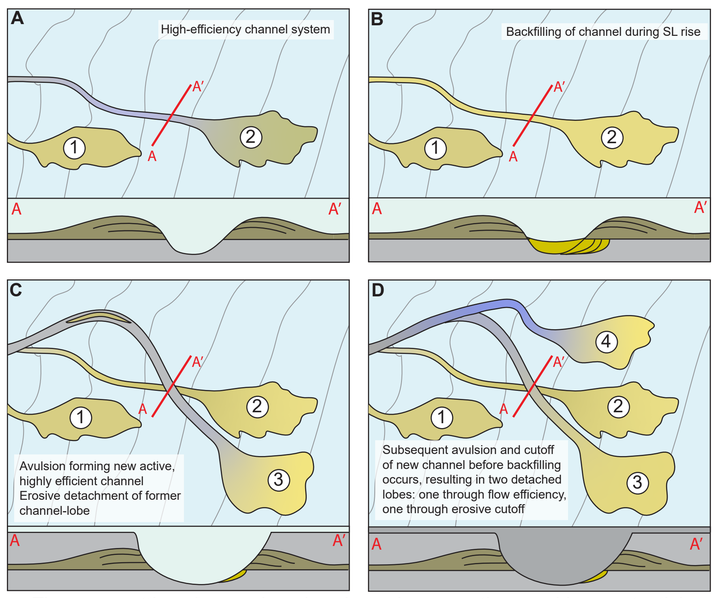

The cross-cutting of one submarine channel over another provides a potential mechanism for the detachment of basin-floor sands. Complete detachment requires that the newer, cross-cutting channel axis be filled only by fines, as sand-on-sand contacts would simply result in an alternate migration path.

Contour Current Erosion

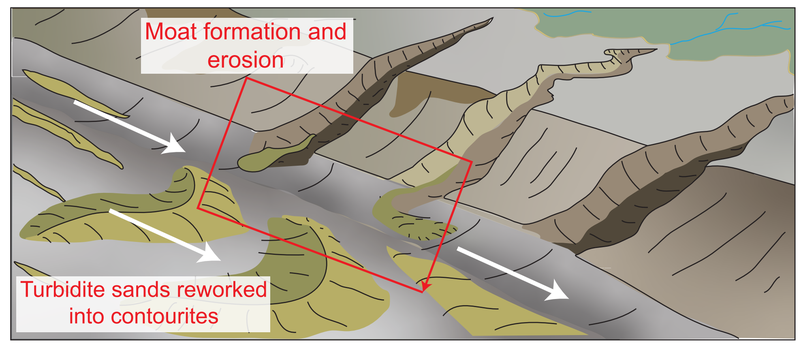

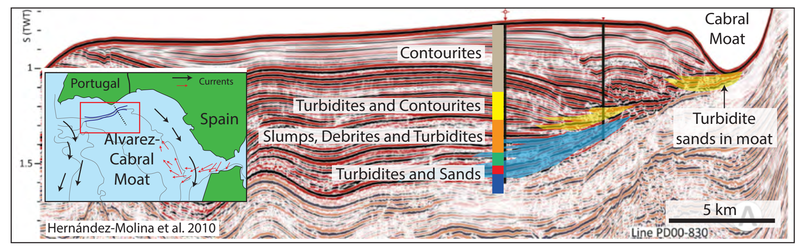

Currents are known to induce erosion of bottom sediments at the bases of along-slope current cores that are forced against the seafloor by Coriolis forces, producing moats, contourite channels, or marginal valleys. Contour current forces, however, are unpredictable at detaching sands from slopes, as they may instead rework sands into contourite bodies that are in contact with more proximal deposits.

MTD Erosion

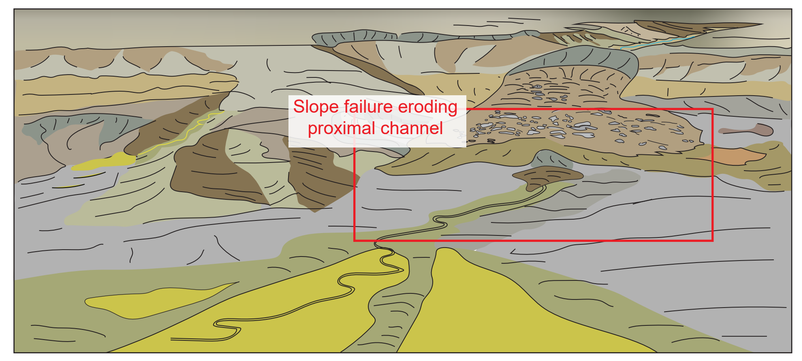

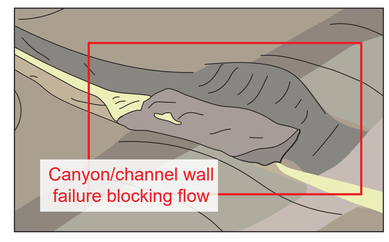

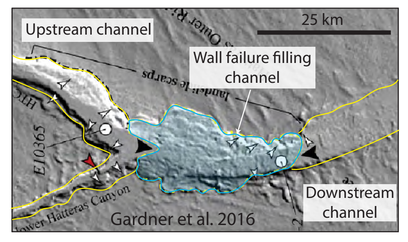

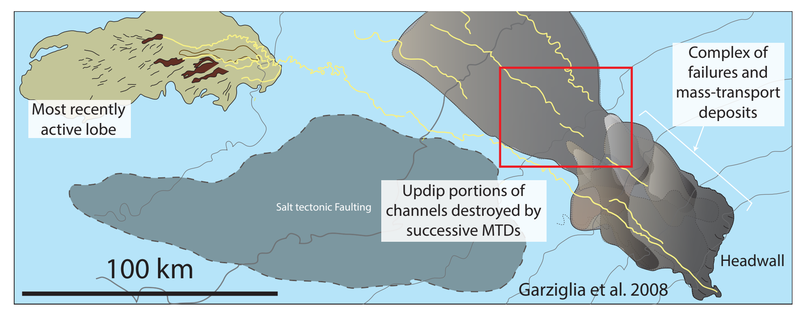

MTDs that occur after canyon or channel-fed turbidite deposition on the basin floor may erode the more proximal portions of deep-sea channels and lobe complexes, resulting in sands that are cut off from their source through both slope erosion and by the emplacement of large-scale debris flows.

Scale, Predictability, Occurrence, and Effectiveness of Detachment Mechanisms

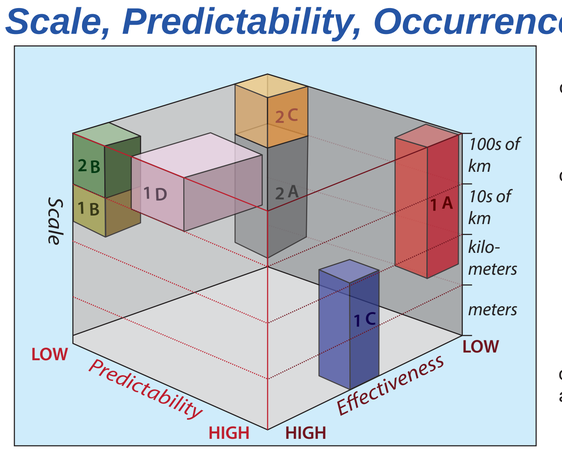

	1A	1B	1C	1D	2A	2B	2C
Effectiveness	Low	High	Moderate	High-Mod.	Moderate	High	Low
Predictability	High	Low	High	Low-Mod.	Low	Low	Low
Scale (km)	High-Mod.	High	Low	High	Low	High	High

- Each detachment process also operates within a certain zone within a proximal-distal system
- Each mechanism is directly controlled by several factors, including the grain size and sorting of input sediment, the height, frequency, and variability of the flows involved, the slope gradient, the size of submarine landslides, and the intensity and direction of bottom currents.
- Controlling factors are, in turn, controlled by the larger-scale geologic and oceanographic setting of the area in question.
- This type of broad correlation can help to predict the occurrence of these mechanisms by favoring or dis-favoring their likelihood in a given location.

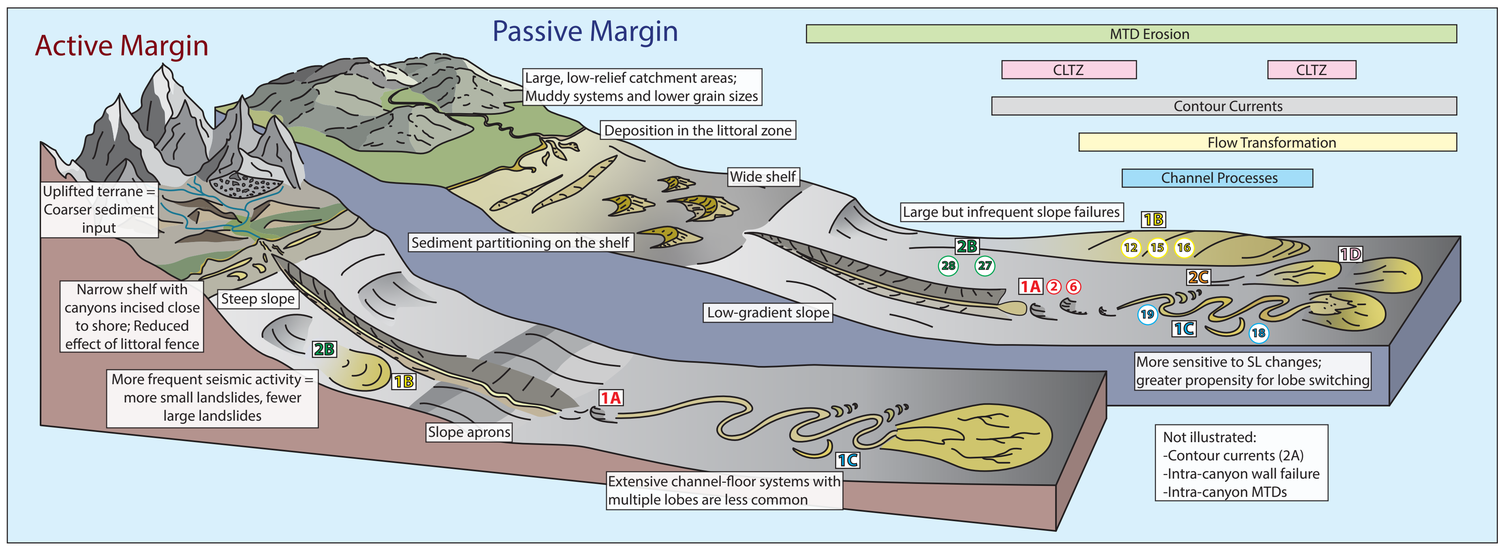

This publication has emanated from research supported in part by a research grant from Science Foundation Ireland (SFI) under Grant Number 13/RC/2092 and is co-funded under the European Regional Development Fund and by PIPCO RSG and its member companies.

Ireland's European Structural and Investment Funds Programmes 2014-2020
Co-funded by the Irish Government and the European Union

European Union
European Regional Development Fund

Science Foundation Ireland sfi For what's next

PIP Petroleum Infrastructure Programme

iCRAG 2019

Resources for a Sustainable Future

PROTECTION FROM EARTH'S HAZARDS

Reconstructing the depositional history of large landslide deposits on the Hikurangi margin, offshore New Zealand

B. Couvin[1]; A. Georgiopoulou[2]; J. J. Mountjoy[3]; L. Amy[1]; G. J. Crutchley[4] and IODP Expeditions 372 and 375 participants[5]

Corresponding author email: **benjamin.couvin@icrag-centre.org**

[1]*Irish Centre for Research in Applied Geosciences (ICRAG), University College Dublin, Belfield, Ireland* [2]*University of Brighton, Brighton, United Kingdom of Great Britain and Northern Ireland* [3]*National Institute of Water And Atmospheric Research (NIWA), Hataitai, Wellington, New Zealand* [4]*GEOMAR Kiel, Germany* [5]*International Ocean Discovery Program, Texas A&M University, College Station, USA*

ABSTRACT

The Tuaheni Landslide Complex (TLC), off the east coast of New Zealand, is uncommonly characterised by areas of compression upslope and extension downslope. It has been thought to consist of a stack of two genetically linked landslide units identified on seismic data. We used 3D seismic reflection, bathymetry data, and IODP core U1517C (Expedition 372), to understand the internal structures, deformation mechanisms and depositional processes of the TLC deposits. Sedimentary Units II and Unit III of core U1517C correspond to two stacked chaotic units in the 3D seismic data. In the core, Unit II shows deformation whereas Unit III appears more like an *in situ* sequence. Variance attribute analysis shows that Unit II is split in lobes around a coherent stratified central ridge, which is bound by scarps. By contrast, we find that Unit III is continuous beneath that central ridge and has an upslope geometry that can be interpreted as a channel-levee system. Both units show evidence of downslope lateral spreading due to the presence of the Tuaheni Canyon downslope, removing support from the toe of the slide. These results suggest Unit II and Unit III are not genetically linked, that they are separated substantially in time and that they had different emplacement mechanisms, but failed under similar circumstances and are possibly liable to continuous deformation.

INTRODUCTION

Submarine landslides are a recognized **hazard** to coastal settlements and marine installations. The **Tuaheni Landslide Complex** (TLC) (fig. 1) is a group of MTDs thought to have an **active creeping behaviour**, which is still **poorly understood** (Mountjoy et al., 2014). In this study, we analyse the **sedimentary character** and **depositional environment** of the TLC, in order to test the hypothesis that the lower landslide unit is actually an *in situ* sedimentary package despite having the seismic characteristics of a MTD, From there, we determine a most likely **depositional history** of the TLC.

GEOLOGICAL SETTING

The TLC is located on the seismically active Hikurangi margin, a subduction zone. It consists of two landslide lobes separated by a central ridge (fig. 1). The structural regime within the landslide is unusual as it is compressional upslope and extensional downslope (Mountjoy *et al.* 2009; Mountjoy *et al.* 2014). In previous studies, the TLC was interpreted as a stack of two MTD units (Mountjoy *et al.* 2014; Gross *et al.* 2018; Kuhlmann *et al.* 2018) that appear separated by a negative impedance reflection with respect to the seafloor reflector (Gross *et al.* 2018).

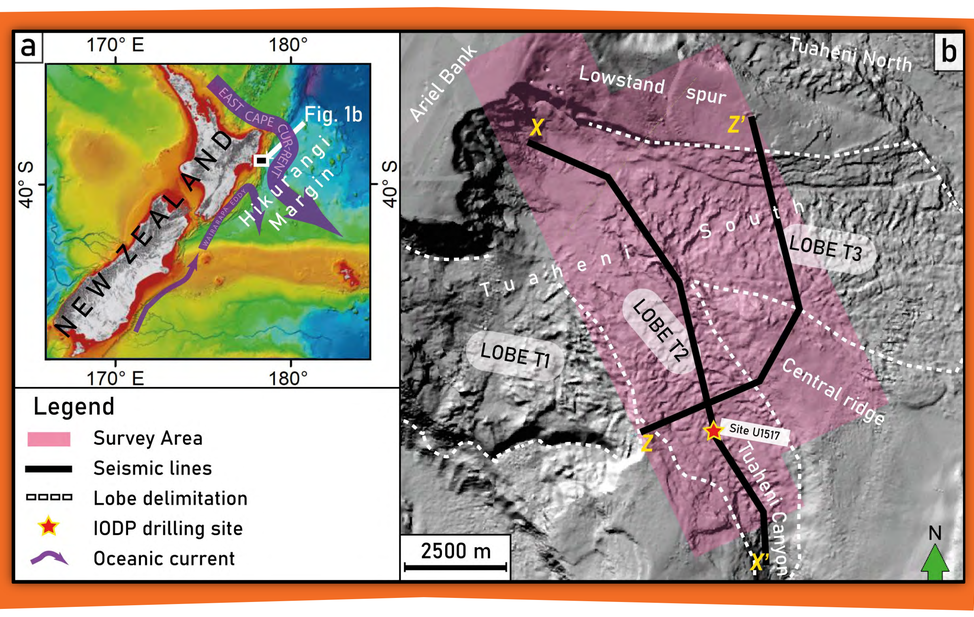

figure 1: (a) map of New Zealand showing local currents, bathymetry and the study area. (b) study area. Inline XX' (fig. 2) and crossline ZZ' (fig. 3) are shown in black. >>

METHODS

Seismic data was acquired during *RV Tangaroa* TAN1404 voyage using a P-Cable system for high-resolution 3D seismic acquisition (Gross et al., 2018). We focused on four major horizons (R1 to R4). Seismic attributes such as variance and gradient attributes provided meaningful results.
A 190 m core (U1517C) was drilled in the distal part of Lobe T2 of the TLC during IODP Expedition 372 (Pecher *et al.* 2018). Five lithological units were defined (I to V). We described and logged Units I, II and III of Core U1517C .

Left - figure 2: Inline XX'. (a) uninterpreted data. (b) interpreted.
Right - figure 3: Crossline ZZ' (a) uninterpreted data (b) interpreted.

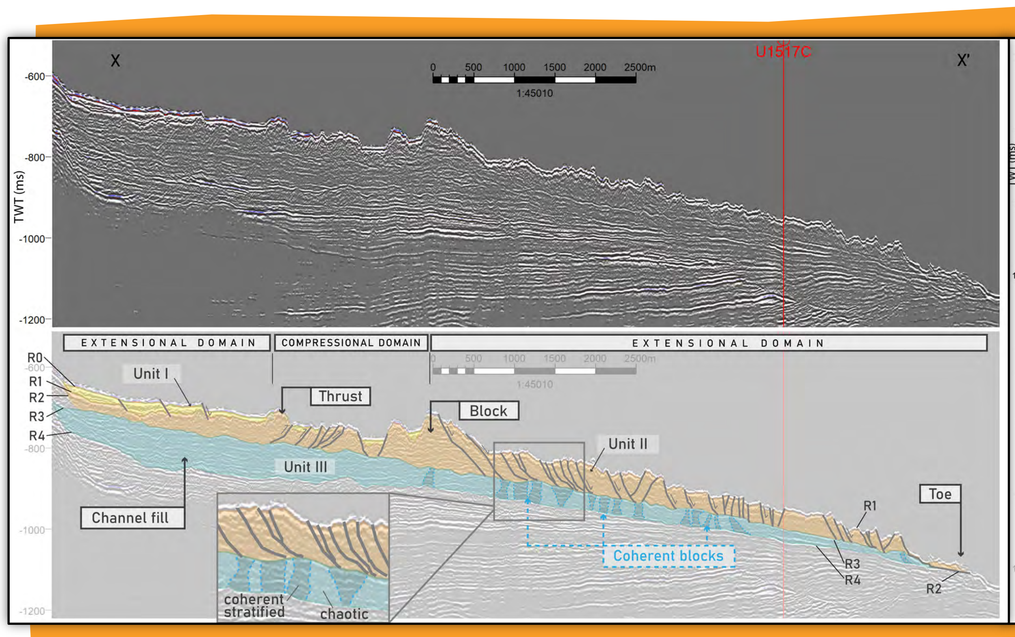

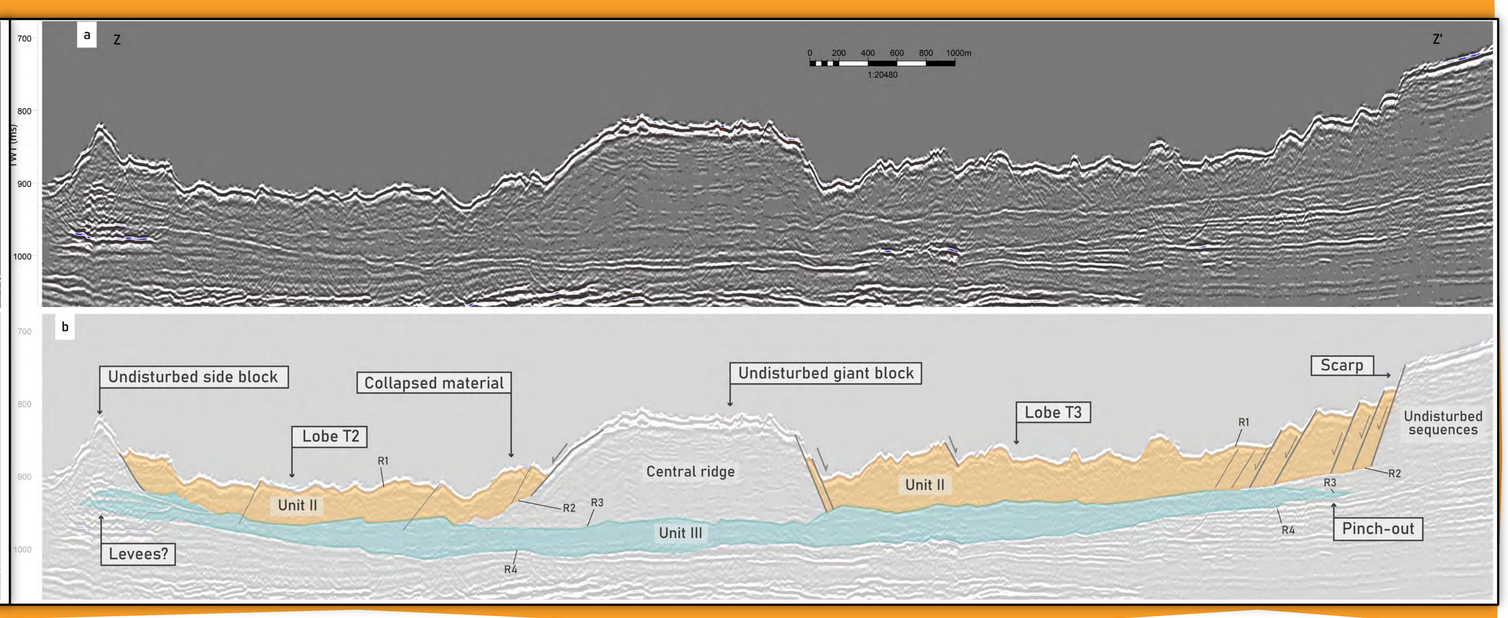

SEISMIC DATA ANALYSIS

Unit II

In seismic data, Unit II is characterised by a chaotic facies. It is faulted, with an area of compression upslope, and extension downslope. It features large blocks (fig. 2). The unit is bound by head scarps and side scarps.

Unit III

The lower unit does not appear faulted but presents lateral variation of seismic facies with blocks of coherent stratified reflectors (fig. 3). This could be interpreted as laterally spreading blocks surrounded by debris. Unit III also seems to extend beyond the margins of the TLC and below the central ridge. The unit can be picked upslope where it seems to feature a channel (fig. 2).

LITHOLOGY

Unit II

In core, Unit II (3 to 40.74 mbsf) consists of alternating very fine sand layers and structureless muds. Sand layers are deformed. Internal structure is either massive or fining upwards (fig. 4).

<< figure 4. Unit II in IODP core U1517C.

Unit III

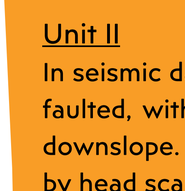

This mostly silty unit (from 40.74 to 66.7 mbsf) is structured in laminae (fig. 5) and presents next to no deformation.

<< figure 5. Unit III in IODP core U1517C.

figure 6: thickness time maps of the TLC units (a) Unit II. (b) Unit III.

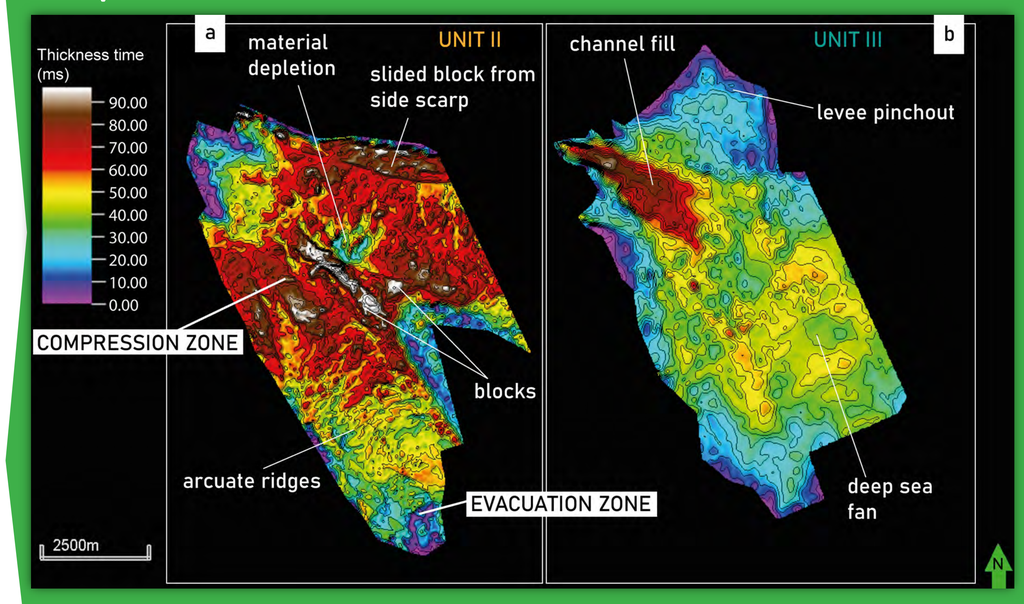

figure 7: variance (or coherency) maps of the TLC units (a) Unit II. (b) Unit III.

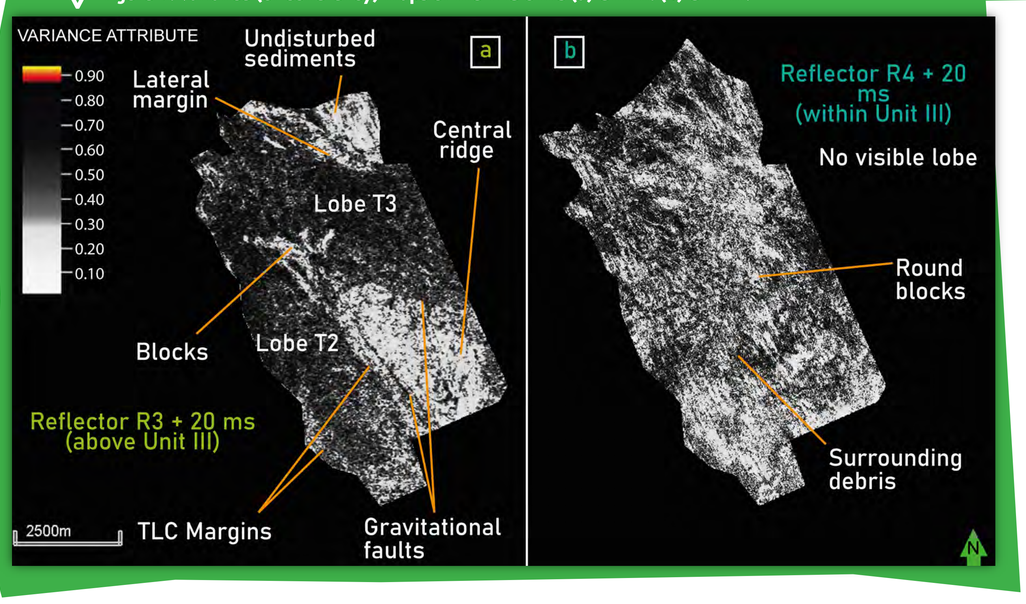

SEISMIC ATTRIBUTES

Thickness

While Unit II is bound within lobes and shows arcuate ridges downslope (fig. 6a), which evidences extension, Unit III presents a geometry that resembles channel-levee systems, with levees that progressively thin out and pinch out beyond the margins of the TLC (fig. 6b).

Variance

In Unit II, the chaotic facies is contained within lobes T2 and T3 and features large blocks (fig. 7a), while Unit III does not show any lobe geometry, but features numerous low-variance patches that are interpreted as blocks (fig. 7b).

CONCLUSIONS

- Unit II and Unit III have different sources and geometries and therefore are **not genetically linked**.
- Unit III being **continuous below the central ridge** means that there is a **significant time interval** between the two units.
- Unit II is **faulted**, while Unit III undergoes **lateral spreading**.
- **Basal shear surface** and possible creeping movement of TLC most likely focused at reflector R2 (**base of Unit II**).

REFERENCES

Böttner, C., Gross, F., Geersen, J., Crutchley, G. J., Mountjoy, J. J., & Krastel, S. (2018). Marine Forearc Extension in the Hikurangi Margin: New Insights From High-Resolution 3-D Seismic Data. Tectonics, 37 (5), 1472–1491. https://doi.org/10.1029/2017TC004906

Gross, F., Mountjoy, J. J., Crutchley, G. J., Böttner, C., Koch, S., Bialas, J., … Krastel, S. (2018). Free gas distribution and basal shear zone development in a subaqueous landslide – Insight from 3D seismic imaging of the Tuaheni Landslide Complex, New Zealand. Earth and Planetary Science Letters, 502, 231–243. https://doi.org/10.1016/J.EPSL.2018.09.002

Mountjoy, J. J., McKean, J., Barnes, P. M., & Pettinga, J. R. (2009). Terrestrial-style slow-moving earthflow kinematics in a submarine landslide complex. Marine Geology, 267 (3–4), 114–127. https://doi.org/10.1016/j.margeo.2009.09.007

Mountjoy, J. J., Pecher, I., Henrys, S., Crutchley, G., Barnes, P. M., & Plaza-Faverola, A. (2014). Shallow methane hydrate system controls ongoing, downslope sediment transport in a low-velocity active submarine landslide complex, Hikurangi Margin, New Zealand. Geochemistry, Geophysics, Geosystems, 15(11), 4137–4156. https://doi.org/10.1002/2014GC005379

Pecher, I. A., Barnes, P. M., Levay, L. J., & Scientists, E. (2018). Expedition 372 Preliminary Report Creeping Gas Hydrate Slides and Hikurangi LWD, (November 2017).

New Zealand map courtesy of NIWA.

This publication has emanated from research supported in part by a research grant from Science Foundation Ireland (SFI) under Grant Number 13/RC/2092 and co-funded under the European Regional Development Fund and by PIPCO RSG and its member companies.

Ireland's European Structural and Investment Funds Programmes 2014-2020 — Co-funded by the Irish Government and the European Union

European Union — European Regional Development Fund

Science Foundation Ireland — For what's next

University of Brighton

NIWA Taihoro Nukurangi

GEOMAR

IODP International Ocean Discovery Program

THREE DIMENSIONAL MODELLING AND WSN MONITORING OF DUBLIN PORT TUNNEL

IRISH CENTRE FOR RESEARCH IN APPLIED GEOSCIENCES

University College Cork, Ireland
Coláiste na hOllscoile Corcaigh

Introduction

Opened in 2006, Dublin Port Tunnel was the largest underground civil infrastructure in Ireland and the longest urban road tunnel in Europe. After in service for more than a decade, the tunnel has developed some structural deteriorations with time, such as concrete spalling, lining cracks, water infiltration, etc., particularly around large vehicle cross passage sections, which may pose a risk to tunnel serviceability and even safety. In the light of tunnel maintenance, a three-dimensional hydro-mechanical coupled finite element analysis is conducted to investigate the long-term ageing structural performance of Dublin Port Tunnel. Meanwhile, a wireless sensor network (WSN) will be deployed at a critical tunnel cross passage for tunnel deformation monitoring.

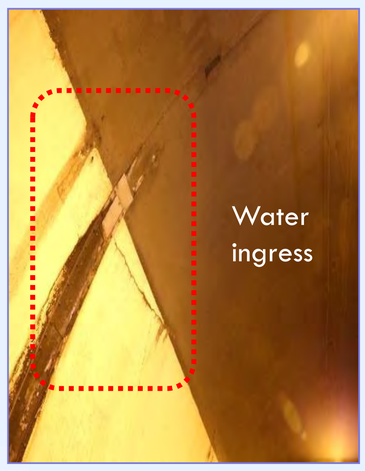

Water ingress

Concrete spalling

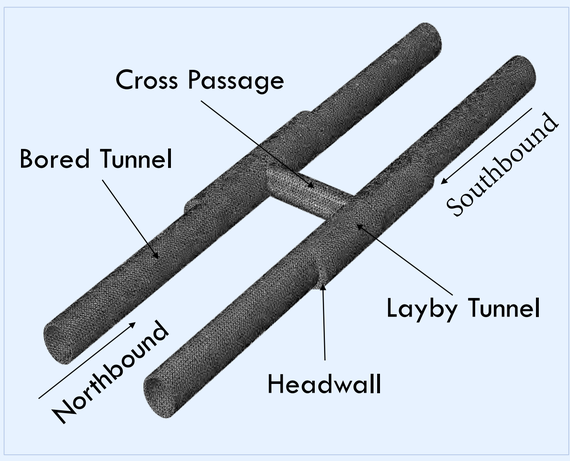

Numerical Model of VCP 16

Numerical Simulation

The coupled FE analysis concentrates on two main sections, the layby tunnel and cross passage. The results will be validated against monitoring data and field observations.

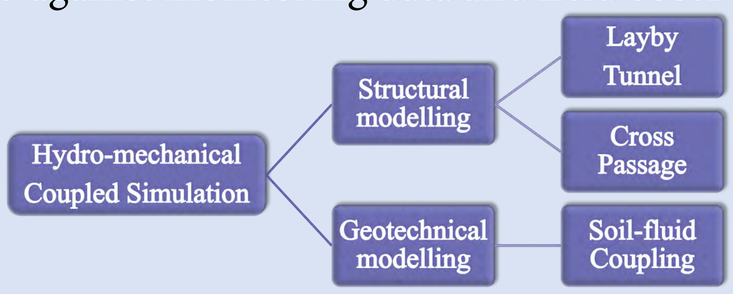

Coupled modelling of Dublin Port Tunnel

Following geological investigation, section VCP 16 mainly goes through hard limestone, with Dublin Boulder Clay, glacial silts, made ground, etc., lying above.

Vehicle Cross Passage 16

Soil Profile around VCP 16
1. Made ground
2. Alluvial gravels, silts and sands
3. Glacial silts, sands and gravels
4. Dublin Boulder Clay
5. Bedrock (Limestone)

Future Work

- Numerical modelling of hydro-mechanical coupled behavior of soil and tunnel linings in the long term, which takes account of the effect of water drainage system configurations.
- Onsite deployment of wireless sensor network system to monitor the tunnel lining inclination, crack development, lining convergence, etc., to assess the performance of tunnel structures.

WSN Monitoring

Wireless Sensor Network (WSN) relies on wireless connectivity and spontaneous formation of networks (Radio frequency and 3/4G network) to ensure data transmission, and features rapid deployment due to elimination of complicated and costly cabling in various applications.

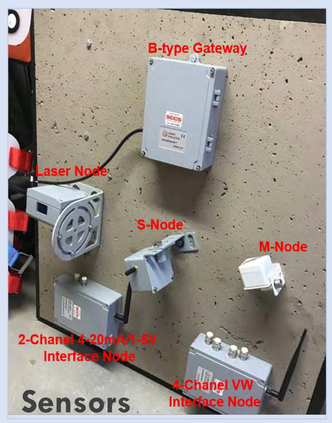

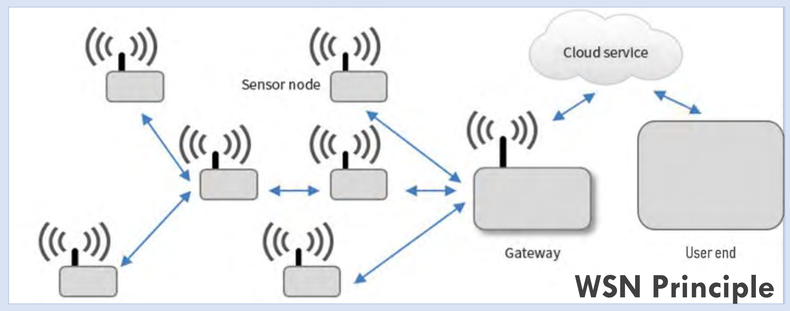

Life expectancy: ≥1.5 years/hour sampling interval
Accuracy: 0.0025° (tilt-meter) / 0.1% reading
Transmission range: 350m underground; further above ground.
Range: -30° ~ +30° (tilt-meter) / 0.05m~100m (laser node)

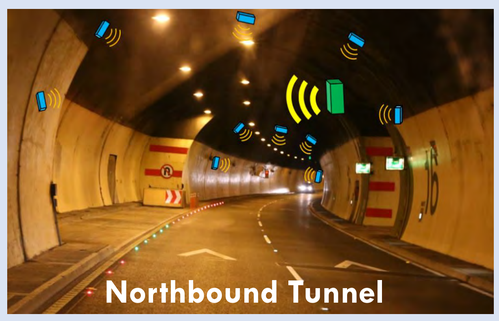

A package of 2 gateways, 16 tilt-meters, 8 crack-meters, and 1 laser node from WISEN Ltd. will be deployed around vehicle cross passage 16 in Dublin Port Tunnel.

Advantages of WSN Monitoring:

- Real-time sensing.
- Save maintenance cost.
- Predict long-term tunnel deterioration.

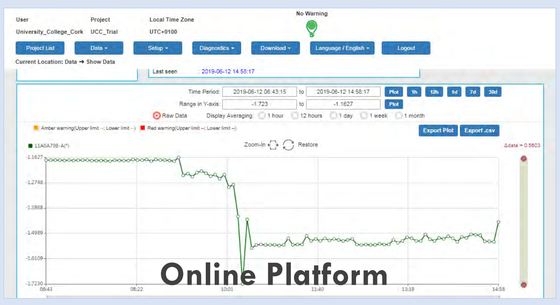

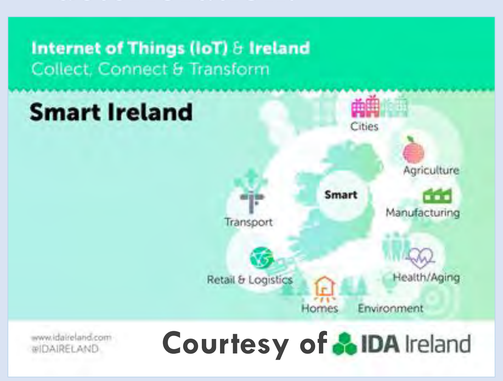

- Guide design, construction and maintenance.
- Deliver whole-life value of civil structures.
- Create a smart sensing network with wider applications.

Dr Z. Li (zili.li@ucc.ie University College Cork)
M. Friedman (miles.friedman@tii.ie Transport Infrastructure Ireland)
Chao Wang (chaowangucc@gmail.com)
University College Cork, Cork, Ireland

This publication has emanated from research supported in part by a research grant from Science Foundation Ireland (SFI) under Grant Number 13/RC/2092 and co-funded under the European Regional Development Fund..

Ireland's European Structural and Investment Funds Programmes 2014-2020
Co-funded by the Irish Government and the European Union
European Union
European Regional Development Fund
Science Foundation Ireland sfi For what's next
Bonneagar Iompair Éireann Transport Infrastructure Ireland

"Automated Crack Classification for Large-scale Tunnel Structure Using Deep Learning"

Authors- Student- Darragh O Brien , Supervisor – DR Zili Li

IRISH CENTRE FOR RESEARCH IN APPLIED GEOSCIENCES

University College Cork, Ireland
Coláiste na hOllscoile Corcaigh

Introduction

Deep Learning is a very vast and rapidly growing area of the computing world its uses span from facial recognition, self-driving cars and even used in finance. In this poster, I will explain how deep learning in the form of a CNN (convoluted neural network) will be utilized to locate cracks and classify the in the tunnel infrastructure at European Centre for Nuclear Research (CERN). The aim is not only to create a CNN that works at this location but that can be slightly altered and used in any tunnel infrastructure across the globe to analyze its structural health.

Convoluted Neural Network(CNN)

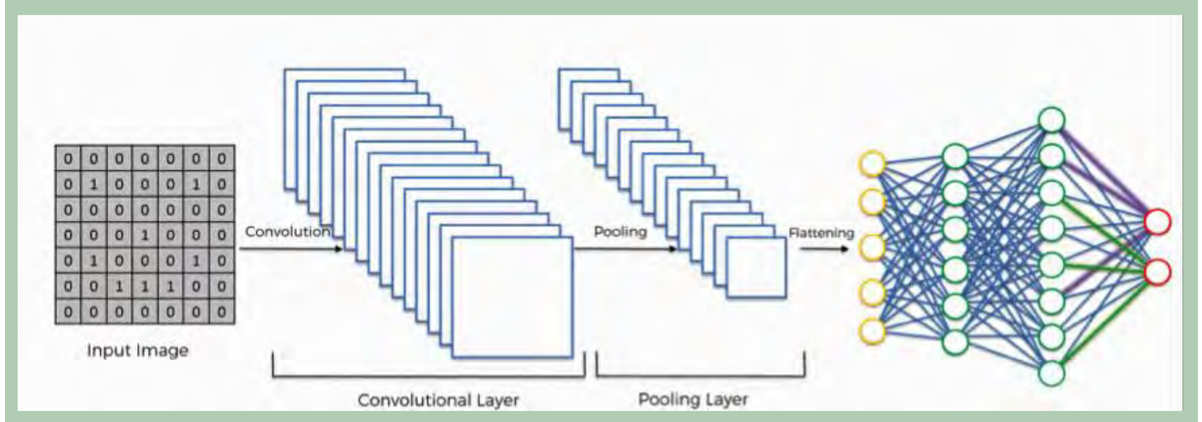

In Deep Learning, the most commonly adopted method of image analyzation is based on Convoluted Neural Networks(CNN). As the CNN takes inspiration from the biological connections of the eye to the brain. A CNN is made up of a predetermined number of layers, they can be made up of a variation convolution, pooling, flattened and dense layers to make to most accurate detection algorithm. A CNN is only as good as the training it receives.

Processed images

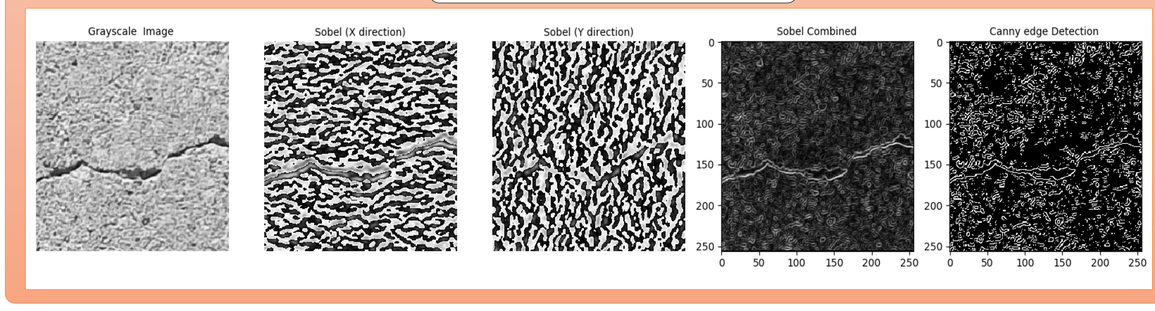

Preliminary Results

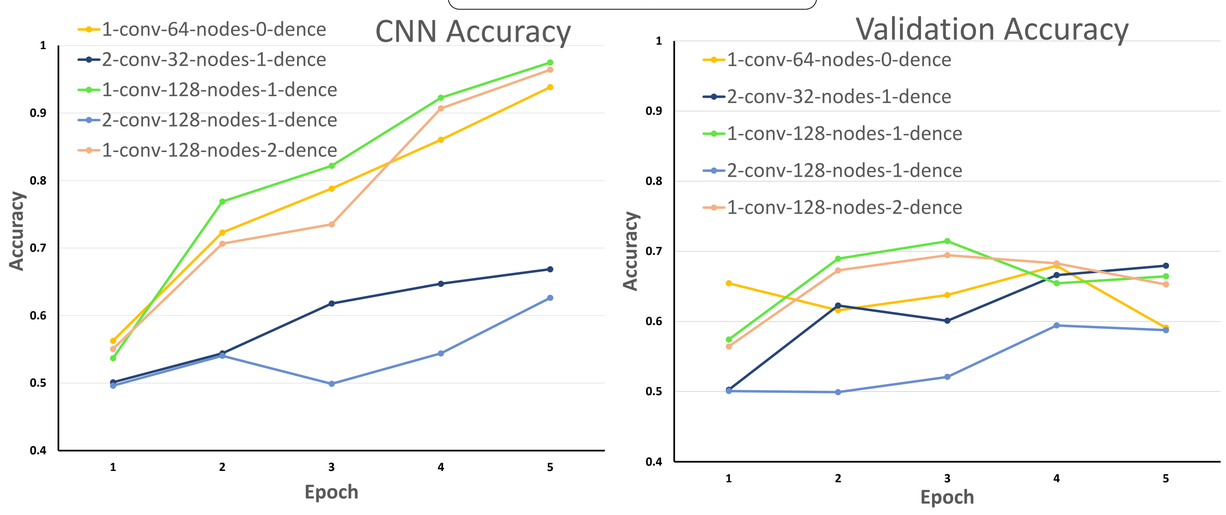

- This is the provisional CNN it is being run off 1996 images form the SDNET2018 data set. The above Graphs show the CNN and Validation accuracy.
- 1-conv-128-nodes-1-dence (green) has a huge of 97.49% but only a 66.44% validation accuracy this is a clearly showing that overfitting is occurring
- 2-conv-32-nodes-1-dence which has more convolutions and less nodes has a CNN accuracy of 67.95% and a validation accuracy of 66.86% although it still has a low accuracy it shows that the CNN under this structure that more epochs will cause a greater accuracy.
- These systems by definition are shallow neural networks and are only the start of the research, in the future the system of layers used will be much deeper and contain 10 or more layers.

Current CNN's for crack detection

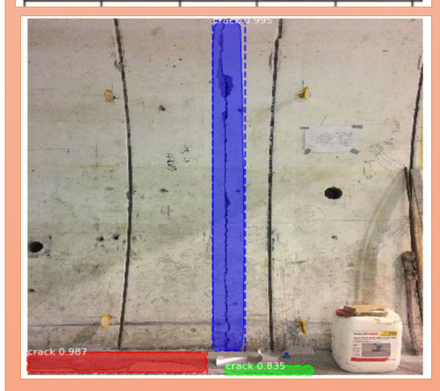

At this moment in time there has been extensive research in the crack detection with the use of CNN in a wide variety of objects . These CNNs can locate and even highlight a crack in an image or even a video frame by frame. However for the crack detection in tunnels the research has been very difficult and limited by the constraints of the tunnels themselves, such as lack of light, shadows caused by light, rounded structure and objects on the tunnel lining. This inhibits a good data base being created without image processing.

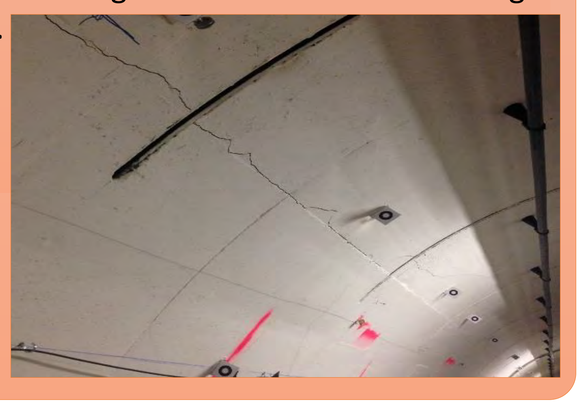

Image Acquisition

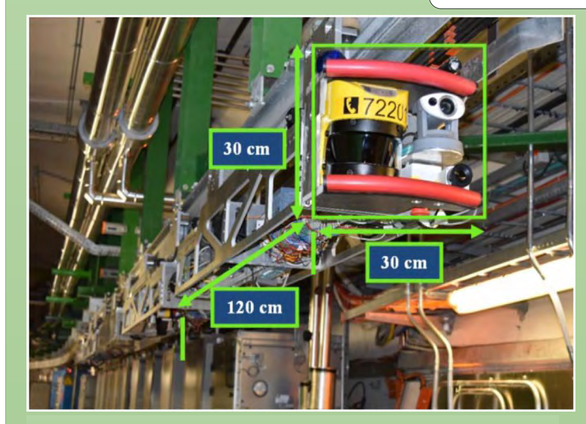

Train Inspection Monorail (TIM)

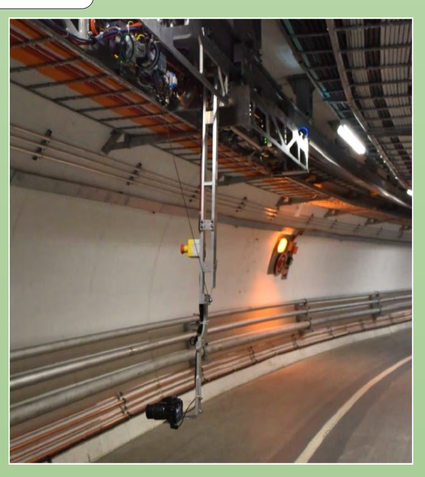

There are currently many different options for image acquisition but the two most useful for this research are the use of the TIM and the Cernbot. These are two mobile platforms that move cameras around the tunnels taking pictures of the walls. These technologies enable uniform and high definition images to create a Data set on which the CNN can be trained/tested on

Cernbot

Image Classification

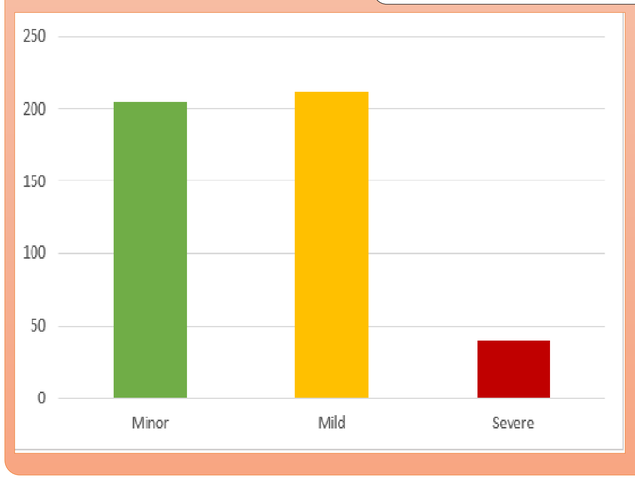

In CERN during the inspectors if a crack is notice a picture is taken an classified in 1 of the 3 sections. In my research I aim to use this data base of pre organised images in order to Create a CNN that classify cracks into these 3 categories. This in turn reduces the subjectivity and increases productivity during inspections.

Future work

The CNN crack classification offers a solution to the problem in the structural health monitoring of a tunnel infrastructure. This problem is the human subjectivity, as currently tunnels are monitored and cracks recorded by a tunnel inspector. With the implementation of this CNN, the human subjectivity will be reduced massively if not elevated with the records of the tunnel will become more accurate and in-depth. As all tunnels do not have the luxury of having a working monorail the hope is that the CNN will be also developed to be able to intake video and decipher cracks. This will allow any tunnel to be examined once a video of the tunnel is provided.

This publication has emanated from research supported in part by a research grant from Science Foundation Ireland (SFI) under Grant Number 13/RC/2092 and co-funded under the European Regional Development Fund..

Ireland's European Structural and Investment Funds Programmes 2014-2020
Co-funded by the Irish Government and the European Union
European Union
European Regional Development Fund
Science Foundation Ireland sfi For what's next
CERN

Investigation of the link between stress, pore pressure, and slow slip earthquakes: implication for geohazard modelling

E. Behboudi[1] (effat.behboudi@ucdconnect.ie),I. Lokmer[1], D.D McNamara[2], T. Manzochi[1], L. Wallace[3], D. Saffer[4], P. Barnes[5], I. Pecher[6], H. Lee[7], G. Kim[8], W. Hung-Yu[9], K. Petronotis[10], L. LeVay[10], Expedition 372 & 375 Scientists[10]

[1] *School of Earth Science, UCD;* [2] *Department of Earth, Ocean and Ecological Sciences, University of Liverpool;* [3] *Natural Hazards, GNS Science, Lower Hutt, New Zealand;* [4] *Department of Geosciences, Penn State, USA*; [5] *NIWA, New Zealand*; [6] *School of Environment, University of Auckland, New Zealand*; [7] *National Institute of Meteorological Research, South Korea*; [8] *Korea Institute of Geoscience and Mineral Resources, South Korea*; [9] *Institute for Research on Earth Evolution, Japan Agency for Marine-Earth Science, Japan*; [10] *International Ocean Discovery Program, Texas A&M University, USA*

What are Slow Slip Earthquakes?

- SSEs release energy on a fault over longer time periods than normal earthquakes (weeks to months).
- Commonly occur along subduction margin interfaces.
- At deeper depths on the interface, plates slowly slide along each other, whereas at shallower depths friction between the plates causes them to become temporarily stuck.
- Every couple of years stress in the stuck portion builds up and is released in a SSE.

Why are Slow Slip Earthquakes Important?

- When the locked portion of the subduction interface experiences a long (hundreds of years) period of being stuck, release of this stress build-up can result in a damaging earthquake.
- SSEs occur next to parts of the subduction interface that experience these damaging earthquakes.
- SSEs may increase stress on the locked part of the interface and trigger damaging earthquakes.
- Understanding this relationship will allow better hazard modelling in regions that experience SSEs.

Hikurangi Subduction Zone (HSM), New Zealand

- SSEs recorded along HSM in New Zealand between 2002 and 2012.
- Discovered using GPS which can detect sub-centimetre changes in land movements.
- In the northern region SSEs are shallow (<15 km) and occur over two weeks approximately every two years.

What is the possible link between the stress regime and subduction interface slip behaviour?

- **Do SSEs and locking impact the character of the stress field?**
- **How are local stress field conditions affected by variable structure across the HSM (frontal thrust, over-riding material, incoming material)?**

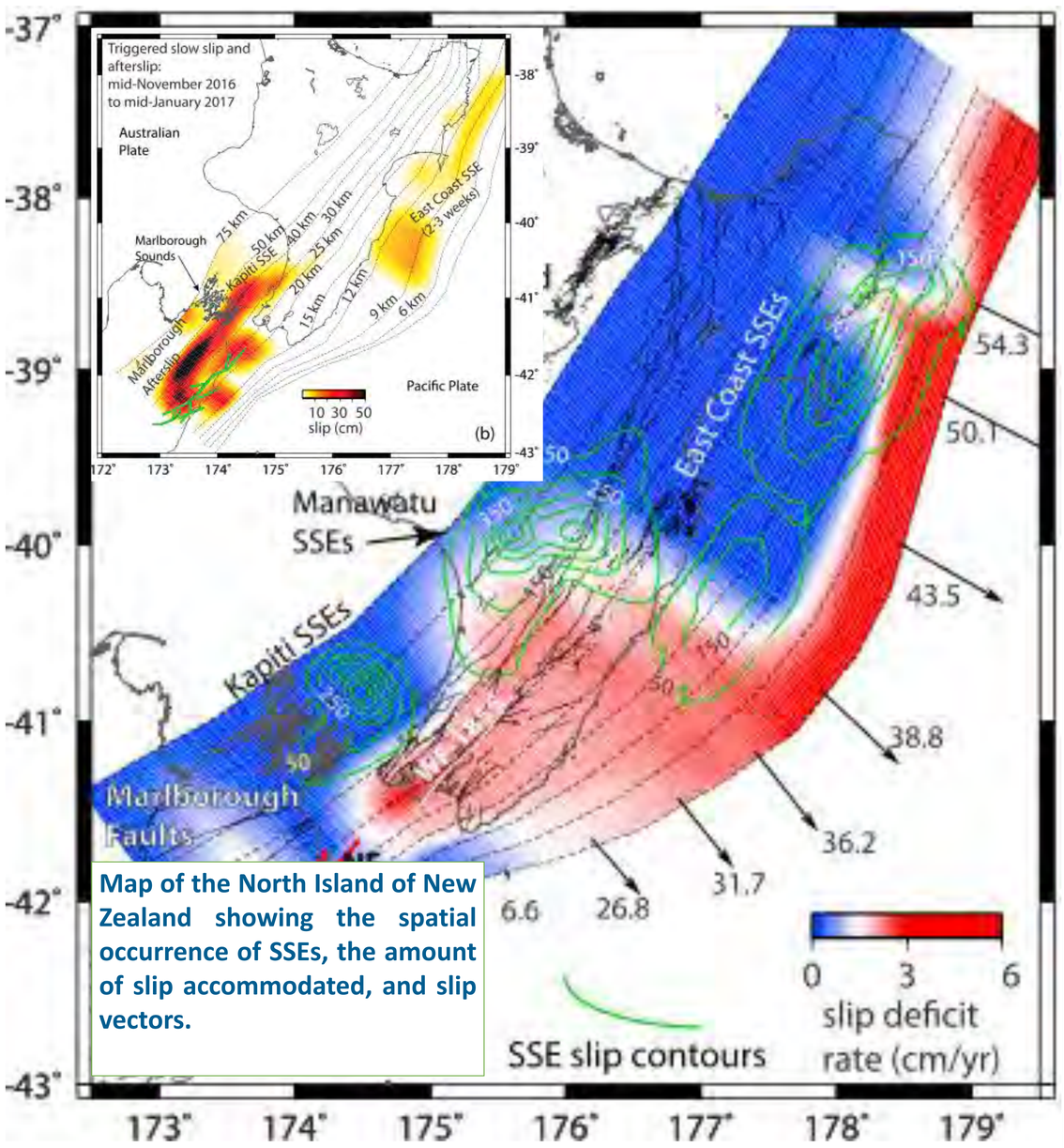

Map of the North Island of New Zealand showing the spatial occurrence of SSEs, the amount of slip accommodated, and slip vectors.

Stress Characterisation

- To determine full tensor of HSM, Borehole breakouts (BOs) and earthquake focal mechanisms are used.
- BOs are well-known indicators that develop perpendicular to the present-day S_{Hmax} orientation and can be observed by Borehole imaging tools in shallow depths (3-4 km).
- for greater crustal depths, S_{Hmax} orientation can be determined from Earthquake focal mechanisms .

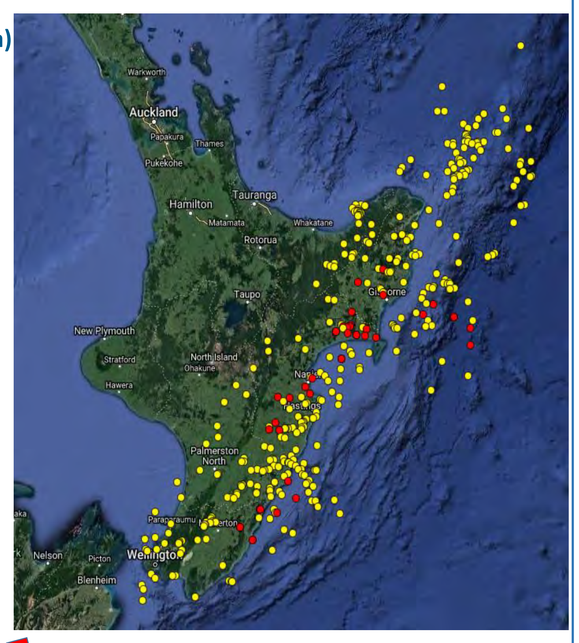

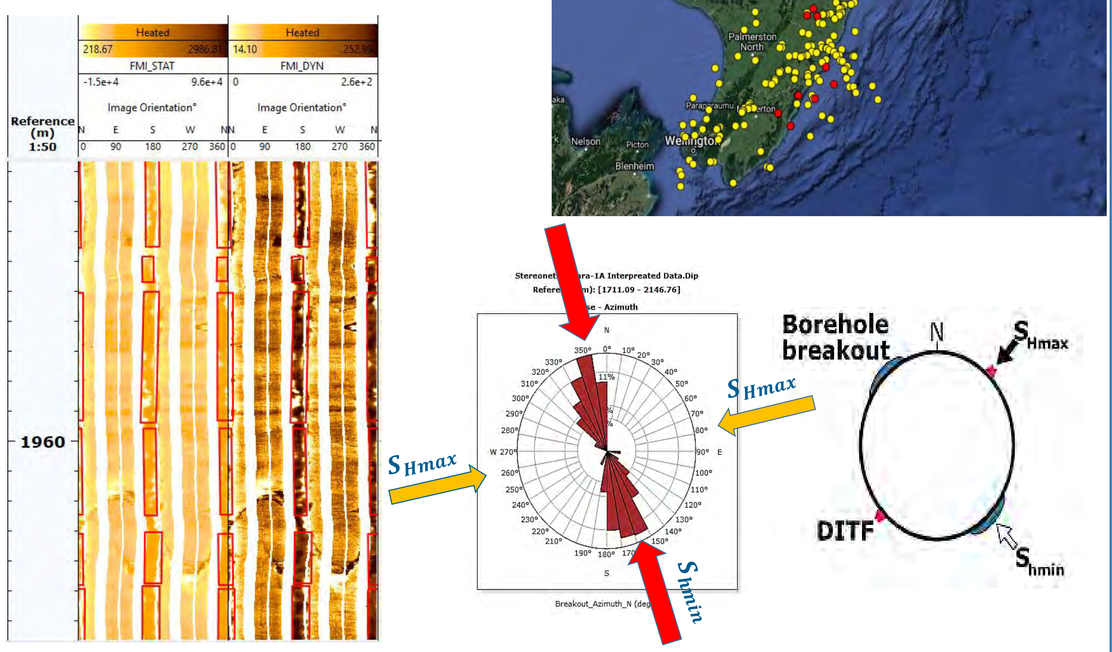

a) Map of the east coast of North Island New Zealand showing locations of industry and IODP wells and earthquake data in this study.

b) Schematic of borehole breakout analysis for S_{Hmax} and S_{hmin} orientation determination for Tuhara-1A.

Future work

- Full analysis of image logs for stress induced fractures and borehole breakout for determination of stress orientation and magnitudes in shallow depths.
- Analysis Moment Tensor data to determine the stress orientation for deep depths.

Preliminary Results – HSM S_{hmin} Orientations

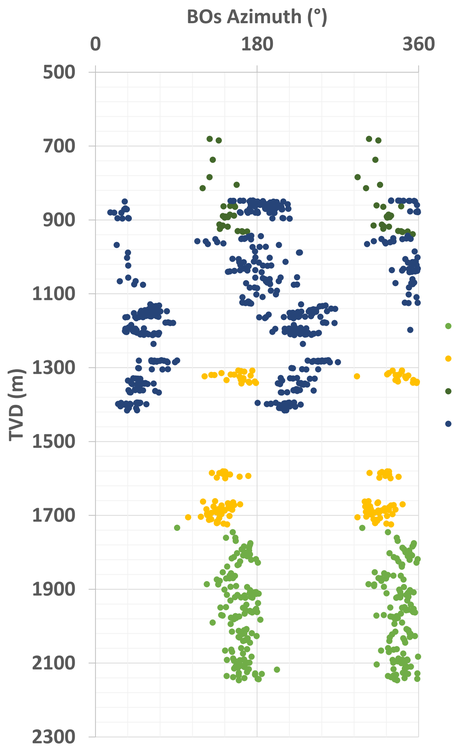

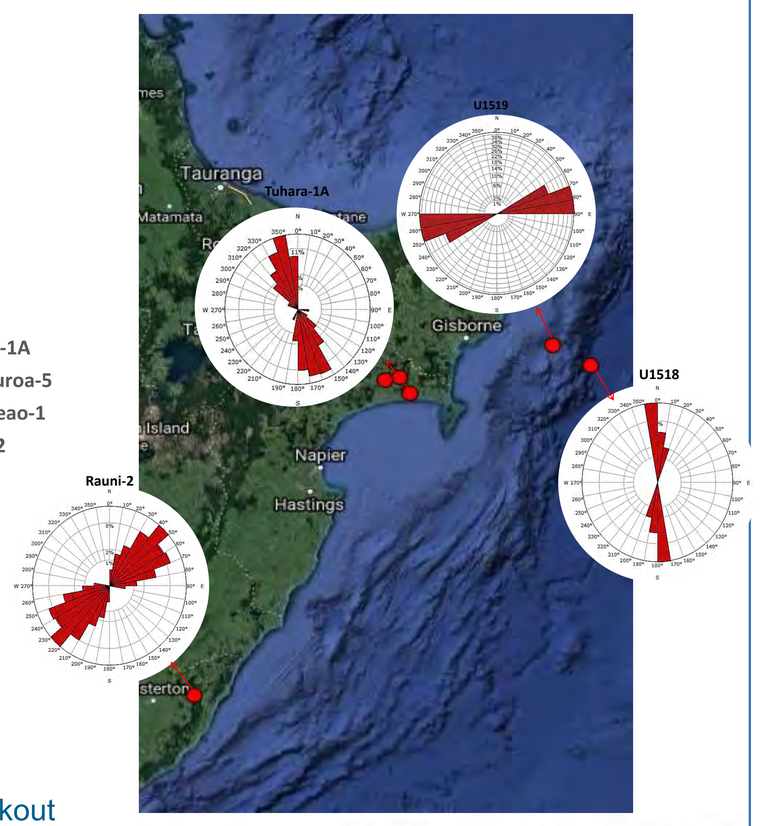

- S_{hmin} orientations from borehole breakout observations vary along the HSM.
- S_{hmin} orientations within individual wells also vary.
- S_{Hmax} orientations at Northern Hawke Bay is sub parallel to HSM trough while in southern East Coast it is almost orthogonal.
- U1518 at the frontal thrust matches stress orientations seen further back in the hangingwall.
- U1519 shows a rotation in stress orientation to the regional trend – related to deformation quiescence in this part of the hangingwall?
- Variations with depth may be due to slip on local structures or changes in pore pressure?

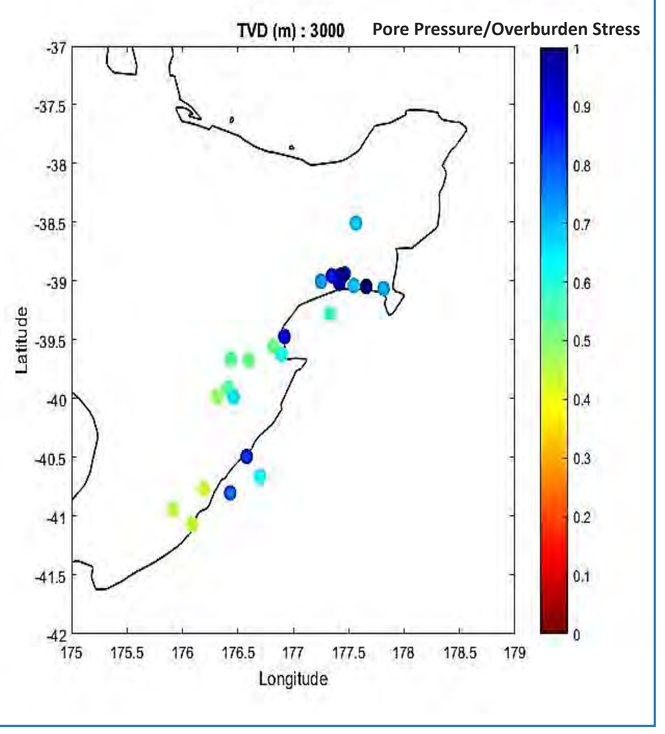

This publication has emanated from research supported in part by a research grant from Science Foundation Ireland (SFI) under Grant Number 13/RC/2092 and co-funded under the European Regional Development Fund.

Ireland's European Structural and Investment Funds Programmes 2014-2020
Co-funded by the Irish Government and the European Union
European Union
European Regional Development Fund
Science Foundation Ireland sfi For what's next
Geological Survey Suirbhéireacht Gheolaíochta Ireland | Éireann

References:

- McNamara, D.D., Wu, H.Y., Lee, H., Wallace, L.M., Lee, G., Heeschen, K.U., Elger, J., Saffer, D.M., Barnes, P., and Pecher, I.A., 2018, December, Borehole stress indicators across the Hikurangi Subduction Margin: Preliminary insights from IODP Expedition 372, AGU Fall Meeting Abstracts.
- Wallace, L.M., Webb, S.C., Ito, Y., Mochizuki, K., Hino, R., Henrys, S., Schwartz, S.Y., and Sheehan, A.F., 2016, Slow slip near the trench at the Hikurangi subduction zone, New Zealand, Science, 352 (6286), 701–04.

Locating sub-surface Karst Conduit Waterflow using Seismic Ground Vibrations

Haleh Karbala Ali and Christopher J. Bean

Geophysics Section, School of Cosmic Physics,
Dublin Institute for Advanced Studies (DIAS)

Email: haleh@cp.dias.ie

Motivation

What is Karst?

Karst is a landscape with distinctive hydrology and landforms that arise when the underlying rock is soluble.

Figure 1. Schematic Karst model (Eoin McCraith, GSI).

The importance of Karst in Ireland

- Karst is an important source of drinking water,
- Groundwater in Karst interacts with surface water systems and may cause groundwater flooding,
- Interfere with water-filled Karst conduits in geotechnical and civil engineering projects creates difficulty.

Current State of the problem

Karst structure has been successfully imaged through different geophysical approaches such as seismic and resistivity. **But**, no study has been done on locating Karst conduits containing waterflow.

What we aim to determine?

- Locate subsurface conduits in Karst that has water flow,
- Determine the flow rate in sub-surface Karst conduits.

How we approach this goal?

- Record the ground vibration induced by the flow of water in sub-surface Karst conduits by deploying seismometers on the ground,
- We start by testing the methodology on surface rivers where the river location and flowrate are known.

Seismic signal generation by waterflow in rivers

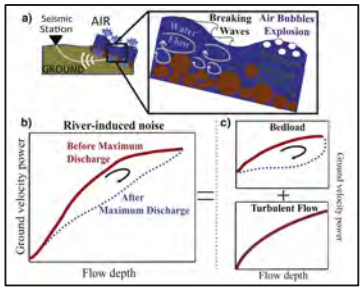

Figure 2.(a) Cartoons showing (left) the deployment technique used to monitor rivers from seismic observations and (right) selected fluvial processes potentially generating ground motion. (b) Schematics of the clockwise hysteresis commonly observed in the river-induced ground power as a function of flow depth. (c) Illustration of the relative contribution of bedload-induced noise versus turbulent-flow-induced noise (Larose, 2015).

Amplitude Ratio Source Location (ARSL) Method

- Successful application of ARSL method for locating the source of volcanic tremors (Taisne et al., 2011; De Barros et al., 2013),
- Based on the decay of amplitude with distance due to geometrical spreading and anelastic attenuation effects,
- Calculation of the ratio of seismic intensities between stations to avoid estimation of intensity at the source.

$$I_i = I_0 \frac{e^{-Br_i}}{r_i^n}, \quad \text{with} \quad B = \frac{\pi f}{QV}$$

Where I is the seismic intensity. f, Q, β and r are freqeuncy, quality factor for attenuation, shear wave velocity and the source to station distance.

$$\frac{I_i}{I_j}\Big|^{r} = \left(\frac{r_j}{r_i}\right)^{n} \exp\left[-B\left(r_i^l - r_j^l\right)\right]$$

n = 0.5 or 1 for the surface and body waves, respectively.

1st SURFACE RIVER EXPERIMENT

Glenmacnass River- Wicklow Mountains (13 Sep. 2019)

- Test experiment to analyze the seismic signal generated by the flow of water,
- 1-hour recording of a seismic signal using 1 Hz. Short-period seismometers at 5 stations near the river.

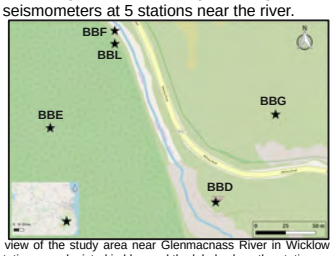

Figure 3. Map view of the study area near Glenmacnass River in Wicklow Mountains. The recording stations are depicted in blue and the labels show the station names.

- **Pre-processing:** Taper, detrend, demean, instrument- response correction.

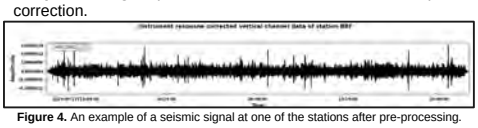

Figure 4. An example of a seismic signal at one of the stations after pre-processing.

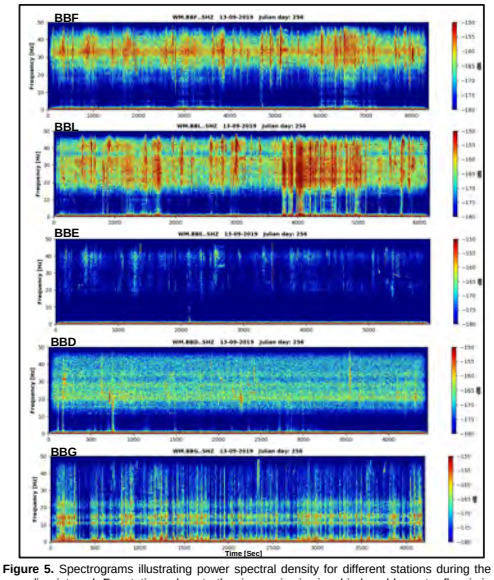

Figure 5. Spectrograms illustrating power spectral density for different stations during the recording interval. For stations close to the river, seismic signal induced by water flow is in the frequency range of 30- 40 Hz.

Application of the ARSL method to Glenmacnass seismic data

1- Band-pass filter in the frequency range of interest,
2- Computation of the envelope of the signal using Hilbert transform,
3- Application of median filtering to remove transient spikes,
4- Minimizing the misfit between observed and theoretical intensities using a grid search method.

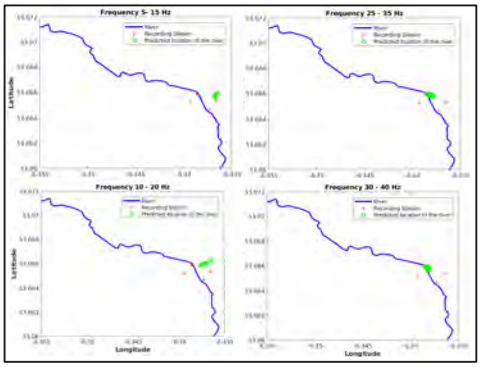

Figure 6. Application of ARSL method to the band-pass filtered Glendassan seismic data. According to the spectrograms in Figure 7, the dominant frequency of the river-induced signal is in 30- 40 Hz. The ARSL method can determine the location of the river correctly when the data is filtered in this frequency range.

2nd SURFACE RIVER EXPERIMENT

Avoca River- Wicklow Council yard (09- 14 Oct. 2019)

- Choice of this site location due to the existence of 2 EPA permanent water level/ flowmeter gauges,
- Design of two extremely dense arrays suitable for array processing applications,
- Deployment of 13 stations to record for 5 days with 4 additional stations added in the 4th day,
- Leaving 2 stations to record for 1.5 months to correlate river-induced signal and flowrate.

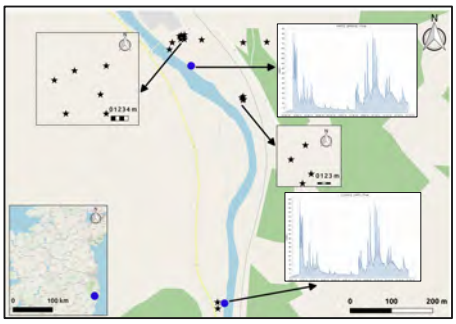

Figure 7. Map view of the study area near Avoca River in Wicklow. We deployed 15 stations upstream near the Whitebridge flowmeter gauge and 2 stations downstream in the Council yard. 2 stations are still deloyed. The black stars depict seismic stations while the blue circles show flowmeter locations.

KARST SITE LOCATION

- A possible location for the seismic deployment in Karst is Pollnagran cave, the only active stream cave of Roscommon,
- The cave goes beneath road N5 which is of importance to Transport Infrastructure Ireland (TII),
- Other candidate locations are caves in Co. Clare and Co. Galway.

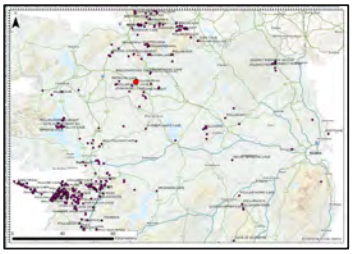

Figure 8. Map view of discovered caves in Ireland depicted as purple dots. The Pollnagran cave in Roscommon is illustrated in red (map provided by GSI).

Future Work

- Application of the ARSL method for locating the Avoca river using all available stations,
- Application of *f-k* and SPAC array processing methods to the Avoca dataset for locating the Avoca river and determining the veocity structure,
- Correlation of the EPA's hydrological data with the two seismic monitoring stations at Avoca site,
- Acquisition design and start of deployment at the Karst site,
- Application of the tested ARSL and array processing methods on surface river to locate the Karst subsurfacw conduits waterflow.

References

- De Barros, L., Bean, C.J., Zecevic, M., Brenguier, F. and Peltier, A., 2013, Eruptive fracture location forcasts from high-frequency events on Piton de la Fournaise Volcano, Geophysical Research Letters, 40, 4599- 4603.
- Larose E., 2015, Environmental seismology: What can we learn on earth surface processes with ambient noise?, 2015, Journal of Applied Geophysics, 116, 62-74.
- Taisne, B., Brenguier, F., Shapiro, N.M. and Ferrazzini, V., 2011, Imaging the dynamics of magma propagation using radiated seismic intensity, Geophysical Research Letters, 38, L04304.

Acknowledgements

The authors greatly acknowledge Geological Survey Ireland (GSI) for financially supporting this project. We are thankful to Dr. David Craig from DIAS for his invaluable help during the two river fieldworks, Dr. Ka Lok Li from DIAS for providing the source code for calculation of the inverse problem for the ARSL method. We are also grateful to Dr. Caoimhe Hickey and Dr. Ted Mccormack from the Groundwater program of GSI for providing the maps of potential Karst site locations and for fruitful discussions. Finally, we acknowledge Dr. Billy O'Keeffe for help with the problem definition.

Ireland's European Structural and Investment Funds Programmes 2014-2020
Co-funded by the Irish Government and the European Union
European Union
European Regional Development Fund
Science Foundation Ireland sfi For what's next
Geological Survey Suirbhéireacht Gheolaíochta Ireland | Éireann
TII Bonneagar Iompair Éireann

Understanding the link between climate warming and increased volcanic eruptions: detecting Icelandic tephra and volcanic aerosols in peat

L. Blennerhassett[1], E.L. Tomlinson[2]

(1) L., Blennerhassett, Department of Geology, Trinity College Dublin, College Green, Dublin 2. **Email:** blennel@tcd.ie
(2) E.L., Tomlinson, Department of Geology, Trinity College Dublin, College Green, Dublin 2. **Email:** tomlinse@tcd.ie

i. Background/Rationale

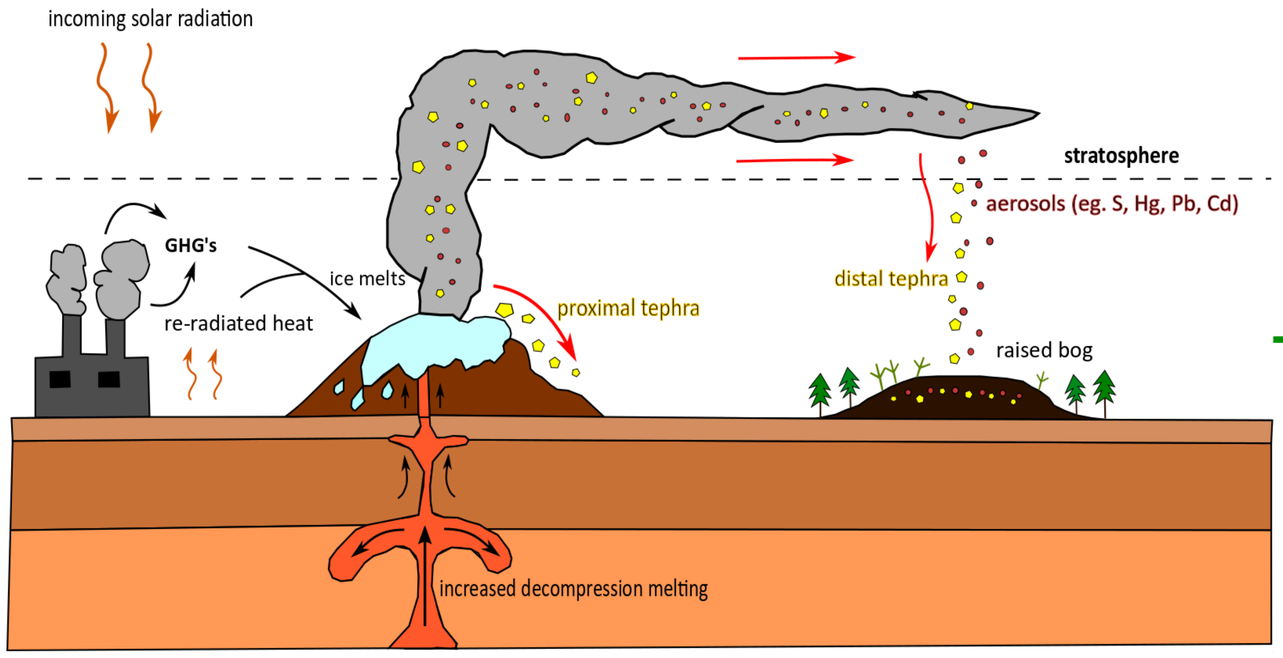

Figure 1: Schematic illustrating the relationship between an increase in planetary warming and the effect on magma production in locations such as Iceland. Raised bogs in distal locations to the volcanic source may record eruption frequency and type through direct atmospheric deposition of tephra and/or aerosols. Especially where stratospheric injection is achieved**.** Note: this relationship has predominantly been observed during the transition from the Last Glacial period into the Holocene (11,700 yrs BP), which may act as an analogue for predicting future eruption frequency due to anthropogenic climate change (Maclennan *et al*. 2002; Schmidt *et al.* 2013). Some tephras are invisible to the naked eye and are known as cryptotephras (Cooper *et al.* 2018).

Research Gaps

- This area of research is relatively novel. The distal tephra record is only just beginning to paint a picture of eruption frequency as a result of climate induced deglaciation in Iceland and in other locations around the world.
- There is notable **spatio-temporal gaps** across the Northern European Icelandic tephra record (Swindles *et al*. 2011; 2018; Lawson *et al.* 2012). More distal tephra and cryptotephra from the Last Glacial-Holocene transition and throughout the Holocene must be discovered to further understand **eruption frequency and type** in response to climate change and changing ice mass.
- The **response time** between melting ice and induced volcanic eruption is also largely unknown.
- There is a significant **basaltic tephra gap**; where most of the distal Icelandic tephra discovered is silicic in composition despite Iceland's predominantly basaltic volcanism.

Figure 1b: Hekla, Iceland - predominantly silicic (Oregon State University, 2019)

Figure 1c: Holuhraun basaltic fissure eruption 2014-2015, Iceland (Extreme Iceland, 2019)

- Further understanding this relationship based on past analogues is key to addressing one of the many **geo-hazards** we may face in response to the climate crisis. Large ash and/or aerosol producing volcanic eruptions have the potential to **seriously disrupt air space and civilization**. Recent history provides us with such examples from Iceland, with the eruption of Eyjafjallajökull in 2010 and the large basaltic eruption of Laki in 1783.

ii. Methodology and Progress

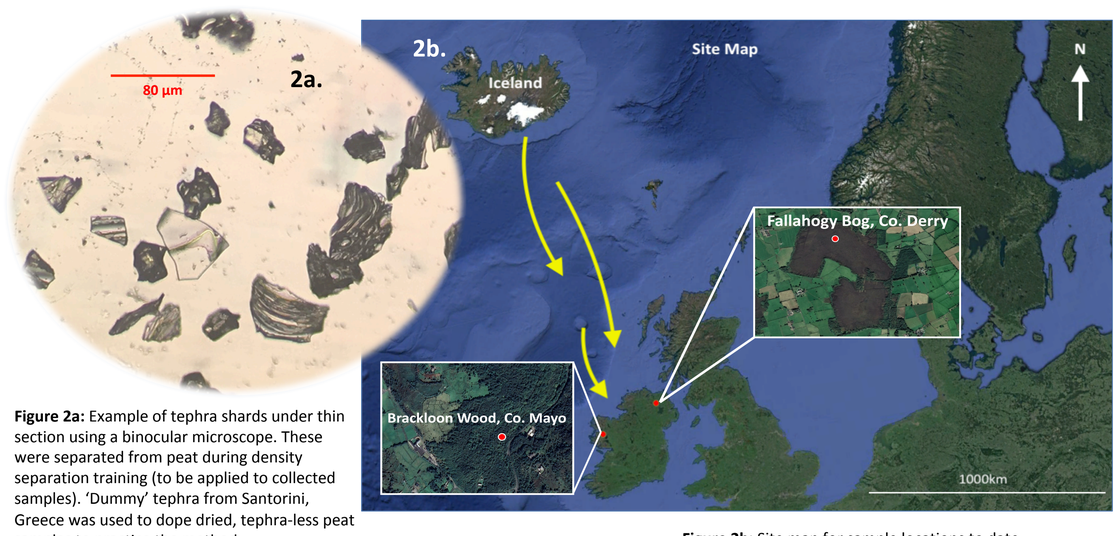

Figure 2a: Example of tephra shards under thin section using a binocular microscope. These were separated from peat during density separation training (to be applied to collected samples). 'Dummy' tephra from Santorini, Greece was used to dope dried, tephra-less peat samples to practice the method.

Figure 2b: Site map for sample locations to date. Both have known tephra horizons. Note: Brackloon wood is known for hosting the basaltic Laki 1783 tephra, which caused widespread aerosol emission and disruption to civilization (Reilly and Mitchell 2015).

Sample Collection

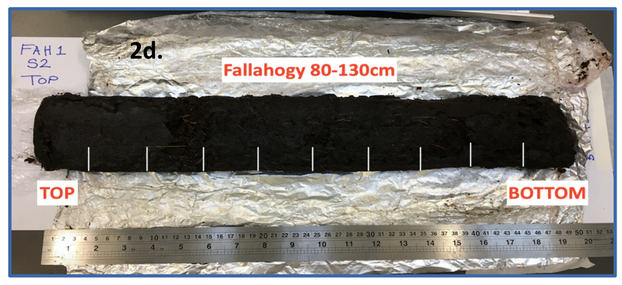

Figure 2c: Coring at Fallahogy Bog, Co. Derry using a Russian corer. A total core length of 7m was achieved. Note: coring at Brackloon Co. Mayo, only penetrated to 50cm as the Laki tephra is known to exist at 13-14cm depth (Reilly & Mitchell, 2015; Rosca, 2018).

Figure 2d: Picture showing one of the cored samples extracted from Fallahogy bog and the initial sampling resolution for loss on ignition and tephra detection (on-going).

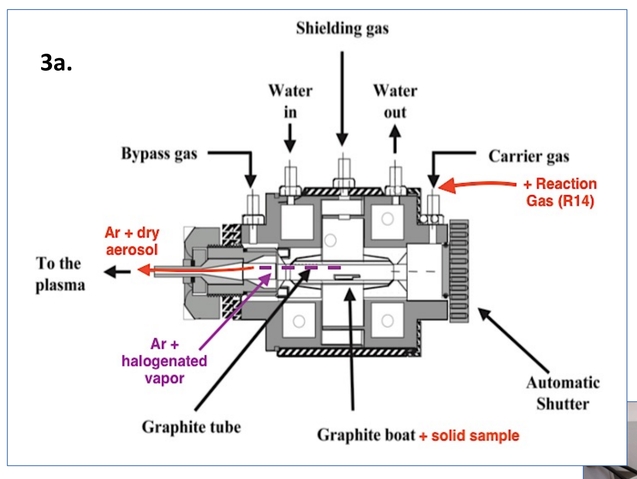

Figure 3a: adapted illustration from Esteban & Slowikowski (2013) showing basic set-up of an Electro-Thermal Vaporisation system (ETV). Solid samples are vaporised to dry aerosols in the presence of a halogen reaction gas and transported to the plasma in OES or MS systems.

ETV-ICP-OES Method Development

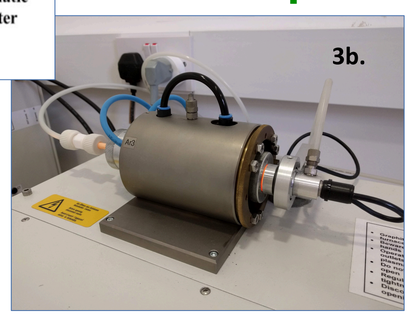

Figure 3b: ETV instrument in TCD in use. The ETV in this case is coupled to an OES. The ETV-ICP-OES method is being refined to allow the detection of volcanic aerosols and possibly altered basaltic tephra horizons in peat. Thus attempting to address spatio-temporal gaps in the Icelandic record over much of the Holocene.

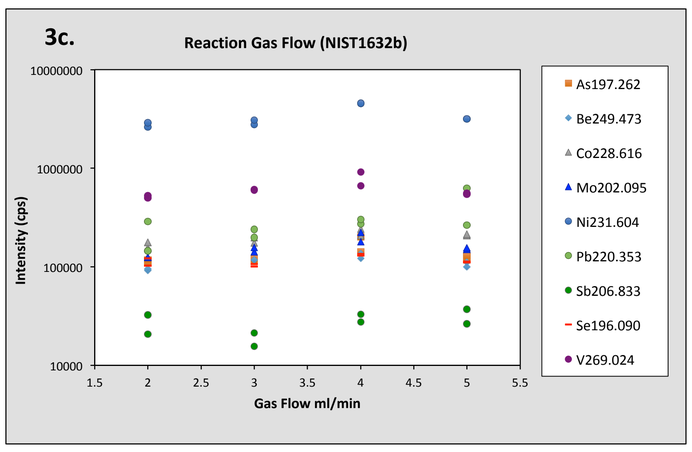

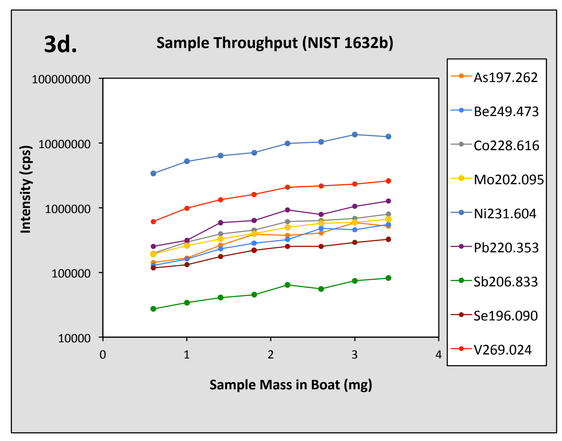

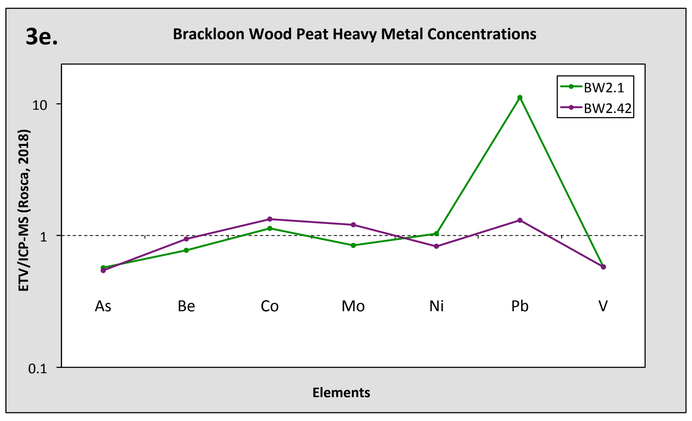

Figure 3c: Changing the reaction gas flow did show some effect on the detection of analyte signals where many elements prefer a flow of 4 ml/min compared to the default setting of 2.5 ml/min.

Figure 3d: Changing the mass of sample in the graphite boats causes loading on the plasma and decreases sensitivity. At approx. 1.8 mg the signal starts to dampen and at approx. 3.4 mg the plasma extinguishes.

Figure 3e: Preliminary comparison of heavy metal detection between the solid sampling ETV method and the conventional solution-ICP method (Rosca, 2018). Values come within close agreement to the solution ICP values except for Pb. This appears to be as a result of Pb anomalies within the graphite boats (as seen from blank analyses), which can be corrected for. Note: solution ICP uses harsh chemical digestion during sample preparation which may preclude the detection of volatiles. However, ETV-ICP-OES offers direct solid sample analyses.

iii. Overall Project Goals

Years 1-4

1. To refine the ETV-ICP-OES method for the detection of volcanic aerosols and altered tephra horizons in peat samples
2. To compare the sensitivity, efficiency, accuracy and precision of the ETV-ICP-OES method to conventional solution ICP-MS methods for tephra and aerosol detection
3. To select the most preferable method and apply to collected peat cores
4. To additionally carry out density separation and explore other tephra detection techniques to isolate crypotephra layers in peat cores
5. To apply radiocarbon dating to tephra-absent sections of the peat cores
6. To employ pollen analysis on the peat cores to act as a local climate signal
7. To create a tephrochronology of the peat cores by geochemical comparison to published tephra records
8. To couple the tephra and/or aerosol findings to the Greenland ice core tephra/aerosol records in order to achieved a time resolved climate signal ($\delta^{18}O$).
9. To use number 8 above; where a link between eruption frequency, type and response to climate warming in Iceland may be assessed in order to help predict future volcanic outcomes of anthropogenic climate change.

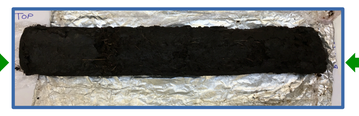

References:

- Cooper, C. L., Swindles, G. T., Savov, I. P., Schmidt, A., & Bacon, K. L. (2018). Evaluating the relationship between climate change and volcanism. *Earth-Science Reviews*, *177*(March), 238–247.
- Climate-NASA (2019) Imagery from: 'Core questions: An introduction to ice cores', assessed 12th November 2019, available at: https://climate.nasa.gov/news/2616/core-questions-an-introduction-to-ice-cores/
- Extreme Iceland (2019) Holuhraun 2014-2015 eruption image, assessed 12th November 2019, available at: https://www.extremeiceland.is/en/blog/1293-eruption-sightseeing-flight-bardarbunga-holuhraun
- Google Earth (2019), Satellite imagery, assessed on 31st October 2019.
- Lawson, I. T., Swindles, G. T., Plunkett, G., & Greenberg, D. (2012). The spatial distribution of Holocene cryptotephras in north-west Europe since 7 ka: implications for understanding ash fall events from Icelandic eruptions. *Quaternary Science Reviews*, *41*, 57–66.
- Maclennan, J., Jull, M., McKenzie, D., Slater, L., & Grönvold, K. (2002). The link between volcanism and deglaciation in Iceland. *Geochemistry, Geophysics, Geosystems*, *3*(11), 1–25.
- Martín-esteban, A., & Slowikowski, B. (n.d.). Critical Reviews in Analytical Chemistry Electrothermal Vaporization — Inductively Coupled Plasma – Mass Spectrometry (ETV-ICP-MS): A Valuable Tool for Direct Multielement Determination in Solid Samples Electrothermal Vaporization — Inductively Coupled, (April 2013), 37–41.
- Oregon State University (2019) Imagery from: 'Volcano World: Hekla – The Gateway to Hell', Tom Pfeiffer photography, assessed 12th November 2019, available at: http://volcano.oregonstate.edu/hekla-gateway-hell
- Photovolcanica.com (2019) Imagery from: 'Eyjafjallajökull volcano 2010', assessed 12th November 2019, available at: http://www.photovolcanica.com/VolcanoInfo/Eyjafjallajökull/Eyjafjallajökull.html .
- Reilly, E., & Mitchell, F. J. (2015). Establishing chronologies for woodland small hollow and mor humus deposits using tephrochronology and radiocarbon dating. *Holocene*, *25*(2), 241–252.
- Rosca, C. (2018) 'Peat bogs as archives of atmospheric metal pollution from natural and anthropogenic sources – A case study from Ireland', *Unpublished Ph.D. Thesis*, Department of Geology, Trinity College Dublin.
- Schmidt, P., Lund, B., Hieronymus, C., Maclennan, J., Árnadóttir, T., & Pagli, C. (2013). Effects of present-day deglaciation in Iceland on mantle melt production rates. *Journal of Geophysical Research: Solid Earth*, *118*(7), 3366–3379.
- Swindles, G. T., Watson, E. J., Savov, I. P., Lawson, I. T., Schmidt, A., Hooper, A., … Carrivick, J. L. (2018). Climatic control on Icelandic volcanic activity during the mid-Holocene. *Geology*, *46*(5), e444–e444.
- Swindles, Graeme T., Lawson, I. T., Savov, I. P., Connor, C. B., & Plunkett, G. (2011). A 7000 yr perspective on volcanic ash clouds affecting northern Europe. *Geology*, *39*(9), 887–890.

This publication has emanated from research supported in part by a research grant from Science Foundation Ireland (SFI) under Grant Number 13/RC/2092 and co-funded under the European Regional Development Fund and by iCRAG industry partners.

Ireland's European Structural and Investment Funds Programmes 2014-2020
Co-funded by the Irish Government and the European Union
European Union
European Regional Development Fund
Science Foundation Ireland sfi For what's next
Geological Survey Suirbhéireacht Gheolaíochta Ireland | Éireann

GIST Survey

Geohazard Investigation in the Irish Sea using Seismic and Seabed Mapping Techniques

Mark Coughlan[1,2], Eoghan Daly[1,3], Jan Majcher[4], Megan Dolan[1,3], Alex Braun[1,2], Shauna Creane[5,6]

1 iCRAG Irish Centre for Research in Applied Geosciences
2 UCD Dublin
3 NUI Galway OÉ Gaillimh
4 Ulster University
5 UCC Coláiste na hOllscoile Corcaigh, Éire University College Cork, Ireland
6 GDG Gavin & Doherty Geosolutions
Dublin Institute for Advanced Studies

RV Celtic Voyager (top left) and GIST survey activities (clockwise): recovering sediment core on deck; acquiring multibeam data; deploying sparker seismic equipment; describing seabed samples; retrieving passive acoustic monitors.

Summary

The GIST Survey was a two-week, multidisciplinary research survey onboard the *RV Celtic Voyager*, gathering geological, geophysical and marine data in the north Irish Sea.

Aims

1. To gather data in support on ongoing iCRAG research
2. To foster collaboration with other research institutes
3. To train iCRAG researchers in offshore data collection techniques

Objectives

1. To collect shallow seismic and core data to better understand the Quaternary development of the Irish Sea
2. To use this information to inform geohazard mapping and foundation engineering studies for offshore wind in the area
3. To examine the physical processes occurring at natural laboratories (i.e. shipwrecks) on the seafloor with respect to seabed morpho- and hydrodynamics using repeat bathymetric surveys and sediment samples
4. To collect data on acoustic noise propagation in the north Irish Sea and its controls

Results

- 390km of sparker seismic data to a depth of 50m was collected
- 9 sediment cores of up to 3m penetration were gathered
- Acoustic noise data were collected at 3 locations
- 6 shipwreck sites were surveyed using high-resolution multibeam echosounder, shallow seismic and current speed profiling
- 59 grab samples were attempted
- 16 CTD profiles for water column properties
- 8 water sample locations for water quality studies

Survey Highlights

1. A significant amount of seismic data was collected, covering 5 planned offshore windfarm projects, with which to identify common engineering challenges to these projects (Fig. A). Including the presence of shallow gas (Fig. B)

2. At the wreck site *SS Polwell*, the scour signature was noted to extend significantly northward, subsequently interacting with the nearby gas interconnector pipeline (Fig. C)

3. In addition to background noise, meaningful acoustic events were recorded including a bottom trawler passing within 2km while towing and our own seismic sparker survey (Fig. D)

A: GIST survey seismic data collection and survey sites with proposed windfarms in the area

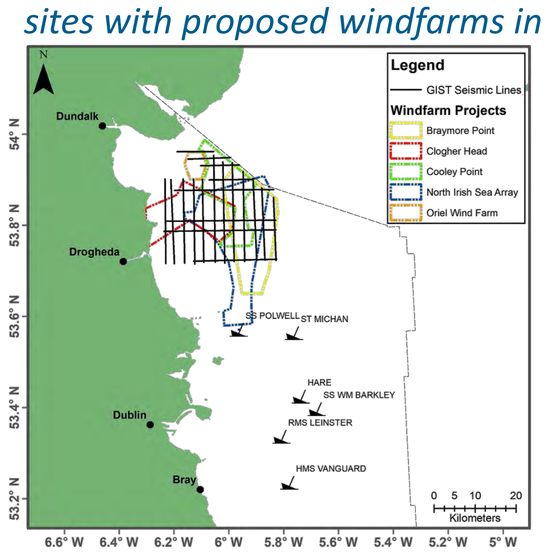

B: Shallow gas on seismic profile

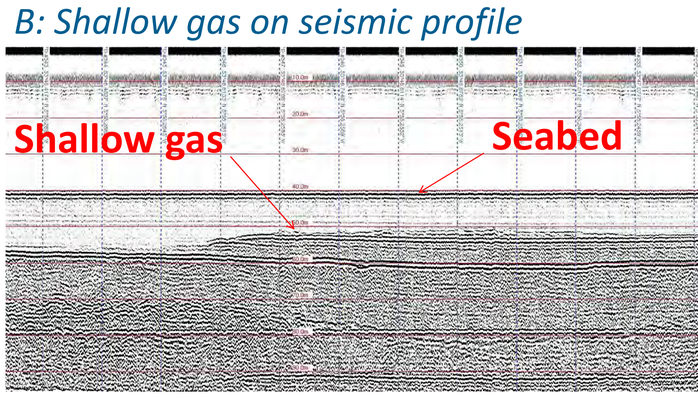

C: Shipwreck and pipeline interaction

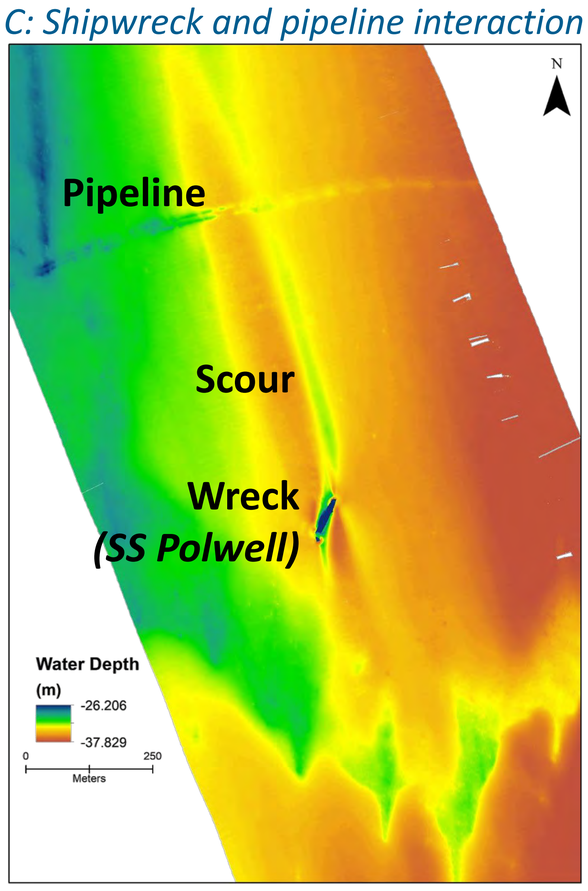

D: GIST survey acoustic events

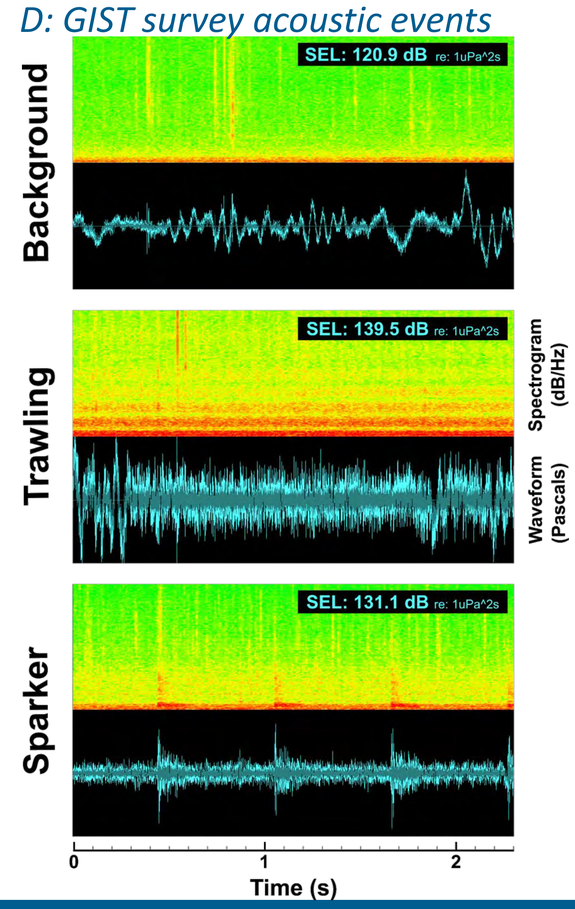

This publication has emanated from research with financial support in part from Science Foundation Ireland (SFI) under grant number 13/RC/2092 and 16/SP/4319 with support from the Geological Survey Ireland (GSI), and is co-funded under the European Regional Development Fund and by iCRAG industry partners.

Ireland's European Structural and Investment Funds Programmes 2014-2020
Co-funded by the Irish Government and the European Union
European Union
European Regional Development Fund
Geological Survey Suirbhéireacht Gheolaíochta Ireland | Éireann
Science Foundation Ireland sfi For what's next

Acknowledgements: Shiptime onboard RV Celtic Voyager for this survey was granted by the Marine Institute, funded under the Marine Research Programme 2014-2020 by the Irish Government. We thank Rosemarie Butler and Aodhán Fitzgerald (Marine Institute) for their work in helping organise the survey. We thank Ruth Plets and Rory Quinn (Ulster University) for their advice and support. We express immense thanks to the Master (Philip Baugh) and crew onboard RV Celtic Voyager for CV19027 for their expertise and experience in assisting data collection.

PIP Petroleum Infrastructure Programme

Implications of fluid migration, shallow gas and seepage in the north Irish Sea

Mark Coughlan[1,2], Srikumar Roy[1,2], Conor O'Sullivan[1,2], Annika Clements[3], Ronan O'Toole[4], Ruth Plets[5]

1 iCRAG Irish Centre for Research in Applied Geosciences
2 UCD Dublin
3 seafish
4 Geological Survey Suirbhéireacht Gheolaíochta Ireland | Éireann
5 Ulster University

1. Shallow gas in marine sediments

- Shallow gas in unconsolidated marine sediments is globally widespread and represents a significant geohazard from an engineering perspective, as well as being important as a tool for frontier exploration of hydrocarbon reservoirs .
- The impacts of shallow gas and its seepage on seabed ecology is variable.
- methane is one of the most important greenhouse gases in the atmosphere and it has been estimated that methane bubbles from the world's shallow shelf areas could account for up to 20% of the total contribution of atmospheric methane (Hovland and Judd, 1992).
- Owing to its significant effects and implications, there is a need for accurate mapping and prediction of where shallow gas and fluid seepage can occur in addition to estimates of gas volume in shallow shelf settings around the world.

2. Examples from north Irish Sea

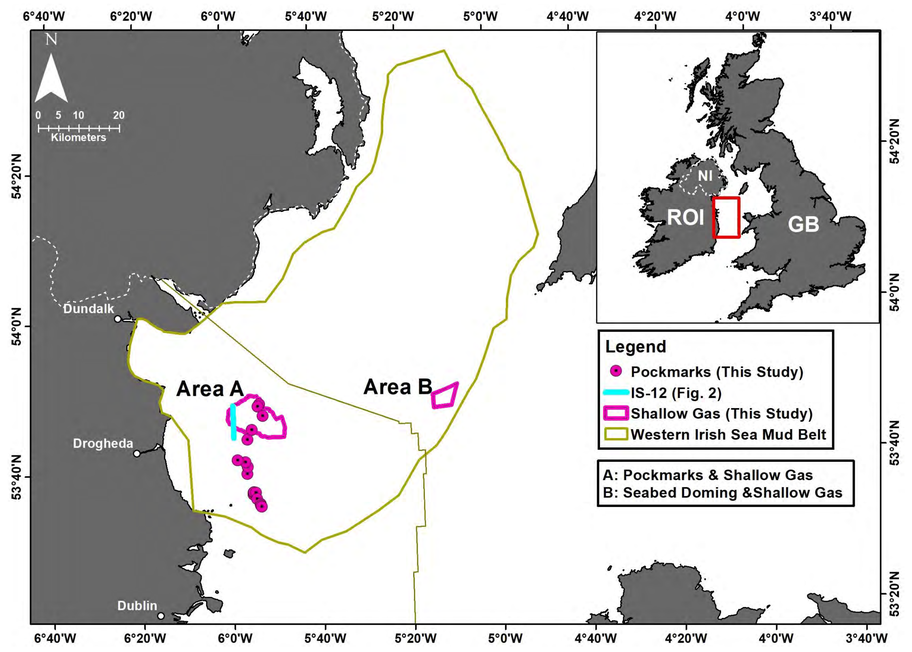

- Evidence for shallow gas accumulations and seepage in the Irish Sea can be detected from direct observation on shallow seismic lines as gas chimneys, enhanced reflectors and acoustic turbidity.
- Seabed morphological evidence includes seabed domes and pockmarks.

Area A: Pockmarks from multibeam echosounder data and shallow gas from sparker seismic profile

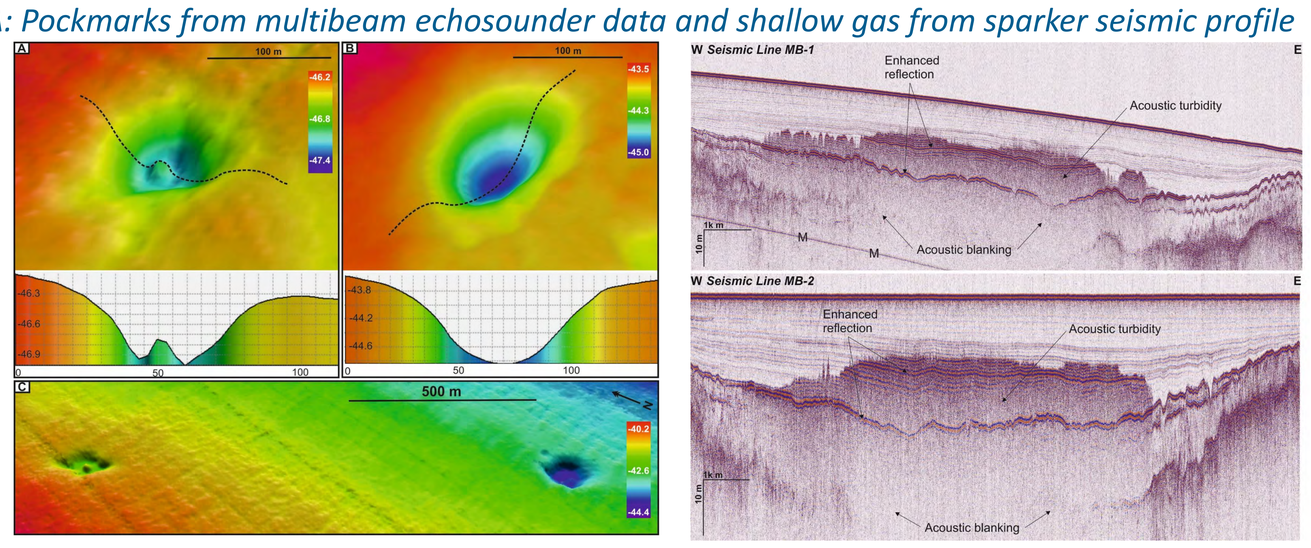

Area B: Seabed doming from multibeam echosounder data (left) and shallow gas from pinger seismic profile (right)

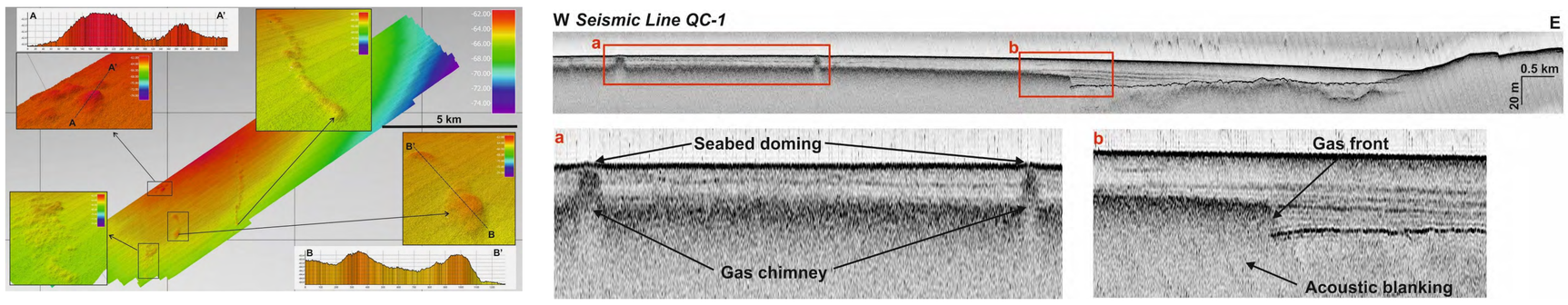

3. Thermogenic source?

- 2D reflection seismic data highlights a small half-graben structure (Fig. 2)
- This minor graben is interpreted as an erosional outlier, and the stratigraphy is inferred to be Permian and Triassic, similar to that of the Peel Basin which is known to be gas bearing.
- The bounding faults of this small graben are observed to offset the Base-Cenozoic surface, indicating relatively recent tectonic activity.
- The areal extent of this graben correlates with the extent of the acoustic turbidity mapped on sub-bottom profiler sections .

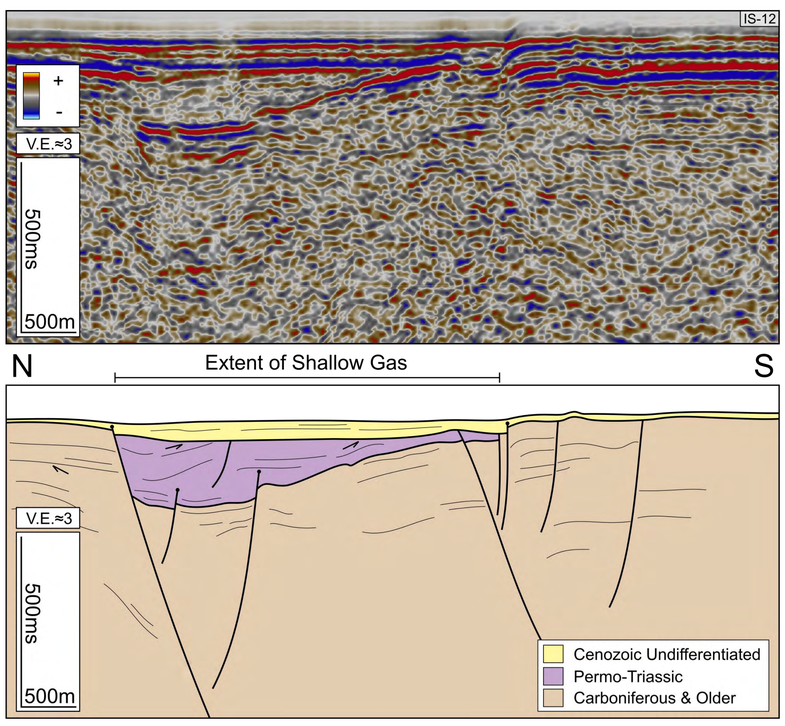

Fig. 2: 2D multichannel seismic line IS-12 and accompanying geoseismic interpretation.

4. Conceptual Model

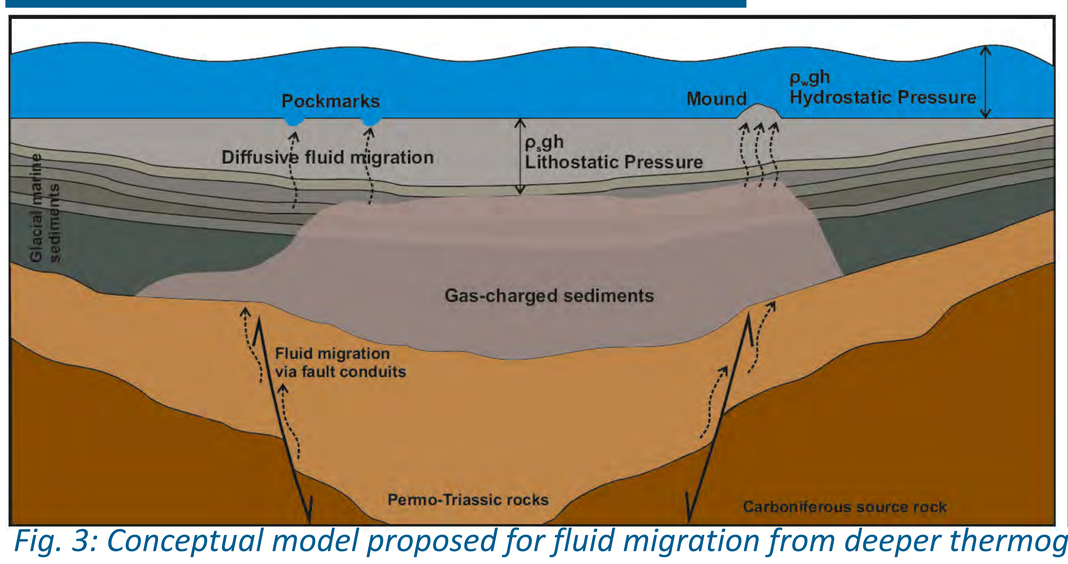

Parameters	Values	Source
Gravitational force	980 cm/s2	Heyl & Cook., (1937)
Density of marine sediments	1.8 g/cm3	Tenzer & Gladkikh., (2014)
Density of seawater	1.029 g/cm3	Millero and Huang., (2009)
Avg. water depth	4750 cm	This study
Avg. height of gas-charged sediments	1300 cm	This study
Lithostatic pressure	229320 kg/m/s	This study
Hydrostatic pressure	478999.5 kg/m/s	This study
Total pressure	708319.5 kg/m/s	This study

Fig. 3: Conceptual model proposed for fluid migration from deeper thermogenic source rocks via recently reactivated fault conduits to shallow Quaternary sediments in the Western Irish Sea Mud Belt. These sediments have become charged/saturated with gas in dissolved and/or free state. Subsequently, some of the gas undergoes diffusive migration to the seafloor, leading to the formation of pockmarks and seabed doming. It illustrates schematically the litho- and hydrostatic pressure required to keep the gas-in-place, more details in the accompanying table

5. Conclusion

Based on this model, with future data collection surveys (e.g. INFOMAR), it may be possible to predict the extent of shallow gas and location of gas seepage structures, which may act as a serious geohazard and constraint on infrastructure development or have significant implications for seabed ecology/conservation efforts.

This publication has emanated from research with financial support in part from Science Foundation Ireland (SFI) under grant number 13/RC/2092 and 16/SP/4319 with support from the Geological Survey Ireland (GSI), and is co-funded under the European Regional Development Fund and by iCRAG industry partners.

Ireland's European Structural and Investment Funds Programmes 2014-2020
Co-funded by the Irish Government and the European Union

European Union
European Regional Development Fund

Geological Survey Suirbhéireacht Gheolaíochta Ireland | Éireann

Science Foundation Ireland sfi For what's next

Acknowledgements: Petroleum Affairs Division (PAD) of the Department of Communications, Climate Action and Environment (DCCAE), Ireland, for providing access to released well, seismic and potential field datasets. Schlumberger for providing academic licenses of Petrel. IHS Markit for providing the academic licence for the KINGDOM. This paper contains Irish Public Sector Data (INFOMAR) licensed under a Creative Commons Attribution 4.0 International (CC BY 4.0) licence. Dr. Matthew Service and Rory O'Loughlin (both Agri-Food and Biosciences Institute, Northern Ireland) for releasing MBES data for Queenie Corner. Rosie Jebb (GSI) and Andy Trafford (UCD) for processing MBES and sub-bottom profile data. The crew and scientists onboard all surveys listed for their work, co-operation and skill in collecting the data.

PIP Petroleum Infrastructure Programme

Karst and the N6 Galway City Ring Road: Infrastructure for a Sustainable City and Community

Dolan, M.* [1,2,3,4], McCabe, B. [1,3,4], Henry, T. [2,3,4], Murray, J. [2,3], Daly, E. [2,4], O'Leary, D. [2,4], Fleming, M. [5]

[1] Civil Engineering, College of Engineering and Informatics, NUI Galway [2] Earth and Ocean Sciences, School of Natural Sciences, NUI Galway [3] Irish Centre for Research in Applied Geosciences (iCRAG)

[4] Ryan Institute, NUI Galway [5] Arup, 50 Ringsend Road, Dublin 4 ***m.dolan16@nuigalway.ie or megan.dolan@icrag-centre.org***

(iv) Sediment Log

BH03

Figure 8
Simplified log

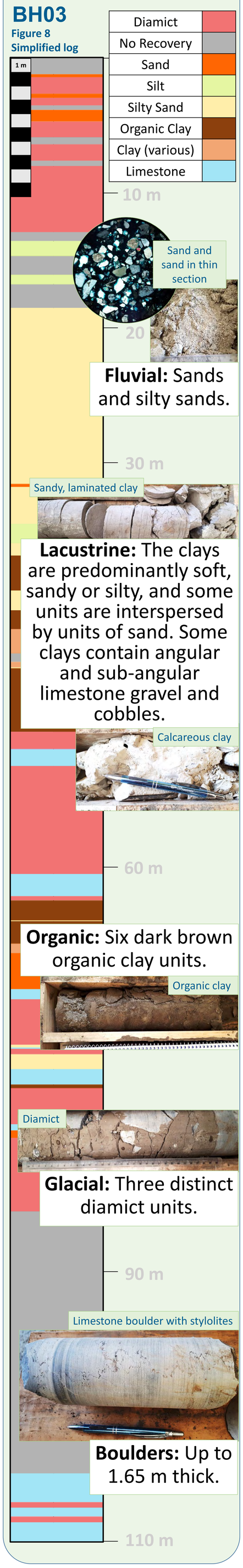

Introduction

A *c*.110 m deep sediment-filled karst feature was discovered during preliminary ground investigation for a proposed tunnelled section (to avoid a local Special Area of Conservation) along the N6 Galway City Ring Road (Fig.1). The discovered feature located between Lough Corrib and Galway City, adjacent to the inactive Coolough Quarry (Fig.2), has prompted a geological investigation to better understand the nature and timing of formation of this karst landform (300 m L x 100 m W). This presentation discusses only the results which provide data that will help inform the construction of the N6 tunnel, which will commence within the western quarry walls, pass through limestone bedrock and emerge within the large karst depression (fields within study site).

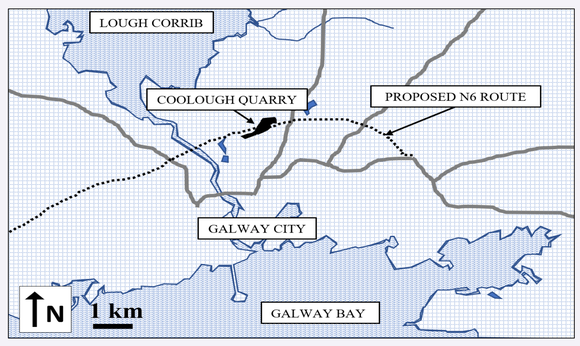

Figure 1 Galway map with proposed N6 route showing location of Coolough Quarry.

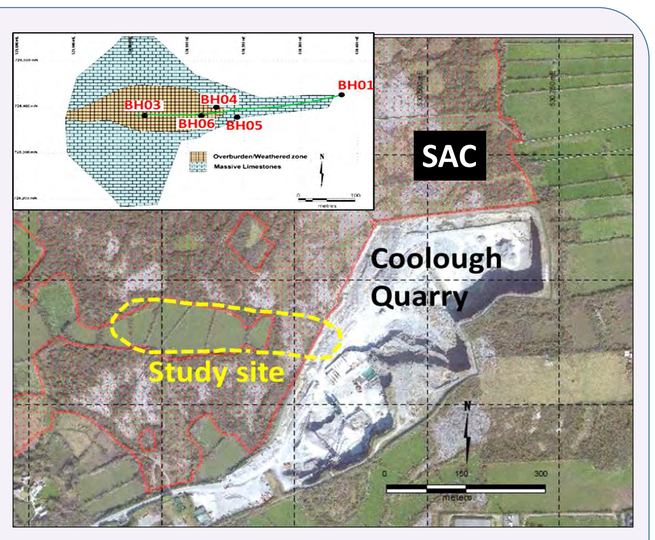

Figure 2 Satellite showing Coolough Quarry, the Special Area of Conservation (SAC) in red hash and the study site in yellow (location of proposed tunnel). Inset: karst feature (brown) as mapped using electrical resistivity & microgravity.

Methodology

(i) Line transects and laser scans were used to collect structural data from the exposed limestone bedrock in Coolough Quarry. **(ii)** 2D electrical resistivity surveys were conducted across the quarry floor to image the subsurface structure. **(iii)** A petrographic analysis determined the lithology of the bedrock. **(iv)** Core from BH03 was used to create a detailed log (Fig.8) of the infilling sediment within the karst feature.

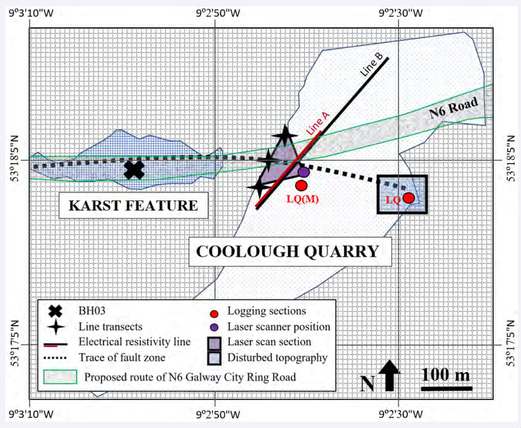

Figure 3 Schematic map of study site showing relevant field work locations and the proposed route of the N6 Galway City Ring Road. Lines included represent the electrical resistivity survey lines (240 m and 480 m) and the trace of an apparent fault damage zone (dashed). Areas highlighted include an area of topographic disturbance and the laser scan section.

(i) Structural Analysis

Line Transects: The bedrock demonstrates fractures from the millimetre scale to major joints. Two vertical/subvertical joint sets strike roughly 050 and 150 (Fig.4).

Terrestrial Laser Scanner: Scan models of the quarry face in which the tunnel will commence give an accurate representation of the joint orientations (and other fractures) and the overall nature of the outcropping limestone bedrock (Fig.5).

This data will help inform the stabilisation of the quarry walls in the construction of the mined tunnel.

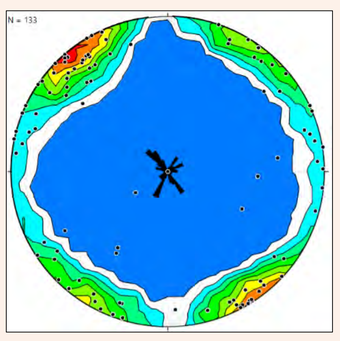

Figure 4 Stereonet with poles to planes and calculated rose diagram for major bedrock joints.

Figure 5 3D model of the scan section as generated in Cyclone software showing two quarry benches in which the mined tunnel will commence.

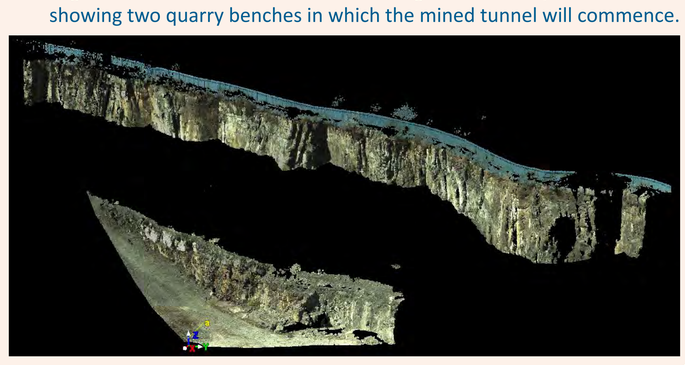

(ii) Geophysics – Karst Assessment

Wenner-Schlumberger and dipole-dipole arrays were used on both line lengths (Line A and Line B). A thick layer interpreted as massive and unweathered limestone ('rock') strongly contrasts the areas of low resistivity in each profile; (i), (ii) and (y). A fault zone (~65 m wide) and deep conduit (i and ii) are interpreted beneath the Coolough quarry floor (Fig.6) from low resistivity readings on the 2D electrical resistivity profiles.

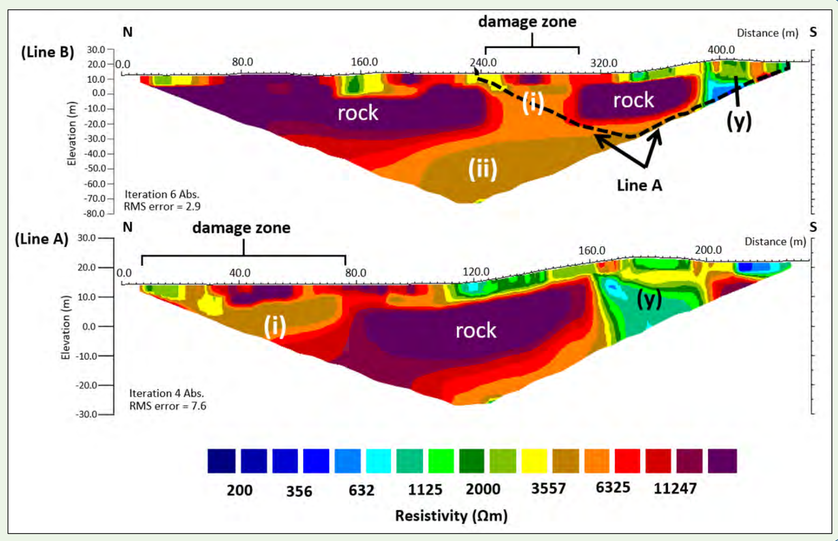

Figure 6 Modelled resistivities for the Wenner-Schlumberger array configuration on Line B and Line A. A dashed black line indicates where the survey extent of Line A overlaps Line B. Areas (i) and (ii) are interpreted as the damage zone of a fault and a conduit with resistivity values between 3557-6325 Ωm. Area (y) yields relatively low resistivity values between 632-2000 Ωm and is interpreted as containing shallow karst with a high volumetric water content.

(iii) Petrography

Limestone bedrock samples were typically grey, fine to medium grained and algal-rich peloidal and skeletal packstones and wackestones. The samples did not exhibit macroporosity. Two ~20-30 cm thick fissile clay units are interbedded within the limestones (documenting sea-level fluctuation) which are thick-bedded to massive. Bioclasts include foraminifera, crinoids, various calcareous algae (including *Konickopora*) and bryozoans (Fig.7). The fossil assemblages are scarce in macrofauna. The bedrock is interpreted as having been deposited in a shallow-water shelf setting.

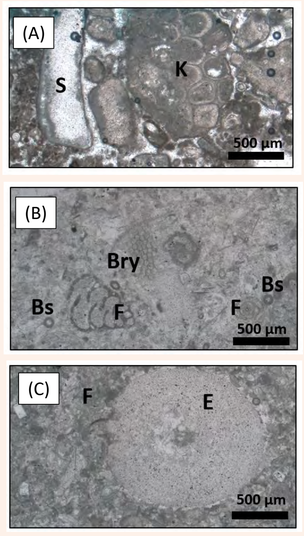

Figure 7 Photomicrographs of limestone samples. *Konickopora* algae (K), Skeletal fragments (S), Foraminifera (F), Brachiopod spines (Bs), Bryozoans (Bry), and Echinoderm (e.g. crinoids) (E).

Conclusions

The proposed N6 Galway City Ring Road is part of an effort to relieve traffic congestion and ensure the sustainable growth of Galway city. Characterisation of the bedrock (structure and petrography) informs the design of the mined tunnel section, part of the N6 road, whilst the detailed log of the sediment infilling the karst feature informs the construction of the open cut tunnel segment. The geophysics results expose structures within the subsurface of the quarry, beneath the proposed route of the N6 road, revealing potential karst-related risks.

Acknowledgements

The authors would like to thank project sponsors; Arup and the Geological Survey Ireland.

This publication has emanated from research supported in part by a research grant from Science Foundation Ireland (SFI) under Grant Number 13/RC/2092 and co-funded under the European Regional Development Fund and by iCRAG industry partners.

iCRAG 2019

Resources for a Sustainable Future

PLATFORM
PUBLIC PERCEPTION AND UNDERSTANDING

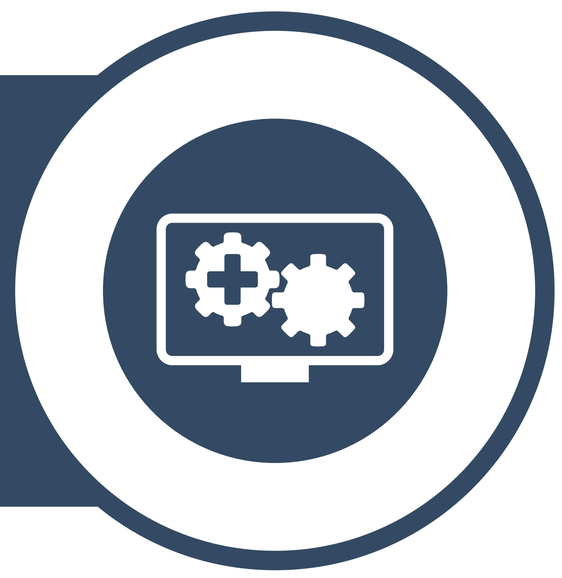

Radon Risk Perception, Communication and Participative Decision-making

Gary Bradley[1], Quentin Crowley[2], David Hevey[3]

1. Irish Centre for Research in Applied Geosciences (iCRAG)
2. Dept. Geology, School of Natural Sciences, Trinity College Dublin
3. Dept Psychology, Trinity College Dublin

Email: gary.Bradley@icrag-centre.org

❖ Context

- Radon-cancer is a global issue and this research supports Goal 3 of the UN Sustainable Development Goals.
- Radon is a naturally occurring radioactive gas present in residential properties. It is the second cause of lung cancer after smoking and is attributed to new 300 cases in Ireland every year.
- Radon is featureless and can only be measured via special detectors. The average Radio level in Ireland is 77 Bq/m^3. EPA recommended action-level for mitigation is >200 Bq/m^3 Highest level in Ireland 49,000 Bq/$m^{3.}$ Despite the risk to health, resident response rate for testing remains low (17-30%).
- Cognitive and emotional (affective) nature of Radon-risk perception not well understood.
- Current behaviour change theories have poor fit / predictability and focus mainly on intention rather than actual behaviour change.

❖ Research Questions

1. **How does risk perception influence personal agency in response to communications?**

a. **Risk-based cognitive-affect:**
- What core affect (affect heuristic) and cognitive aspects of risk perception contextualises affect and influences decision-making motivation towards testing and mitigation behaviour?

b. **Message customisation and optimisation:**
- How can message selection, framing and presentation influence participatory decision-making?
- Are factors such as socio-economic status or location important?
- Are layered and/or sequenced messages more effective that single-instance delivery?

2. **How can improved testing and mitigation be achieved through risk communications?**
- Custom model and delivery design
- Locally supported, shared decision-making
- Can online systems support behaviour change?

❖ Challenges

- To profile key factors in stake holder decision-making behaviour (Policy-makers, local government and residents).
- Determine representative populations and sampling strategy
- Understand how Radon perception, exposure and dosimetry constructs influence risk perception and decision-making..
- Determine process-orientated factors that promotes shared decision-making and engagement.

❖ Methodology

1. Profile stakeholder groups via survey & focus group

2. Design targeted, customised communications to support shared decision-making

3. Evaluate for effectiveness

This publication has emanated from research supported in part by a research grant from Science Foundation Ireland (SFI) under Grant Number 13/RC/2092 and co-funded under the European Regional Development Fund..

Ireland's European Structural and Investment Funds Programmes 2014-2020
Co-funded by the Irish Government and the European Union
European Union
European Regional Development Fund
Science Foundation Ireland sfi For what's next

The Tephra Bag Experiment - Five steps for a successful citizen science project

Kamila Kwasniewska[1], Geertje Schuitema[2], Jennifer C. McElwain[1]

[1]Botany Department, Trinity College Dublin, Dublin, Ireland

[2]Marketing Department, College of Business, University College Dublin, Dublin, Ireland

1 Scope the problem

Climate change *is a global scale challenge for humanity that requires a multilateral solution on a planetary scale.*

- The mechanisms by which we can reduce the greenhouse gas levels in the atmosphere requires some form of **geoengineering solution** or rapid development and deployment of negative carbon emission technology.
- Implementation of **negative carbon emission technology** will only be possible if there is broad citizen engagement and implementation acceptance of the proposed solutions.

2 Design a meaningful and engaging project

Plant-enhanced chemical weathering *could increase the rate at which CO_2 helps to weather calcium silicate, that in turn increases the rate at which the carbonates are deposited and stored in the oceans.*

- The Tephra Bag Citizen Science projects aims **to evaluate the chemical weathering potential of tephra** (volcanic ash) placed in a tea bag which is buried in the soil together with planted ryegrass, one of the most common plants in Ireland.
- The secondary aim is to **educate the citizen scientist on potential geological–based solutions** for climate change by reducing the greenhouse gas concentration in the atmosphere.

TephraBAG citizen science

3 Build a citizen science community

- Recently, education and **engagement with the public has become an equally important aim of citizen science** projects, as there is a need for a dialogue between scientist and the public.
- The project focuses on **engaging with teachers, school children and their families in science.**

Citizen scientists *are volunteers who collaborate with a scientific process, for example by collecting data. They observe and record information about the natural world and contribute to a growing need of environmental data.*

4 Manage the data

- To ensure for a good quality data set the **volunteers must be provided with the training** for the data collection or data analysis.
- A website incorporating the instructions for experimental set-up, data collection and data upload is designed on a citizen science platform e.g., Zooniverse.

Collection of meaningful data *is a primary goal of most citizen science projects.*

5 Sustain and Improve

Successful citizen science projects require sustained participation and funding, as well ***as sound methods of evaluating progress toward goals.***

- The project aims to **investigate school children's engagement and knowledge around climate change** and carbon emission reduction.
- To systematically assess the school children's commitment and education, **a protocol to design and evaluate the project is developed.**

This publication has emanated from research supported in part by a research grant from Science Foundation Ireland (SFI) under Grant Number 13/RC/2092 and is co-funded under the European Regional Development Fund and by iCRAG industry partners.

Ireland's European Structural and Investment Funds Programmes 2014-2020 — Co-funded by the Irish Government and the European Union

European Union — European Regional Development Fund

Science Foundation Ireland — For what's next

contact:

The human side of geoscientists: comparing geoscientists' and non-geoscientists' cognitive and affective responses to geology

Anthea R Lacchia*[1], Geertje Schuitema[1], Peter Haughton[1], Patrick Shannon[1] & Fergus McAuliffe[1]
[1] iCRAG, Irish Centre for Research in Applied Geosciences, UCD School of Earth Sciences, Dublin, Ireland
*e-mail: anthea.lacchia@icrag-centre.org

Study motivations and relevance to sustainable development goals

Geoscientists and non-geoscientists often struggle to **communicate**, especially around complex or contentious geoscience issues connected to **sustainable resource consumption and production**, clean **energy**, as well as **climate action**. This hinders communication processes that are essential to **sustainable development**.

United Nations Sustainable Development Goals (SDGs) of relevance to this study

For true dialogic communication between experts and non-experts to take place, both groups must understand the audience they are engaging with. Here, we focus on understanding the differences in **thoughts** and **feelings** between experts and non-experts.

Approach

Research questions

1. What is the perception and understanding of geology on the part of local people in Clare?
2. How well do the mental images of members of the local community match those of geoscientists?

We adopted **a "mental models" psychological approach** (see Gibson *et al*, 2016) to investigate the perception of people living in rural communities in County Clare and of experts across Ireland.

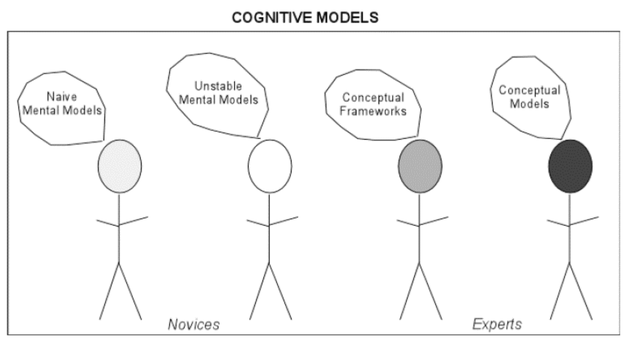

Four categories of cognitive models in Libarkin *et al* (2003)

Mental models

Mental (or cognitive) models are an individual's representation of a phenomenon, or a way for people to interpret and navigate the world (Libarkin *et al*, 2003).

Libarkin *et al* (2003) recognize four categories of mental models in the context of science education, categorised into novices' and experts' mental models (see left).

Mixed methods approach

A face-to-face **survey** was conducted with experts (recruited across Ireland) and non-experts (recruited in a rural community in Ireland) to compare their mental models of the **subsurface** of the Earth, applied-geoscience processes, i.e. **mining**, **quarrying** and **drilling**, and **flooding**. To establish their mental models, respondents were asked to make **sketches** of the processes, geohazard, and of the subsurface to any depth.

Respondents
Total = 62
Non-geoscientists = 38
Geoscientists = 24

The sketches were analysed by means of **thematic analysis** to identify themes that were common to some or all of them. Three dominant themes were identified in the sketches using thematic analysis:

1. Degree of **knowledge & familiarity** with the topics
2. Presence of **human interactions**
3. **Perceived impact** on the economy or environment

Thematic analysis of sketches

KNOWLEDGE & FAMILIARITY

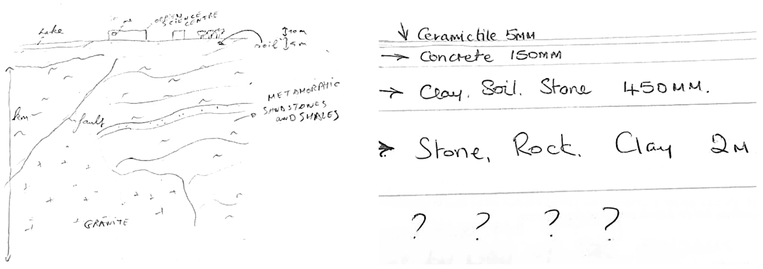

Geoscientist — Non-geoscientist

Compared to non-experts, experts' mental models incorporated:

- More technical jargon, $F(1,42) = 6.776$, $p<.05$
- More labels, $F(1,54) = 8.294$, $p<.01$
- More layers, $F(1,54) = 9.083$, $p<.005$
- A greater sense of scale, $F(1,54) = 4.229$, $p<.05$
- A greater depth, $F(1,58) = 25.392$, $p<.001$

- While experts have a higher level of knowledge and familiarity with geoscience processes and concepts, non-experts possess local knowledge and lay expertise

HUMAN INTERACTIONS

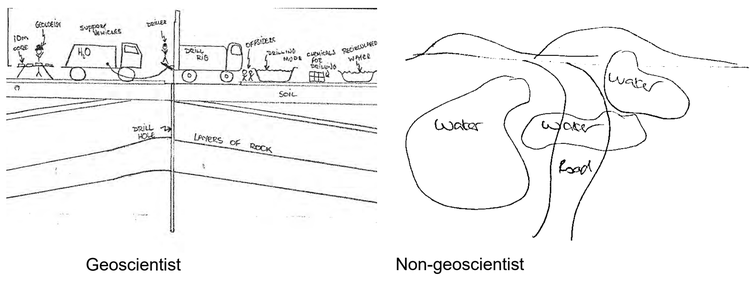

Geoscientist — Non-geoscientist

- Experts included more human interactions than non-experts in their mental models, $F(1,54) = 24.610$, $p < 0.001$

- Human interactions were particularly present in the mental models of experts

IMPACT ON ENVIRONMENT & ECONOMY

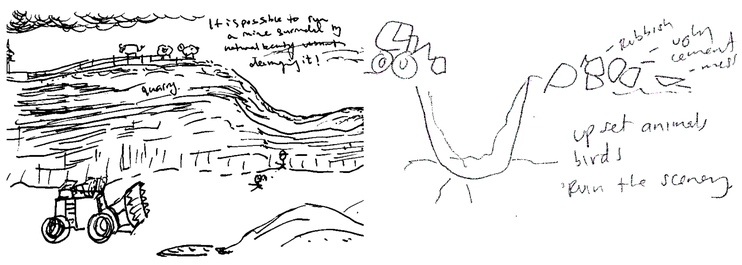

Geoscientist — Non-geoscientist

- An environmental or economic impact theme was present in the mental models of both experts and non-experts

- Experts tended to highlight the positive impacts, often in a defensive tone, whereas non-experts tended to dwell on the negative ones (e.g. labels: 'ruins the scenery', 'upset animals')

Recommendations

THEORY

Non-experts' mental models focus on environmental and economic **impacts** of geoscience, while **experts** focus more on **human** interactions, as well as having more familiarity and technical knowledge about geoscience.

The is no clear dichotomy of 'naïve' versus 'complex' mental models. Instead, the mental models of *both* groups incorporate **affective** (based on feelings) and **cognitive** (based on rational thoughts) components. We thus argue that mental models should be defined as the cognitive and affective representation of a phenomenon.

PRACTICE

In order for inclusive **dialogue** to take place, experts and non-experts may wish to focus on **commonalities** rather than differences in their mental models in order to find common ground. By acknowledging the affective components of their mental models, and including **feelings** in their chosen form of communication, experts may reach wider audiences. Overall, showcasing geoscience as a **human activity** should result in successful communication strategies. Our results can help to enable dialogue around **sustainable** use of Earth's resources.

References

Gibson, H., Steward, I., Pahl, S., & Stokes, A. 2016. A "mental models" approach to the communication of subsurface hydrology and hazards. *Hydrology and Earth System Sciences*, 20, 1737-1749
GSI, 2015. Review of key issues around social acceptance of geoscience activities and earth resources in Ireland. Geological Survey of Ireland, Dublin.
Libarkin, J., Beilfuss, M., & Kurdziel, J. 2003. Research methodologies in Science Education: mental models and cognition in education. *Journal of Geoscience Education*, 51(1), 121-126.
SFI Evaluation Toolkit, 2015. Available at: http://www.sfi.ie/discover-science-engineering-dse/guidance-and-best-practice/evaluation-toolkit.html
UN Sustainable Development Goals website. Available at: https://sustainabledevelopment.un.org/

Acknowledgements

We are very thankful to the people of County Clare and to the geoscientists who took part in the survey. Thank you to the iCRAG EPE Think Tank for piloting the survey and to iCRAG staff for taking part in the expert consultation. Thank you to SFI for funding this research. Ethical approval for the study was obtained from University College Dublin (Ethical Exemption Reference Number HS-E-17-84-Lacchia-Haughton).

This publication has emanated from research supported in part by a research grant from Science Foundation Ireland (SFI) under Grant Number 13/RC/2092 and co-funded under the European Regional Development Fund and by PIPCO RSG and its member companies.

Ireland's European Structural and Investment Funds Programmes 2014-2020
Co-funded by the Irish Government and the European Union
European Union
European Regional Development Fund
Science Foundation Ireland sfi For what's next
PIP Petroleum Infrastructure Programme

GeoPlan: A new engagement framework for decision-making on coastal geohazards

Dr Daniel Tubridy*, Dr Mick Lennon, Prof Mark Scott

*UCD School of Architecture, Planning and Environmental Policy - daniel.tubridy@ucd.ie – geoplan.ucd.ie - twitter.com/Geoplan_UCD

Background

- Due to the effects of climate change, **geohazards such as coastal erosion will have increasingly severe impacts on coastal areas and communities in Ireland** [1].
- There are significant risks including damages to infrastructure and property, built heritage and sites with ecological designations.

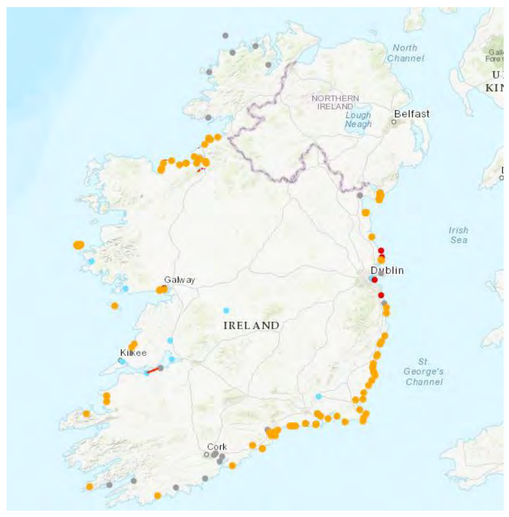

Properties at risk from coastal erosion in Ireland in medium term (CCMA, 2017)

Coastal erosion and property damage, Donaghmore, Co, Wexford (Wexford CC, 2019)

- However, there are **important uncertainties and knowledge gaps** regarding local impacts and about what management strategies should be adopted.
- Conventional strategies which rely on the construction of new coastal defences will be inadequate due to **technical limits, resource constraints and ecological impacts** [2].

Landscape impacts and technical limitations of conventional coastal defences in Portrane, Co, Dublin and Rosses Point, Co. Sligo (credit: the authors)

- Evidence also shows that identifying and implementing more sustainable adaptation strategies, such as 'managed retreat' from at-risk areas, requires **extensive community engagement** [3].
- Further research is required to understand how this can be achieved.

Aims and objectives

The aim of the research is to develop a new knowledge sharing and participatory decision-making framework capable of integrating conflicting understandings of risk and vulnerability amongst different stakeholder groups. The associated research objectives are:

- To explore whether managed retreat could be a viable adaptation strategy in an Irish context,
- To develop and trial an innovative **knowledge co-production and co-design process** in the real-world setting,
- To **develop guidelines** to inform planners and policy-makers across different sectors of adaptation planning in Ireland regarding methods of risk assessment and community engagement.

O'Raw et al. 2017

NUIG, 2019

Work plan

In order to address the project's aim of developing and trialling a new participatory decision-making framework, a range of intermediate work packages and deliverables are being progressed. These include

- A review of academic and grey literature on **coastal climate change adaptation and managed retreat**
- A review of the **Irish planning and policy context** for coastal planning and climate adaptation
- Developing the methodology and workshop materials through the **application of principles of knowledge co-production and co-design.**
- A scoping exercise to identify relevant case studies and desk research on local context and coastal management challenges.

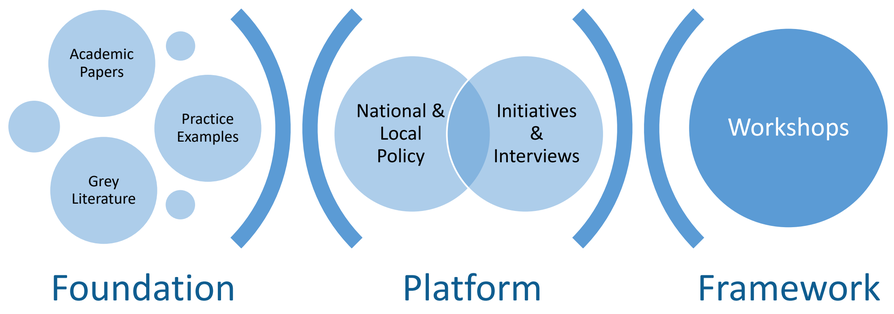

- Within the case studies, the research process will involve the trialling of the participatory decision-making framework through a series of three workshops facilitated by the research team.
- Each workshop will involve distinct stages of **measuring** participants' views on risk, vulnerability and coastal management, **co-designing** workshop materials and **supporting and professionalising** the workshop outputs.

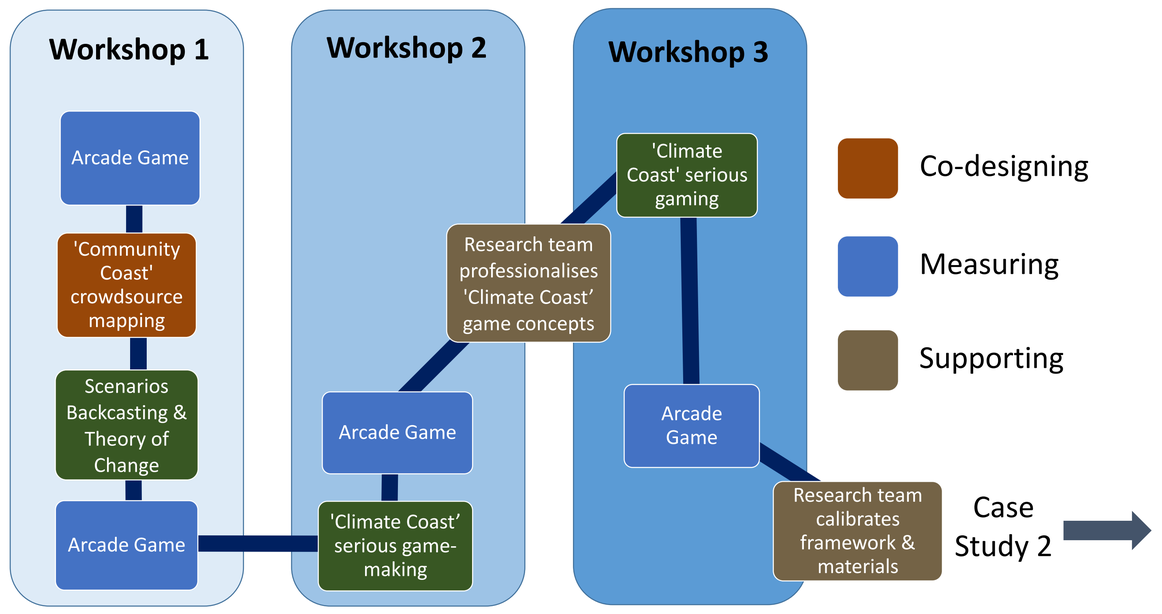

Dissemination

The outputs of the research project will include knowledge transfer events, evidence-based policy and practice recommendations regarding community engagement in the management of coastal geohazards as well as academic publications. The specific dissemination methods are:

- **A project website (geoplan.ucd.ie) and twitter account (twitter.com/Geoplan_UCD)** which provide background information and regular updates on the progress of the research project
- A **one-day workshop** to communicate key project outputs to policymakers and planners, as well as contributions to national and international academic conferences
- **Academic publications** including a review of planning challenges associated with 'managed retreat' from climate hazards (currently in preparation).

References

[1] Climateireland.ie (2019) "Hazard tool: Coastal Erosion" (https://www.climateireland.ie/#!/tools/hazardTool/hazardscopingCoastalErosion

[2] O'Connor, M. C., Lymbery, G., Cooper, J. A. G., Gault, J., & McKenna, J. (2009). Practice versus policy-led coastal defence management. *Marine Policy*, *33*(6), 923-929.

[3] Blunkell, C. T. (2017). Local participation in coastal adaptation decisions in the UK: between promise and reality. *Local Environment*, *22*(4), 492-507.

This publication has emanated from research supported in part by a research grant from Science Foundation Ireland (SFI) under Grant Number 13/RC/2092 and co-funded under the European Regional Development Fund and by iCRAG industry partners.

Ireland's European Structural and Investment Funds Programmes 2014-2020
Co-funded by the Irish Government and the European Union
European Union
European Regional Development Fund
Science Foundation Ireland sfi For what's next

A Feat of Clay: Palaeontology Engagement through Art

Elspeth Wallace[1.], Anthea Lacchia[1.], Elaine Harrington[2.],
Fergus McAuliffe[1.], Emma Morris[1.], Peter Haughton[1.]
[1.] Irish Centre for Research in Applied Geosciences, University College Dublin
[2.] University College Dublin Parity Studios

Figure 1: A ceramic dish inspired by a fossil echinoid.

Palaeontology: a gateway to the Earth Sciences?

There is little doubt that palaeontology can be an effective tool in engaging publics with the geosciences. Fossils are charismatic and capable of inspiring publics regardless of age, ethnicity, gender and other factors. Despite this, audiences reached by palaeontological engagement are often limited to recurring groups, such as families with young children and adults with a pre-held interest in the sciences.

A Feat of Clay

A Feat of Clay is an exciting interdisciplinary project which aims to broaden the audiences reached by palaeontological engagment through collaboration with the arts. The pilot workshop has been developed and run in collaboration with University College Dublin Parity Artist in Residence Elaine Harrington, and was made possible through a University College Dublin seed funding grant (grant number SF1734).

In the workshop, participants were introduced to a range of fossils and the geoscience involved in producing clay for ceramics. They were then encouraged to create a fossil-inspired artwork from the clays that were provided (figure 1). The most popular method of artwork creation was a fossil imprint in the manner of a trace fossil. This raised the question: what trace will humans leave on the Earth?

We chose to run the 2.5-hour workshop on a Saturday afternoon at a community centre in rural Western Ireland, an area classified as having low levels of scientific engagement by Science Foundation Ireland (Science In Ireland Barometer, 2015).

Each year, approximately 200 geologists visit West Clare, in Western Ireland, for education and training (more than 10,000 over the decades), and it is an ideal location for non-geoscientists to take part in public engagement activities around geoscience. This is why we chose to pilot our project there. This also diversified the audience that could be reached by the workshop.

Expanding Audiences

Twenty five people attended the Feat of Clay workshop. The audiences reached could be split into two distinct groups:

1. Predominantly female non-scientists between the ages of 30-60 (figures 2 and 3).
2. Ceramic artists interested in learning more about the technical and professional side of ceramics and geology. Though they also had chance to make a ceramic piece, they preferred to engage with the scientists in attendance to learn more.

Audiences wil be monitored to evaluate their expansion from those traditionally reached by iCRAG's public engagement activities.

Figures 2 and 3: Workshop attendees preparing clay for imprints and sculpting their creations from the provided clay.

Motivation

Figure 4: Fossils available for inspiration and trace making.

Art-science collaborations have the ability to bring together different perspectives to create new and unique forms of public engagement. A Feat of Clay capitalises on this perspective in order to increase public learning.

Artists, geoscientists and publics hold a diversity of views of the Earth and clay as the materials that make up rocks, fossils, utensils and art. As geoscientists and artists, we work with the same materials, but the significance we apply to them, and how we work with them are different. To explore these different viewpoints, and educate publics in geology and palaeontology, we designed the workshop to examine the material journey from Earth to pot.

Figures 5, 6 and 7: Creations made during the Feat of Clay workshop.

What's next?

We will build on the success of this event by repeating this workshop in 2020 in other STEM target communities and locations as identified by the Science in Ireland barometer (2015).

A further and important part of the project (seed funding grant SF1734) is to develop transportable ceramic models of the subsurface which can be used to engage different groups of non-geoscientists with geoscience.

These models are inspired by cores of Carboniferous- aged rocks which were drilled in Co. Clare, Ireland, by Equinor (Statoil) in a joint project with University College Dublin (figure 8). The cores illustrate how strata get deposited as well as the main principles of biostratigraphy.

Fossil models and impressions (of ammonoids) will also be developed for use in teaching and public engagement by University College Dublin Parity Artist in Residence Elaine Harrington with the other co-authors.

We will evaluate the efficacy of the models in increasing STEM understanding and literacy in schools in Ireland and also bring them to festivals and events such as the University College Dublin Festival in 2020.

We intend the models and materials to be permanently available to University College Dublin for public engagement events in the future.

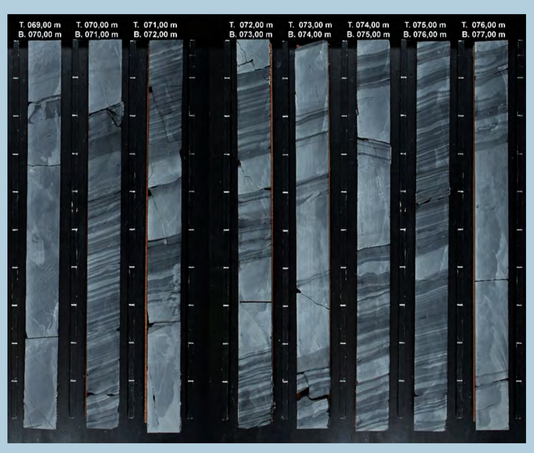

Figure 8: Core of Carboniferous rocks (Ross Sandstone Formation UCD/Equinor core) that are the inspiration for the models of the subsurface that will be created in 2020.

This publication has emanated from research supported in part by a research grant from Science Foundation Ireland (SFI) under Grant Number 13/RC/2092 and is co-funded under the European Regional Development Fund and by PIPCO RSG and its member companies.

Ireland's European Structural and Investment Funds Programmes 2014-2020
Co-funded by the Irish Government and the European Union
European Union
European Regional Development Fund
Science Foundation Ireland sfi For what's next

Background artwork credit: Gillian Lewarne, photographs: Elspeth Wallace, core display: Anthea Lacchia
This project was made possible thanks to UCD Seed Funding (Grant number SF1734). We would like to thank participants to our workshop, the Elliott Centre in Kilkee for providing access to the facilities and iCRAG volunteers to helping during the event.

iCRAG 2019

Resources for a Sustainable Future

PLATFORM
3D IRELAND

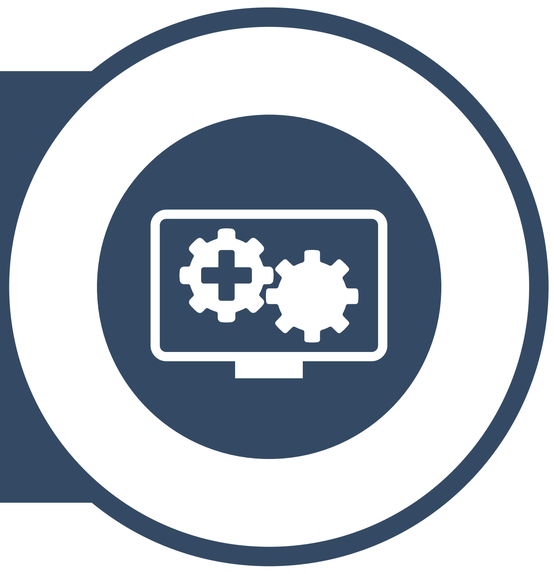

The ‘Blue Book’ revamped: Towards a tectono-stratigraphic framework of the Tournaisian & Viséan of Ireland

R. Doyle[1], M. Philcox[1,2], J. Murray[3] , E. McGrath[4], K. Torremans[1], J. Guven[1], M. Pracht[4], J.J. Walsh[1]

[1] iCRAG (Irish Centre for Research in Applied Geosciences), University College Dublin, Belfield, Dublin 4; [2] Consultant Geologist; [3] iCRAG (Irish Centre for Research in Applied Geosciences), National University of Ireland, Galway; [4] Geological Survey Ireland, Beggars Bush, Haddington Road, Dublin 4

1. Introduction

The past half-century of mineral exploration and research activity in Ireland has generated a considerable amount of lithostratigraphic data. Philcox (1984) produced an extremely valuable compilation of this work in an Irish Association for Economic Geology (IAEG) publication titled **“Lower Carboniferous Stratigraphy of the Irish Midlands”**. Colloquially known within the industry as ‘**The Blue Book**’, it focused on the Tournaisian of the Irish Midlands, which proved influential amongst exploration geologists. In the intervening 30+ years, an updated synthesis of this work, incorporating more recent discoveries, has not, however, been produced.

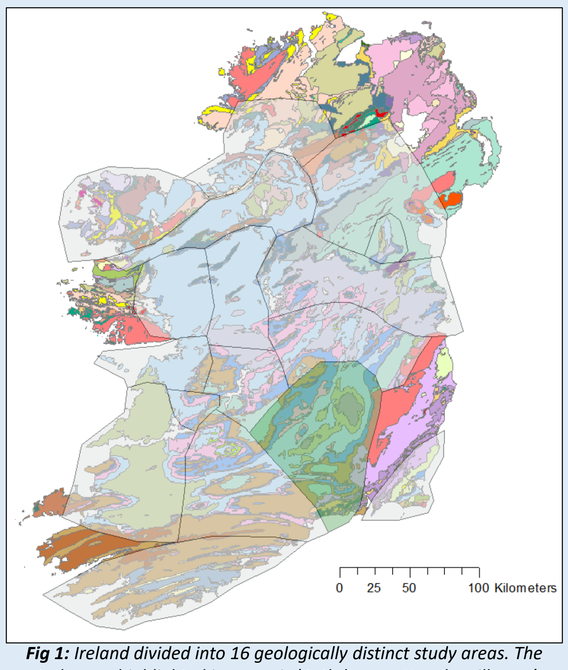

Fig 1: *Ireland divided into 16 geologically distinct study areas. The study area highlighted in green is ‘Rathdowney Trend – Kilkenny’. This is where work will commence. – (Base map from the GSI 1:500,000 Bedrock Geological Map of Ireland)*

Since 1984, **exploration of Carboniferous strata has expanded both regionally and at depth**, placing **greater demands on our understanding of the Mississippian lithostratigraphy of Ireland**. The proposed project will produce a revised dynamic stratigraphy of the **Tournaisian and Viséan**, with a comprehensive account of the lithostratigraphy linked to the considerable quantity of unpublished data collected in the last 3 decades.

The final product, with a working title of “**The New Blue Book**” would not be possible without funding from GSI and iCRAG UCD. It will be made **publically available as a GSI publication** via **a series of online chapters on distinctive geological provinces**, combining detailed lithological descriptions, colour photographs with hyperspectral scanning data and correlative sections of lithofacies.

2. Core Scanning

- High quality RGB photographs with additional hyperspectral information (SWIR) will be captured for each of the most representative drillholes using the new core scanner at the GSI core storage facility.
- Specific hyperlinks which can be found in-text will lead the reader to HD photographs of the particular core they are interested in.
- We work in close relationship with companies and consultants for stratigraphic interpretations in each study area. We aim to get the best and most relevant drillholes and stratigraphic information.
- Updateable: Text and hyperlinks can easily be updated as new data and drillholes come in, because it is an online resource.

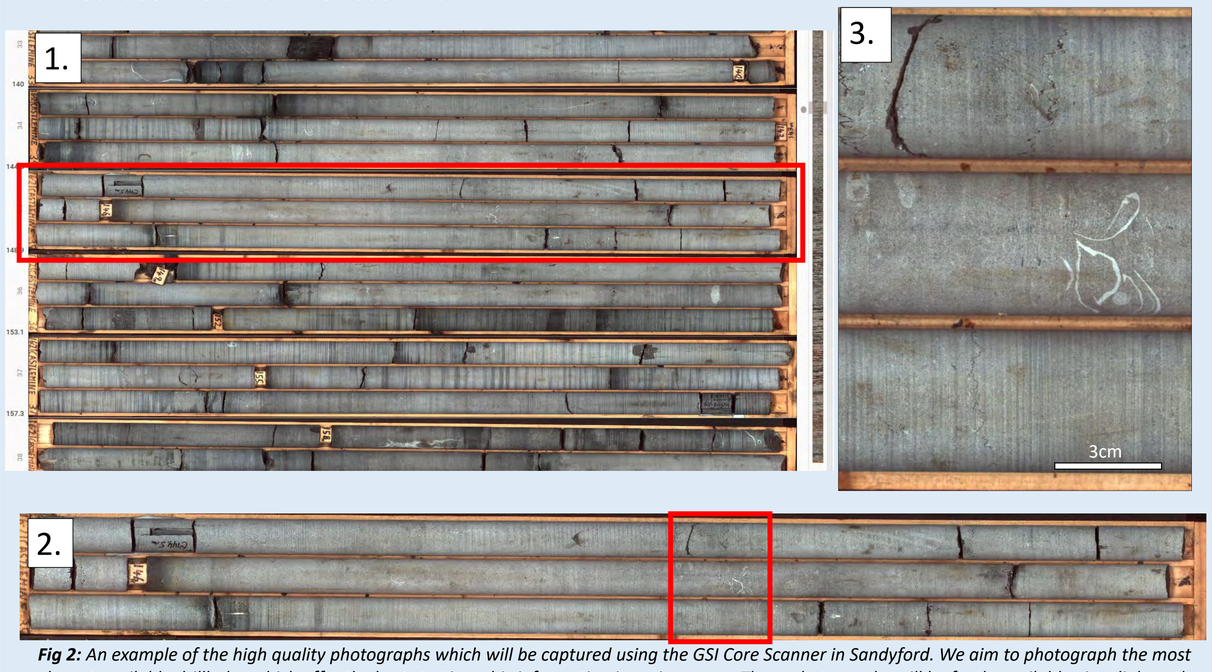

Fig 2: *An example of the high quality photographs which will be captured using the GSI Core Scanner in Sandyford. We aim to photograph the most relevant available drillholes which offer the best stratigraphic information in a given area. These photographs will be freely available via a link on the GSI website.*

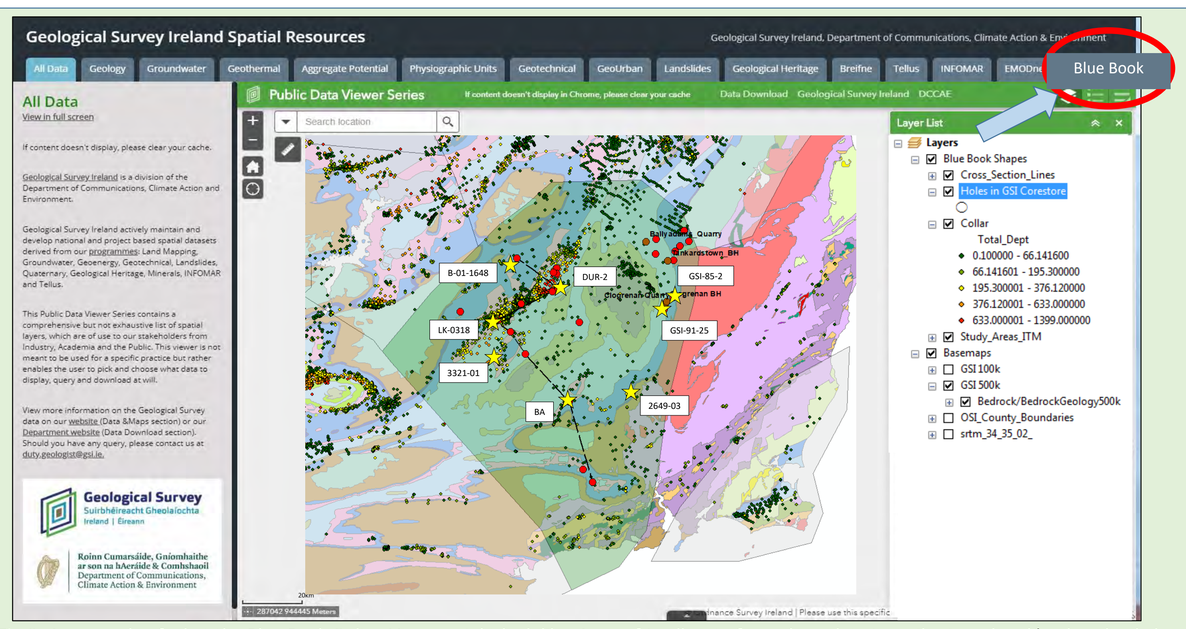

Fig 3: *An example of what the Blue Book Online Viewer might look like. A user-friendly interface where data is easily viewed and/or downloaded. Modified from: GSI Spatial Resources Online Viewer*

3. Online Interactive Viewer

- An online interactive viewer to be developed which can be used in tandem with online chapters to give the reader a wealth of additional information about a particular area they are interested in.
- All data referred to in the chapters can be viewed spatially on a user-friendly interface.
- Interactive layers enable the user to click on an object and download/view the relevant available information (e.g. HD core photos, correlative sections, drillhole logs, reports).
- The online viewer will be publically available, hosted on the GSI website.

4. Progress: Rathdowney Trend – Kilkenny

- Work on Study Area 1 (The Rathdowney Trend – Kilkenny) is coming to a close.
- Large scale data compilation of the area has been completed.
- Representative drillholes have been compiled and identified for correlation across the stratigraphic region. A selection of these will be scanned at the GSI core store.
- Text for the Tournaisian stratigraphy has been completed and is currently underway for the Visean stratigraphy.
- Data transfer and metadata protocols have been established between iCRAG and GSI for inclusion in GOLDMINE.
- Draft correlative sections are currently being put together. Expert feedback is being requested regarding style and format.
- Drillhole ‘LK-0318’ (T.D@ 804.5m) has been transported from Lisheen core store and scanned in Sandyford. Drillhole ‘DUR-2’ (T.D@ 1050.25m), BA (T.D@328m), GSI-85-2 (T.D@217.4m), GSI-91-25 (T.D@275m), 2649-03 (T.D@204.2m), B-01-1648 (T.D@183.2m), 3321-01 (T.D@274m) have also been scanned (see *Fig 3* for locations).

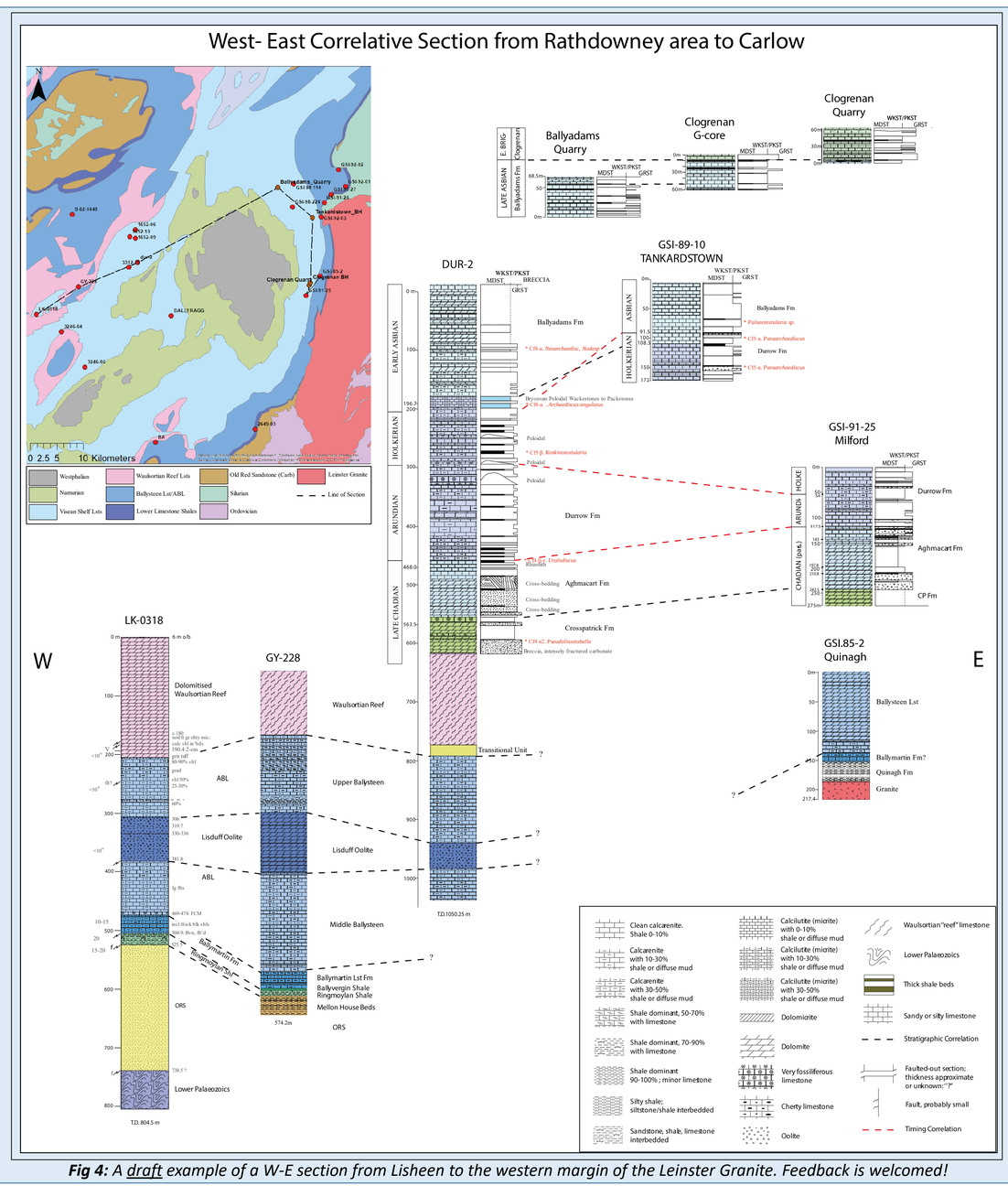

Fig 4: *A draft example of a W-E section from Lisheen to the western margin of the Leinster Granite. Feedback is welcomed!*

5. Next steps…

- Work has already commenced on Study Area 2: Wexford Syncline, Hook.
- Why Wexford?
  - Compilation of key data has already been completed previously.
  - Small area and should be completed relatively quickly.
- A shortlist of most representative drillholes is currently being made.
- Correlative sections will be drafted and we will begin writing text for the area.

This publication has emanated from research supported in part by Geological Survey Ireland and in part by a research grant from Science Foundation Ireland (SFI) under Grant Number 13/RC/2092 and co-funded under the European Regional Development Fund and by iCRAG industry partners.

Ireland’s European Structural and Investment Funds Programmes 2014-2020
Co-funded by the Irish Government and the European Union
European Union
European Regional Development Fund
Science Foundation Ireland sfi For what’s next

iCRAG’s Raw Materials research partners
GEOSCIENCE IRELAND Exploring Developing Sustaining
Hannanmetals
BOLIDEN
Teck
GROUP ELEVEN RESOURCES LTD.
lundin mining
Trevali MINING CORPORATION
PIP Petroleum Infrastructure Programme

iCRAG 2019

Resources for a Sustainable Future

PLATFORM GEOCHEMISTRY

Laser-ablation isotope and trace element geochemistry for the iCRAG Energy Security and Supply of Raw Materials Challenges

Eszter Badenszki[1,2] and J. Stephen Daly[1,2]

1: UCD School of Earth Sciences, University College Dublin, Dublin, Ireland
2: Irish Centre for Research in Applied Geosciences, Dublin, Ireland
NCIGPD1A - Geochemistry Platform

Introduction

The National Centre for Isotope Geochemistry (NCIG, Fig. 1) at UCD is a dynamically developing laboratory that collaborates primarily with the Energy Security and Supply of Raw Materials Challenges (Fig. 4) within iCRAG as well as working with external users (e.g., Cambridge Arctic Shelf Programme, CASP-UK, Fig. 2b; Dr. Donnelly Archibald, St. Francis Xavier University - Canada; Martin Whitehouse, NORDSIM – Sweden; Zengjie Zhang, Fig. 2a, Sun Yat-sen University – China).

This project focuses on analytical techniques where sampling is carried out by laser ablation. The main objectives of this project is to support users working with methods already established in the lab and to set up new analytical protocols (e.g., laser ablation split-stream system, LASS). The main scientific challenge of this project is assessing the involvement of the deep crust, using Irish deep crustal xenoliths, in the formation of the Irish Carboniferous-hosted Pb-Zn deposits.

Methods supported by this project

Pb isotopes in K-feldspar

This method is mostly used to investigate the provenance of detrital feldspar in order to reconstruct palaeo-drainage systems and to understand sedimentary basin development (Fig. 2a- b). This technique can also of help to understand better formation of igneous intrusions. Within iCRAG, this technique supports projects in the Energy Security Challenges, e.g., HC4.1PhD1 – Franklin. External users e.g., B. Anders – NUIG; M. Flowerdew - CASP; and D. Archibald - St. Francis Xavier University – Canada.

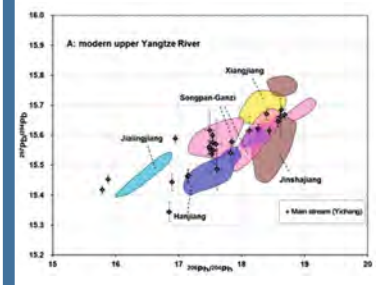

Figure 2a. Detrital K-feldspar Pb isotopic data of modern Yangtze River sands compared with putative sources (Zhang *et al.* 2016)

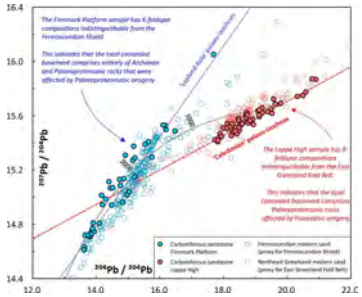

Figure 2b. Detrital K-Feldspar compositions measured from two Carboniferous samples and compared with those recorded from modern sand collected from the Fennoscandian Shield and the East Greenland Fold Belt (Flowerdew *et al.*, in prep)

Zircon analyses

In situ U-Pb and Lu-Hf isotope analyses of zircon are routinely done by laser ablation coupled with Q-ICP-MS and MC-ICP-MS, respectively. The combined results of these methods are used in petrogenetic and provenance studies (e.g., NCIGPD1A-Badenszki).

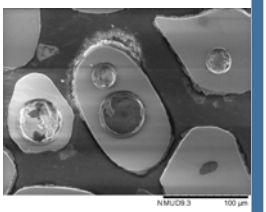

Figure 3. Laser ablation pits in zircons for U-Pb and Lu-Hf isotopic analysis (Badenszki *et al.*, 2019).

Trace element analyses and mapping

Trace element spot analyses and trace element mapping of silicate minerals provide petrogenetic information that have a wide range of application. Within iCRAG this method was used in projects in the Energy Security Challenges (e.g., HC4.1PD2 – Zimmermann) and in Supply of Raw Materials Challenge (RM1.2PhD4 – Kaeter).

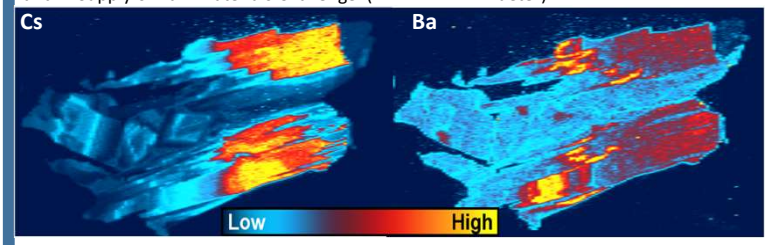

Figure 4. Cs and Ba trace element maps of hydrothermally altered muscovite from a lithium pegmatite, Nova Scotia (Kaeter *et al.*, in preparation).

Ongoing developments: Laser Ablation Split Stream system (LASS)

In the LASS system, laser-ablated material will be fed to and analysed in both the Neptune and iCAP Q instruments simultaneously. Hence precise isotopic ratios and multi-elemental concentrations or inter-elemental ratios can be obtained from the same sample region. This is especially valuable for fine-grained samples or complex mineral grains where two analyses from the same domain is often. The LASS system will allow simultaneous analysis of

- trace elements (e.g., Rb, Sr, Ba, Mn, U and Th) and Pb isotope ratios, potentially improving provenance resolution.
- zircon U-Pb and Lu-Hf isotopic systems or a combination of trace element and Hf isotopic composition analysis.

Figure 1. One of the NCIG labs at UCD; The NCIG at UCD is equipped with:

- Analyte G2 excimer laser ablation system from Teledyne Cetac Technologies (funded by iCRAG)
- Thermo Scientific Neptune (multiple collector inductively-coupled plasma mass spectrometer (MC-ICP-MS, funded by SFI), upgraded with Jet interface (funded by PRTLI5)
- Two new Thermo Scientific iCAP Q quadrupole inductively-coupled plasma mass spectrometers (Q-ICP-MS, funded by PRTLI5); one for solution analysis, one for laser ablation work.
- Thermo Scientific Triton thermal ionization mass spectrometer (TIMS, funded by HEA)
- New Wave Micromill (funded by SFI)

Ongoing research

Can the lower crust be a metal source for the Carboniferous-hosted Zn-Pb deposits?

Shallow (<10 km depth) hydrothermal circulation within upper crustal rocks is widely accepted as the main metal source for the giant Irish Carboniferous-hosted Zn-Pb orefield (Wilkinson & Hitzman 2015).

However, isotopic analysis for several elements in deep crustal xenoliths, including Pb in K-feldspar, are comparable with data (especially galena Pb) from the base metal deposits. This, along with other evidence (e.g., Davidheiser-Kroll *et al.*, 2014; Elliott 2015; Hnatyshin *et al.,* 2015) suggests involvement of the deep crust as a metal source.

Laser ablation mapping in TCD shows that garnet and biotite have high Zn contents that are substantially reduced by hydrothermal alteration, thus suggesting a metal extraction mechanism (Fig. 5), and supporting a role for the lower crust in ore genesis.

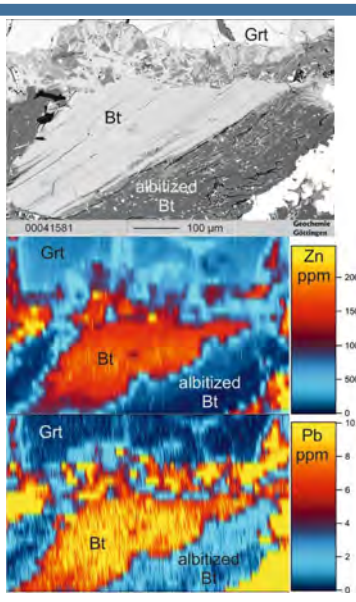

Figure 5. BSE (top) and laser-ablation ICPMS elemental images (with D. Chew, TCD) show high Zn contents in biotite in a lower crustal xenolith, substantially reduced by albitization during hydrothermal alteration

References

Zhang, Z. *et al.* 2016. *GSA Bulletin*, 128, 1339–1351; **Badenszki *et al*. 2019. J. Pet.** (in press); **Wilkinson, J.J. & Hitzman, M.W. 2015**. In: Archibald, S.M. & Piercey, S.J. (eds) *Current Perspectives on Zinc deposits*. IAEG, pp. 59-72; **Davidheiser-Kroll, B. *et al.* 2014.** *Min. Deposita*, 49, 547–553; **Elliott, H. 2015**. *Unpubl. PhD thesis*, Univ. Southampton; **Hnatyshin, D. *et al.* 2015**. *Geology*, 43, 143-146.

This publication has emanated from research supported in part by a research grant from Science Foundation Ireland (SFI) under Grant Number 13/RC/2092 and co-funded under the European Regional Development Fund..

iCRAG 2019

Resources for a Sustainable Future

PLATFORM GEOPHYSICS

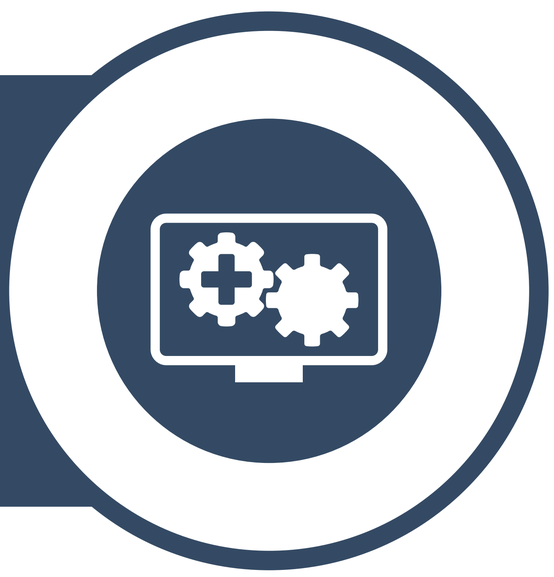

3-D Magnetotelluric Assessment of the Geo-resources Potential of the Irish Crust

Duygu Kiyan[1,2] (duygu@cp.dias.ie), J. Campanyà[1,3*], C. Hogg[1], C.J. Bean[1], J. Fullea[4], S.P. Blake[3**], V. Rath[1], R. Delhaye[1], P.T. Gallagher[1,3], A.G. Jones[1***] and R. Scanlon[5]

iCRAG Irish Centre for Research in Applied Geosciences

Trinity College Dublin, Coláiste na Tríonóide, Baile Átha Cliath, The University of Dublin

DIAS Institiúid Ard-Léinn | Dublin Institute for Advanced Studies

Geological Survey Suirbhéireacht Gheolaíochta Ireland | Éireann

An Roinn Cumarsáide, Gníomhaithe ar son na hAeráide agus Comhshaoil, Department of Communications, Climate Action & Environment

I. INTRODUCTION

In the framework of Space Weather ElectroMagnetic Database for Ireland (SWEMDI), project funded by the Geological Survey Ireland, we acquired long-period magnetotelluric (LMT) data at over twenty stations in 2018. The locations of these stations are represented with orange inverted triangles on the map (on the right-hand side). These LMT data together with the existing data set at over thirty stations (blue inverted triangles, ISLE-MT – Irish Magnetotelluric Lithosphere Experiment, Rao et al., 2014) across Iapetus Suture Zone (ISZ) have been modelled in 3-D. Since June 2019, new LMT data are being acquired at 12 stations (yellow solid circles).

This study aims to construct an island-wide 3-D electrical conductivity map of Ireland's crust and uppermost mantle. Deep probing magnetotelluric imaging yields information on the structure, composition and temperature of the crust and upper mantle, and can detect processes associated with mineralisation and areas of high temperature and or permeability related to promising geothermal targets. Here, we present for the first time 3-D electrical conductivity distribution in the lower crust and the uppermost mantle of the entire island.

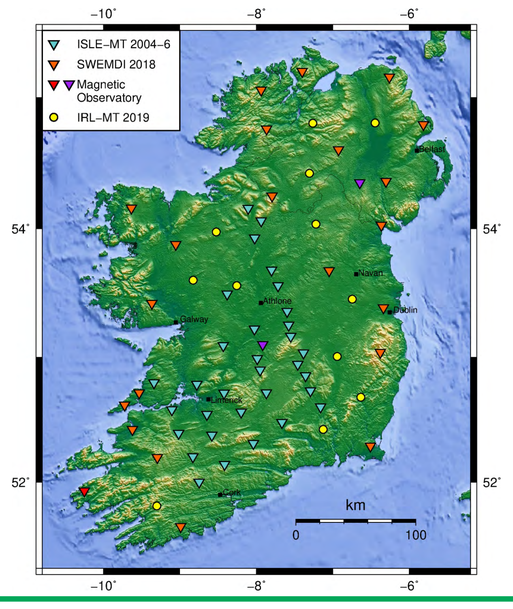

EXAMPLES of LMT RESPONSE CURVES

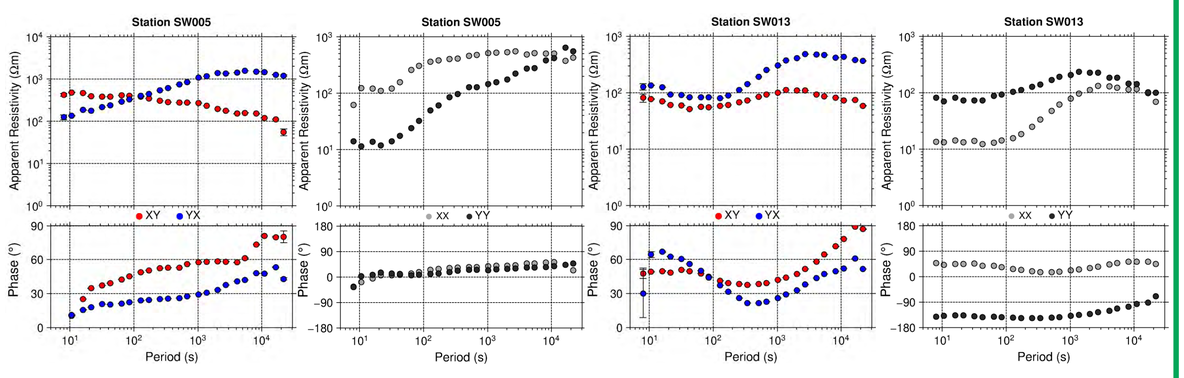

Figure showing examples of LMT data. The data were acquired using DIAS Lviv LEMI-417M recording systems. We processed the data using the codes BIRRP (Chave & Thompson, 2004) and ELICIT (Campanyà et al., 2014) was used when either the electric and magnetic channels stopped recording data. The ISLE-MT project used LiMS systems (Andreson et al., 1988; Narod & Bennest 1990) and GEOMAGNET systems from the Geophysical Intrument Pool Potsdam for data collection. Stations SW005 and SW013 are located in Kerry and Donegal , respectively.

II. MT DATA ANALYSIS and MODELLING

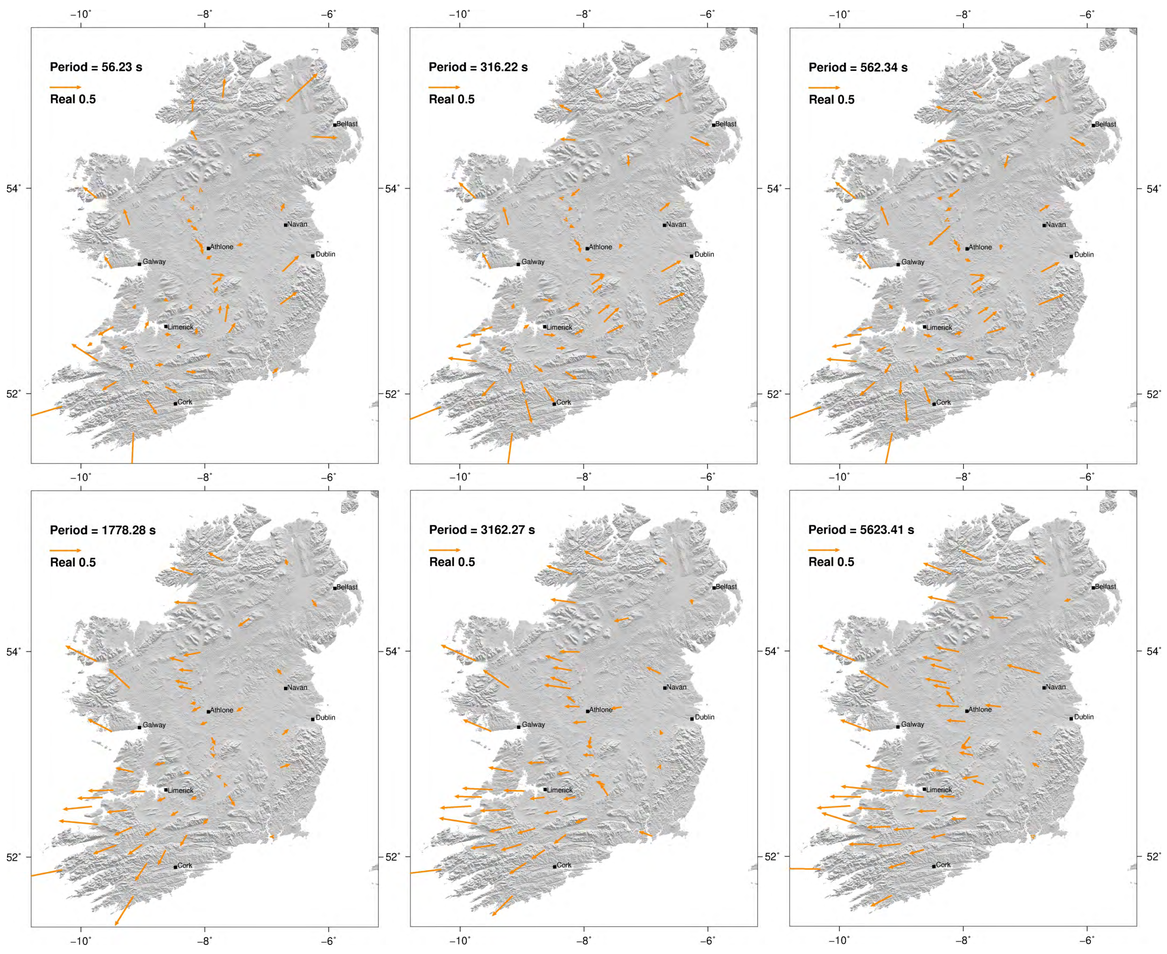

INDUCTION VECTOR MAPS (PARKINSON CONVENTION)

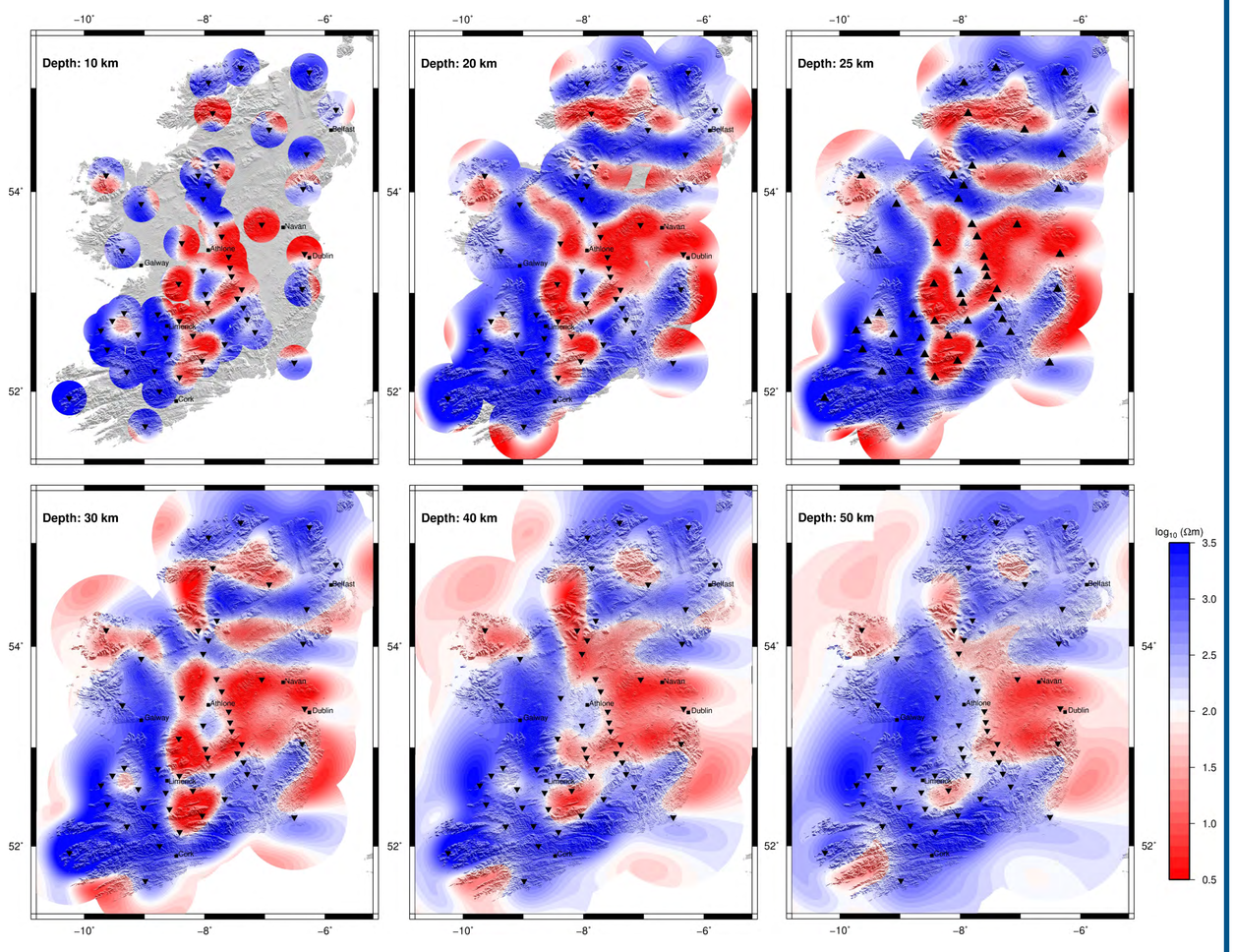

HORIZONTAL ELECTRICAL CONDUCTIVITY DEPTH SLICES

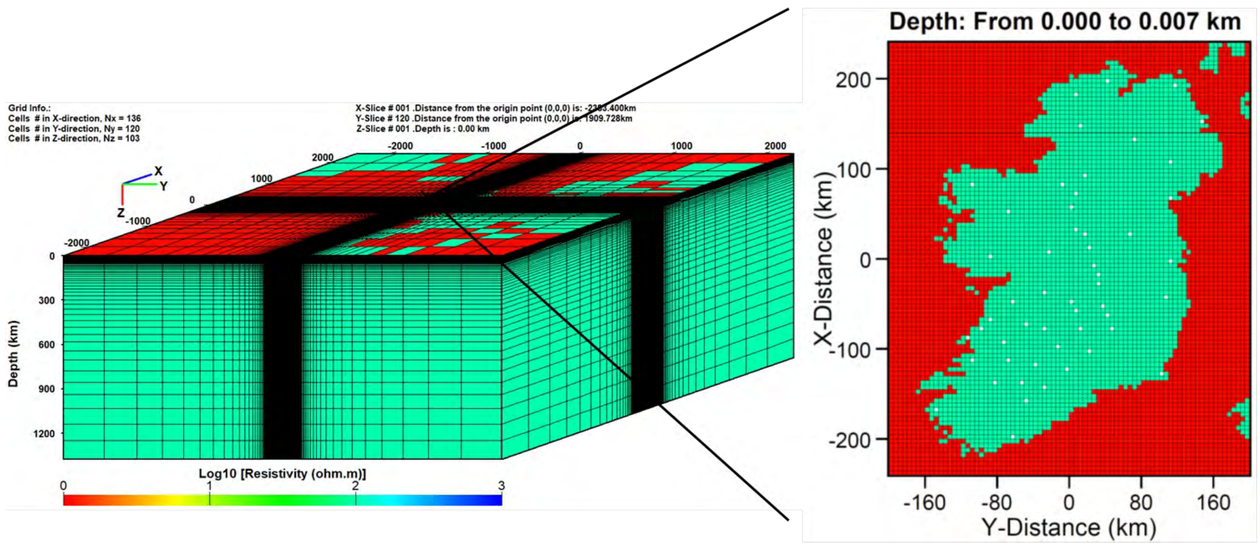

3-D MT MODEL MESH

The 3-D mesh extends laterally from ~-2400 km to ~2400 km in the north-south and east-west directions and to a depth of ~1300km. The green cells have the values of 100 Ωm and will be modified during the inversion, and red cells represent the Irish Sea and the Atlantic Ocean and are fixed to 0.3 Ωm. In total, the mesh consists of 136 x 120 x 103 cells in the north-south, east-west and vertical directions, respectively. The centre of the mesh comprised a uniform mesh of 96 x 80 x 103 cells, with a horizontal cell size of 5 km x 5 km. The lateral extends of the padding cells, 20 planes in each of the north, south, east and west directions, increased by a factor of 1.25. In the vertical direction, the cell thickness is of 7.5 m and the subsequent layer thicknesses are increased by a factor of 1.1. The newly acquired long-period MT data covers the period range of 10 – 20,000 s with good data quality. These data together with the legacy MT data were decimated to 14 periods per site with regular distribution for periods from 10 s to ~18,000 s.

In total, 52 sites were used in the inversion process. The 3-D inversions were run with full impedance tensor elements (Zxx, Zxy, Zyx, and Zyy) and vertical magnetic transfer functions. Error floors were set to an absolute value of 5% of $(Zxy \times Zyx)^{1/2}$ and 0.02 for the impedance data and vertical magnetic transfer functions, respectively. The starting model resistivity was set to 100 Ωm with the resistivities of the Irish Sea and the Atlantic Ocean are being fixed to 0.3 Ωm. ModEM code (Egbert and Kelbert, 2012; Kelbert et al., 2014) was used to obtain the electrical resistivity model of Ireland's lithosphere. The inversion results are summarised above. The presented resistivity model converged to an RMS of 2.52 after 176 hours of computation on the cluster of ICHEC. We are currently testing the nested mesh approach implemented in ModEM (described and first applied by Meqbel et al., 2014). Applying this approach will reduce the required computational time for inversion runs.

III. ON-GOING & FUTURE WORK

In the Earth's crust, the primary conducting mineral phases are saline water, graphite, sulphides, iron oxides and in tectonically active regions, partial melt, while in the upper mantle, electrical conductivity is sensitive to temperature and minor highly conductive phases, such as water, melt, mantle graphite (cratonic lithosphere) and mantle sulphides. The on-going and future work comprises (i) performing 3-D inversions including data acquired in the second half of 2019, (ii) interpretation of the 3-D inversion results and (ii) combining MT data with seismic, gravity, elevation and surface heat flow data sets to update the works by Fullea et al. and Jones et al. (2014) on thermal and compositional structure of present day Ireland's lithosphere. To that aim, an integrated geophysical-petrological approach (LitMod3D) will be used, where electrical conductivity, density and seismic velocities are dependent on modal mineralogy, temperature, composition, water content, and presence of melt.

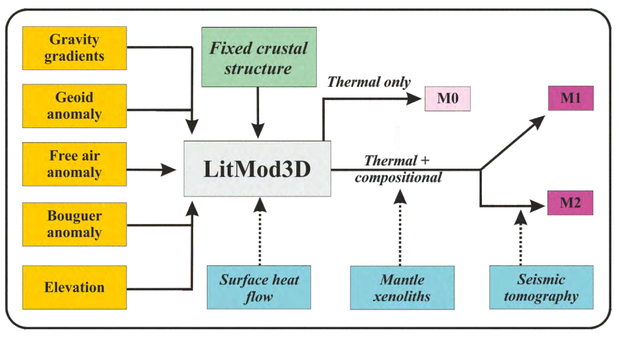

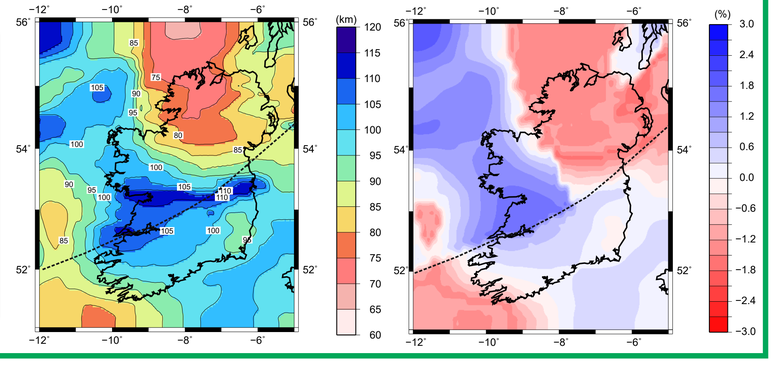

This publication has emanated from research supported in part by a research grant from Science Foundation Ireland (SFI) under Grant Number 13/RC/2092 and co-funded under the European Regional Development Fund and iCRAG industry partners.

Ireland's European Structural and Investment Funds Programmes 2014-2020
Co-funded by the Irish Government and the European Union
European Union
European Regional Development Fund
Science Foundation Ireland sfi For what's next

Acknowledgements

The lithospheric research leading to these results also received funding from Geological Survey Ireland (GSI) under 2017 GSI Short Call Research Programme (2017-sc-037). We would like to thank Coillte (www.coillte.ie) and the farmers for allowing us to install temporary long-period MT stations. Gary Egbert, Anna Kelbert and Naser Meqbel are gratefully thanked for making their ModEM 3-D inversion code available to us. We thank Naser Meqbel for sharing the visualisation code 3D-Grid with us. Numerical computations were carried out on Kay cluster of the Irish Centre for High Performance Computing (www.ichec.ie). The maps are plotted using the Generic Mapping Tools (GMT) of Wessel and Smith (1991) and Wessel and Smith (1998).

[1] Dublin Institute for Advanced Studies (DIAS)
[2] Irish Center for Research in Applied Geosciences (iCRAG)
[3] Trinity College Dublin
[4] Complutense University of Madrid, Spain
[5] Geological Survey Ireland
[*] Now at the Geological Survey Ireland
[**] Now at NASA Goddard Space Flight Center, USA
[***] Now at Complete MT Solutions, Canada

Receiver function imaging above an underground mine

Senad Subašić[1,3], Nicola Piana Agostinetti[2], Christopher J. Bean[1]

1) Geophysics Section, Dublin Institute for Advanced Studies; 2) Department of Geodynamics and Sedimentology, University of Vienna, Austria;
3) School of Earth Sciences, University College Dublin, Ireland

Introduction

The aim of the project is to image the shallow structure around the Boliden Tara Mines area in Navan, Ireland, using passive seismic methods. To accomplish that, we installed an array of 21 broadband seismometers, arranged in a square 5 by 5 km area. During this one year deployment, we recorded 600 strong and distant earthquakes (Mw>5), and we use them as our passive sources for probing the shallow crust. We calculate high frequency receiver functions (up to 12 Hz) and invert them using a trans-dimensional reversible jump Markov Chain Monte Carlo algorithm. The recovered velocity profiles are compared with sonic log data, and are shown to split the area into two distinct regions. Stations in the southeastern part of the array match the (filtered) borehole data remarkably well, while stations in the northwest image different structures. These results demonstrate the ability of receiver function analysis in providing qualitative and quantitative information in an exploration environment.

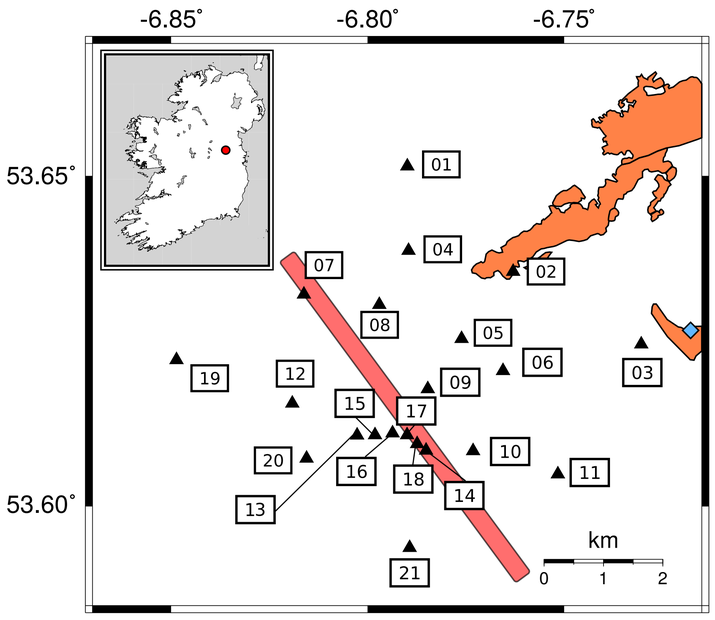

Figure 1: 21 seismometeres deployed in a square 5 by 5 km area. Approximate location of the known orebody marked in orange. Blue diamond marks the location of the borehole used for comparisons later. Red line is a profile on which station results will be projected later on. Red circle in the inset shows the array location within Ireland.

Receiver functions

Usually employed to image strong and deep velocity contrasts such as the Mohorovičić discontinuity or the lithosphere-asthenosphere boundary. However, it has been shown (e.g. Subašić et al, 2019) that receiver functions (RFs) contain information at higher frequencies (up to 8 Hz) as well, and can be used for shallow crustal imaging. We compute RFs using Gaussian low pass filters ranging from 0.5 to 12 Hz. We perform harmonic decomposition (Bianchi et al., 2010), and focus on the zero order harmonics (k=0; bulk isotropic variation of seismic velocities with depth (Figure 2).

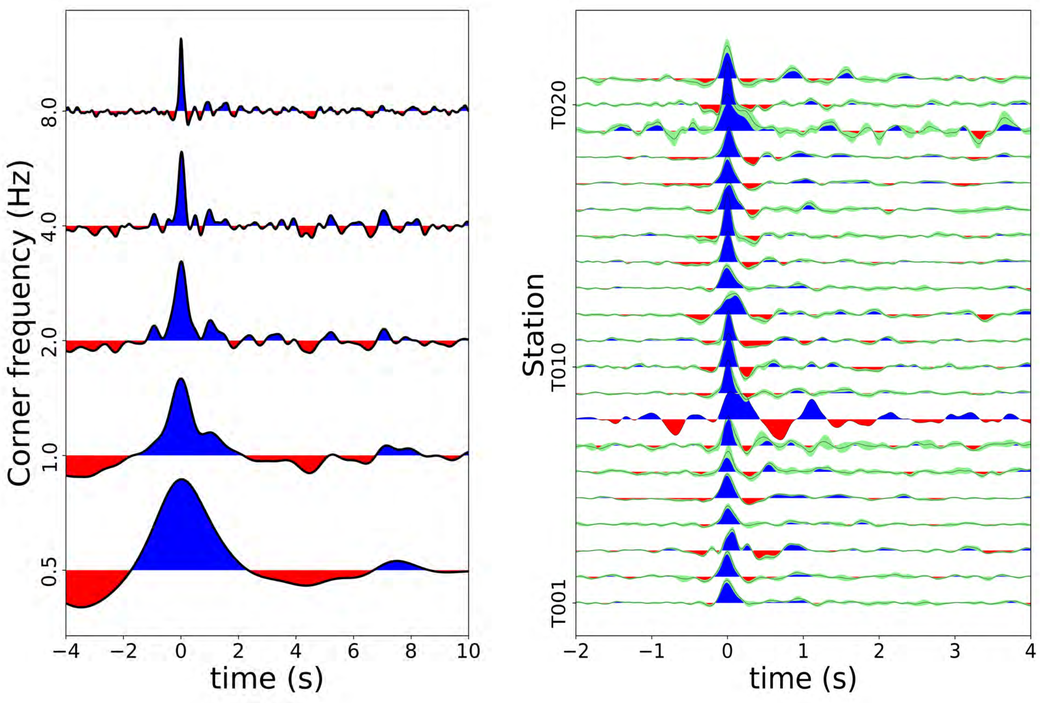

Figure 2: left: receiver functions for station T009, calculated using different corner frequencies for the low pass filter (from 0.5 to 8 Hz). Features sharpen as the frequency increases - one blue pulse at 0.5 Hz resolves into four at 4 and 8 Hz. Right: zero-order harmonics computed from 8 Hz RFs. The green shaded area is the standard deviation. The majority of stations are in a noisy environment (people's backyards, near roads, industrial and farm equipment), which limits the number of usable RFs.

Inversion

Zero order harmonics are the input for RF inversion. We use a trans-dimensional Reversible jump Markov Chain Monte Carlo (RjMCMC) algorithm, developed by Piana Agostinetti and Malinverno (2010), with 600.000 models and 92 independent parallel chains (55 million models per station). The final results are expressed in terms of posterior probability distributions (PPDs) of the investigated parameters, e.g. S-velocity at depth and depth of seismic interfaces (Figure 3).

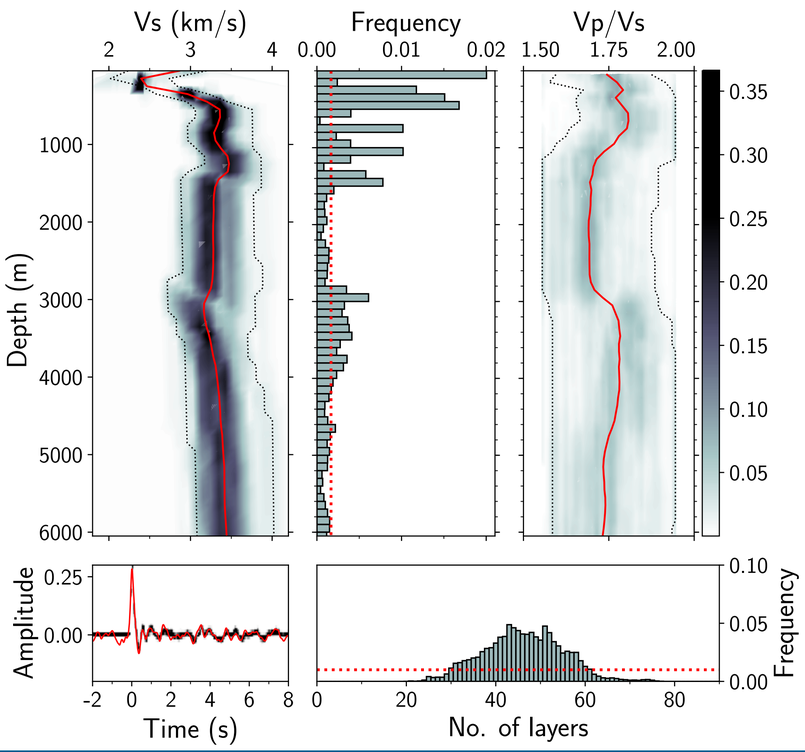

Figure 3: inversion results for station T015; left: density plot of marginal PPD of S-wave velocity, mean S-wave velocity (red line), and 95% confidence intervals (dotted black lines); middle: histogram of interface depths in the sampled models; right: PPD of Vp/Vs; bottom left: fit between observed (red) and posterior RF; bottom right: histogram of the number of layers

Results

We compare our inversion results for each station to the available borehole data (Figures 4 and 5). The match between our results and the filtered sonic log is excellent for stations in the southeast, with both the trend and absolute velocity being recovered in most cases.

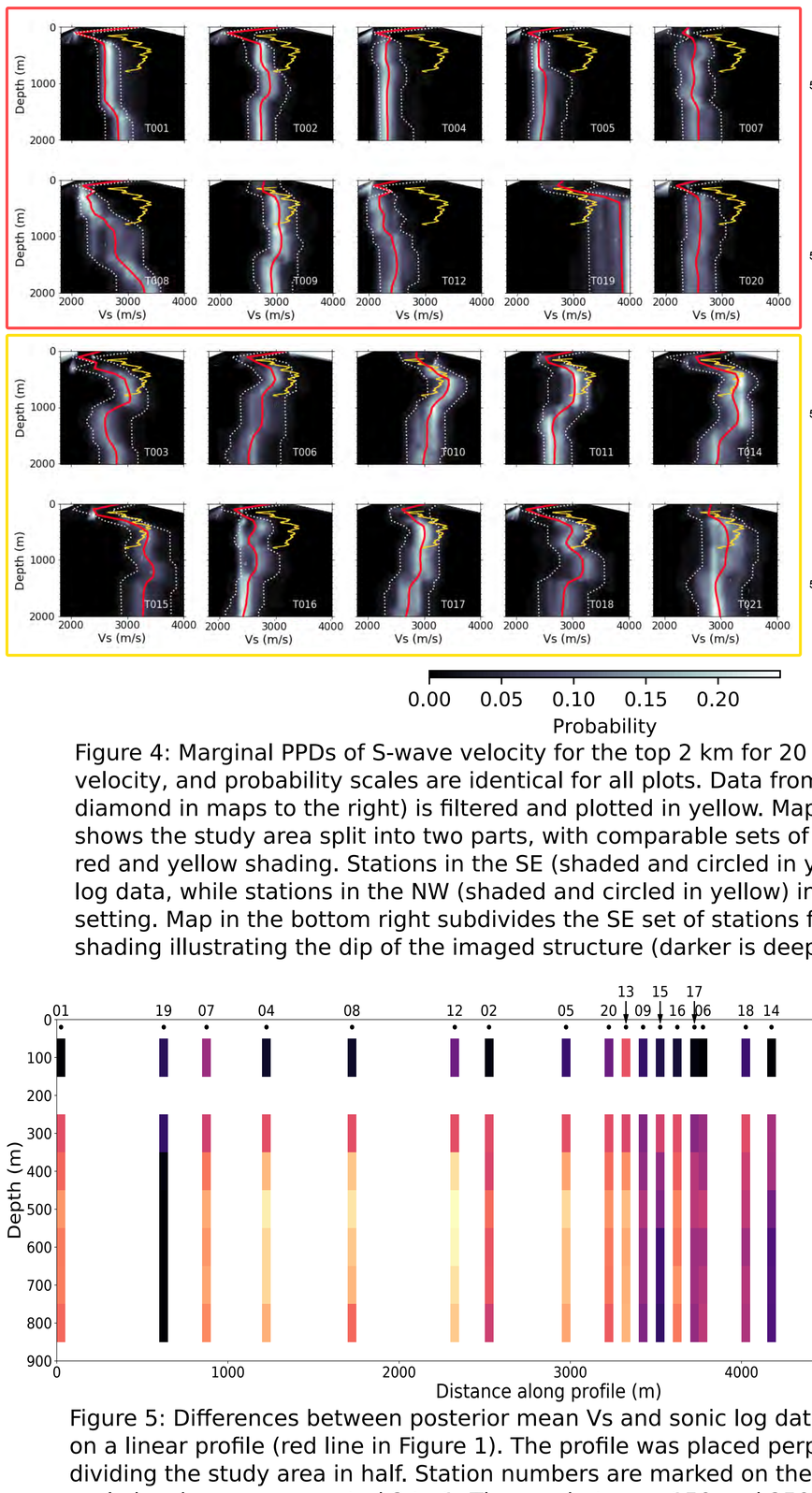

Figure 4: Marginal PPDs of S-wave velocity for the top 2 km for 20 stations in the array. Depth, velocity, and probability scales are identical for all plots. Data from a nearby borehole (green diamond in maps to the right) is filtered and plotted in yellow. Map in the top right corner shows the study area split into two parts, with comparable sets of stations emphasised using red and yellow shading. Stations in the SE (shaded and circled in yellow) agree with the well log data, while stations in the NW (shaded and circled in yellow) indicate a different structural setting. Map in the bottom right subdivides the SE set of stations further, with the gradient shading illustrating the dip of the imaged structure (darker is deeper).

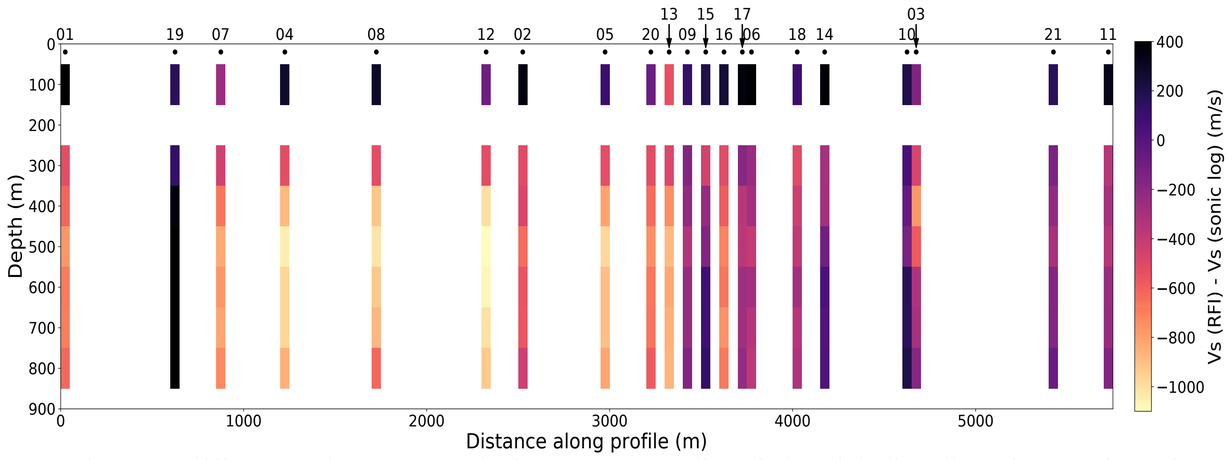

Figure 5: Differences between posterior mean Vs and sonic log data for all stations projected on a linear profile (red line in Figure 1). The profile was placed perpendicular to the line dividing the study area in half. Station numbers are marked on the top of each column. Vertical scale has been exaggerated 2 to 1. The gap between 150 and 250 m is due to a corresponding gap in the sonic log.

Conclusions

The study area is split down the middle based on the velocity profile differences. We attribute this split to the Navan fault, a large normal fault trending NNE and dipping SE. Qualitative information on this bimodal nature of the area can be obtained from a stack of several strong events during a month, without any inversions.
RFs are a low cost passive seismic tool able to proble the shallow structure underneath the receiver. Each seismometer acts as a borehole, providing a velocity profile similar to a low resolution sonic log.

Acknowledgments:
Boliden Tara Mines is thanked for their support and publication permission.
This work has been carried out using the ResearchIT Sonic cluster which was funded by UCD IT Services and the Research Office.
We would like to thank Giuseppe Maggio, Clara Gómez García, Clare Horan, and Martin Möllhoff for their efforts during the planning, deployment, and maintenance of the array.

References

1) Bianchi, I., Park, J., Piana Agostinetti, N. and Levin, V. (2010), Mapping seismic anisotropy using harmonic decomposition of receiver functions: An application to Northern Apennines, Italy, J. Geophys. Res., 115, B12317, doi:10.1029/2009JB007061
2) Di Bona, M (1998), Variance estimate in frequency-domain deconvolution for teleseismic receiver function computation, Geophysical Journal International, 134: 634-646, doi:10.1111/j.1365-246X.1998.tb07128.x
3) Piana Agostinetti, N., Malinverno, A. (2010), Receiver function inversion by trans-dimensional Monte Carlo sampling, Geophysical Journal International, 181: 858-872, doi:10.1111/j.1365-246X.2010.04530.x
4) Subašić, S., Piana Agostinetti, N., Bean, C.J., (2019), Estimating lateral and vertical resolution in receiver function data for shallow crust exploration, Geophysical Journal International, 218: 2045-2053, doi:10.1093/gji/ggz262

This publication has emanated from research supported in part by a research grant from Science Foundation Ireland (SFI) under Grant Number 13/RC/2092 and co-funded under the European Regional Development Fund, and partially conducted with the financial support of Science Foundation Ireland under Grant Number 14/IFB/2742. N.P.A. research is funded by Austrian Science Foundation (FWF) under Grant Number M2218-N29.

email: senad@cp.dias.ie

GEO-URBAN: Preliminary Application of Passive Seismic and Electromagnetic Methods in the Dublin City

Giuseppe Maggio, Duygu Kiyan, Colin Hogg, Robert Delhaye, Chris Bean

Dublin Institute for Advanced Studies, Dublin, Ireland

GEO-URBAN PROJECT OBJECTIVES:

- To image the subsurface of the Dublin City in order to better understand the local geology and and structures in the effort of the geothermal exploration
- To apply a wide range of geophysical techniques in the urban environment: Cross-correlation, H\V, MagnetoTelluric and Controlled-Source methods
- To create a resistivity model of the Dublin Basin
- To create a velocity model of the Dublin Basin from the sediments down to the deeper crust
- To investigate the characteristics and feasibility of passive seismic and electromagnetic methods in the Dublin urban area

STUDY AREA AND GEOLOGICAL BACKGROUND

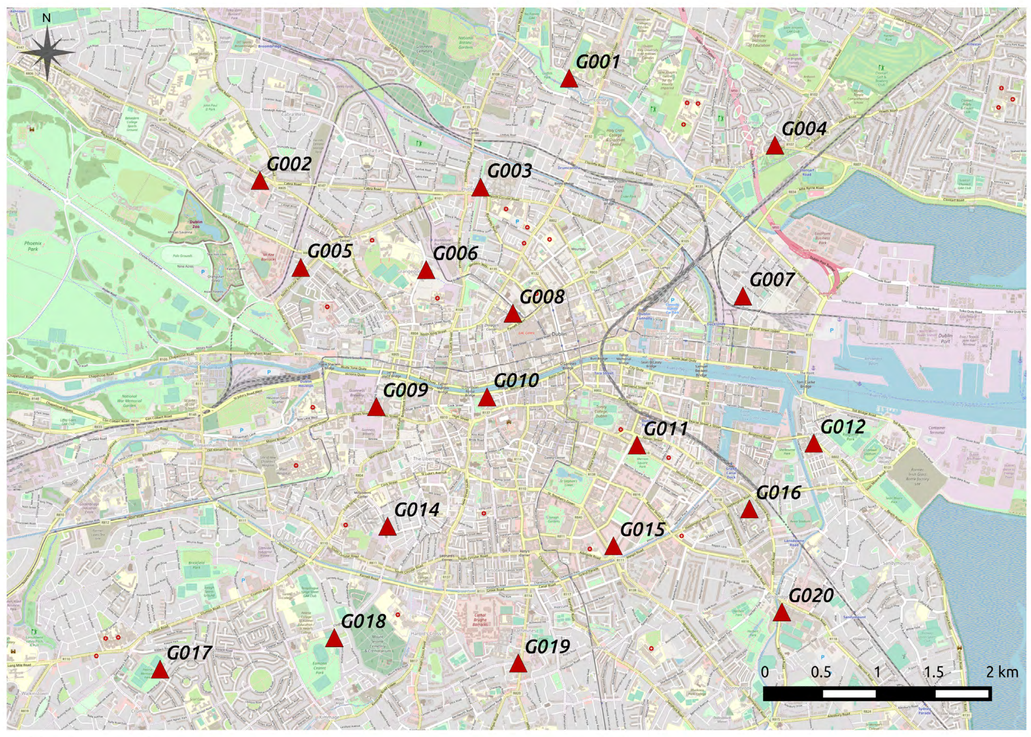

Dublin City : Deployment Map

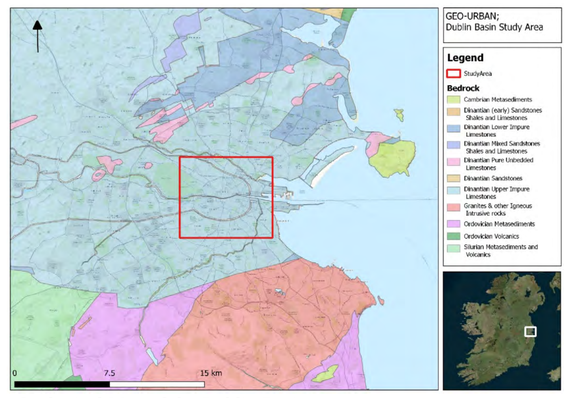

Geological Map of the Dublin Basin

19 Broadband stations:

- GURALP 6TD 30s-100Hz
- GURALP T40 60s-50Hz

- Duration: from April to August 2019
- Average interstation distance: 0.9 km
- Array Aperture: 7.2 Km

FREQUENCY CONTENT AND CROSS-CORRELATION OF SEISMIC NOISE

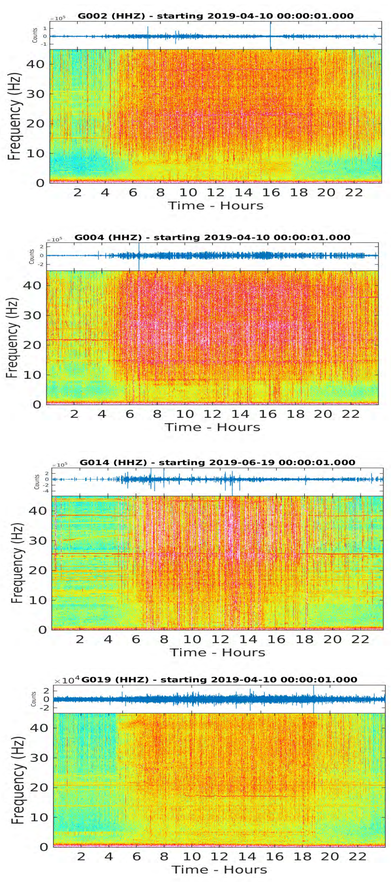

Spectrograms

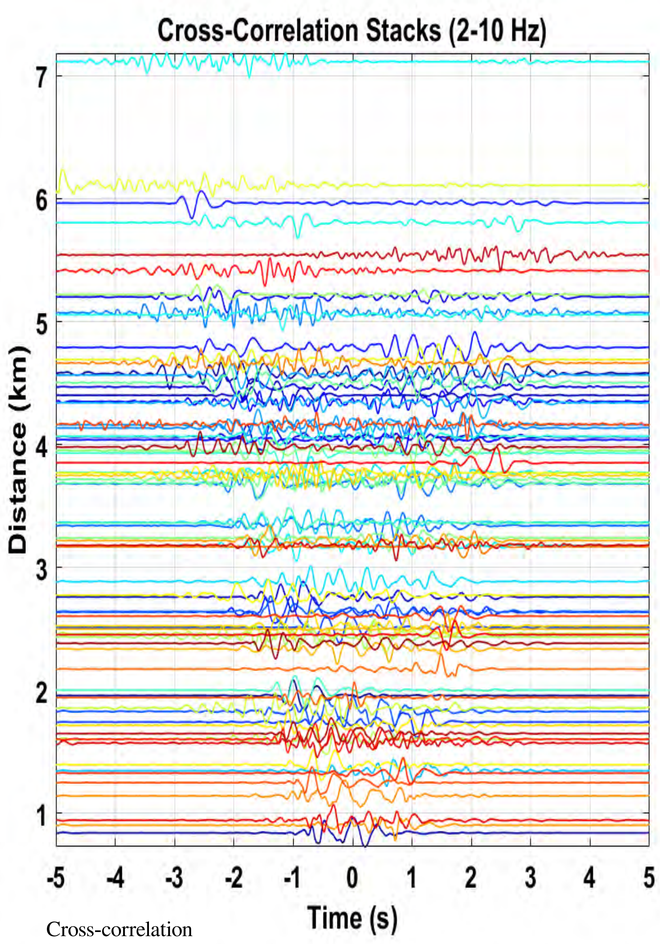

Cross-correlation

- We apply the cross-correlation to extract the empirical Green's function by assuming that each pair of stations acts as virtual-shot source and receiver.
- Workflow:

1) Data Collection
2) Frequency Analysis
3) Cross-Correlation
4) Dispersion Analysis
5) Inversion
6) Velocity Model

H/V METHOD:

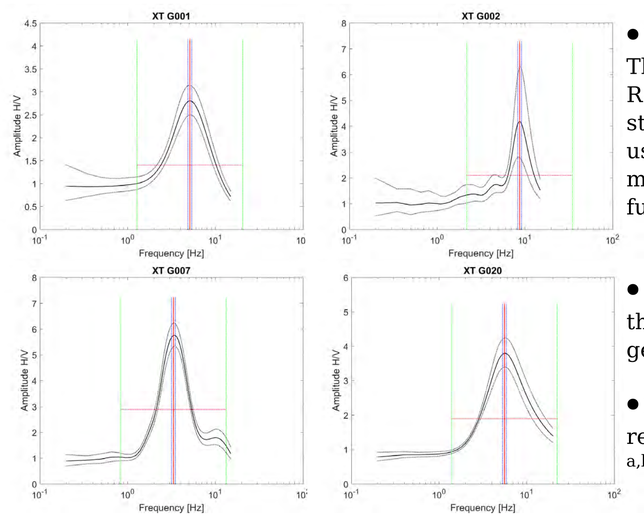

H\V curves at station G001, G002, G007, G020

- H/V spectral ratio method: The Horizontal-to-Vertical Spectral Ratio (H\V) method, is a single-station approach using ambient vibration measurements to estimate the fundamental frequency of a site
- The method is used to estimate the sediment thickness and the geometry of the bedrock surface
- Frequency peak- depth relationship: Depth(h)= $_a f^b$

a,b: Empirical regression coefficients

- Depth to Bedrock profiles of Dublin City:

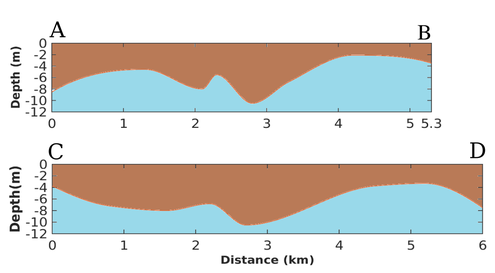

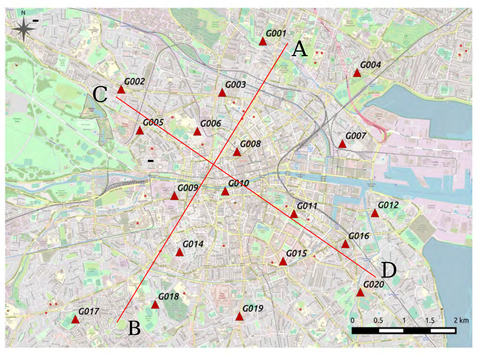

ELECTROMAGNETIC METHODS: Merrion Square MT Data Acquisition

- The electromagnetic methods are, namely, magnetotellurics (MT) and controlled-source electromagnetics (CSEM). The natural-source MT method utilises natural variations in electromagnetic energy to infer the electrical conductivity (or its inverse resistivity) properties of rocks within the Earth.
- The first MT data acquisition was undertaken in the Merrion Square Park in Dublin City centre using Phoenix Geophysics equipment, namely MTU-5A recording boxes and MTC-50 induction coils.
- Magnetic time-series data were simultaneously recorded at a remote reference site (electrically quiet area) about 45 km away. At the site, the two horizontal, perpendicular magnetic field components were recorded, as well as the vertical magnetic field component. The two horizontal, perpendicular electric field components were measured using non-polarising Pb–PbCl (lead–lead chloride) electrodes laid out in a cross with a dipole length of 60 m.
- This first data acquisition has highlighted some issues with anthropogenic noise in the urban area. The MT time-series, particularly the electric fields, were heavily contaminated and distorted due to electromagnetic noise from Dublin City tram/railway systems and other infrastructure.

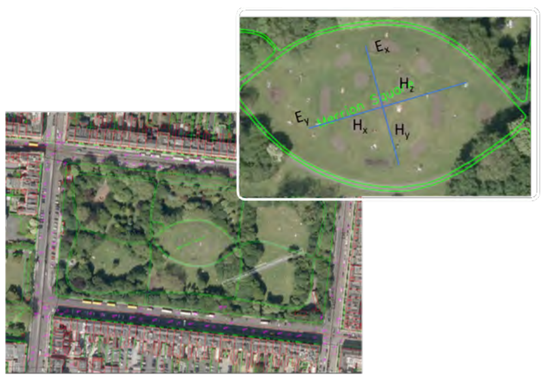

Merrion Square Park deployment map

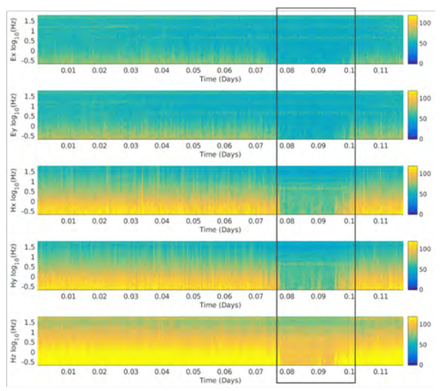

Time series from the Merrion Square park

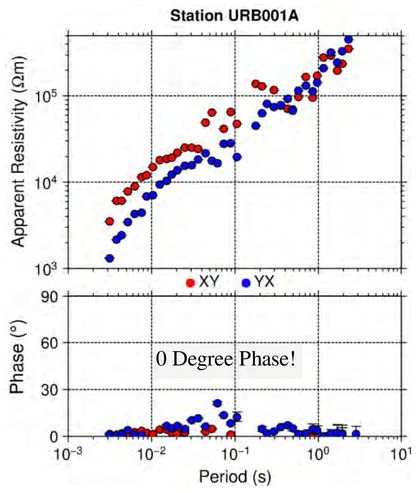

The MT response

NEXT STEP: Seismic Railway Noise Test

- Test the feasibility of exctracting body waves from the noise generated by trains
- In the late 2019, we will deploy 15 sensors c.a along the railway in Newcaste village.
- Study area rationale: Presence of a major geological structure and previous geophysical observations are available (RF, MT, active seismic profiles and deep boreholes).

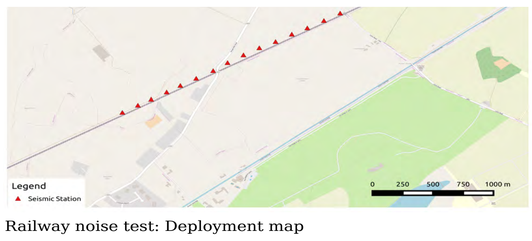

Railway noise test: Deployment map

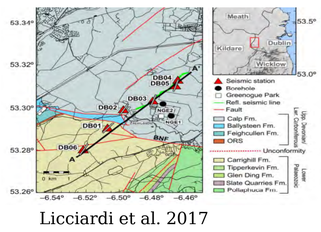

Licciardi et al. 2017

NEXT STEP: Controlled-Source AMT Data Acquisition

- In areas where natural high frequency MT signal quality is poor, it is possible to instead emit a signal from a location at a distance from the survey area (transmitter, Tx). The controlled-source audiomagnetotelluric (CSAMT) method is most effective at detecting and mapping resistivity contrast in the top 1 km of the Earth's surface.

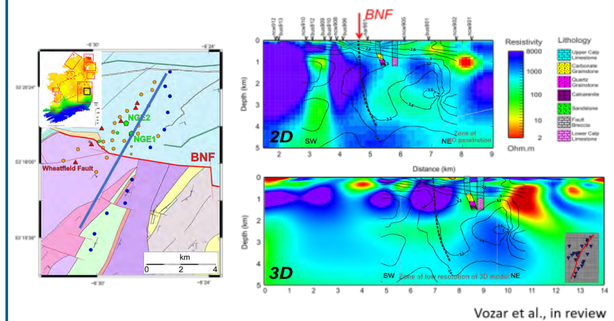

Vozar et al., in review

Prior to data acquisition in Dublin city, electrical resistivity measurements using Phoenix Geophysics CSAMT instrument will be performed in the highly urbanised Dublin suburb, Newcastle. The Newcastle area has already been investigated using multi-geophysical methods (e.g., natural-source MT (Vozar et al., in review)) between the years of 2009 and 2012 with an aim of the development of geothermal energy. The Newcastle area will therefore be an excellent test bed for the CSAMT data acquisition.

This project has been subsidised through the ERANET Cofund GEOTHERMICA (Project no. 731117), from the European Commission and the Department of Communications, Climate Action and Environment / Geological Survey Ireland.

Ireland's European Structural and Investment Funds Programmes 2014-2020
Co-funded by the Irish Government and the European Union
European Union
European Regional Development Fund

References:

- Bensen, G. D., Ritzwoller, M. H., & Shapiro, N. M. (2008). Broadband ambient noise surface wave tomography acro ss the United States. Journal of Geophysical Research: Solid Earth, 113(5), 1-21. https://doi.org/10.1029/2007JB005248
- Nakamura, Y. (1989) A method for dynamic characteristics estimation of subsurface using microtremor on the ground surface. Quaterly Report of the Railway Technical Research Institue 30 (1), 25-30
- Chave, A. D. and Jones, A. G., Eds. 2012. The MT method: Theory and Practice, Cambridge University Press.